

**The role of MLL/AF4  
in  
leukaemic cell biology**

**Lars Buechler**



**A thesis submitted in part requirement for the degree of  
Doctor of Philosophy from the Faculty of Medicine, Newcastle  
University, Newcastle upon Tyne, UK June 2010**

Fusion Gene Research Group

Northern Institute for Cancer Research

Paul O' Gorman Building

Medical School

Framlington Place

Newcastle upon Tyne

NE2 4HH

## Abstract

T(4;11) acute lymphoblastic leukaemia (ALL) presenting the fusion gene *MLL/AF4* is a hallmark of infant ALL. The 5 year event free survival is less than 40%. It was shown that *MLL/AF4* is important for cell cycle progression, proliferation, clonogenicity, engraftment in mice and repression of apoptosis. However, in order to improve treatment *MLL/AF4* needs to be examined in contexts closer to the leukaemic situation *in vivo*.

To investigate the fusion gene, *MLL/AF4* positive SEM, generated from an ALL patient, were depleted for *MLL/AF4* by RNAi. The consequential changes in gene expression patterns were analyzed using cDNA- and Oligo- arrays. These gene expression patterns were assigned to biological functions and pathways using the Ingenuity platform. A set of significantly differently expressed genes such as N-CADHERIN and *FGFR1*, both described for the adherence and regulation of haematopoietic stem cells (HSC), was identified and validated by qRT-PCR.

The HSC niche context was further investigated by establishment of a leukaemic - bone marrow feeder cell-to-cell interaction assay. Increased cell death, cell cycle arrest and prolonged growth curves caused by *MLL/AF4* depletion in SEM could also be shown on feeders. Additionally, culturing of *MLL/AF4* positive patient material on feeders allowed for long-term culture.

An imaging method using fluorescent *MLL/AF4* positive cells in mouse xenograft models was employed to monitor the distribution and biology of *MLL/AF4* positive cells, showing colonisation of bone marrow rich spinal, femoral and cranial bones.

Finally, in order to analyze the function of identified target genes of MLL/AF4 by over-expression, a novel lentiviral expression system allowing transduction of stem cells and tightly regulating induction of expression, was initiated.

In conclusion, these data indicate a central role of MLL/AF4 in leukaemogenesis while the systems established in this work are of relevance for drug development assays.

## **Acknowledgement**

I would like to thank my supervisor Dr. Olaf Heidenreich for this interesting and challenging project and for his technical and theoretical support.

Prof. Josef Vormoor I would like to thank for funding and supporting my work.

I am grateful to the Jose Carreras Stiftung and the NECCR for funding my work.

Also I would like to thank Christian Berens for supplying plasmids including mCherry, pWHE and others as well as his input in the two vector design.

Furthermore I would like to thank Dr. Johann Greil for his support and for providing us with primary SEM.

Importantly, additional thanks go to Vasily Grinev for his expertise in the lentiviral protocol and for the generation of transduced cell lines such as SEMcami, Kasumi-1 DC and for his experimental support.

I am thankful to the NICR and Prof. Andy Hall for providing a state of the art and productive scientific environment.

Most importantly would like to thank Patricia Garrido-Castro for her extensive experimental and scientific support (too much to list here).

I also thank Mike Batey for his support in mouse work and Hesta McNeill for sorting.

Furthermore I thank Kerrie Wilson for her support in FLOW CYTOMETRY analysis, mouse work and reading the manuscript. Additionally I thank Kieran O'Toole for his help in performing the histological sections and Chris Bacon for his pathology expertise in interpreting data.

For reading the manuscript I also thank Simon Bomken and Lisa Russell.

Finally I thank several members of different groups for their scientific and collegial support, these are: Andreas Gessner, Natalia Martinez, Karel Fiser, Svetlana Mysina and Frida Ponthan. I apologise to anyone I forgot.

## **Statement**

All work shown in this thesis was performed by myself, with the exception of “Test of the Teton vector”, chapter 5, which was performed by Vasily Grinev using the Teton vector cloned by myself.

Several experiments included technical assistance of colleagues, these were:

i.f. and i.v. injections and imaging in mice by Mike Batey

sorting of transduced cells by Hesta McNeill

setting and adjusting co-culture flow cytometry by Patricia Garrido Castro and

i.f. injections and flow cytometry compensation by Kerrie Wilson

## Abbreviations

AF4	ALL-1 fused gene on chromosome 4
AL	Acute leukaemia
ALL	Acute lymphoblastic leukaemia
ALF	TFIIA-alpha/beta-like factor
AML	Acute myeloid leukaemia
APC	Allophycocyanin
APS	Ammonium persulfate
BCR	Breakpoint cluster region
BM	Bone marrow
BMP	Bone morphogenic protein
bp	base pair
BSA	Bovine serum albumin
cALL	common ALL
cAMP	cyclic AMP
CD	Cluster of differentiation
cDNA	complementary DNA
CFSE	Carboxyfluorescein succinimidyl ester
CHD	C-terminal homology domain
CIAP	Calf intestinal alkaline phosphatase
CLL	Chronic lymphocytic leukaemia
CLP	Committed lymphoblastic progenitor
CML	Chronic myeloblastic leukaemia
CMP	Committed myeloid progenitor
CMV	Cytomegalo virus (promoter)
CNS	Central nervous system

CP	Committed progenitor
CT	cycle threshold
CXCR	Chemokine receptor
dH <sub>2</sub> O	distilled H <sub>2</sub> O
DJ	Diverse Joining gene segment recombination
DMSO	Dimethylsulfonic acid
DNA	Deoxyribonucleic acid
DNA-PK	DNA protein kinase
dNTP	Deoxynucleotide triphosphate
Dox	Doxycycline
ds	double strand
DSB	Double strand break
DUSP6	Dual specificity phosphatase 6
EB	Elution buffer
EDTA	Ethylene diamine tetra acetate
EGF	Epidermal growth factor
eGFP	enhanced GFP
ERK	Extracellular signal regulated kinase
ES	Embryonic stem cell
FACS	Fluorescence activated cell sorting
FCS	Fetal calf serum
FGF	Fibroblast growth factor
FITC	Fluorescein isothiocyanate
FSC	forward scatter
fw	forward
GAPDH	Glycerine aldehyde 3 phosphate dehydrogenase
G-CSF	Granulocyte colony stimulating factor

GFP	Green fluorescent protein
Gln	Glutamine
GM-CSF	Granulocyte - macrophage colony stimulating factor
GMP	Granulocyte macrophage progenitor
GOI	Gene of interest
Gp	Glycoprotein
Gy	Gray
H3K4	Histone 3 lysine 4
HDAC	Histone deacetylase
HOXA	Homeobox cluster A genes
HSC	Haematopoietic stem cell
i.f.	intra femoral
i.h.	intra hepatic
i.v.	intra venous
ICAM	Intracellular adhesion molecule
IGF	Insulin like growth factor
IL	Interleukin
IN	Integrase
IRES	Internal ribosomal entry site
I- $\kappa$ B	NF- $\kappa$ B inhibitor
KB	Knowledge Base
LB	Luria broth
LEF-1	Lymphoid enhancer-binding factor 1
LFA	Lymphocyte function associated antigen
LIF	Leukaemia inhibitory factor
LMPP	Lymphoid primed multipotent progenitor
LPS	Lipopolysacharide



LSC	Leukaemic stem cell
LT-HSC	Long term HSC
LTR	Long terminal repeat
LXR	Liver X receptor
MAPK	Mitogen activated protein kinase
M-CSF	Macrophage colony stimulating factor
MEF	Murine embryonic fibroblast
miRNA	micro RNA
MkEP	Megakaryocyte erythroid progenitor
MLL	Mixed lineage leukaemia
mRNA	messenger RNA
MSC	Mesenchymal stem cell
MT	Methyltransferase domain
nef	negative factor
NF- $\kappa$ B	Nuclear factor of kappa light polypeptide gene enhancer in B-cells
NHD	N-terminal homology domain
NHEJ	Non homologous end joining
NK	Natural killer cells
NLS	Nuclear localisation sequence
NOD	Non obese diabetic
nt	nucleotide
ORF	Open reading frame
PAA	Poly acryl amide
PAGE	Polyacrylamide gel electrophoresis
PBS	Phosphate buffered saline
PBS	Primer binding site

PBSA	PBS plus BSA
pcG	Polycomb group
PCR	Polymerase chain reaction
PE	Phycoerythrin
PE-Cy7	Phycoerythrin-cyanin7
PEG	Poly ethylene glycol
Pen/Strep	Penicillin/Streptomycin
PerCP	Peridinin chlorophyll protein
PGK	Phospho glycine kinase (promoter)
PHD	Plant homeodomain
PI	Propidium iodide
PIC	Preintegration complex
ppt	poly purine tract
Ptc	Patched
Rag	Recombination activating gene
R region	Repeat element
RAR	Retinoid acid receptor
rev	reverse
RISC	Ribonucleic acid induced silencing complex
RISC	RNA induced silencing complex
RNA	Ribonucleic acid
RNAi	RNA interference
rpm	rounds per minute
RRE	rev response element
RT	Real time (PCR)
RT	Reverse transcriptase (viral enzyme)
RT	room temperature

RTC	Reverse transcriptase complex
rtTA	tet controlled transactivator
RXR	Retinoid X receptor
s.c.	subcutaneous
SCID	Severe combined immunodeficient
SET	Su(var)9-3, Enhancer of Zeste and trithorax histone methyltransferase domain
SFFV	Spleen focus forming virus (promoter)
Shh	Sonic hedgehog
shRNA	short hairpin RNA
SIN	Self inactivating vector
siRNA	short interfering RNA
Smo	Smoothened
SOX	Sry-related HMG box (gene)
ss	single strand
SSC	sideward scatter
ST-HSC	Short term HSC
SV40	Simian virus 40 T antigen
t(a;b)	reciprocal translocation between chromosome a and chromosome b
TAT	Transcriptional transactivator
TCF	T-cell factor
TEMED	Tetramethylethylene diamine
TERT	Telomerase reverse transcriptase
TetO	Tetracyclin operator
teton	rtTA expressing
TGF- $\beta$	Tumour growth factor beta
TRE	tet responsive element

tRNA	transfer RNA
trx	Trithorax
trxG	Trithorax group
TSAP	Thermosensitive shrimp alkaline phosphatase
U region	Unique element 5' or 3'
u / $\mu$ l	unit (enzymatic) / microliter
UTR	Untranslated region
VDJ	Variable Diverse Joining gene segment recombination
VJ	Variable Diverse gene segment recombination
VDR	Vitamin D receptor
Wnt/WNT	wint, wingless and int
WPRE	Woodchuck posttranscriptional regulatory element
X-Gal	staining substrate for $\beta$ -galactosidase

## List of tables

Table 1 Staining protocol for the Annexin-V – PI assay .....	71
Table 2 Oligo-array Ingenuity analysis: The top 5 subcategories of Diseases and Disorders sorted on p-value, generated using Ingenuity Pathway Analysis; Ingenuity Systems Inc. ....	95
Table 3 Oligo-array Ingenuity analysis: The top 5 of Molecular and Cellular Functions .....	97
Table 4 Oligo-array Ingenuity analysis: The top 5 of Physiological System Development and Function sorted on p-value, generated using Ingenuity Pathway Analysis; Ingenuity Systems Inc. ....	98
Table 5 Oligo-array Ingenuity analysis: The top 5 of Associated Network Functions	101
Table 6 Oligo-array Ingenuity analysis: The 16 most significant Canonical pathways .....	103
Table 7 Genes overlapping in cDNA- and oligo array analysis of MLL/AF4 depleted leukaemic SEM cells.....	114
Table 8 Selected genes affected by MLL/AF4 depletion.....	129
Table 9 Cells counts of M210B4, SEMTeton and co-cultures .....	157
Table 10 Cells counts of M210B4, MV4;11Teton and co-cultures .....	160
Table 11 Statistics of Figure 66 and Figure 67 .....	164
Table 12 Statistics of Figures 88 and 89 .....	187
Table 13 Summary of quadrant cell numbers from Figures 94 and 95.....	196
Table 14 GFP positivity of different MV4;11 sorts .....	241
Table 15 GFP positivity of SEMTeton .....	242

## List of figures

Figure 1 Basic model of Haematopoiesis .....	2
Figure 2 Composite model of Haematopoiesis .....	3
Figure 3 Pappenheim stains from patients with ALL .....	6
Figure 4 B-cell development .....	7
Figure 5 Delayed infection hypothesis .....	9
Figure 6 Treatment of leukaemia .....	12
Figure 7 Chemotherapeutic agents .....	14
Figure 8 Chemotherapeutic agents 2 .....	16
Figure 9 Kaplan-Meier estimates of event-free survival .....	17
Figure 10 Kaplan-Meier analysis of event-free survival 2 .....	18
Figure 11 Balanced translocation .....	19
Figure 12 Non-homologous end joining .....	21
Figure 13 The MLL protein and gene .....	22
Figure 14 The processing of the MLL protein .....	24
Figure 15 The frequency of <i>MLL</i> associated chromosomal abnormalities .....	25
Figure 16 Schematic representation of the protein AF4 .....	26
Figure 17 The <i>MLL</i> , <i>MLL/AF4</i> and the <i>AF4/MLL</i> gene .....	27
Figure 18 siRNA mediated RNAi .....	32
Figure 19 shRNA Mechanism .....	33
Figure 20 Comparison of the siRNA and the miRNA RNAi .....	35
Figure 21 Dilution of CFSE staining in cell membranes due to proliferation .....	66
Figure 22 CFSE staining pattern .....	66
Figure 23 The cell cycle .....	72
Figure 24 Typical Cell cycle analysis .....	73
Figure 25 Schematic of Lentivirus generation and transduction .....	84
Figure 26 Flow chart of using Ingenuity Pathway Analysis for array data analysis .....	93
Figure 27 IPA Network Generation, Ingenuity Feature descriptions .....	100
Figure 28 Pie chart of canonical pathways .....	105
Figure 29 Early signalling in hepatic stellate cells .....	106
Figure 30 G-protein coupled receptor signalling .....	107
Figure 31 cAMP mediated signalling .....	108
Figure 32 Wnt / $\beta$ -Catenin signalling .....	109
Figure 33 Role of Oct4 in Mammalian embryonic stem cell pluripotency .....	110
Figure 34 VDR / RXR activation .....	112
Figure 35 <i>MLL/AF4</i> depletion in SEM .....	113
Figure 36 Genes affected by <i>MLL/AF4</i> Knockdown .....	115
Figure 37 qRT-PCR validation of <i>DAAMI</i> and <i>BNIP3</i> .....	116
Figure 38 <i>DUSP6</i> expression analysis .....	117
Figure 39 <i>HOXA7</i> expression analysis .....	118
Figure 40 <i>FGFR1</i> expression analysis .....	119
Figure 41 N-cadherin expression analysis .....	120
Figure 42 N-CADHERIN surface expression analysis .....	121

Figure 43	Model of the haematopoietic stem cell niche .....	134
Figure 44	Regulation of a HSC in the bone marrow niche .....	135
Figure 45	Schematic of the regulation of a HSC .....	139
Figure 46	Pathways regulating the HSC in the endosteal and vascular niche .....	141
Figure 47	Summary of niche interactions .....	142
Figure 48	HS-5 feeder layers treated with Mitomycin C .....	146
Figure 49	Cell cycle analysis dot plots of HS-5 .....	148
Figure 50	Cell cycle analysis Histogram of HS-5 .....	148
Figure 51	HS-5 cell cycle Modfit Analysis using Aneuploid and Diploid mode .....	149
Figure 52	HS-5, MV4;11 and co-culture .....	150
Figure 53	Cellcycle Dotplots of untreated M210B4 cells .....	151
Figure 54	Cellcycle histogram of untreated M210B4 .....	151
Figure 55	Cell cycle Dotplots of M210B4 cells irradiated at 80 Gy .....	152
Figure 56	Cell cycle of irradiated M210B4 .....	152
Figure 57	SEMTeton cultured on M210B4 feeder layers .....	154
Figure 58	SSC – FSC Dot-Plots for M210B4 and SEMTeton .....	155
Figure 59	Flow cytometric analysis of M210B4, SEMTeton and co-cultures .....	156
Figure 60	Flow cytometric analysis of M210B4 - SEMTeton co-cultures .....	156
Figure 61	Cell counts of M210B4 and SEMTeton and co-cultures .....	158
Figure 62	M210B4 and MV4;11Teton controls .....	159
Figure 63	M210B4, MV4;11Teton and co-cultures analysed by flow cytometry .....	159
Figure 64	Flow cytometric analysis of M210B4 - MV4;11Teton co-cultures .....	159
Figure 65	Cell counts of M210B4, MV4;11Teton and co-cultures .....	161
Figure 66	Flow cytometry discrimination of Feeders and SEMTeton .....	162
Figure 67	Flow cytometry discrimination of SEMTeton dilutions on feeders .....	163
Figure 68	Niche proliferation standard curve .....	165
Figure 69	Co-culture images of Mv4;11Teton on M210B4 feeders .....	166
Figure 70	Co-culture images of SEMTeton on M210B4 feeders .....	167
Figure 71	Images of M210B4 co-cultures with Kasumi-1 or SKNO-1 .....	168
Figure 72	Inversion experiment on M210B4 Feeder .....	169
Figure 73	<i>AML/MTG8</i> knockdown in Kasumi-1 DC .....	171
Figure 74	<i>MLL/AF4</i> expression in siRNA treated SEM and SEMTeton .....	171
Figure 75	SEM electroporated and co-cultured on feeder in 1/20 dilution .....	173
Figure 76	SEM electroporated and co-cultured on feeder in 1/40 dilution .....	173
Figure 77	siRNA treated SEM seeded in dilutions with and without feeders .....	175
Figure 78	siRNA treated Kasumi-1 seeded in dilutions with and without feeders .....	176
Figure 79	<i>MLL/AF4</i> depletion in SEMTeton on feeders .....	178
Figure 80	Cell numbers of <i>MLL/AF4</i> depleted SEMTeton without feeders .....	179
Figure 81	Cell numbers of <i>MLL/AF4</i> depleted SEMTeton on feeders .....	180
Figure 82	Fusion gene depletion in Kasumi-1 DC on feeders .....	181
Figure 83	Relative cell numbers of Kasumi-1 DC treated with siMA6 without feeders .....	182
Figure 84	Relative cell numbers of Kasumi-1 DC treated with siMA6 on feeders .....	182
Figure 85	Gene expression changes of <i>MLL/AF4</i> depleted SEM kept on feeders .....	183

Figure 86 Gene expression changes of MLL/AF4 depleted SEM without feeders .....	184
Figure 87 SEM controls for PI and Annexin-V staining.....	185
Figure 88 Apoptosis in siMA6 treated SEM.....	186
Figure 89 Apoptosis in siAGF1 treated SEM .....	186
Figure 90 Feeder Influence on MLL/AF4 derived apoptosis.....	187
Figure 91 CFSE tracking of daughter populations in siRNA treated SEM .....	189
Figure 92 Gene expression levels of a 96h timecourse in siRNA treated SEM without feeders .....	190
Figure 93 Gene expression levels of a 144h timecourse in siRNA treated SEM .....	192
Figure 94 Infant –MLL/AF4 patient viability.....	195
Figure 95 Cell viability fibroblast control.....	195
Figure 96 MLL/AF4 patient cells CD19 shifts .....	197
Figure 97 MLL/AF4 patient cells after 3 weeks on M210B4 feeders .....	198
Figure 98 Baltimore Classification of Viruses Classes I-VII .....	212
Figure 99 HIV Lifecycle .....	215
Figure 100 Reverse transcription of lentiviral RNA .....	216
Figure 101 Lentiviral DNA integration.....	218
Figure 102 Genomic structure of HIV .....	220
Figure 103 The development of lentiviral vectors .....	224
Figure 104 Tet-on system .....	226
Figure 105 Scheme of Lentiviral two vector system .....	228
Figure 106 Schematic of the protocol for the lentiviral two vector system.....	229
Figure 107 Scheme of Lentivirus 1 (Teton vector) cloning.....	232
Figure 108 Map of pUHrt62-1 .....	233
Figure 109 Map of pHR-SINcPPT-SIEW (SIEW) vector .....	234
Figure 110 Restriction analysis of pUHrT62-1 oligo ligation .....	235
Figure 111 Restriction analysis of Teton vector clone.....	236
Figure 112 Functionality test of vector 1 (Teton vector).....	237
Figure 113 Transduction rates of Vector 1 in SEM and MV4;11.....	239
Figure 114 MV4;11 as negative control for transduction.....	240
Figure 115 Sorts of Teton transduced MV4;11.....	240
Figure 116 GFP positivity SEM and sorted SEMTeton .....	241
Figure 117 Cloning of the Tet-PGK-cherry cassette .....	244
Figure 118 Scheme of SIEW-Tre-PGK-cherry cloning.....	244
Figure 119 Map of pTRE-Tight vector .....	245
Figure 120 Map of pWHE1105 vector.....	245
Figure 121 Map of pTre-PGK vector.....	246
Figure 122 Map of pcDNA3.1-mcherry vector.....	246
Figure 123 Map of pTre-PGK-cherry vector (PPC) .....	247
Figure 124 Restriction digest of pTre-PGK clones.....	248
Figure 125 Restriction digest of pTre-PGK cherry clones.....	249
Figure 126 Intra-femoral injection (i.f.) into a mouse .....	261
Figure 127 GFP fluorescence.....	265
Figure 128 Early SEM and engraftment in R2G mice.....	269



Figure 129 Bone marrow of a 2nd transplanted R2G mouse.....	271
Figure 130 Early SEM control 2 .....	271
Figure 131 Peripheral blood of a transplanted NSG mouse.....	273
Figure 132 Bone marrow of a NSG mouse.....	273
Figure 133 Sections of NSG mouse spleens .....	275
Figure 134 NSG mouse with fur and with Veet hair removal .....	277
Figure 135 NSG mouse i.f. transplated with SEMcami.....	278
Figure 136 NSG mouse injected i.f with SEMcami.....	279
Figure 137 Panel of a control mouse and an i.f. transplanted NSG mouse.....	280
Figure 138 NSG mouse 1 transplanted i.v. with SEMcami .....	281
Figure 139 NSG mouse 2 with i.v. transplant of SEMcami.....	282
Figure 140 NSG mouse 3 injected i.v. with SEMcami .....	283
Figure 141 NSG mouse injected i.v. with SEMcami .....	284
Figure 142 Cranium and brain of NSG mouse .....	285
Figure 143 NSG mouse injected s.c. with SEMcami.....	286
Figure 144 NSG mouse injected s.c. 2nd panel from Figure 143 .....	286

# Contents

<b>CHAPTER 1: INTRODUCTION .....</b>	<b>1</b>
<b>1.1 Haematopoiesis .....</b>	<b>1</b>
<b>1.2 Leukaemia .....</b>	<b>4</b>
1.2.1 AML .....	5
1.2.2 ALL .....	6
1.2.2.1 ALL epidemiology and aetiology .....	7
1.2.2.2 ALL Development .....	9
1.2.2.3 Treatment .....	11
1.2.2.3.1 Chemotherapeutic agents .....	13
1.2.2.4 Outcome .....	16
<b>1.3 Recurrent chromosomal rearrangements .....</b>	<b>19</b>
<b>1.4 MLL.....</b>	<b>21</b>
<b>1.5 AF4 .....</b>	<b>25</b>
<b>1.6 MLL/AF4 ALL .....</b>	<b>27</b>
<b>1.7 The RNAi pathway and siRNA.....</b>	<b>31</b>
<b>1.8 General aims.....</b>	<b>38</b>
<b>CHAPTER 2: MATERIALS AND METHODS.....</b>	<b>40</b>
<b>2.1 General Materials .....</b>	<b>40</b>
2.1.1 Materials.....	40
2.1.2 Equipment .....	40
2.1.3 Plastics .....	42
2.1.4 Chemicals.....	42
2.1.5 Buffers .....	43
2.1.6 Molecular Cloning.....	45
2.1.6.1 Restriction Enzymes.....	45
2.1.6.2 Modifying Enzymes.....	45
2.1.7 Cell analysis .....	46
2.1.8 Real Time RT-PCR .....	47
2.1.9 Kits .....	47
2.1.10 Synthetic Oligonucleotides .....	47
2.1.11 Cell-lines .....	51
2.1.12 Bacteria.....	54
2.1.13 Mice .....	55
<b>2.2 Methods .....</b>	<b>56</b>
2.2.1 Methods chapter 3: Array validation.....	56

2.2.1.1 Array analysis Ingenuity.....	56
2.2.1.2 Hybridization of siRNA.....	57
2.2.1.3 RNAi and Electroporation.....	57
2.2.1.4 RNA isolation.....	57
2.2.1.5 cDNA synthesis.....	58
2.2.1.6 Primer design.....	58
2.2.1.7 Quantitative Real Time PCR analysis.....	59
2.2.1.8 Amplicon control.....	61
2.2.1.9 Cell culture.....	62
2.2.1.10 Freezing and thawing of cells.....	62
2.2.1.11 Counting cells.....	63
2.2.1.12 Flow cytometric analysis.....	63
2.2.1.13 Compensation.....	64
2.2.1.14 CFSE staining.....	64
2.2.2 Methods Chapter 4 - Bone Marrow Feeders.....	67
2.2.2.1 Growth arrest with MMC.....	67
2.2.2.2 Growth arrest with AMD.....	67
2.2.2.3 Growth arrest with Irradiation.....	67
2.2.2.4 Collagen coating.....	68
2.2.2.5 Co-culture.....	68
2.2.2.6 Inversion Test.....	69
2.2.2.7 Discriminating count.....	69
2.2.2.8 Flow cytometric analysis based cell count on Feeder.....	69
2.2.2.9 Primary Material co-culture.....	70
2.2.2.10 Determination of viable cells with Annexin-V and PI.....	70
2.2.2.11 Cell cycle analysis.....	71
2.2.3 Methods Chapter 5 - Lentiviral cloning, production and transduction.....	73
2.2.3.1 DNA- restriction Digest.....	73
2.2.3.2 Gel electrophoresis.....	74
2.2.3.3 Gel extraction.....	74
2.2.3.4 Modification.....	75
2.3.3.4.1 Blunting.....	75
2.3.3.4.2 Dephosphorylation.....	76
2.3.3.4.3 Phosphorylation.....	77
2.2.3.5 Oligo design and synthesis.....	77
2.2.3.6 Ligation.....	78
2.3.3.6.1 sticky end.....	78
2.3.3.6.2 blunt end.....	78
2.2.3.7 Transformation.....	79
2.3.3.7.1 JM109.....	79
2.3.3.7.2 STBI3.....	79
2.2.3.8 DNA Purification.....	80
2.3.3.8.1 Quick plasmid isolation.....	80
2.3.3.8.2 Mini kit, midi kit and maxi kit.....	80
2.2.3.9 Lentivirus Production.....	81
2.2.3.10 Lentivirus Transduction.....	83
2.2.3.11 Measurement of Transduction rate.....	85
2.2.3.12 Sort.....	85
2.2.3.13 Test of Function.....	86

2.3.4 Methods Chapter 6 - Mouse work.....	86
2.3.4.1 Handling.....	86
2.3.4.2 Injections .....	87
2.3.4.2.1 Intraperitoneal injection, i.p. ....	87
2.3.4.2.2 Intrafemoral injection, i.f. ....	87
2.3.4.2.3 Intrahepatic injection, i.h. ....	87
2.3.4.3 Section .....	88
2.3.4.4 Cell harvest .....	88
2.3.4.5 Imaging .....	89
<b>CHAPTER 3 ARRAY ANALYSIS AND VALIDATION.....</b>	<b>91</b>
<b>3.1 Introduction.....</b>	<b>91</b>
<b>3.2 Aims .....</b>	<b>92</b>
<b>3.3 Results Array Analysis and validation .....</b>	<b>93</b>
3.3.1 Array analysis.....	93
3.3.1.1 Oligo array (Affimetrix U133 Plus 2.0) Ingenuity analysis.....	93
3.3.1.2 Array comparison and validation of possible target genes .....	112
3.3.1.3 Evaluation of N-cadherin Surface expression .....	121
<b>3.4 Discussion Array Chapter .....</b>	<b>122</b>
<b>CHAPTER 4 BONE MARROW FEEDER INTERACTION.....</b>	<b>132</b>
<b>4.1 Introduction and Theory .....</b>	<b>132</b>
4.1.1 Stem cells.....	132
4.1.2 The haematopoietic niche.....	132
4.1.3 Surface molecules regulating the niche .....	136
4.1.3.1 Neuronal cadherin .....	136
4.1.3.2 Fibroblast growth factor .....	137
4.1.3.3 $\beta$ -catenin.....	138
4.1.3.4 Notch .....	138
4.1.3.5 BMP .....	140
<b>4.2 Aims .....</b>	<b>143</b>
<b>4.3 Results Bone marrow feeder interactions.....</b>	<b>144</b>
4.3.1 Establishment of Feeder layer .....	144
4.3.2 Examination of HS-5 for feeder layer properties.....	144
4.3.3 Test of M210B4 .....	150
4.3.3.1 Growth arrest .....	151
4.3.3.2 Incubation of M210B4 feeders with SEMTetron.....	153
4.3.3.3 Establishment of a flow cytometry based cell count assay .....	161
4.3.3.4 Co-cultures of SEMTetron and MV4;11Tetron on M210B4 .....	166
4.3.3.5 Inversion test .....	168
4.3.4 Fusion gene knock down and feeder interaction .....	170

4.3.5 Investigation of feeder influence on fusion gene depletion derived gene expression and viability .....	178
4.3.6 Track of daughter populations after MLL/AF4 knockdown .....	188
4.3.7 The feeder as an assay system for interactions.....	190
4.3.7.1 MLL/AF4 influence on <i>HOXA7</i> and <i>TERT</i> .....	190
4.3.7.2 The feeder and primary patient material .....	193
<b>4.4 Discussion Feeder Chapter .....</b>	<b>199</b>

## **CHAPTER 5 LENTIVIRAL CLONING, PRODUCTION AND TRANSDUCTION .....211**

<b>5.1 Introduction and Theory .....</b>	<b>211</b>
5.1.1 Lentiviruses.....	213
5.1.2 Reverse Transcription.....	215
5.1.3 Integration.....	217
5.1.4 Genomic structure.....	219
5.1.5 HIV derived Lentiviral vectors.....	221
5.1.6 IRES .....	224
5.1.7 WPRE .....	225
5.1.8 Tet-on .....	225
5.1.9 Two vector system design .....	227
<b>5.2 Aims .....</b>	<b>230</b>
<b>5.3 Results.....</b>	<b>232</b>
5.3.1 Generation of the TetOn Vector.....	232
5.3.2 Cloning of the TetOn vector .....	233
5.3.2.1 Test of the TetOn Vector .....	236
5.3.2.2 Virus generation and transduction of TetOn .....	238
5.3.2.2.1 Validation of Transduction.....	238
5.3.2.2.2 Sorting of Transduced cell populations.....	239
5.3.2.2.3 Test for accessibility of MLL/AF4 Knockdown.....	242
5.3.2.2.4 Test on bone marrow feeders.....	243
5.3.2.2.5 Test of clonogenicity .....	243
5.3.3 Cloning of expression vector .....	243
<b>5.4 Discussion lentiviral results .....</b>	<b>250</b>

## **CHAPTER 6 MOUSE WORK .....257**

<b>6.1 Introduction: mouse models for leukaemia .....</b>	<b>257</b>
6.1.1 SCID .....	257
6.1.2 NOD SCID .....	258
6.1.3 NSG .....	258
6.1.4 Rag2 knockout mice.....	259
6.1.5 R2G .....	260
6.1.6 The use of mouse models for studying leukaemia .....	260
6.1.7 Imaging .....	265

<b>6.2 Aims .....</b>	<b>267</b>
<b>6.3 Results mouse work .....</b>	<b>268</b>
6.3.1 SCID mice i.f. injections with early SEM .....	268
6.3.1.1 Flow cytometric analysis.....	268
6.3.1.2 Histological examinations.....	274
6.3.2 Establishment of an SEM <i>in vivo</i> monitoring in mice .....	276
6.3.2.1 SEM cami injections i.f., i.v. ....	276
6.3.2.1.1 Hair removal .....	277
<b>6.4 Discussion mouse results.....</b>	<b>288</b>
<b>CHAPTER 7 GENERAL DISCUSSION.....</b>	<b>296</b>
<b>7.1 Summary of thesis .....</b>	<b>296</b>
<b>7.2 Overall summary.....</b>	<b>306</b>
<b>REFERENCES.....</b>	<b>307</b>
<b>APPENDIX.....</b>	<b>336</b>
cDNA array data .....	336
oligo array data .....	337
Conferences .....	338
Publication .....	339
Courses .....	340

# **Chapter 1**

## **General introduction**

# Chapter 1: Introduction

## 1.1 Haematopoiesis

Haematopoiesis is the formation (greek: poiesis) of blood (greek: haima) cells. This process provides all blood cells which originate from haematopoietic stem cells (HSC). Haematopoietic stem cells are able to self-renew and are multipotent meaning they can differentiate into all types of blood cells. In human adults they are located in the bone marrow. In principle, haematopoietic stem cells can divide indefinitely and maintain the stem cell pool, whilst producing progenitor cells. This function of dividing to form at least one identical daughter cell with full differentiation potential is called self-renewal. In contrast progenitors are already restricted, meaning they cannot differentiate into all types of blood cells anymore. Progenitor cells and subsequently differentiated cells show increasing restriction to specific cell types and increasing proliferation potential, while HSCs divide only rarely. More and more differentiated blood cells are amplified by proliferation and continuously provide the cellular components of blood (Figure 1).

Fetal haematopoiesis occurs mainly in the liver. However, other organs can harbor haematopoiesis if necessary, including the thymus and spleen. These are known as extramedullary sites of haematopoiesis.



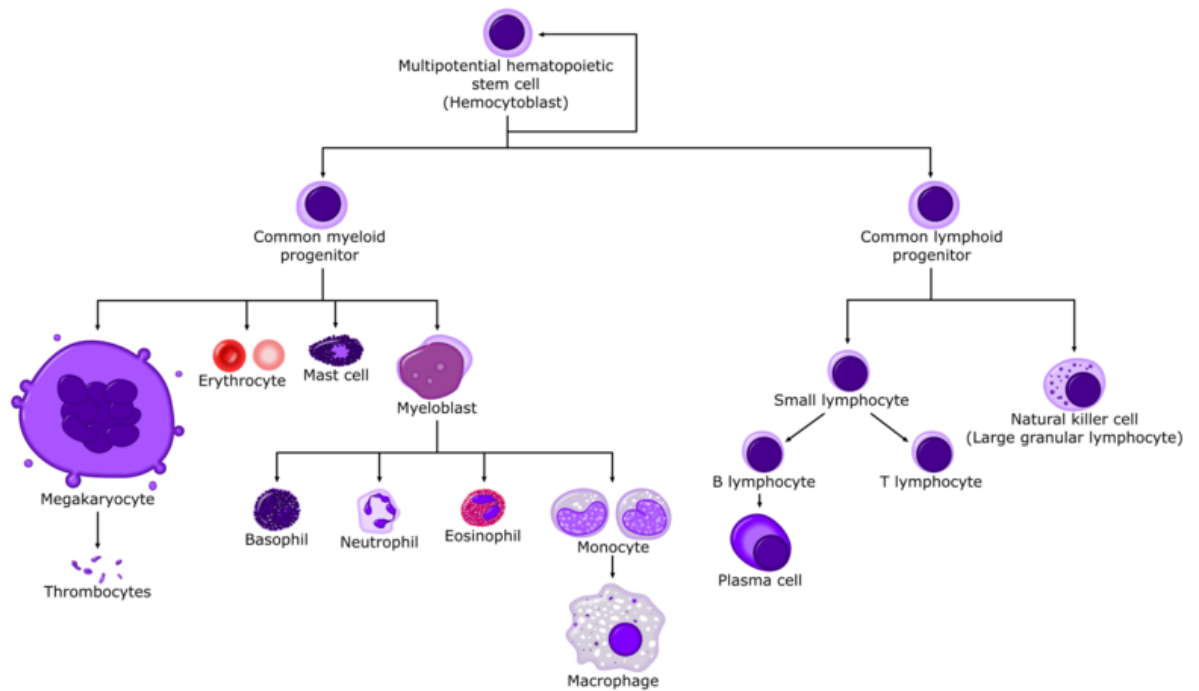


Figure 1 Basic model of Haematopoiesis

A haematopoietic stem cell can differentiate into progenitor cells which can further differentiate into fully mature lymphoid and myeloid blood cells. There are two major types of blood cells: myeloid cells which derive from the common myeloid progenitor and comprise cells such as Erythrocytes and Granulocytes and lymphoid cells which derive from the common lymphoid progenitor and comprise cells such as B and T lymphocytes from [scioly.org/w/index.php?title=Anatomy](http://scioly.org/w/index.php?title=Anatomy)

There are two main subgroups of blood cells:

- the myeloid which comprise the macrophages, monocytes, granulocytes (basophil, neutrophil and eosinophil), mast cells, erythrocytes and thrombocytes (fragments of megakaryocytes)
- the lymphocytes which comprise natural killer cells, T-lymphocytes and B-lymphocytes.

The myeloid cells are derived from a common myeloid progenitor while the lymphoid derive from a common lymphoid progenitor.

A more up to date model from Adolfsson et al 2005 (Adolfsson, Mansson et al. 2005) slightly changes the position of the progenitor cells (see Figure 2).

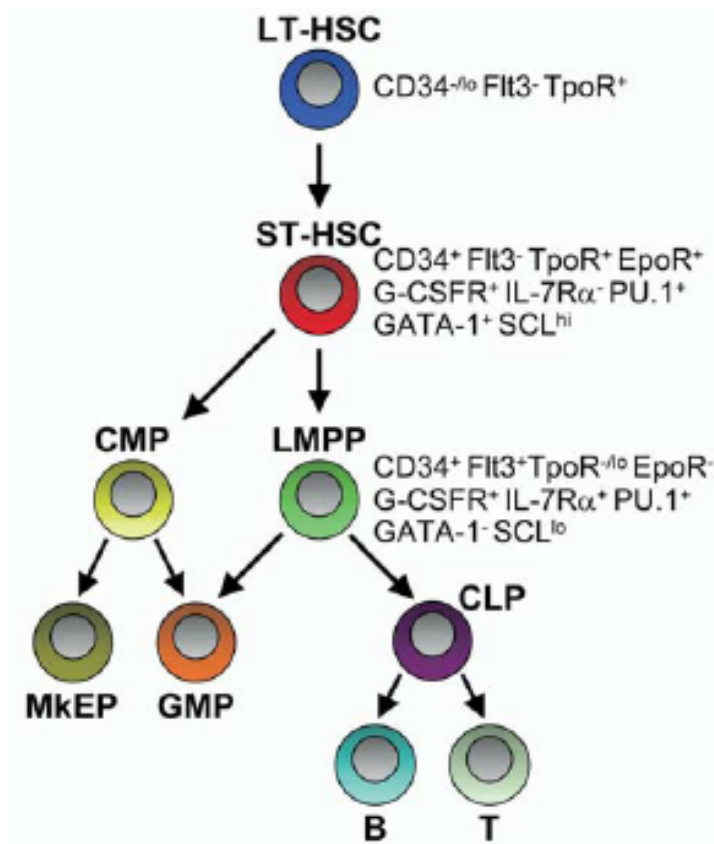


Figure 2 Composite model of Haematopoiesis

A longterm Haematopoietic stem cell (LT-HSC) differentiates into a short term HSC (ST-HSC) which can further differentiate into a common myeloid progenitor (CMP) and a lymphoid primed multipotent progenitor (LMPP). CMPs give rise to megakaryocyte/erythroid progenitors (MkEP) and granulocyte/macrophage progenitors (GMP). LMPP give rise to GMPs as well as to CLPs which differentiate into B and T cells. So far this was shown in mice. from Adolfsson et al 2005

This model further specifies longterm HSCs (LT-HSC), with full self renewal capacity and short term HSCs (ST-HSC), with reduced self-renewal capacity compared to LT-HSCs, but still full myelo-lymphoid differentiation potential (Figure 2). Most importantly, the existence of a so called lymphoid-primed multipotent progenitor (LMPP) with high proliferation potential and combined myelo-lymphoid differentiation potential, but an ablated ability to generate erythroid and megakaryocyte lineages,

changed the current model (Adolfsson, Borge et al. 2001; Adolfsson, Mansson et al. 2005). However, the existence of a LMPP was shown in mice so far.

Lymphoid organs such as spleen, thymus and lymph nodes are important in the maturation, activation and proliferation of certain lymphoid cells. The old model consisted of a lymphoid restricted progenitor which should migrate to lymphoid organs for the maturation into fully differentiated cells, however the newer finding of the LMPP in mice, which can also give rise to GMPs (granulocyte macrophage progenitors) questions if such a LMPP would migrate to lymphoid organs.

The various sub branches of haematopoiesis can be activated and thus regulated by certain growth factors such as colony stimulating growth factors and interleukins. Haematopoietic stem cells, progenitors and fully differentiated blood cells show a characteristic set of surface expression markers by which they can be identified.

## **1.2 Leukaemia**

Leukaemia is a term constituted of the two greek words leukos for “white” and hamia for “blood”. Leukaemia is a haematological malignancy, a type of cancer which affects blood cells. Leukaemias are divided onto two main groups: the chronic and the acute leukaemias. In chronic leukaemia, mature but abnormal white blood cells accumulate over a long period, the progression usually takes months to years and is often monitored for evidence of substantial disease progression before being treated. Chronic leukaemia is mainly found in older patients.

In contrast, acute leukaemia is characterized by a fast progression. Immature cells accumulate and interfere with the production of normal blood cells in the bone marrow,

resulting in bone marrow failure syndrome – the combination of low levels of erythrocytes, leukocytes and platelets. Early initiation of treatment is required due to the fast progression of the disease. The extreme enrichment of malignant cells leads to a spill over in the blood and organ infiltration. These two features result in the common presenting symptoms:

fatigue; breathlessness; susceptibility to infections; excessive bruising; petechiae; (little spots or lines in the skin due to low platelets); bone pain; joint pain and enlargement of lymph nodes, liver and spleen.

Acute leukaemia is subclassified into acute myeloid leukaemia (AML) and acute lymphoblastic leukaemia (ALL).

### **1.2.1 AML**

Acute myeloid leukaemia (AML) affects white blood cells from the myeloid lineage. Similar to ALL it is characterized by a rapid growth of abnormal myeloid cells which accumulate in the bone marrow and interfere with the generation of normal blood cells. This results in fatigue, shortness of breath, bruising, bleeding and a higher risk for infections. The symptoms are caused by the replacement of normal cells, the drop in red blood cells and platelets. One subgroup are AMLs with recurrent genetic abnormalities like translocations, e.g. t(8;21) where a RUNX1 / RUNX1T1 fusion protein is present.

## 1.2.2 ALL

Acute lymphoblastic leukaemia (ALL) affects white blood cells of the lymphoid lineage.

The symptoms are the same as for acute leukaemia in general.

ALL is diagnosed by analysis of the complete blood count, blood smears and the white cell count. Blood smears show blasts in the majority of ALL cases (see Figure 3).

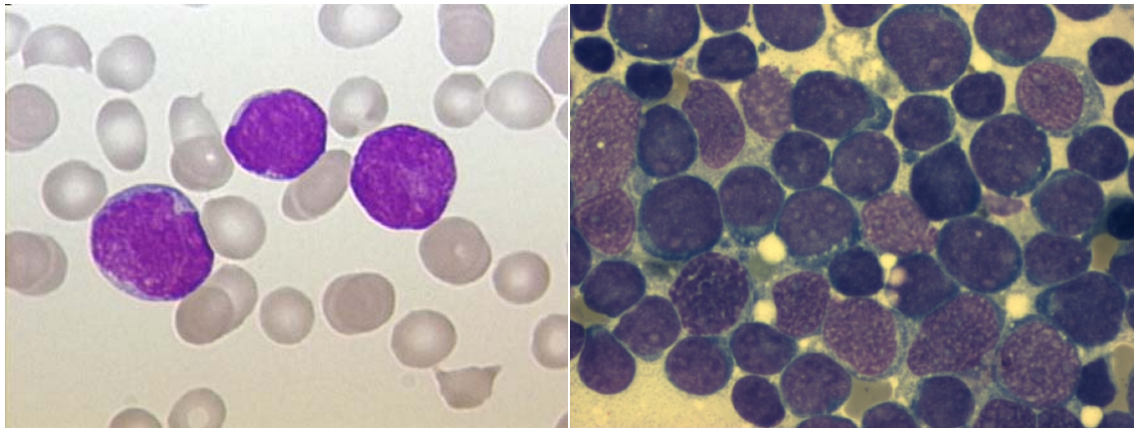


Figure 3 Papanheim stains from patients with ALL

(Left) Peripheral blood of a child (magnification x100), 3 violet stained bigger cells are lymphoblasts, grey cells are erythrocytes (Right) Bone marrow smear (large magnification). Bone marrow containing numerous lymphoblasts. free to publish

Bone marrow biopsies are used to prove ALL. Further diagnostics include cytogenetics and immunophenotyping to subclassify if blasts derive from B or T-cells, determining T- or B-cell ALL. But also imaging methods such as ultrasound and CT are used to investigate if organs such as lungs, liver, spleen, lymph nodes, kidneys and brain were infiltrated.

B lineage ALL can be further subdivided by surface marker expression into progenitor cells (see Figure 4).

In precursor B cell ALL (CD10+, cytIgM+) a precursor, a partially differentiated, unipotent cell, often called blast as well is affected. Subtypes of precursor B-cell ALL comprise translocation generated forms (see chapter 1.3) such as t(12;21)-ETV, t(1;19)-E2A/PBX1, t(9;22)-BCR/ABL and t(v;11q23)-*MLL* rearrangement.

Pro-B ALL (CD10-) is one of the most immature ALL subtypes. Approximately 30% show the t(4;11) translocation (see chapter 1.3 ).

Finally common ALL (cALL) (CD10+, cytIgM -) which is more mature than pro B-ALL is found to be connected to t(9;22), t(12;21) and hyperploid B-cells. cALL comprises for 20% of childhood ALL. It shows a high recurrence of chromosomal translocations such as t(1;19)(q23;p13).

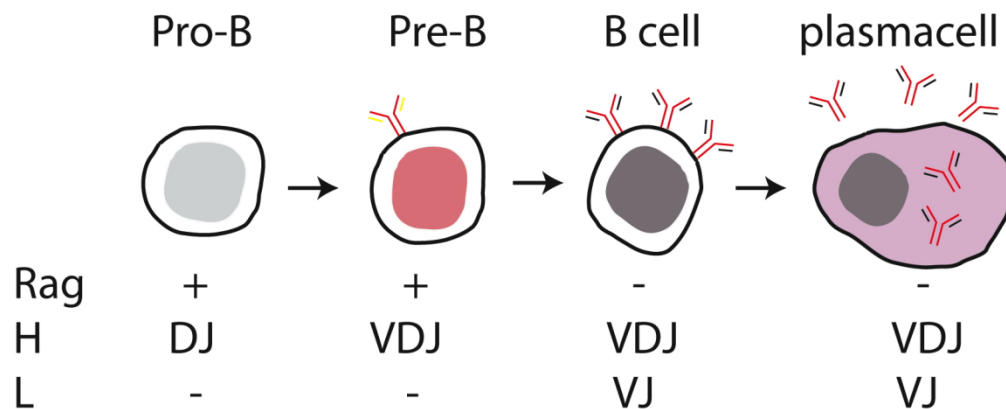


Figure 4 B-cell development

A B-cell differentiates starting from a pro-B cell to a pre B cell, to a B cell and finally a plasmacell. These stages correspond to genetic processes. Rag (recombination active gene) involved in recombination and rearrangement; H Heavy chain, L light chain of immunoglobuline; DJ, VJ, VDJ Diverse (D), Variable (V) and Joining (J) gene segment events. from [nfs.unipv.it/.../immunology/bcelldif](http://nfs.unipv.it/.../immunology/bcelldif)

### 1.2.2.1 ALL epidemiology and aetiology

The majority of the ALL cases occur in children with a peak age of 2 to 5 years with a 1:1.3 predominance in males. Although a few cases are connected to inherited diseases

such as Down syndrome, Bloom's syndrome, Ataxia telangiectasia and Nijmegen breakage syndrome they only account for less than 5% (Pui, Robison et al. 2008). Studies have shown that ALL is also associated to ionizing radiation, exposure to chemotherapy and a high birth weight (Hjalgrim, Westergaard et al. 2003). Overall a relation to industrialization was found. Additionally, it is known that there is a prenatal origin for some childhood leukaemias (Wiemels, Cazzaniga et al. 1999).

Flavonoids such as Quercetin found in fruits and vegetables could, according to a hypothesis, act as Topoisomerase II inhibitors and could increase the risk of childhood leukaemias as discussed by Juli A. Ross 2000 (Ross 2000) .

Twin studies in *TEL/AML1 (ETV6/RUNX1)*-positive ALL revealed that although there is a much higher prevalence for ALL of about 100 times (Mori, Colman et al. 2002) the concordance of developing ALL in identical twins who bear this fusion is only 10%. This can be explained by the concept that additional events to a first hit are required after birth to induce leukaemia (Greaves and Wiemels 2003).

The delayed infection hypothesis from Greaves relies on a minimum two-hits model connecting prenatal events to second hits (see Figure 5). Because of the increased hygienic situation in industrialized countries a pre-leukaemic cell would have low exposure to antigens. If a delayed, meaning later in life, infection occurs it could trigger an aberrant response of the pre-leukaemic cell. This response is induced by cytokines produced from activated T-cells, which lead to a suppression of haematopoiesis and a selective outgrowth of preleukaemic cells. Secondary mutations can then generate "overt leukaemic cells" (Greaves 2006).

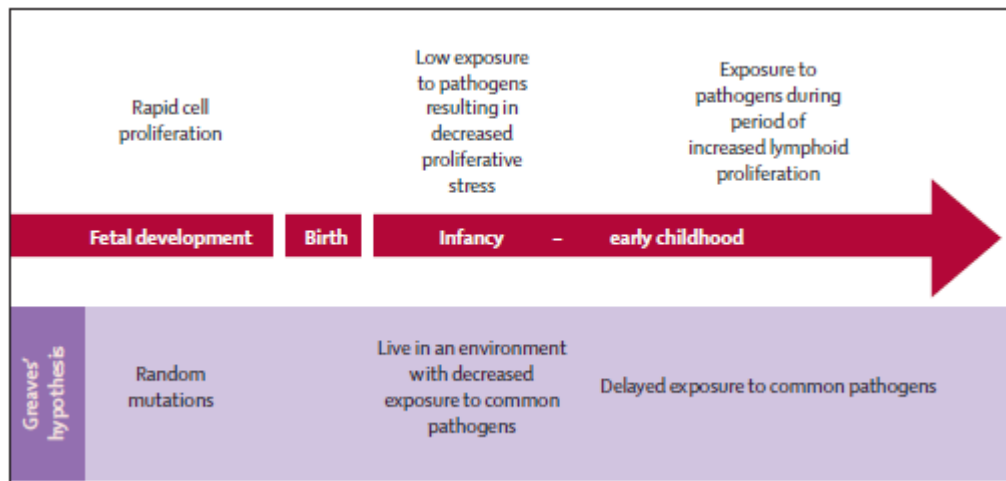


Figure 5 Delayed infection hypothesis

Greaves' hypothesis is based on a pre-leukaemic cell which is exposed to low antigen levels after birth due to higher hygiene in industrialized countries. It assumes that infections in early childhood could trigger the growth of such a pre-leukaemic cell. from Pui et al. 2008

### 1.2.2.2 ALL Development

The development of ALL is thought to begin in committed blood progenitor cells that received events such as mutations, deletions and translocations. Committed haematopoietic progenitors in general can be of the myeloid (CMP, MkEP, GMP) the lymphoid branch (CLP) or mixed lympho-myeloid (LMPP). If genetic lesions such as mutations occur in a B or T-cell, they can produce a stage specific developmental arrest or an impaired capacity for unlimited self renewal (Armstrong and Look 2005). But such mutations can have already occurred in haematopoietic stem cells providing those with multi-lineage capacities (Wang and Dick 2005).

A recent study investigated bone marrow mesenchymal stem (BM-MS) cells of children with B-ALL for different cytogenetic abnormalities with fusion genes like *TEL/AML1*, *BCR/ABL*, *AML/MTG8*, *MLL/AF9*, *MLL/AF10* and *MLL/ENL* (Menendez P, Catalina P 2009). Only *MLL/AF4* patient mesenchymal stem cells were positive for the corresponding fusion gene and its expression. In this context the fusion could be



generated early in the stem cell hierarchy while the leukaemic blast is arrested in the later stage of a pro B cell (Menendez P, Catalina P 2009).

Although chromosomal abnormalities are a hallmark of ALL, additional genetic events are necessary to induce leukaemia. In 40% of B-cell precursor ALLs events such as amplifications, point mutations and deletions are located in B-cell regulating genes (Mullighan, Goorha et al. 2007). The B cell developmental genes are frequent targets for mutation, these include TCF3, LEF1 and IKZF1 and most frequently PAX5, which is mutated in about 30% of precursor ALLs (Mullighan, Goorha et al. 2007). The sequential expression of these and other transcription factors drives the B-cell through its several developmental stages.

The Knudson 2-hits model is based on observations in retinoblastoma but was generalized to all cancers. According to this model, cancer is the result of accumulated mutations to a cell's DNA. As retinoblastoma cases showed, children with early disease onset had inherited a first event and just needed a second event for the generation of retinoblastoma. Older patients should have acquired two mutations before they developed this cancer type (Knudson A 2001). Later this model was expanded, stating that carcinogenesis is dependent on tumour suppressor genes, which control cell growth, and on proto-oncogenes, which stimulate cell growth (Tomlinson, Roylance et al. 2001).

Beside the HSC as cell of origin for ALL, previous models also state that leukaemia is established by a rare leukaemic stem cell (LSC) within the leukaemic cell population. In contrast to the rare LSC (leukaemic stem cell) model, Le Viseur et al. have shown that sorted primary blast populations from B precursor ALL, representative of several stages of B precursor maturation, are able to initiate leukaemia in a NSG mouse model, even

with restricted numbers transplanted (Le Viseur 2008). This has led to the development of a new ALL stem cell model, where almost every cell has the potential to activate stem cell phenotype, as discussed by Vormoor (Vormoor 2009).

### **1.2.2.3 Treatment**

Following diagnosis of the subgroup of leukaemia and the allocation into the low, high or very high risk group treatment is started with the remission induction phase. This first phase aims to kill 99% of the leukaemic cells while allowing normal haematopoiesis to proceed. The standard treatment is a 3 drug protocol consisting of a glucocorticoid (prednisone or dexamethasone) vincristine and asparaginase, whilst adults and children with a high risk receive a 4 drug treatment induction (Pui and Evans 2006) with addition of an anthracycline. The second phase is the consolidation phase in which the treatment is intensified to kill remaining more resistant leukaemic cells, such as remaining cells from the marrow or in the CNS. This treatment reduces the risk of relapse and frequently includes high doses of methotrexate plus mercaptopurine. The last phase is the continuation/maintenance treatment and is mainly thought to prevent relapse (see Figure 6) (Pui, Robison et al. 2008).

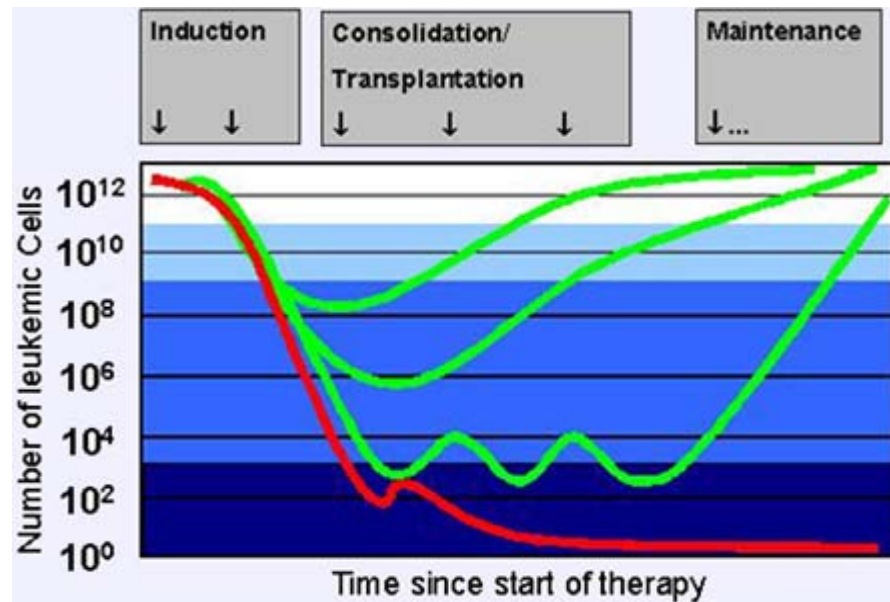


Figure 6 Treatment of leukaemia

A general treatment protocol for leukaemia is shown. Induction of treatment aims to kill the majority of cells initially present leading to a strong decrease in leukaemic cell numbers. Consolidation aims to further reduce more resistant leukaemic cells and maintenance treatment aims to prevent relapse from outgrowth of surviving leukaemic cells. Red curve cured patient, green curves relapsing patients from [www.atlasgeneticsoncology.org/Deep/MinResDiseaseA...](http://www.atlasgeneticsoncology.org/Deep/MinResDiseaseA...)

ALL patients receive chemotherapy for 2 (girls) to 3 years (boys), in which daily mercaptopurine and weekly methotrexate are the basic drugs.

For patients with very high risk, relapsed or refractory disease, treatment may also include radiation to the CNS or allow stem cell transplantations. Prior to transplantation a myoablative therapy is given which should kill all haematopoietic stem cells. An HLA (tissue type) matched donor is required, and may be an identical twin, sibling or unrelated person. However, this treatment modality has significant and potentially life threatening side effects including prolonged bone marrow suppression and such as graft versus host disease.

### 1.2.2.3.1 Chemotherapeutic agents

Chemotherapy is in principle a treatment with chemicals to eradicate microorganisms or cancer cells, nevertheless the term chemotherapy is widely used for anti-neoplastic drugs, which are cytotoxic or cytostatic and mainly harm cells with a high proliferation rate. The inhibition of highly proliferating cells can also harm hair follicles, the bone marrow and the digestive tract leading to alopecia (hair loss), myelosuppression and mucositis (inflammation in the intestines). Nausea is a common acute side effect of treatment.

Listed below are the most common therapeutic agents for the treatment of ALL.

Prednisolone (Figure 7A) is an anti-inflammatory corticosteroid. It inhibits functions such as leukocyte migration and capillary proliferation. It is thought to induce apoptosis in lymphoid cells. Long term side effects include cushing syndrome, glaucoma, osteoporosis, diabetes mellitus.

Dexamethasone (Figure 7 B) is an anti-inflammatory alternative corticosteroid. It is believed to provide better penetration into the CNS but has a higher incidence of side effects including psychological disturbance and avascular necrosis.

Vincristine (Figure 7 C) is a vinca alkaloid from the *Catharanthus roseus* plant. It acts as a mitotic inhibitor by binding to tubulin and inhibition of microtubule assembly. Long term side effects include neuropathy.

Asparaginase (no image) is an enzyme that catalyzes the hydrolysis of asparagine to aspartic acid. The principle of its function is that, in contrast to healthy cells, the non-essential aminoacid asparagine cannot be synthesized by ALL cells.

Cyclophosphamide (Figure 7 D) is a nitrogen mustard compound which alkylates DNA at the N7 of the base guanine. Long term side effects include the increased risk for bone marrow and lymph node cancers.

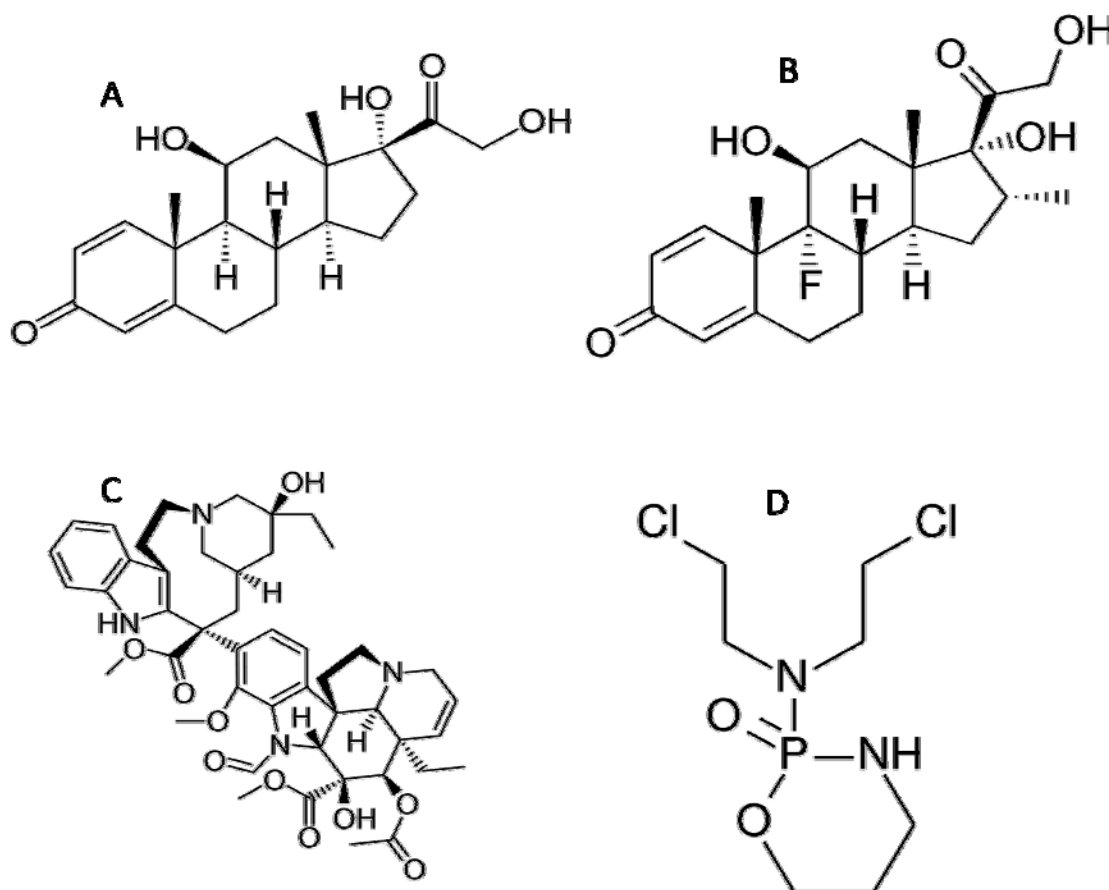


Figure 7 Chemotherapeutic agents

Structural formulas of (A) Prednisolone (B) Dexamethasone (C) Vincristine and (D) Cyclophosphamide free to publish

Cytarabine (Ara C) (Figure 8 A) is a nucleoside analogue which damages DNA making S-phase cells especially susceptible. As long term effects secondary malignancy and infertility are reported

(<http://pubchem.ncbi.nlm.nih.gov/summary/summary.cgi?cid=6253>).

Etoposide (Figure 8 E) is an inhibitor of Topoisomerase II whose natural function is to unwind the DNA double helix by cutting and re ligating both strands and is essential in

replication. This inhibitor targets the re ligation. A known long term side effect is the induction of secondary AML.

6-Thioguanine (Figure 8 B) is an antimetabolite which interferes with the purine and pyrimidine biosynthesis. It can possibly interfere with epigenetic gene regulation by perturbing cytosine methylation. Identified side effects include veno-occlusive disease of the liver (hepatotoxicity) and secondary malignancies.

6-Mercaptopurine (Figure 8 C) is a 6-Thioguanine prodrug and a purine derivate which inhibits nucleotide synthesis and metabolism as well. It affects nucleotide interconversion and glycoprotein synthesis. Possible long term side effects are diseases such as lymphomas.

Methotrexate (Figure 8 D) is an antimetabolite which inhibits the metabolism of folic acid. Side effects are hepatotoxicity and cytopenia, meaning decreased blood cell production.



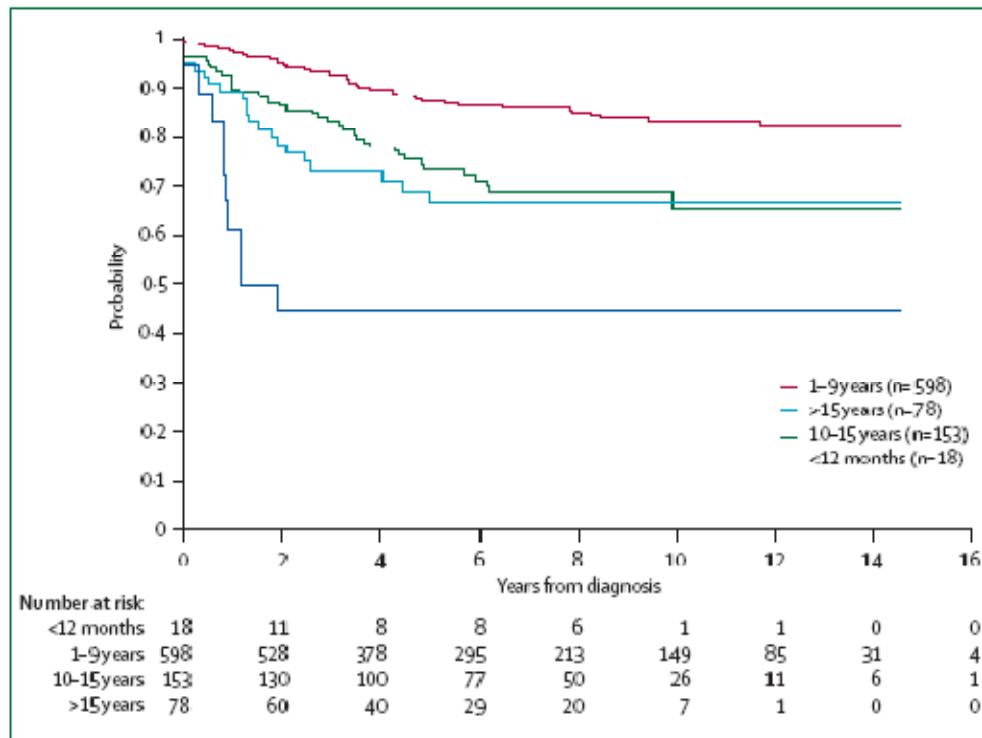


Figure 9 Kaplan-Meier estimates of event-free survival

Kaplan-Meier estimates of event-free survival according to age at diagnosis of acute lymphoblastic leukaemia. The table below the diagram shows the number of patients assessed corresponding to the years on the x-axis. from Pui, Robinson et al. 2008

A low risk of relapse is found in patients aged 1 to 9 and a leukocyte count below  $50 \times 10^9/l$  (Pui, Campana et al. 2001) while patients with more than  $400 \times 10^9/l$  are hyperleukocytic and are at high risk for early complications (Lowe, Pui et al. 2005).

Additionally genetic factors determine the prognosis of a patient. The 5 year event free survival is 91% for hyperploidy, 89% for TEL/AML1, 86% for E2A/ PBX1 fusion, 82% for other B-lineage leukaemias, 73% for T-cell ALL, 37% for BCR/ABL and 32% for MLL/AF4 (Pui, Robison et al. 2008) (see Figure 10).



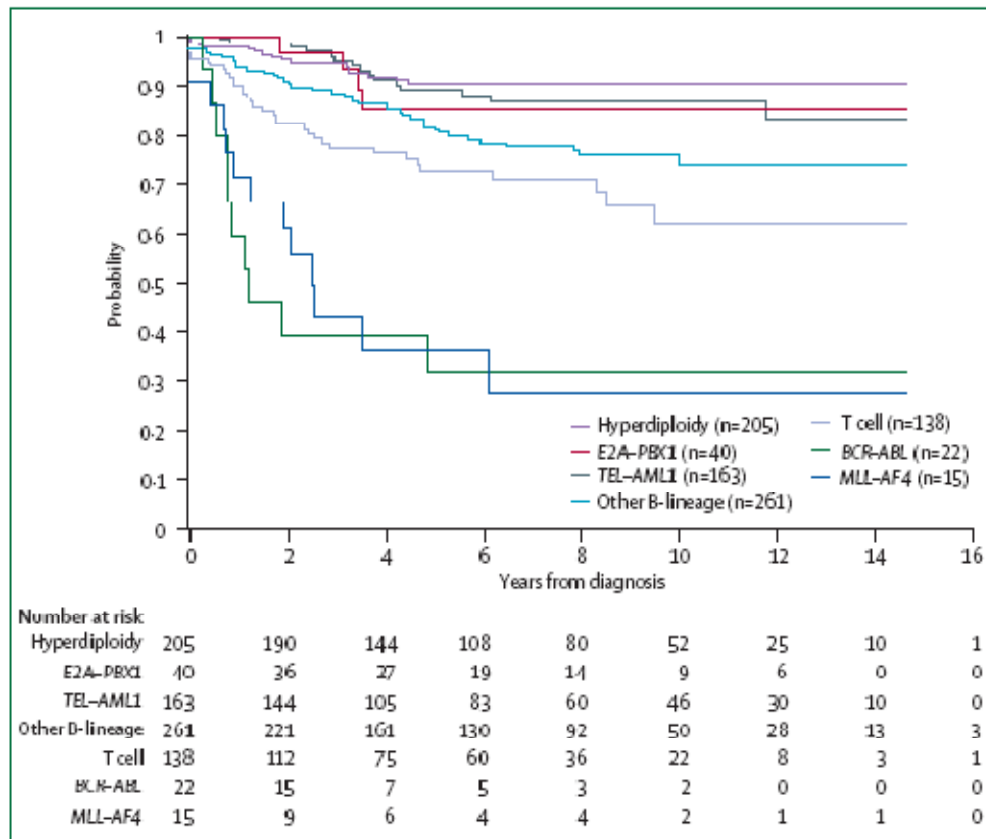


Figure 10 Kaplan-Meier analysis of event-free survival 2

Kaplan-Meier analysis of event-free survival according to biological subtype of leukaemia  
 The table below the diagram shows the number of patients assessed corresponding to the years on the x-axis. from Pui, Robinson et al. 2008

## 1.3 Recurrent chromosomal rearrangements

Genetic lesions such as mutations, deletions, duplications, inversions, insertions and translocations are very common in leukaemias. In a translocation a chromosomal region is located to another chromosome. This chromosomal rearrangement with a non-homologous chromosome is called reciprocal if, chromosomal segments are exchanged between these chromosomes (see Figure 11). They occur in 0.16% of all newborns, but in the majority of the cases they have no consequences due to the lack of secondary mutations. These would be required to induce leukaemia according to the two hit model.

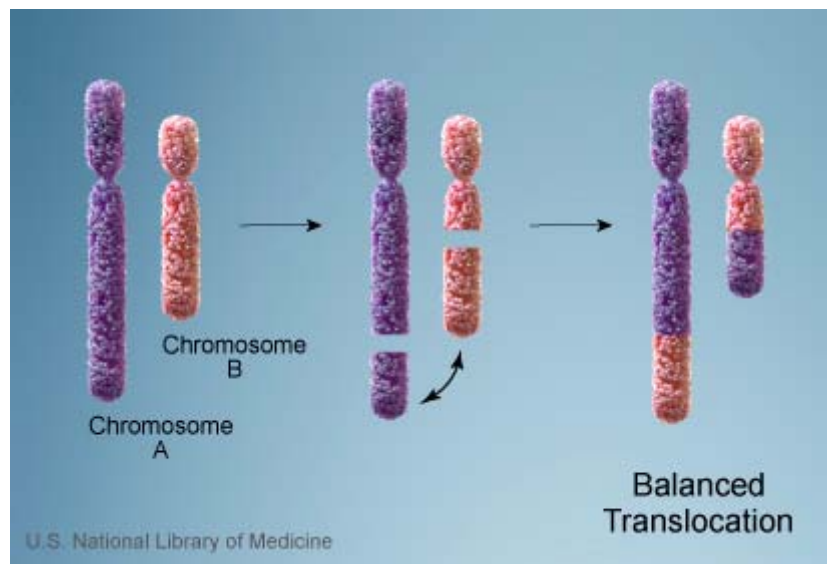


Figure 11 Balanced translocation

In a balanced translocation portions of chromosome “A” and chromosome “B” are exchanged and fused leading to two newly fused chromosomes but no loss of genetic material. from U.S. National Library of Medicine

Chromosomal translocations can result in the generation of fusion genes. These are generated if the breakpoint of one chromosome segment lies within a gene and this is fused to the breakpoint of another gene, which can give rise to a unique gene translating into a fusion protein with novel properties. Common examples are the CML-associated  $t(9;22)(q34;q11)$  reciprocal translocation which generates *BCR/ABL* fusion gene and the

t(4;11) translocation which generates two reciprocal fusion genes *MLL/AF4* and *AF4/MLL*.

Reciprocal translocations are responsible for the generation of different leukaemias of which the majority are generated *de novo*. Elliot and Jasin suggested that repair mechanisms accidentally produce translocations while trying to repair an extended DNA damage (Elliott 2002). In contrast therapy related leukaemias are known to be caused by chemotherapeutic agents. Especially several cases of AML are connected to Topoisomerase II inhibitors. Uninhibited Topoisomerase II controls double-strand breaks and helps maintain the structure of DNA throughout different cell phases. The blockage of this enzyme supports non-homologous recombinations, creating various *MLL* rearrangements and inducing relatively therapy resistant leukaemias. (Andersen, Christiansen et al. 2001). Etoposide, a commonly used Topoisomerase II inhibitor, was shown to induce *MLL* rearrangements in fetal liver cells (Moneypenny, Shao et al. 2006).

The mechanism of aberrant translocation relies on two or more double strand breaks followed by incorrect rejoining of the broken ends. Many of those new junctions show loss of substantial DNA material at the breakpoints, suggesting DNA degradation before joining. The non-homologous end joining (NHEJ) pathway employing DNA-dependent protein kinase (XRCC4) and DNA ligase IV (Povirk 2006), is used to repair double strand breaks. Unlike the homologous recombination, no homologous sequence is required to ligate the ends of the breaks. After a double strand break DNA dependent protein kinase (DNA-PK) and several other proteins are required to prepare the ends of the DNA for subsequent ligation (see Figure 12).

## Non-homologous end-joining

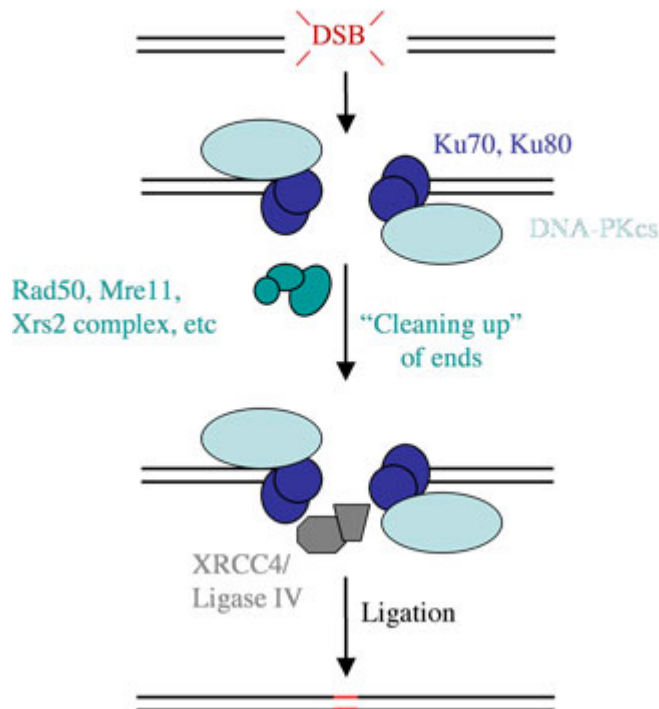


Figure 12 Non-homologous end joining

After a double strand break DNA-PK and other proteins prepare the ends of double strand broken DNA for ligation. DSB double strand break; Ku70, Ku80 autoantigens forming a heterodimer; DNA-PK DNA dependent protein kinase, Rad50 RAD50 homolog, Mre11 meiotic recombination 11 homolog A , XRCC4 X-ray repair complementing defective repair in Chinese hamster cells 4 from [www.gurdon.cam.ac.uk/.../research\\_interests.htm](http://www.gurdon.cam.ac.uk/.../research_interests.htm)

## 1.4 MLL

Mixed lineage leukaemia gene *MLL*, also called *ALL1*, is a proto-oncogene which is translocated in various ALLs. *MLL* belongs to the human trithorax gene family and is homologous to the *Drosophila* trithorax (*trx*). Amongst others the *Drosophila* trithorax stimulates gene expression during embryogenesis. The polycomb genes act antagonistically to *trx*, repressing target genes (Popovic and Zeleznik-Le 2005). Polycomb proteins can act in epigenetic silencing of genes such as HOX genes. In

contrast trithorax genes (*trx*) maintain gene expression by influencing the chromatin structure.

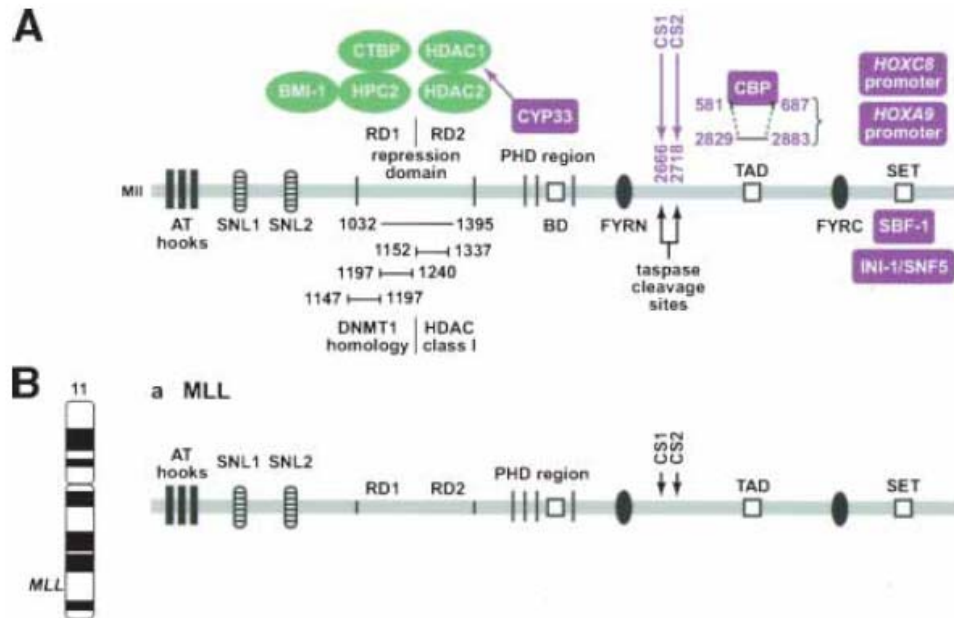


Figure 13 The MLL protein and gene

(A) MLL protein; shown in green are protein interactions that are present after translocations and shown in purple are protein interactions lost in the *MLL* fusion proteins. (B) Mll gene left chromosome 11 and the position of *MLL* and right schematic of *MLL* gene AT hooks regions of DNA binding, SNL1,2 nuclear localization signals, RD1,2 repression domains, DNMT1 DNA methyl transferase 1, HDAC Histone deacetylase, PHD plant homology domain, FYRN and FYRC N and C terminal domain for heterodimerisation, TAD transcriptional activation domain and SET histone methylase from Daser et al. 2004

The gene locus of *MLL* is positioned at the long arm band q23.3 of chromosome 11. The gene comprises 36 exons. The transcribed 11.9 kb long mRNA translates into a 3969 amino acids long protein which contains many domains with regions homologous to various proteins (see Figure 13). Three AT-hooks are located close to the MLL N-terminus. These promote binding to AT-rich DNA in the minor groove (N.J. Zeleznik-Lee 1994). By binding to DNA, MLL can recruit proteins to the DNA by protein-protein interactions. The AT hooks are followed by SNL1 and SNL2, which are nuclear localization signals. Further downstream RD1 and RD2 are located, two repression domains of different function, which can be found in all MLL fusions and which are

necessary for the fusion gene-mediated transformation (Slany, Lavau et al. 1998). Then Polycomb repressor proteins HPC2 and BMI-1 and the co repressor CTBP are recruited by the DNA methyltransferase homology domain located in RD1 (Xia, Anderson et al. 2003). The histone deacetylases HDAC1 and HDAC2 are recruited by RD2 and cause repression (Xia, Anderson et al. 2003). Taspase 1 cleaves the MLL protein at CS1 and CS2 into 2 polypeptides, of N-terminally 2666 and C-terminally 1251 amino acids size. They form a heterodimer by connection of the FRYN and FRYC domains (Hsieh, Ernst et al. 2003) (see Figure 14). MLL, or more exactly cleaved MLL, is important for HOX gene expression, as knockdown of Taspase 1 was linked to loss of Hox gene expression (Hsieh, Cheng et al. 2003). Regions including the PHD domain (plant homology domain), downstream TAD (transcriptional activation domain) and the C-Terminal SET domain are not retained in *MLL* fusions such as *MLL/AF4*. TAD interferes with acetylation and HOX gene expression while SET possesses a histone methylase activity for histone 3 at lysine 4 (Milne, Briggs et al. 2002). H3K4 methylation represents an active state of transcription, which is probably induced at HOX gene promoters by the SET domain of MLL. (Daser and Rabbitts 2004).

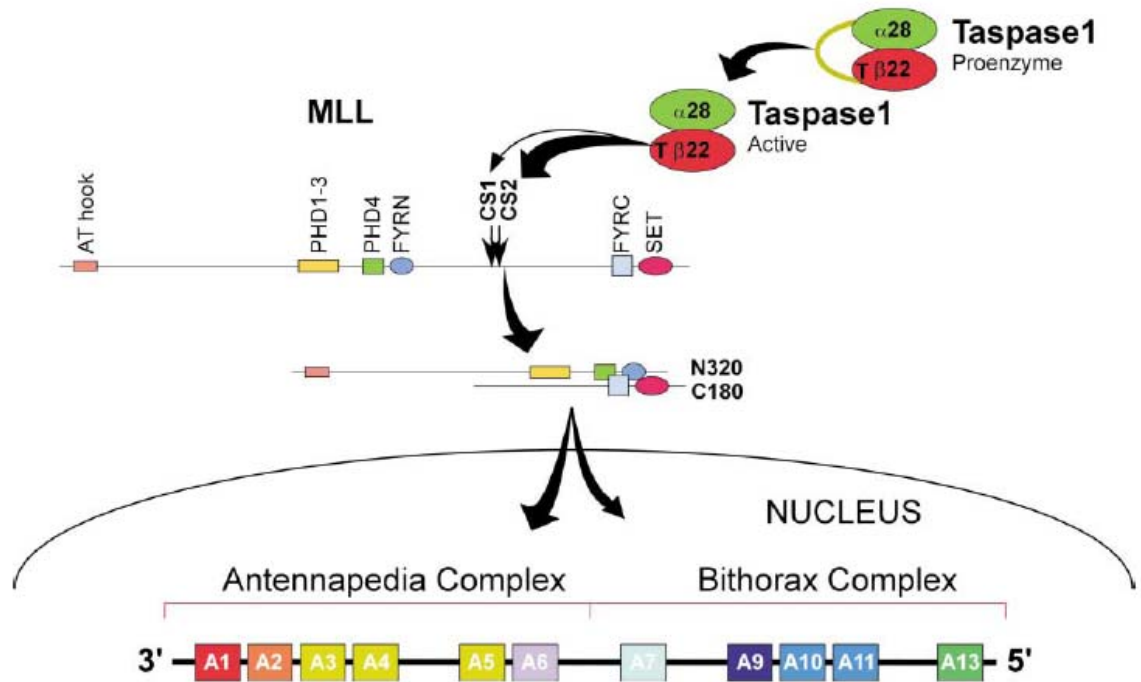


Figure 14 The processing of the MLL protein

MLL is cleaved by Taspase 1 leading to the heterodimerisation of the N and C terminal fragment which can locate into the nucleus and regulate gene expression, here the HOX gene exons are shown AT hooks regions of DNA binding, PHD plant homology domain, FYRN and FYRC N and C terminal domain for heterodimerisation and SET histone methylase. from Hsieh et al. 2003

The *MLL* gene contains a breakpoint cluster region (BCR). This 8.3kb spanning region is known to produce several different breakpoints and related translocations. For the *MLL* gene more than 100 translocation partners are known. Within a single translocation partner, such as t(4;11), translocation produces slightly different fusion genes due to the variety of *MLL* Breakpoints. *MLL* rearrangement is the most common translocation in childhood ALL. A prominent fusion partner of *MLL* is *AF4* (see Figure 15).

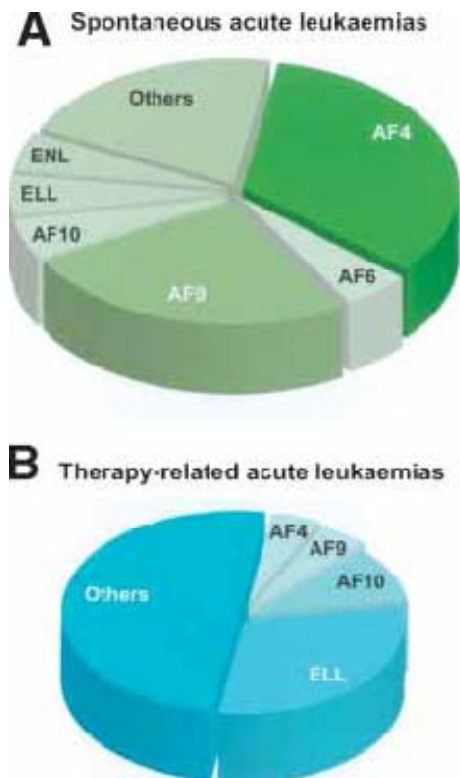


Figure 15 The frequency of *MLL* associated chromosomal abnormalities

The frequency of *MLL* associated chromosomal abnormalities in (A) Spontaneous acute leukaemia (B) Therapy related acute leukaemia MLLT myeloid/lymphoid or mixed-lineage leukemia (trithorax homolog, *Drosophila*); translocated to 4 (AF6), 3 (AF9), 10 (AF10), 1 (ENL); ELL elongation factor RNA polymerase II from Daser et al 2004

## 1.5 *AF4*

The *AF4* gene encodes a 125 to 145 kDa protein from a 10.5 kb mRNA, which is transcribed from 23 exons covering 300kb on chromosome 4 band q21 (Bursen, Moritz et al. 2004). The ubiquitous protein AF4 localizes to subnuclear compartments and is expressed in various haematopoietic and non-haematopoietic cells (Li, Frestedt et al. 1998).





Figure 16 Schematic representation of the protein AF4

NHD N terminal homology domain, ALF AF4/LAF4/FMR2 protein family, pSer serine and proline rich region, NLS Nucleus localization signal and CHD C terminal homology domain from Bursen et al 2004

The NHD (N-terminal homology domain), the CHD (C-terminal homology domain), ALF, pSer and NLS are all conserved protein domains (see Figure 16). ALF is the consensus domain for the members of the ALF protein family which include AF4/LAF4/FMR2 (ALF) and encode for transcription cofactors which are frequently translocated in childhood leukaemia. The downstream pSer domain is a proline and serine rich region. Finally, upstream of CHD is the NLS, a nuclear localization region. Because AF4 has DNA binding and transcriptional activation properties it is thought to act as a nuclear transcription factor (Prasad, Yano et al. 1995; Ma C 1996; Nilson I 1997). The interaction of AF4 with ubiquitin ligases SIAH1 and SIAH2 regulates its proteasomal degradation. These two ubiquitin ligases and the N-terminal portion of AF4 are thought to be involved in the oncogenic mechanism of AF4/MLL (Bursen, Moritz et al. 2004).

AF4 inactivation in mice causes defects in the development of B and T cells, such as lower expression of CD4 and CD8 and reduced numbers of mature and pre B cells in the bone marrow (Isnard, Core et al. 2000).

Isnard et al assumed that the translocation of *AF4* with *MLL* could orientate the oncogenic process towards the lymphoid lineage. Interestingly the *MLL/AF4* fusion protein has the same sub cellular distribution as AF4 (Li, Frestedt et al. 1998).

## 1.6 MLL/AF4 ALL

*MLL/AF4* is a fusion gene which is generated by the translocation of chromosome 4 and 11 - t(4;11)(q21;q23) (see Figure 17).

MLL/AF4 ALL has the worst outcome in infants and adults while children do better (Mancini, Scappaticci et al. 2005). It is also the most common translocation in infant leukaemia, being present in 70-80% of cases. Infant MLL/AF4 cases are considered as high or very high risks patients.

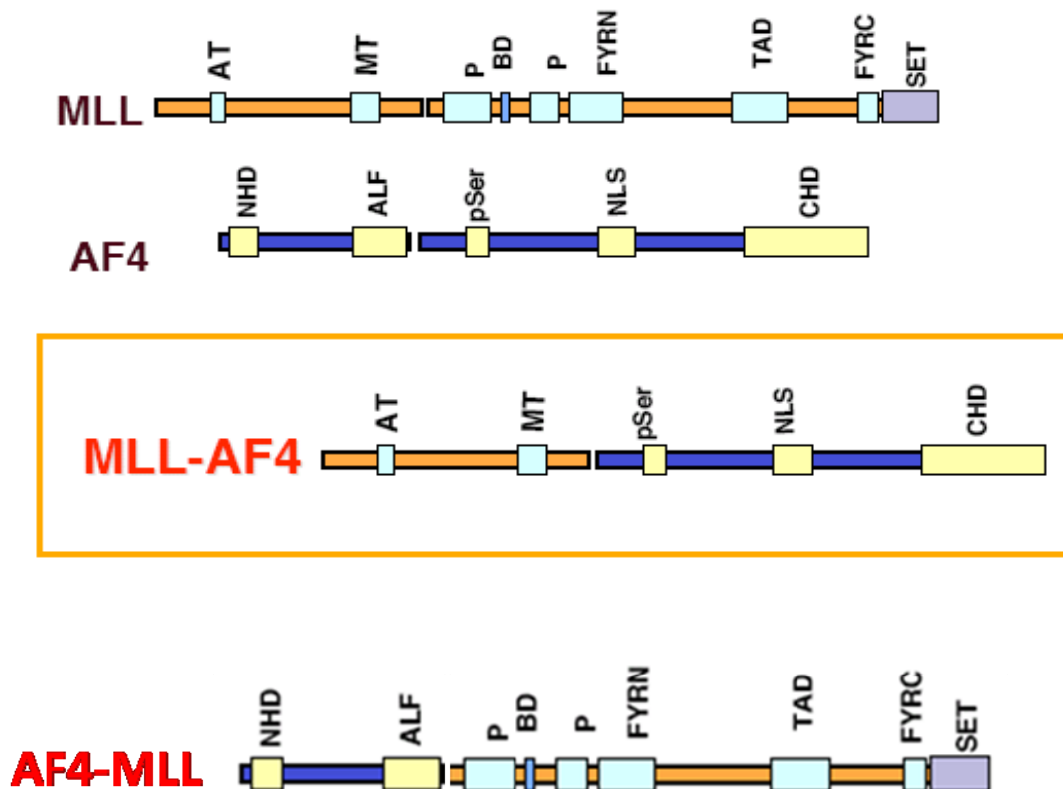


Figure 17 The *MLL*, *MLL/AF4* and the *AF4/MLL* gene

(Top) the *MLL* gene (2<sup>nd</sup> from top) the *AF4* gene (3<sup>rd</sup>) *MLL-AF4* fusion gene and (4<sup>th</sup>) the *AF4-MLL* fusion gene; NHD N terminal homology domain, ALF AF4/LAF4/FMR2 protein family, pSer serine and proline rich region, NLS Nucleus localization signal and CHD C terminal homology domain, AT hooks regions of DNA binding, PHD plant homology domain, FYRN and FYRC N and C terminal domain for heterodimerisation and SET histone methylase

However, the t(4;11) translocation produces a second fusion gene *AF4/MLL* which fuses the C terminal part of *MLL* to the N terminal part of *AF4* (see Figure 17). This fusion gene was associated with oncogenic potential and other properties which are mentioned later, paradoxically it is only present in 80% of the *MLL/AF4* patients.

An interesting indication for the cause of such *MLL* rearrangements and thereby resultant leukaemias, is the occurrence of *MLL* rearrangements in secondary leukaemias (see Figure 15 B) following Topoisomerase II inhibitor treatment (Pui and Relling 2000). It was speculated that *MLL* rearrangements could be caused by Topoisomerase II inhibitors from environmental, medical or dietary exposure (Biondi, Cimino et al. 2000).

Leukaemic translocations such as t(4;11) often activate genes that encode for master oncogenic transcription factors that are developmentally regulated, controlling cell differentiation and encoding proteins in important transcription cascades (Armstrong and Look 2005). They are aberrantly expressed in leukaemic cells and regulate downstream responder genes positively or negatively (Pui, Relling et al. 2004).

The biological function of *MLL/AF4* was studied by several ways *in vivo* and *in vitro*, by knock-in, over expression and by knock down.

An *MLL/AF4* knock-in mouse model showed that *MLL/AF4* expression in young mice resulted in a lymphoid and myeloid deregulation, while bone marrow colonies showed unique mixed pro-b lymphoid colonies (Chen, Li et al. 2006). After 520 days (median) incubation time mice developed mixed lymphoid and myeloid hyperplasia, B-cell lymphomas and haematopoietic malignancies. The white blood count was increased and immature cells were found in the blood. Despite these symptoms the long time for the onset of the haematological malignancy suggested that a second hit was missing (Chen, Li et al. 2006).

In an alternative model the conditional expression of *MLL/AF4* resulted in large, diffuse B-cell lymphomas and in a long latency. The tumours were transplantable but *MLL/AF4* knock-in mice seemed, as in the previous model, to lack the 2<sup>nd</sup> hit. The authors concluded that only in lymphoid cells *MLL/AF4* can act as an oncogene (Metzler, Forster et al. 2006).

The group of Scott Armstrong has created a conditional mouse knock-in model for *MLL/AF4* which generates precursor B cell ALL or AML. The immunophenotype and gene-expression profile of induced *MLL/AF4* ALL cells confirmed the pre B ALL status. This model could resemble the phenotype of the human disease and its gene expression patterns, proving that *MLL/AF4* is sufficient to induce leukaemia (Andrei V. Krivtsov, Zhaohui Feng 2008).

The Heidenreich group has already shown that *MLL/AF4* can be investigated by depletion of the corresponding fusion transcript with RNAi without affecting the transcript levels of native *MLL* and native *AF4*. With the decrease in *MLL/AF4* mRNA, protein levels have been reduced by 67% in the relapsed childhood ALL cell line, SEM. Most importantly mouse engraftment of SEM depleted for *MLL/AF4* prolonged median survival to 82 days compared to 52 days in controls. These findings showed that *MLL/AF4* is important in engraftment (Thomas, Gessner et al. 2005). Although previous mouse models implied that *MLL/AF4* lacks a second hit to be carcinogenic, our data agreed with the recent Armstrong model, which shows the importance of *MLL/AF4* in inducing leukaemia. They also agreed with other mouse models showing a lymphoma phenotype, which could be promoted by the strong anti-apoptotic effect of *MLL/AF4*.

Timecourse experiments suggested that the half life for the MLL/AF4 protein is shorter than 48h. Depletion of *MLL/AF4* transcript resulted in inhibited clonogenicity, proliferation and cell cycle progression. Furthermore this depletion induced apoptosis 3fold compared to controls; this finding was supported by the activation of pro-apoptotic Caspase 3 and reduced BCL-Xl which in contrast is anti-apoptotic (Thomas, Gessner et al. 2005). MLL/AF4 induces expression of HOX genes, shown in *HOXA7*, *HOXA9* and *MEIS1* levels being reduced after MLL/AF4 knockdown. CD133 a marker for haematopoietic stem and early progenitor cells was reduced 2 fold in transcript levels following MLL/AF4 depletion, but also in surface expression (Thomas, Gessner et al. 2005).

2 years later the group of R. Marschalek investigated the effect of MLL/AF4 and its reciprocal fusion gene product, AF4/MLL, in leukaemogenesis by over expressing them separately and in combination *in vitro* and *in vivo*. Using murine embryonic fibroblast cells they observed that co-transfected cells gained the highest number of cycling cells and lowest levels of apoptosis. Both fusion proteins showed oncogenic properties, but *AF4/MLL* transfected cells showed higher proliferation than MLL/AF4 and alone induced focus formation. Therefore, the authors suggested AF4/MLL to be of greater significance in inducing growth transformation. Their conclusion was that t(4;11) represents two hits; MLL/AF4 and AF4/MLL (Gaussmann, Wenger et al. 2007).

Very recently the same group published results showing mice which were engrafted with Lin<sup>-</sup>Sca1<sup>+</sup> positive cells which had been transduced with onco-retroviruses encoding AF4/MLL and / or MLL/AF4. Within the observation period of 13months, only the AF4/MLL and MLL/AF4 + AF4/MLL transduced cells induced a pro B-ALL. These data suggest that AF4/MLL has a different function than MLL/AF4 in leukaemogenesis. In particular, these data imply that AF4/MLL may be the driver at

least at the early phases of leukaemogenesis. However as previously mentioned AF4/MLL is present in only 80% of t(4;11) derived leukaemias. Explaining the role of these two fusion proteins, it was stated that they correspond to two hits, explaining the early onset of the disease in infants (Bursen, Schwabe et al. 2010).

## 1.7 The RNAi pathway and siRNA

RNA interference (RNAi) has probably evolved to protect the genome against aberrant RNA or dsRNA deriving from active transposons or viruses in the cell (Ketting, Haverkamp et al. 1999; Tabara, Sarkissian et al. 1999). The transposon and virus replication is antagonized by degradation of their corresponding mRNA. RNAi was originally discovered in *C.elegans* (Fire, Xu et al. 1998) and subsequently in the frog (Oelgeschlager, Larrain et al. 2000) and mouse (Svoboda, Stein et al. 2000; Wianny and Zernicka-Goetz 2000). Today it is accepted as to be relevant across a wide range of eukaryotic organisms. The mechanism has similarities to the posttranscriptional gene-silencing (PTGS) which is found in plants and fungi (Smardon, Spoerke et al. 2000).

RNAi is induced by double strand RNA (dsRNA), which is cleaved by the dsRNA-specific ribonuclease Dicer into small dsRNA fragments of 21-23 nt in length called short interfering RNAs (siRNAs) (Zamore, Tuschl et al. 2000). These siRNAs are separated into single strands by a protein component of the RNA-induced silencing complex (RISC) (Matranga, Tomari et al. 2005) (see Figure 18). RISC contains endonucleases and cleaves mRNA complementary to the included siRNA strand. Only one of the two siRNA strands becomes part of RISC, this strand is called the guide strand. The other strand is called passenger strand and is degraded during RISC

activation (Gregory, Chendrimada et al. 2005). The catalytic components of RISC are argonaute proteins; they are located in cytoplasmic P-Bodies which show high rates of mRNA degradation (Sen and Blau 2005). Of the argonaute 1-4 proteins included in the RISC complex only the hsAgo2 has Slicer activity and is therefore responsible for mRNA cleavage (Liu, Carmell et al. 2004).

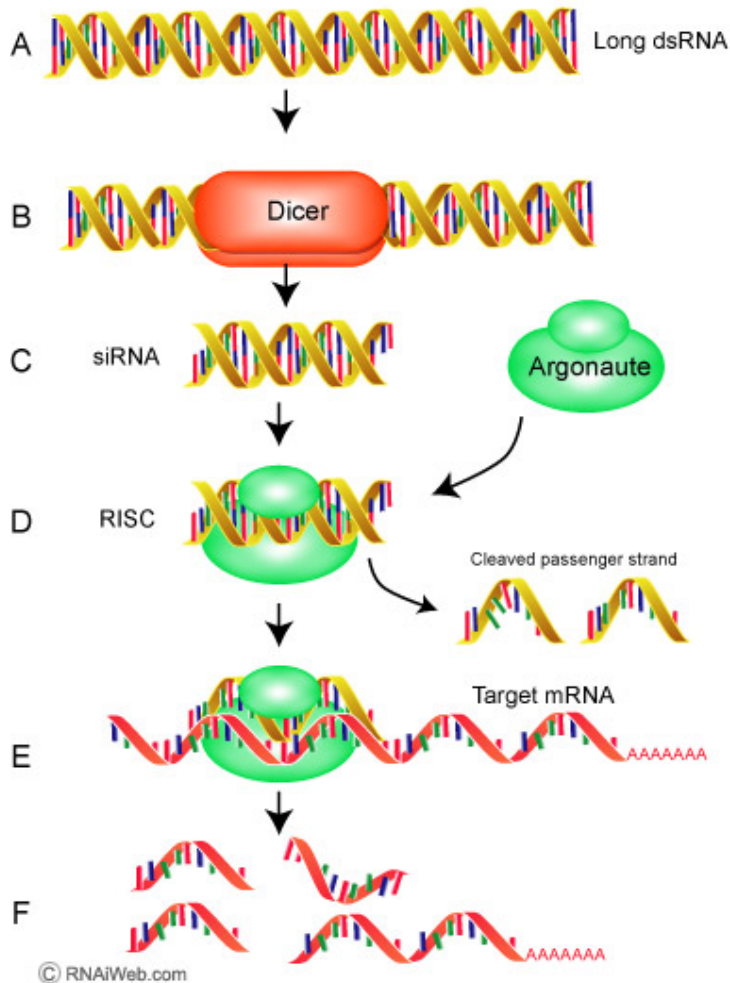


Figure 18 siRNA mediated RNAi

A long double stranded RNA sequence (A) is bound by the nuclease Dicer which cuts the long dsRNA strand into short dsRNA generating siRNA of 21-23 nt length (B). siRNA and Argonaute proteins form the RISC complex (C). By this RISC complex the passenger strand is cleaved (D). The guide strand leads the RISC complex to target mRNA (E) and target mRNA is cleaved (F) resulting in no translation of the mRNA into protein from <http://www.genome.ou.edu/5853/rnai/RNAi.jpg>

siRNA can originate from virally transduced shDNA, encoding for shRNA which is then processed into siRNA, from long dsRNA precursors or delivered directly from

outside the cell. The latter is important in functional studies, where the expression of certain genes is abrogated (see Figure 19).

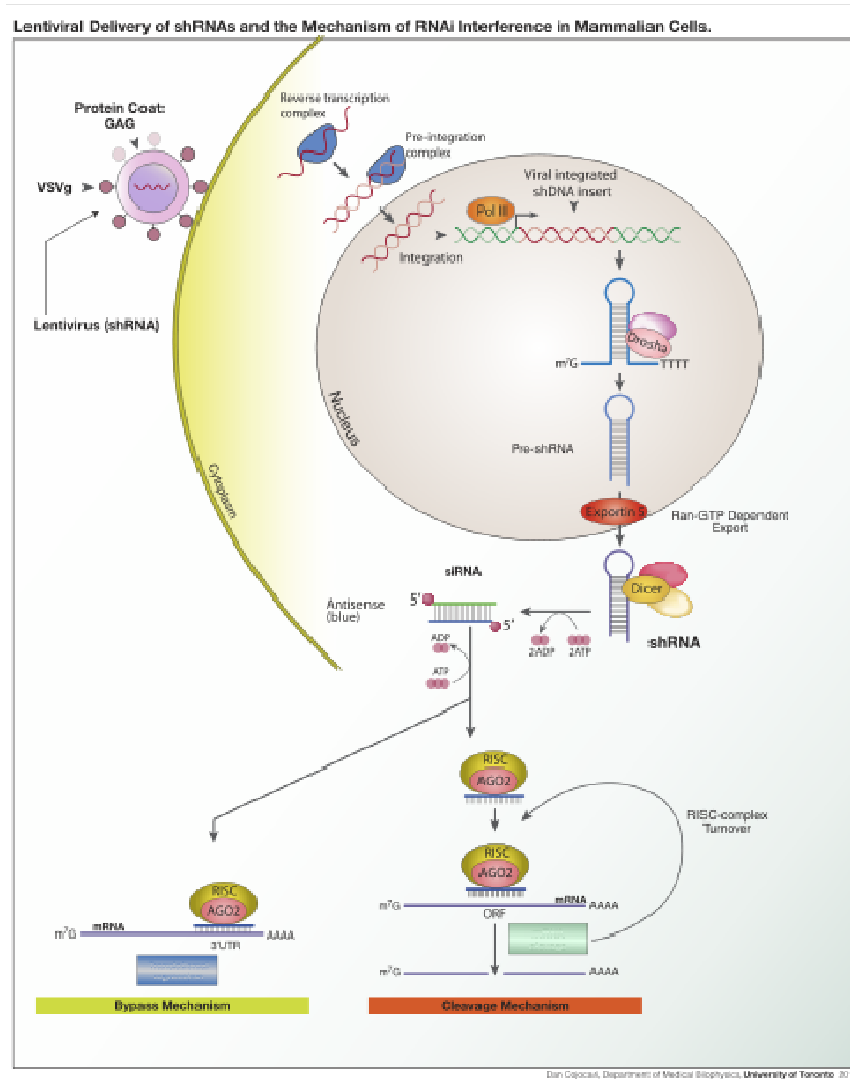


Figure 19 shRNA Mechanism

By lentiviral infection a shDNA sequence is inserted into the genome. This shDNA transcribes for a RNA strand which forms a hairpin structure. After this hairpin is processed by Drosha it is exported into the cytosol where Dicer trims it into siRNA which is incorporated into the RISC complex generating cleavage of the target mRNA. The bypass mechanism shown is a cleavage independent mechanism and rather reported for miRNA from Dan Cojocari, free to publish

The two main actors of RNAi are siRNA (short interfering RNA) and miRNA (microRNA). miRNA is not translated but encoded in the genome, controls gene expression and is important in development (Zhao, Ransom et al. 2007). The RNA coding gene is much bigger than the miRNA sequence itself, expressing the pri miRNA,



a primary transcript which is processed to pre-miRNA by Drosha, an RNase III like enzyme, and Pasha, a dsRNA binding protein, in the nucleus. This pre-miRNA has a stem-loop structure of about 70 nucleotides length and is exported from the nucleus by binding to Exportin 5, which serves as a shuttle through the nucleus pore complex (Yi, Qin et al. 2003). Dicer binds and cleaves the dsRNA part of this pre-miRNA producing mature miRNA, which integrates into the RISC complex. miRNA and siRNA use the same machinery following incorporation in the RISC complex (Gregory, Chendrimada et al. 2006) (see Figure 20).

Unlike siRNAs, miRNAs often bind to partial complementary to mRNA and rather inhibit translation, while siRNA is perfectly complementary and leads to degradation of their target mRNA (Pillai, Bhattacharyya et al. 2007). However prior to degradation, mRNA is cleaved by RISC subsequently inducing P- body components. P-bodies (processing bodies) are granules in the cytoplasm which show high mRNA decay (Parker and Sheth 2007).

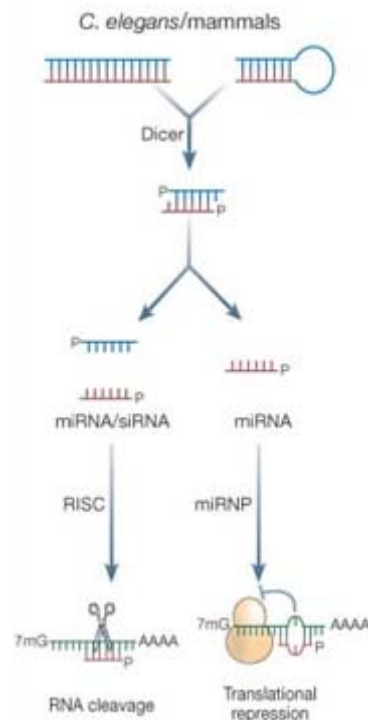


Figure 20 Comparison of the siRNA and the miRNA RNAi

miRNA can lead to translational repression without RNA cleavage. The siRNA RNAi pathway is dependent on this target mRNA cleavage, however miRNA may also use this RISC facilitated cleavage; siRNA silencing RNA, miRNA micro RNA, RISC RNA induced silencing complex, miRNP microRNA-containing ribonucleoprotein complexes from (Meister and Tuschl 2004)

Following degradation of the mRNA the translation is interrupted and the corresponding protein levels decrease.

A substantial problem of siRNA mediated RNAi are off target effects describing the unintended regulation of genes apart from the target gene. Important for this is the seed region at the 5' end of the siRNA guide strand (Lin, Ruan et al. 2005) which comprises 6 nucleotides in the positions 2-7 of the antisense siRNA strand of the siRNA duplex. Sequence complementary of any transcripts to the seed region of siRNAs can lead to off target effects and this also applies to shRNA driven RNAi (Jackson, Burchard et al. 2006).

siRNA and shRNA mediated RNAi is used in functional studies. One basic approach is to deplete a gene of interest and run a subsequent array analysis to monitor corresponding changes in expression of other genes or transcripts. A more complex functional study is to screen numerous genes in one assay. Libraries of siRNA or shRNA are used to identify groups of genes which are of functional relevance in special biological processes or in disease metabolisms. Such libraries can contain thousands of siRNAs or shRNAs targeting numerous genes. By high-throughput RNAi screening huge numbers of genes, pathways and networks can be identified. Often such libraries also contain several different si/shRNAs per gene. Recently published work showed the combinative use of siRNA and shRNA RNAi; genes identified by shRNA screens were further functionally tested by siRNA treatment (Shtutman, Maliyekkel et al. 2010). Supporting this a recent publication showed that siRNA and shRNA RNAi can be useful for functional studies in signalling molecules (Lee, Santat et al. 2009). RNAi library screens are widely used in functional genomics and drug target validation.

Nowadays siRNA depletion is a common research tool to investigate protein functions and it is expected to be used in the future for treatment of diseases. It can be used to deplete important molecules for certain cancer cells thus improving therapy. Cancer cells with fusion genes offer unique targets to efficiently specify treatment to the target cancer cell. Very recently published work showed the delivery of siRNA by nanoparticles to melanoma cells in human patients (Davis, Zuckerman et al. 2010). Most importantly they showed the cleavage of target RNA in the patient cells.

Overall siRNA mediated RNAi is a well established method to investigate target gene functions and a potential and specific tool in treating cancers.

## Hypotheses

- 1. MLL/AF4 controls engraftment and homing by modulating target genes such as FGFR1 and N-cadherin*
- 2. Interaction with the niche affects consequences of MLL/AF4 depletion*

## 1.8 General aims

The general aim of this thesis was to investigate the functions of MLL/AF4 in thereby associated leukaemia, which is commonly an Acute Lymphoblastic Leukaemia. Understanding the manner of how the fusion gene is involved in the generation and maintenance of the disease requires the knowledge of its functions. These are the regulation of target genes by transcriptional or non-transcriptional mechanisms. The assignment of the downstream functions of those target genes to a fusion gene-derived response and the understanding of how those actions influence the malignancy and ultimately the disease itself is a prerequisite to further improvements.

Overall, a better understanding of MLL/AF4 will facilitate the development of better treatments which are highly needed, due to the poor prognosis in infant MLL/AF4.

# **Chapter 2**

## **Materials and Methods**

## **Chapter 2: Materials and Methods**

### **2.1 General Materials**

#### **2.1.1 Materials**

All details and specifications are standard unless stated otherwise.

General lab equipment was purchased from Scientific Laboratory Supplies (Nottingham, UK), VWR (Lutterworth, Leicestershire, UK) or Fisher Scientific (Loughborough, Leicestershire, UK).

#### **2.1.2 Equipment**

ABI 7000 Real Time detection system Applied Biosystems, Darmstadt, DE

ABI 7500 Fast Real-Time PCR system Applied Biosystems, USA

ABI 7000 SDS program Applied Biosystems, USA

ABI 7900HT Sequence detection system Applied Biosystems, USA

ABI SDS 2.2 Applied Biosystems, USA

Agarose gel electrophoresis unit BIO-Rad, Hemel-Hempsted, Herts., UK

Allegra® X-12 benchtop centrifuge Beckman Coulter, High Wycombe, UK

Centrifuge 5415C Eppendorf, Hamburg, DE

Centrifuge 5415R Eppendorf, Hamburg, DE

Class II microbiological safety cabinet BIOMAT-2, Medical Air technology Ltd., UK

D3300 X-ray System, RS320 Chamber, Tube MXR 321, Gulmay Medical, Camberley, Surrey, UK

Electroporation-Impulsegenerator EPI 2500 Heidelberg, DE

Eppendorf Thermomixer comfort, Eppendorf, Hamburg, DE

FACSCalibur Beckton Dickinson, Heidelberg, DE

FACSscan Beckton Dickinson, Oxford, UK

FACS Canto II Beckton Dickinson, Oxford, UK

Fluorescent microscope: Nikon Eclipse TE2000-U and camera: Digital Sight DS-2MBWc, Amstelveen, NL

Hamilton Gastight #1702, 25 $\mu$ L volume, Bonaduz AG, Switzerland

L870M Ultracentrifuge Beckman, High Wycombe, UK

Medimachine + Medicon, sterile, 35 $\mu$ m, BD, Oxford, UK

MINI-PROTEAN II electrophoresis cell BIO-Rad, Hemel-Hempstead, UK

Mouse imager: LT-9MARCOIMSYS: Macro Imaging System, Lighttools, Canada

ND-1000 spectrophotometer Nanodrop technologies Ltd., USA

Spectramax 250 Multiwell plate reader Molecular Devices, Crawley, UK



Scanscope CS/GL, Aperio Technologie Inc., USA

Tissue culture incubator, Heraeus Equipment Ltd., Essex, UK

Universal Hood II, Gel Doc, BIO-Rad, Hemel-Hempsted, Herts., UK

Vortex Genie 2, scientific industries Bohemia, New York, USA

### **2.1.3 Plastics**

All plastics were purchased from Greiner Bio-one (Frickenhausen, DE), Eppendorf (Hamburg, DE) and Becton Dickinson (New York, USA) unless stated otherwise.

Thickwall-style polyallomer conical tubes, Beckman Instruments Inc, High Wycombe, UK

Derlin PKGED'1 adapters, Beckman Instruments Inc, High Wycombe, UK

Falcon culture slide 8 chamber polystyrene vessel, BD, Oxford, UK

### **2.1.4 Chemicals**

All standard chemicals have been purchased either from Fisher

Scientific (Leicestershire, UK), SIGMA (Poole, Dorset, UK)

or BDH (Dorset, UK).

## 2.1.5 Buffers

DNA-PAGE (Polyacrylamide gel electrophoresis)

TBE for 1 l

53 g of Tris base

27.5 g of boric acid

20 ml of 0.5 M EDTA pH 8.0

E.coli transformation

LB-Medium

10 g/l Bacto-Trypton (Applichem, Darmstadt)

5 g/l Yeast Extract

10 g/l NaCl

pH 7.4

sterilised by autoclaving

LB-Agar

10 g/l Bacto-Trypton

5 g/l Yeast Extract

10 g/l NaCl

15 g/l Agar

pH 7.4

sterilised by autoclaving

Hybridisation of siRNAs

siRNA Hybridisation buffer

100 mM NaCl

25 mM Tris-HCl, pH7.5

Cell cycle analysis

Citrate buffer

0.25 M Saccharose

40 mM Natriumcitrate, pH 7.6

DNA-staining and lysis buffer

PBS

20 µg/ml PI

0.5% NP-40

0.5 mM EDTA

Cell cycle wash buffer

PBS

0.5% BSA

FACS-buffer

PBS

2 mM EDTA

0.1% BSA

## 2.1.6 Molecular Cloning

### 2.1.6.1 Restriction Enzymes

Most enzymes were purchased from Fermentas apart from ApoI, BsrGI, PciI and SnaBI which were purchased from New England Biolabs NEB. The standard activity was 10u/ $\mu$ l apart from SnaBI which was 5u/ $\mu$ l.

Aat II	MunI(MfeI)
Apa I	NcoI
Apo I	NheI
AscI	Not I
BamHI	PagI(BspHI)
Bgl II	PciI
Bsp1191 (BstBI)	PmeI (MssI)
BspTI(Afl II)	Pst I
BsrGI	Pvu I
Bsu15I(ClaI)	Pvu II
Cfr42I(Sac II)	Sac I
Cfr9I (XmaI)	Sall
DraI (AhaIII)	ScaI
Eco147I (StuI)	Sgs I(Asc I)
EcoR I	Sma I
EcoR V (Eco321)	SnaBI
HinCII (HindII)	StuI
Hind III	Xba I
Kpn I	Xho I
MssI (PmeI)	

### 2.1.6.2 Modifying Enzymes

Klenow fragment, DNA Polymerase I, 5u/ $\mu$ l NEB

Mung bean nuclease, 10u/ $\mu$ l NEB

T4 DNA Polymerase, 5u/μl Fermentas

T4 DNA Ligase, 5u/μl Fermentas

T4 PNK, Poly Nucleotide Kinase, 10u/μl Fermentas

CIAP, Calf Intestine Alkaline Phosphatase, 10u/μl Fermentas

TSAP, Thermo sensitive Alkaline Phosphatase, 1u/μl Promega

## 2.1.7 Cell analysis

Collagen type I, rat tail, BD Biosciences

Matrigel, Oxford, BD Biosciences

Antibodies were purchased from Becton Dickinson Pharmingen

	clone	dilution used
CD45 PE-Cy7	30-F11	2.5μl / million cells
TER-119 PE-Cy7	TER119	2.5μl / million cells
CD19-APC	SJ25C1	2.5μl / million cells
CD34-PerCP	8G12	10μl / million cells
CD133 PE	293C3 (Miltenyl)	10μl / million cells
CD38 FITC	HB7	10μl / million cells

## **2.1.8 Real Time RT-PCR**

SYBR Green QCR Supermix w/ROX Invitrogen, Paisley, UK

RevertAid™H Minus First Strand cDNA Synthesis Kit Fermentas, York, UK

Electroporation cuvettes 4mm par 50 sans pipet Eurogentec, Southampton, UK

## **2.1.9 Kits**

The following kits were purchased from Qiagen, Crawley, West Sussex, UK

RNeasy Total RNA Isolation Kit

QIAquick PCR Purification Kit

QIAquick Gel Extraction Kit

Miniprep Plasmid Isolation Kit

Maxiprep Endofree Plasmid Isolation Kit

## **2.1.10 Synthetic Oligonucleotides**

Oligonucleotides were purchased from Purimex (Grebenstein, DE), Alnylam Europe

(Kulmbach, DE), VHBio (Gateshead, UK), Eurofins-MWG-Operon (London, UK) or

Qiagen (Crawley, UK)

## siRNA

siMA6 (si <i>MLL/AF4</i> ) sense;	5'-AAGAAAAGCAGACCUACUCCA-3'
siMA6 antisense;	5'-UGGAGUAGGUCUGCUUUUCUUUU-3'
siMM sense;	5'-AAAAGCUGACCUUCUCCAAUG-3'
siMM antisense;	5'-CAUUGGAGAAGGUCAGCUUUUCU-3'
siAGF1 (si <i>AML/MTG8</i> ) sense;	5'-CCUCGAAAUCGUACUGAGAAG-3'
siAGF1 antisense;	5'-UCUCAGUACGAUUUCGAGGUU-3'
si <i>HOXA7</i> sense;	5'-CCGUUCCGGGCUUAUACAAUG-3'
si <i>HOXA7</i> antisense;	5'-UUGUAUAAGCCCGGAACGGUC-3'
siMARS (si <i>MLL/AF4</i> ) sense;	5'-ACUUUAAGCAGACCUACUCCA-3'
siMARS antisense;	5'-UGGAGUAGGUCUGCUUAAAGUCC-3'

## Primers for RealTime-PCR

<i>HoxA7</i> forward	5'-GAG GCC AAT TTC CGC ATC TA-3'
<i>HoxA7</i> reverse	5'-GCG GTT GAA GTG GAA CTC CTT-3'
<i>GAPDH</i> forward	5'-GAA GGT GAA GGT CGG AGT C T-3'
<i>GAPDH</i> reverse	5'-GAA GAT GGT GAT GGG ATT TC-3'
<i>HPRT</i> forward	5'-TGA CAC TGG CAA AAC AAT GCA-3'
<i>HPRT</i> reverse	5'-AGC TTG CGA CCT TGA CCA TC-3'

---

<i>TERT</i> forward	5'-GGA GAA CAA GCT GTT TGC GG-3'
<i>TERT</i> reverse	5'-AGG TTT TCG CGT GGG TGA G-3'
<i>DUSP6</i> forward	5'-AGC TCA AGG ACG AGG GCT G-3'
<i>DUSP6</i> reverse	5'-GGA GAA CTC GGC TTG GAA CTT-3'
Self designed primers:	
<i>ATP2B3</i> forward	3'-AGAAAGGCGAGATAGAACAG-5'
<i>ATP2B3</i> reverse	3'-GATGCTGGTGAAGTTGTC-5'
<i>BNIP3</i> forward	3'-CTCCTGGGTAGAACTGCAC-5'
<i>BNIP3</i> reverse	3'-ATCTTCCTCAGACTGTGAGC-5'
<i>CD69</i> forward	3'-CTCCAGCAAAGACTTTCCTG-5'
<i>CD69</i> reverse	3'-TGTATTGGCCCACTGATAAGG-5'
<i>DAAMI</i> forward	3'-CCACAAATGCCCTGAAATCC-5'
<i>DAAMI</i> reverse	3'-TCACAAAGAAATCCTGCTGTC-5'
<i>DCT</i> forward	3'-ATCTCCAGCGACTCATTGG-5'
<i>DCT</i> reverse	3'-TTACCTATCACAGACAGTTTCCC-5'
<i>ECE1</i> forward	3'-CAAGAGCATAGCCACCGA-5'
<i>ECE1</i> reverse	3'-TCCTCATCCATCCACTTCAG-5'
<i>FLJ13639</i> forward	3'-CCGAGTGATAACCGTCTCC-5'
<i>FLJ13639</i> reverse	3'-TTTGTGCATAGACCATAGTTCC-5'



---

<i>GLEIL</i> forward	3'-GAAACAGAATGAAGACCTCCAG-5'
<i>GLEIL</i> reverse	3'-GCCCACCAGATTGAACAG-5'
<i>NAP1L4</i> forward	3'-GAACCAATCTTGAAACACCT-5'
<i>NAP1L4</i> reverse	3'-GTCAATAGTACACCCGTCAC-5'
<i>PLAT</i> forward	3'-TGCCTGGAAACTTAAAGGAG-5'
<i>PLAT</i> reverse	3'-CGTCCCTTAAATTCACGG-5'
<i>PRDM2</i> forward	3'-CCTTCCCTCCACTCTTACAG-5'
<i>PRDM2</i> reverse	3'-GATTACATGAACCCTCAGTCTC-5'
<i>SCD</i> forward	3'-CCCACCTACAAGGATAAGGA-5'
<i>SCD</i> reverse	3'-CCATTCATAGACATCATTCTGG-5'
<i>SLC16A3</i> forward	3'-CTACTCCGTCTACCTCTTCAG-5'
<i>SLC16A3</i> reverse	3'-CATCCAGGAGTTTGCCCTC-5'
<i>TRIM31</i> forward	3'-GTAGCAAGAAACAGTATCCAC-5'
<i>TRIM31</i> reverse	3'-GCCATGACAGAACAACAG-5'
<i>STS-1</i> forward	3'-ACGACTCCTCTTACTATCATCTG-5'
<i>STS-1</i> reverse	3'-TCTAATAAGGCTTCACCCAC-5'
<i>IGFBP2</i> forward	3'-TCAAGTCGGGTATGAAGGAG-5'
<i>IGFBP2</i> reverse	3'-ACATCTTGCACTGTTTGAGG-5'
<i>CIP1</i> forward	3'-GGACATATCAGGTACATCAGG-5'
<i>CIP1</i> reverse	3'-GGTCAATTCTACATCCTTGCT-5'

<i>BUB3</i> forward	3'-TCCCAGTTCCTGCTTGTC-5'
<i>BUB3</i> reverse	3'-GCGTTGGATCGTAGAAGG-5'
<i>CDK1</i> forward	3'-TGGAGTTGTGTATAAGGGTAGAC-5'
<i>CDK1</i> reverse	3'-AGCACATCCTGAAGACTGAC-5'
<i>FBXL11</i> forward	3'-GGCTATACCTTCGTCATTCC-5'
<i>FBXL11</i> reverse	3'-TTAACTCCAAATCCATGCTG-5'
<i>IRX3</i> forward	3'-TCACAGACTGGTCTCAGC-5'
<i>IRX3</i> reverse	3'-CACTACAGCGATCTGTTCC-5'
<i>CDH2</i> forward	3'-GCAGCTGGACTTGATCGAGAA-5'
<i>CDH2</i> reverse	3'-GTGGCTGTGTTTGAAAGGCC-5'
<i>FGFR1</i> forward	3'-GAGATGGAGGTGCTTCACTT-5'
<i>FGFR1</i> reverse	3'-CATGCAGGAGATGAGGAAG-5'

### 2.1.11 Cell-lines

#### SEM

The cell line SEM was established from the peripheral blood of a 5 year old girl at relapse of ALL. The human B cell precursor leukaemic cells carry the t(4;11) translocation with *MLL* and *AF4* gene portions being fused. This cell line was established by Johann Greil in 1989 (Greil, Gramatzki et al. 1994).

### Primary SEM

Primary SEM are an early passage of the patient cells from which the SEM cell line had been established later. They show a slower growth than cell line SEM described above (Greil, Gramatzki et al. 1994).

### SEMcami

SEMcami are SEM cells transduced with pHR-CMV-DRep/amiAML1-ETO, a lentiviral HIV based vector constitutively expressing the *EGFP* and *Dsred* reporter genes and an AML1-ETO shRNA, the latter target is not present in SEM. SEMcami served as control cells for this vector. The vector and the transduction was performed by Vasily Grinev.

### SEMTeton

SEMTeton were transduced with vector 1 /Teton vector generated in this work with a lentiviral HIV based system. Transduced cells express the reporter gene *EGFP* (see chapter 5).

### RS411

The RS4;11 cell line was established from the bone marrow of a 32 year old female ALL patient. These lymphoblast cells carry the t(4;11) translocation with *MLL* and *AF4* gene portions being fused (Stong and Kersey 1985) .

### MV4;11

MV4;11 cells were isolated from the peripheral blood of a 10 year old boy with biphenotypic B myelomonocytic leukemia expressing both myeloid and lymphoid markers. This is one of the few t(4;11) positive myeloid cell lines (Lange, Valtieri et al. 1987).

#### MV4;11Teton

MV4;11Teton were transduced with vector 1 / Teton vector generated in this work with a lentiviral HIV based system. Transduced cells express the reporter gene EGFP (see chapter 5).

#### Kasumi-1

The Kasumi-1 cell line was established from the peripheral blood of a 7 year old boy with acute myeloid leukaemia. The myeloblast cells bear the t(8;21) translocation with the AML1 and MTG8 genes being fused (Asou, Tashiro et al. 1991).

#### Kasumi-1 DC

Kasumi-1 DC are Kasumi-1 cells transduced with pHR-CMV-DRep, a lentiviral HIV based control vector expressing the Dsred and EGFP reporter genes but no other genes. The vector was generated and transduced by Vasily Grinev.

#### SKNO-1

SKNO-1 cells were isolated from the bone marrow of a 22 year old Japanese woman with AML. Myeloblast cells are GM-CSF dependent and bear the t(8;21) translocation with the AML1 and MTG8 genes being fused (Matozaki, Nakagawa et al. 1995).

#### 293T

The 293T cell line is derived from human embryonal kidney cell line 293. 293T additionally express the large T antigen, are of fibroblast morphology and highly transfectable (Rio, Clark et al. 1985).

#### HS-5

HS-5 are bone marrow stromal cells from a 30 year old caucasian man. They were immortalised with the amphotropic retrovirus vector HPV. The cells of fibroblast

morphology produce several haematopoietic growth factors, cytokines and interleukins (Roecklein and Torok-Storb 1995).

#### M210B4

M210B4 are murine bone marrow stromal cells. These fibroblasts are known to support human and murine myelopoiesis in long term culture (Lemoine, Humphries et al. 1988).

## 2.1.12 Bacteria

#### JM109

JM109 are E. Coli competent cells lacking *recA* (improves DNA yield in Plasmid isolation) and are beta-gal deficient. Genotype: *endA1, recA1, gyrA96, thi, hsdR17* ( $r_k^-$ ,  $m_k^+$ ), *relA1, supE44, Δ( lac-proAB)*, [*F' traD36, proAB, laq1<sup>q</sup>ZΔM15*], Promega, Madison USA.

#### HB101

HB101 are E.Coli competent cells are lacking *recA*, but are not suitable for blue - white screening. Genotype: *F<sup>-</sup>, thi-1, hsdS20* ( $r_B^-$ ,  $m_B^-$ ), *supE44, recA13, ara-14, leuB6, proA2, lacY1, galK2, rpsL20* ( $str^r$ ), *xyl-5, mtl-1*, Promega, Madison USA.

#### STBL3

STBL3 are E.Coli competent cells for the cloning of direct repeats found in lentiviral expression vectors. They show a reduced frequency of unwanted homologous recombinations. Genotype: *F<sup>-</sup> mcrB mrr hsdS20* ( $r_B^-$ ,  $m_B^-$ ) *recA13 supE44 ara-14 galK2 lacY1 proA2 rpsL20* (*Strr*) *xyl-5 - leu mtl-1*, Invitrogen, UK.

#### Self produced JM 109

Self produced JM 109 were made competent using a  $CaCl_2$  / PEG protocol.

### 2.1.13 Mice

NSG

NOD.Cg-*Prkdc*<sup>scid</sup> *Il2rg*<sup>tm1Wjl</sup>/SzJ immune deficient mice also called NOD SCID gamma; NOD-SCID, *Il2Rgamma*<sup>null</sup>; NOD-SCID *Il2Rg*<sup>null</sup> or NSG, were purchased from Jackson Laboratory, USA. In this thesis they are referred to as NSG mice.

Rag2/*Il2rg* double knockout

B10;B6-*Rag2*<sup>tm1Fwa</sup> *Il2rg*<sup>tm1Wjl</sup> immune deficient mice were retrieved from Markus Manz Laboratory, Switzerland (Traggiai, Chicha et al. 2004). In this thesis they are referred to as R2G (Rag2 knockout, Gamma knockout) mice.

## 2.2 Methods

### 2.2.1 Methods chapter 3: Array validation

#### 2.2.1.1 Array analysis Ingenuity

The HG-U133 Plus 2.0 oligo array data were provided pre-analysed with Affimetrix MAS analysis. Using a perfect match and a mismatch probe on the array, MAS calculates if a transcript is present, marginal or absent. Using positive and negative probe sets, MAS also calculates the positive / negative ratio which is a performance indicator for each probe set. Finally the average difference for expression intensities of the transcripts is calculated.

These pre-analysed data sets from the oligo-array were sorted for strength of fold change and only genes with a fold change higher than 2 were used. The Probe ID and the gene names were imported together with the mRNA changes. The Ingenuity Pathway 8.5 analysis identified the role of genes sensitive to the depletion of *MLL/AF4* and connected them (transcripts) to functions, diseases, physiological systems, networks and canonical pathways.

The results were sorted by p-value which the platform generated from data including the strength of the expression level alteration and the ratio between affected genes from the array and the number of genes in that group (pathway, system, etc.) (For further detail see chapter 3.3).

### **2.2.1.2 Hybridization of siRNA**

The sense and the antisense strand were combined in hybridization buffer at a concentration of 20 $\mu$ M each. The mixture was then incubated on a heating block for 30 sec at 95°C, cooled to room temperature and stored at -20°C.

### **2.2.1.3 RNAi and Electroporation**

To knockdown transcripts by RNAi the cells of interest were adjusted to 1x10<sup>7</sup> cells / ml in full medium and pipetted into an electroporation cuvette (between 100 $\mu$ l and 800 $\mu$ l per cuvette). The appropriate siRNA was added to the desired concentration typically 500nM for siMA6. After addition of the siRNA the mixture was quickly flicked and then electroporated usually at 350V, 10msec with the pulse generator EPI2500 (Dr. L. Fischer, Heidelberg). The mixture was incubated for 15min and then normally diluted 1/20 in full medium.

Different cell-lines, siRNAs or experiments required different siRNA concentrations and voltages for optimal results.

For sequential electroporations with siMa6 and control siRNA, cells were electroporated every 48h and if required, cell material was harvested 48hours after each electroporation. Up to 3 sequential electroporations were performed.

### **2.2.1.4 RNA isolation**

To isolate RNA from cells the Qiagen RNeasy Kit was used. According to the manufactures guidelines up to 5x10<sup>6</sup> pelleted cells were lysed in RLT +  $\beta$ -



mercaptoethanol (10 $\mu$ l/ml RLT). This lysate was then added to a Qias shredder column and spun for 2min at full speed. The flow through was then diluted with 350 $\mu$ l of 70% ethanol and the mixture loaded on an RNeasy column which was spun for 1min at full speed. After washes and elution according to the manufacturer's protocol the RNA yield was determined by the Nanodrop ND-1000 UV-Vis measurement.

### **2.2.1.5 cDNA synthesis**

To analyse the mRNA after isolation it had to be converted into cDNA by reverse transcription. For this the RevertAid<sup>TM</sup>H Minus First Strand cDNA Synthesis Kit from Fermentas was used. 1 $\mu$ g of RNA was used, 1  $\mu$ l random hexamers added and the volume adjusted to 12 $\mu$ l with RNase free H<sub>2</sub>O. The mixture was incubated in PCR tubes in a PCR machine for 5min at 70°C followed by the addition of 4 $\mu$ l reaction buffer, 2 $\mu$ l dNTP mix, 1 $\mu$ l RiboLock RNase Inhibitor and 1 $\mu$ l of MuMLV reverse transcriptase polymerase. Then the mixture was put back into the PCR machine and incubated at 25°C for 10min, at 42°C for 60min and finally at 70°C for 10min. After the cDNA synthesis was completed 30 $\mu$ l of RNase free water was added and the samples were stored at -20°C.

### **2.2.1.6 Primer design**

The primers were designed with Primer Express 2.0 using standard parameter for RT-primer design; a melting temperature of 60°C and an amplicon length of typically 50-150bp, but up to 250bp in length.

### 2.2.1.7 Quantitative Real Time PCR analysis

In the real time PCR the multiplication of the PCR product was monitored via Sybrgreen, which intercalates into double strand DNA, in real time. The evaluation of the template amount, here an mRNA transcript, is made by calculating the cycle threshold (CT) values and plotting on a graph.

The molar amount of DNA molecules (total DNA or cDNA) multiplied by the time correlates to the CT value, which means that the more substrate there is, the earlier a signal is detected. Using the CT the amount of mRNA extracted from the cells and ultimately the expression levels can be determined.

Standard primers were diluted from 100 $\mu$ M to 375nM final concentration. The

*MLL/AF4* primers were diluted from 5 $\mu$ M to a final concentration of 62.5nM. The real time PCR was performed in two different real time PCR machines. When using the ABI PRISM 7000 from Applied Biosystems following protocol was used:

Following mix was prepared before pipetting into a 96-well plate.

Master-mix using standard PCR primers:

SYBR©Green	(2x)	7.5	$\mu$ l
Primer fw	(100 $\mu$ M to 375nM)	0.05	$\mu$ l
Primer rev	(100 $\mu$ M to 375nM)	0.05	$\mu$ l
dH2O		4.4	$\mu$ l
$\Sigma =$		12	$\mu$ l

For MLL/AF-4 primers the following mix was prepared:

SYBR©Green	(2x)	7.5	μl
Primer fw	(5μM to 62.5nM)	0.15	μl
Primer rev	(5μM to 62.5nM)	0.15	μl
dH2O		4.1	μl
Σ =		12	μl

The samples were analyzed in triplets. In each 96-well plate well 12μl PCR-Mix + 3μl qRT-PCR cDNA was mixed. After loading, the plates were sealed with foil, spun down briefly and put into the real time PCR machine (ABI PRISM 7000 Sequence Detection System, Applied Biosystems).

The program included 2min at 50°C, 10min at 95°C followed by 40 cycles of 15sec 95°C and 1min 60°C. At the end of the run usually a melting curve was performed. The data was analyzed with the programs ABI 7000 SDS and Microsoft Excel.

The ABI 7900HT Sequence detection system offers analysis of up to 384 samples in one PCR run. The protocol was changed to reflect the smaller well size however the primer concentrations did not change and each sample was prepared in triplets as before.

Master-mix for all standard primers (except *MLL/AF4*)

SYBR©Green	(2x)	5	μl
Primer fw	(100μM to 375nM)	0.03	μl
Primer rev	(100μM to 375nM)	0.03	μl
dH2O		2.94	μl
Σ =		8	μl

Master-mix for *MLL/AF4* primers only:

SYBR®Green	(2x)	5 $\mu$ l
Primer fw	(5 $\mu$ M to 62.5nM)	0.1 $\mu$ l
Primer rev	(5 $\mu$ M to 62.5nM)	0.1 $\mu$ l
dH <sub>2</sub> O		2.8 $\mu$ l
$\Sigma =$		8 $\mu$ l

Per multi-plate well 8 $\mu$ l master-mix and 2 $\mu$ l cDNA were combined. For analysis of the acquired data the SDS version 2.2 program from Applied Biosystems was used. As before a melting curve was performed. Here the temperature was gradually increased and a decrease in signal shows the melting point of the amplicon due to SYBR-Green only intercalating into double strands. Usually specific primers lead to amplicons with a dissociation point of 80°C to 85°C. An unspecific product like primer dimers would be expected at a lower temperature.

### **2.2.1.8 Amplicon control**

In addition to dissociation point analysis, the PCR product can be confirmed by DNA-PAGE. Here the DNA pieces are separated according to length and the size can be measured using a DNA ladder of appropriate size. For this an 8% polyacrylamide gel was made. A 5ml mix contained 1ml 40% Acrylamide / Bisacrylamide, 1ml 5xTBE buffer and 3ml H<sub>2</sub>O. After mixing 10 $\mu$ l TEMED and 50 $\mu$ l 10%APS were added, mixed and the gel poured. Samples were loaded with 6xDNA loading buffer and the gel was run in 1xTBE buffer.

### **2.2.1.9 Cell culture**

Suspension cell-lines SEM, SEMTeton, SEMcami, MV4;11, MV4;11Teton RS4;11 Kasumi-1 DC and Kasumi-1 were fed with RPMI1640 (SIGMA, HEPES Modification), supplemented with 10% FCS (SIGMA) and 2mM Glutamine (SIGMA). SKNO-1 cells were fed RPMI1640 containing 20% FCS, additionally supplemented with GM-CSF (7 ng/ml). Cells were maintained at a concentration of 0.2 to  $1 \times 10^6$  cells / ml. If cells were maintained in culture, part of the suspension was discarded and replaced with fresh medium. Depending on the growth, the start concentration and the cell-line cells were fed twice to thrice a week.

Adherent cells such as HS-5 and M210B4 were fed with RPMI1640 containing 10% FCS and 2mM Glutamine, whereas 293T cells were fed with DMEM (SIGMA) containing 10% FCS and 2mM Glutamine.

To seed or maintain cells, the adherent cell layer was washed with warm PBS, which was then removed and the cells were subsequently incubated with a sufficient amount of 1xTrypsin/EDTA (5mg Trypsin/ml, 2mg EDTA/ml, Sigma) at RT and incubated for 5min or until the cells lost adhesion. Trypsinisation was stopped by addition of FCS containing medium. The cells were then split according to their growth rate and experiment design usually 1/10. All cells were kept at 37°C, 5% CO<sub>2</sub> and 95% air humidity.

### **2.2.1.10 Freezing and thawing of cells**

Cells were frozen by resuspending between  $5 \times 10^6$  to  $1 \times 10^7$  cells in culture medium with 10% DMSO and 20% FCS. The mixture was transferred to cryo-vials (Nunc) on ice and

slowly frozen, packed in cotton in a -80 freezer. After 2 days they were transferred to a liquid nitrogen tank for long term storage.

For thawing cell vials were removed from liquid nitrogen, transported on ice, quickly thawed by hand and resuspended in a larger volume of warm medium as soon they began to thaw. Then the cells were spun down and resuspended in medium to remove the DMSO.

### **2.2.1.11 Counting cells**

For counting a cell suspension was mixed well by pipetting, an aliquot was taken, diluted  $\frac{1}{2}$  with Trypan-blue (dilution from 0.4% to 0.2%, Sigma) and a Neubauer improved counting chamber was loaded with the mixture. Viable cells exclude Trypan blue. Dead cells, however, show intracellular staining with Trypan blue. The chamber had been prepared by attaching a cover glass to the moist chamber. The number of cells in 4 large squares corresponds to  $10^4$  cells/ml.

### **2.2.1.12 Flow cytometric analysis**

Cells were counted, volume adjusted to 200-300 $\mu$ l and saturating volumes of antibody were added (see 2.1.7 ). The samples were then left in the dark for 20min with vortexing in between. Then 2.5ml 0.2% PBSA was added and the samples centrifuged for 5min at 500g and 4°C. The supernatant was subsequently discarded and the cells resuspended in 500 $\mu$ l 0.2% PBSA. The analysis was done on the FACS Canto II machine with DiVa v6.1.2 software, using compensation if several dyes had been applied.

### **2.2.1.13 Compensation**

If a combination of two or more fluorochromes was used in flow cytometric analysis a possible overlap of one fluorochrome emission into another detection channel has to be compensated for, otherwise an over spilling signal could be recorded and a false-positivity for a marker generated.

To accomplish this, a sample was stained with an antibody combination, but also unstained and single stains for each antibody/fluorochrome were prepared. For each channel the threshold and PMT voltages were set using the unstained sample. Then the single stained samples were recorded. The Diva software used these data to identify percentage overspill for each fluorochrome into other channels and automatically generated a mathematical compensation matrix. Once the compensation was set double or more stained samples could be recorded.

### **2.2.1.14 CFSE staining**

Due to toxicity of CFSE and the additional stress by electroporation the concentration of CFSE, incubation times and other parameters had to be changed from the standard protocol. SEM at  $1 \times 10^6$  cells/ml and RS4;11 at  $1.5 \times 10^6$  cells/ml were stained with 0.5 - 1.5  $\mu$ M CFSE. Cells were washed with PBS, resuspended in warm PBS with the CFSE addition and incubated for 10min at 37°C. Then the cells were spun down at 300g for 5min and the pellet was resuspended in medium containing FCS. After 30min the standard cell culture medium (RPMI1640, 10% FCS, 2% Gln) was changed again. One day later the stained cells were electroporated with siMA6 or siAGF1 at  $1 \times 10^7$  cells/ml, 350V and 10msec. They were then diluted 1/40 and incubated in 6-wells. At different

time points aliquots were taken, fixed in PBS + 2% formaldehyde and stored in the fridge.

At the end of the experiment the samples were analysed by flow cytometric analysis detecting the CFSE signal in the FITC channel. These flow cytometric analysis data was analysed by ModFit setting the parent population (generation 0) and the increment (width of each population in the fluorescence scale (x-axis), see Figure 21 and Figure 22).



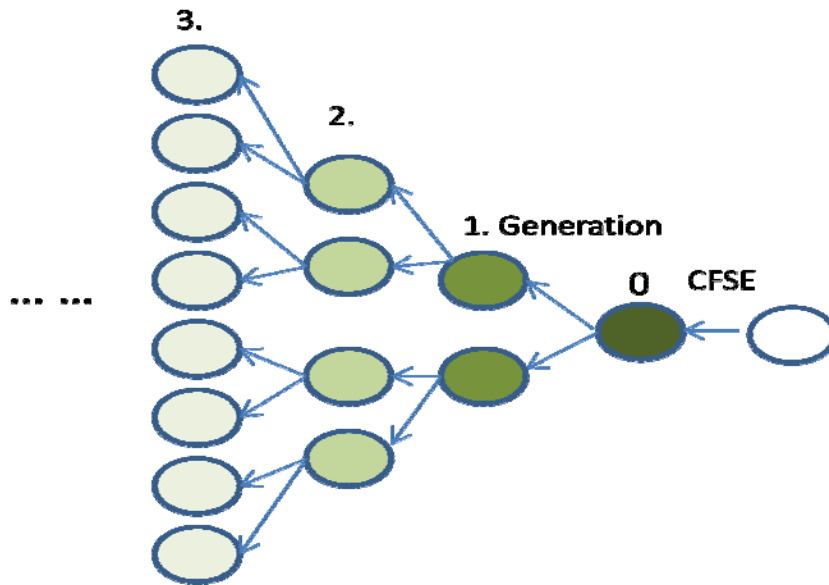


Figure 21 Dilution of CFSE staining in cell membranes due to proliferation

The membrane of a cell is stained with CFSE (0. generation, left) after each division the signal is weakened, CFSE Carboxyfluorescein succinimidyl ester

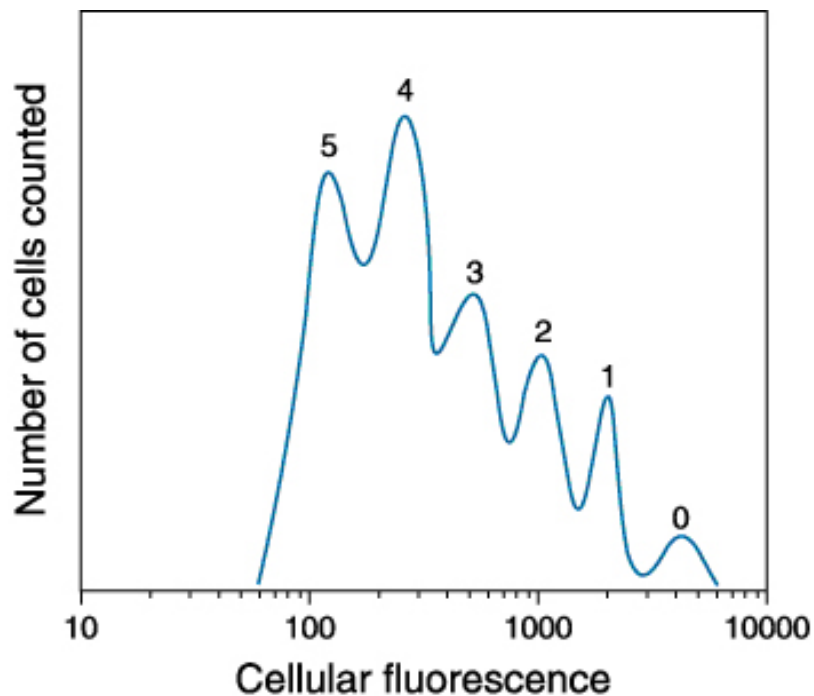


Figure 22 CFSE staining pattern

Successive populations of CFSE stained cells 1 first generation after staining, 2 second generation etc., CFSE Carboxyfluorescein succinimidyl ester from [www.mcg.edu/cancer/shared/flow/fluorophores.html](http://www.mcg.edu/cancer/shared/flow/fluorophores.html)

## **2.2.2 Methods Chapter 4 - Bone Marrow Feeders**

### **2.2.2.1 Growth arrest with MMC**

HS-5 layers were incubated with Mitomycin C (MMC) at a concentration of up to 200 µg/ml medium in 1ml per well (12well) for 5min incubation, subsequently washed twice with PBS and then medium was added. The layers were monitored for apoptosis and growth over the following weeks.

### **2.2.2.2 Growth arrest with AMD**

A dilution of Actinomycin D dissolved in DMSO was prepared to a concentration of 1µM and subsequently strongly diluted in medium. Final concentrations from 0.2 to 6.7nM were used on highly confluent HS-5. The effect on the growth was monitored over 2 weeks.

### **2.2.2.3 Growth arrest with Irradiation**

M210B4 were grown to almost 100% confluence which is approximately  $2.5 \times 10^6$  cells per T25 flask. Then they were washed and trypsinised. After cells lost adhesion 10ml of medium was added and the cells spun down at 1200rpm for 5 minutes. The cell pellet was resuspended in 2.8ml medium which results in 1mm depth in a T25 flask when lying horizontal. The flasks were irradiated for 19.17min at 10mA and 320kV with the D3300 X-ray system resulting in a radiation dose of 60Gy.

The irradiated cells were then diluted in a bigger volume depending on the desired final concentration. Typically they were seeded at  $0.5 \times 10^6$  cells/ml and 1ml per 48well-plate well. The wells had been collagen coated beforehand. For smaller and bigger wells the amount was adjusted proportional to the increased surface. This concentration created an excess of cells, but due to apoptosis taking place an equal layer was achieved after 3 days of incubation. Then the feeder layer was ready for co-culture.

#### **2.2.2.4 Collagen coating**

A fresh solution of rat tail collagen (BD) was prepared at 0.2mg/ml in 0.1N acetic acid under sterile conditions. For 48-well plates 100 $\mu$ l per well were aliquoted and for 6-well plates 800 $\mu$ l per well. The plates have then been left to dry over night under a sterile hood. The next morning the lids were put on the plates and they were stored at room temperature.

#### **2.2.2.5 Co-culture**

Leukaemic cells were incubated on growth arrested feeder layers. According to the experimental setup the required concentration of the cells was adjusted from  $1 \times 10^3$  to  $5 \times 10^6$  cells/ml. When medium colour shifted towards yellow, the upper part of medium in the well was replaced by fresh medium. Density and state of the co-cultured cells was monitored by microscope.

### **2.2.2.6 Inversion Test**

For the inversion test an 8-well chamber slide was collagen coated. Irradiated M210B4 were seeded and left to form a layer for 2 days. Then non-adherent leukaemic cells were co-cultured in various concentrations on the feeder. After one day the wells were carefully washed with medium to remove cells in suspension and the lowest layer on top of the feeders was photographed under magnification. The chambers were then filled with medium to the very top, 2 layers of parafilm were pressed onto the wells and the lid put on top of it, ensuring that no air bubbles remained in the chambers. The slide was then turned upside down and left for 2 hours standing like this. Cells which had not physically attached to the feeder were separated from it by gravity. After the incubation the chamber was opened still being upside down, removing the medium with non attached cells. Following this the feeder layer was again photographed and the before and after images compared for cell-numbers.

### **2.2.2.7 Discriminating count**

Leukaemic cells can be distinguished from the feeder cells by microscopy. Cells like SEM, RS4;11, MV4;11 and Kasumi-1 are much smaller, round instead of fibroblast shaped and less granular than the feeders. For training, feeders alone and feeders with several concentrations of leukaemic cells were used.

### **2.2.2.8 Flow cytometric analysis based cell count on Feeder**

SEM, SEMTeton, irradiated M210B4 and SEMTeton – M210B4 co-cultures with different ratios of SEMTeton were prepared. A characteristic green shift was gated

using native SEM. M210B4 were used as negative control and the zero concentration point for SEMTeton. The SSC-FSC plot was set allowing to display M210B4 and SEMTeton in the same diagram. Furthermore two gates (for M210B4 and SEMTeton) were adjusted using size and fluorescence. A standard curve was generated using the ratios of counted M210B4 to SEMTeton. These setting were saved and used for further determinations of SEMTeton cell numbers on M210B4.

### **2.2.2.9 Primary Material co-culture**

Primary material from patient blood, mouse blood or isolated from mouse organs was washed several times with PBS, full RPMI1640 medium with 2-5% Penicillin / Streptomycin mix was added and the cells incubated on feeder layers. Due to a high number of cells dying high start concentrations were adjusted to  $2 \times 10^6$  cells/ml. Used medium was carefully removed by aspirating  $\frac{1}{2}$  of the well volume from the top and replacing it with fresh medium.

### **2.2.2.10 Determination of viable cells with Annexin-V and PI**

Necrotic cells can be identified using PI incorporation, early apoptotic cells by Annexin-V staining, while late apoptotic cells are positive for both. To set up the assay several controls were used. Unstained cells were used for all cell-types. As positive controls cells were incubated at 65°C for 10min and stained either with PI or with Annexin-V to set the shift of necrotic or apoptotic cells into their quadrant. The samples which had been analysed for viable cells were stained with both Annexin-V and PI (see Table 1).

The following table summarises the protocol.

Unstained cells	PI positive control	Annexin-V positive control	Double stained control cells	Double stained samples
-	Cook 10min 65°C spin	Cook 10min 65°C spin	-	-
-	-	250µl +	Binding 0.325µl	Buffer (BB) Annexin-V FITC
250µl BB	250µl BB + 5µl PI		+ 5µl PI 15min	+ 5µl PI 15min

Table 1 Staining protocol for the Annexin-V – PI assay

BB Binding buffer, PI Propidium iodide

To detect viable leukaemic cells on feeders a more advanced protocol had been established using CD19 staining and gating to select leukaemic cells before detecting necrotic and apoptotic cells. This demanded extra CD19 controls. Cells were stained with 5µl CD19-APC for 20min and then washed as described for the flow cytometric analysis. In the triple stained samples the CD19 staining took place before Annexin-V and PI staining.

### 2.2.2.11 Cell cycle analysis

Cell cycle analysis relies on the principle that the DNA amount in one cell changes according to its phase in the cell-cycle. After a cell-division a cell is small and contains

a single genome, this corresponds to the the G<sub>0</sub> or the G<sub>1</sub> phase. In G<sub>1</sub> mainly cell growth and protein expression takes place. This is followed by the S phase where the DNA is synthesized, so that the amount of DNA rises until doubled. The cells enter the G<sub>2</sub> phase where the cells are growing and protein is expressed. Finally with the same high DNA content as the G<sub>2</sub> phase the M-phase takes place, preparing the cell for segregation, before a new cell cycle starts (see Figure 23).

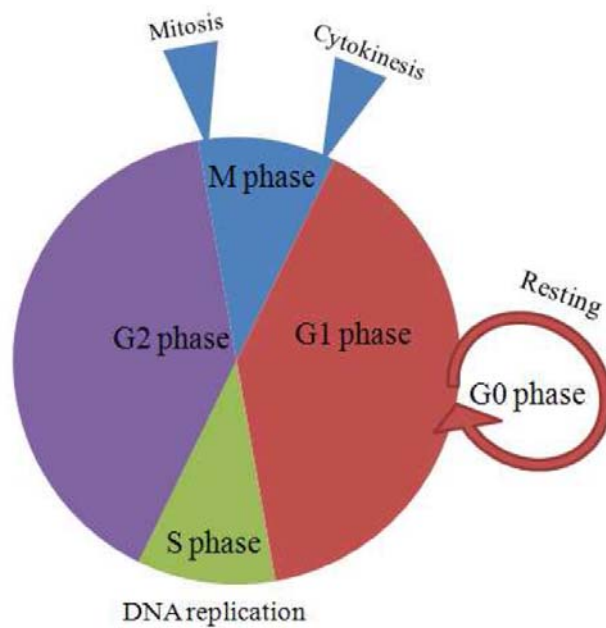


Figure 23 The cell cycle

Shown is the length and order of cell phases. M Mitosis, G growth, S DNA synthesis from Bruce Alberts et al., *Molecular Biology of the Cell*, 4th edition, Wiley-VCH Verlag GmbH&Co.KGAA, Germany

Propidium iodide (PI) is a red fluorescent dye which stains DNA. Its signal can be used to measure the amount of DNA in a cell. To analyse samples  $5 \times 10^4$ - $1 \times 10^5$  cells were washed in PBS and resuspended in 100  $\mu$ l cold citrate buffer. A mix of 400  $\mu$ l propidium iodide and 3  $\mu$ l RNaseA was prepared and added to the citrate buffer cell suspension. The samples were incubated on ice for 5 min and then subsequently analyzed using the FACS canto II machine with the software FACS-Diva v6.1.2. (see Figure 24).

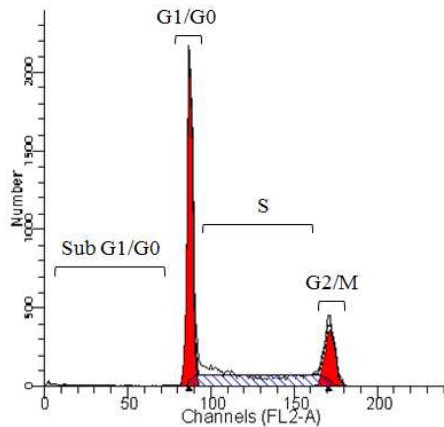


Figure 24 Typical Cell cycle analysis

Shown is a typical FACS Histogramm from a cell cycle analysis, Sub G1/G0 mostly dead and apoptotic cells, G1/G0 phase, S phase, G2/M phase from Varity Software House

## 2.2.3 Methods Chapter 5 - Lentiviral cloning, production and transduction

### 2.2.3.1 DNA- restriction Digest

To cut DNA, sequence specific endonucleases were used. The digest was carried out at 37°C for 1h with 10U of enzyme and 0.5µg to 1µg of DNA was the standard condition. Suitable buffer was chosen according to the manufactures recommendations, normally at 1 fold concentration and a final volume of 20µl. The reactions were stopped by heat inactivation at 65°C or 85°C for 15 minutes.

If DNA had to be digested by two enzymes an appropriate buffer and conditions including enzyme and buffer concentration were chosen using a web tool from Fermentas (<http://www.fermentas.com/doubledigest/>). Sometimes sequential digests had to be performed if the buffer requirements were too different or the enzymes needed different digest temperatures.



### **2.2.3.2 Gel electrophoresis**

After heat inactivation of the digest the mixture was diluted with loading buffer usually 1/6 for a 6xDNA-LB. An agarose gel was made by heating agarose with TAE buffer until agarose was dissolved and the gel was poured into a tray with a comb. Normally 1% agarose for products between 100 and 10000bp were chosen. After the gel had set it was transferred into the electrophoresis chamber with TAE buffer and the wells were loaded with the digest mixture. The gel was covered with buffer. typically electrophoresis was performed at 80V with the positive pole at the opposite end to the loaded mixture. After the bands had run far enough the electrophoresis was stopped and the gel put into an ethidium bromide bath while shaking. Usually 15min of staining in the bath was sufficient, the gel was then taken out of the bath and visualised in a gel visualisation device fitted with a camera able to detect the signal emitted by ethidium bromide.

### **2.2.3.3 Gel extraction**

Following separation by agarose gel electrophoresis DNA fragments were isolated by staining the gel in an ethidium bromide bath, and the desired bands were cut out on a UV-light box. The DNA was extracted using the Qiagen Gelextraction Kit Qiaquickspin. The gel band was dissolved in the same volume of QC buffer and incubated at 50°C for 10min while vigorously shaking. The dissolved gel piece was loaded on the kit column, spun down, washed with 0.5ml QC buffer and 0.75ml PE buffer and resuspended in 50µl EB buffer. The amount of DNA was estimated.

## **2.2.3.4 Modification**

### **2.3.3.4.1 Blunting**

#### **2.3.3.4.1.1 Klenow**

The Klenow enzyme is a fragment from DNA Polymerase I. It was used to fill in protruding 5' ends and cut off protruding 3' ends. As a standard protocol for the fill-in of 5' protruding ends 10 - 15 $\mu$ l (0.1 - 4 $\mu$ g) of digested DNA (aqueous solution), 2 $\mu$ l of 10x reaction buffer for Klenow fragment, 0.5 $\mu$ l of dNTP mix, (2mM each), 0.1 - 0.5 $\mu$ l (1-5u) Klenow fragment were mixed and topped up to 20 $\mu$ l with nuclease free water. The reaction was incubated at 37°C for 10 min and the reaction stopped by heating for 10min at 75°C.

#### **2.3.3.4.1.2 T4 Polymerase**

T4-Polymerase was also used to fill in protruding ends. For blunting DNA with 5' or 3' protruding Termini 4 $\mu$ l 5x reaction buffer for T4 Polymerase, 1 $\mu$ g of digested DNA ,1 $\mu$ l dNTP mix (2mM each), 0.2 $\mu$ l (1u) T4 DNA Polymerase were combined and topped up with nuclease free water to 20 $\mu$ l. The reaction was incubated at 11°C for 20min, or at room temperature for 5 min and stopped heating for 10min at 75°C.

#### **2.3.3.4.1.3 Mung bean nuclease**

Mung bean exonuclease was used to remove ssDNA from a mixture also containing double stranded DNA (dsDNA). For the removal of single-stranded extensions DNA

(0.1 µg/µl) was suspended in 1x Mung Bean Nuclease buffer or 1x NEB buffer 1, 2 or 4. 1.0 units of Mung Bean Nuclease per µg DNA were added and the mixture incubated at 30°C for 30 minutes. The enzyme was inactivated by phenol/chloroform extraction or by addition of SDS to 0.01%. The DNA was recovered by ethanol precipitation.

### **2.3.3.4.2 Dephosphorylation**

#### **2.3.3.4.2.1 Calf Intestine Alkaline Phosphatase**

Calf Intestine Alkaline Phosphatase (CIAP) was used for dephosphorylation of DNA in restriction endonuclease buffer. One unit of CIAP was added to the digest. 3' protruding and blunt ended DNA was incubated at 50°C for 5min while 5' protruding ends were incubated at 37°C for 5min.

Next CIAP was inactivated by addition of EDTA, pH 8 in equal molar concentration to the MgCl<sub>2</sub> and incubated at 65°C for 15min.

#### **2.3.3.4.2.1 Thermo Sensitive Shrimps Alkaline Phosphatase**

Thermo Sensitive Shrimps Alkaline Phosphatase (TSAP) is similar to the CIAP but derived from arctic shrimps. The main advantage is that it can be easily heat inactivated by heating due to its lower thermostability.

For streamline restriction digestion and dephosphorylation 15 units of restriction enzyme for up to 1µg of DNA were used and 1µl of TSAP added. This mixture was

incubated at 37°C for 15min. The reaction was brought to 74°C for 15min to heat inactivate TSAP and restriction enzymes.

#### **2.3.3.4.3 Phosphorylation**

For ligating oligos or small DNA fragments into a vector-fragment, particularly if the vector backbone ends were dephosphorylated, phosphorylation of the oligo / insert was used to increase the likelihood of a successful ligation. A reaction mix of 100-200pmole DNA, 2µl 10x T4 Kinase buffer, 1µl 10mM ATP and 4u T4 polynucleotide Kinase (PNK) was pipetted and topped up with H<sub>2</sub>O to 20µl. The reaction was incubated at 37°C for 1h and heat inactivated at 70°C for 10min.

#### **2.3.3.5 Oligo design and synthesis**

If a cassette had to be inserted into a new vector backbone, but contained no compatible restriction sites to cut the cassette and open the vector this was overcome by the generation of an oligonucleotide. A site in the vector where the cassette should be included was chosen. Restriction sites needed but not present in the vector were chosen. The oligo was designed with the restriction sequences, usually two bases space left in-between the sites and two sticky end overhangs created one at each end. To avoid carrying out additional phosphorylation step, oligos have also been ordered with phosphorylated ends. The sequence was checked for additional restriction sites generated and for methylation sensitive restriction sites. The two strands, sense and antisense, were hybridised at equal molar concentrations in hybridisation buffer, comparable to the siRNA hybridisation protocol.

### **2.3.3.6 Ligation**

#### **2.3.3.6.1 sticky end**

Vector DNA and insert DNA were used in a molar ratio of 1/1 to 1/3 together not exceeding 10 $\mu$ l in a 20 $\mu$ l ligation. Then 2 $\mu$ l T4 ligase buffer, 1u T4 ligase (Fermentas) and H<sub>2</sub>O were added to a final volume of 20 $\mu$ l. The ligation was incubated for 2h at 14°C and subsequently been stopped by heating to 65°C for 15min. A negative control, for example vector DNA without insert DNA was always included.

#### **2.3.3.6.2 blunt end**

For the blunt end ligation it had to be considered that the insert could be ligated into the vector backbone in 2 directions and that the vector could also be religated without insert. Therefore the vector fragment was dephosphorylated. To ligate such blunt ended fragments dephosphorylated vector DNA and insert DNA were used in a molar ratio of 1/1 to 1/3 together not exceeding 10 $\mu$ l in a 20 $\mu$ l ligation. Then 2 $\mu$ l T4 Ligase Buffer, 1 $\mu$ l of PEG, 5u T4 ligase (Fermentas) and H<sub>2</sub>O were added to a final volume of 20 $\mu$ l. The reaction was incubated overnight at 4°C and stopped by heating to 65°C for 15min.

### **2.3.3.7 Transformation**

#### **2.3.3.7.1 JM109**

The most frequent method of transformation used was heat shock. Bacteria were heat shocked at 42°C, which denaturises some proteins, producing gaps in the cell wall. This allowed DNA to diffuse in. JM109 cells are endonuclease (*endA*) deficient, greatly improving the quality of miniprep DNA, and are recombination (*recA*) deficient, improving insert stability.

Cells were removed from -80°C, and placed on ice for 5 minutes then 1–50ng of DNA per 100µl of competent cells was added and the tubes quickly flicked several times. The tubes were immediately put on ice for 10 minutes and heat-shocked for 45–50 seconds at exactly 42°C. Immediately the tubes were returned to ice for 2 minutes. 900µl of cold (4°C) SOC medium was pipetted to each transformation reaction and the tubes were incubated for 60 minutes at 37°C while shaking at approximately 225rpm. To increase the yield of clones the bacteria were briefly spun and the supernatant discarded leaving a small volume remaining in the tube (50-200µl). The pellet was resuspended in this small volume and plated on LB-Agar plates with the required selective antibiotic. The plates were incubated upside-down overnight in an 37°C incubator.

#### **2.3.3.7 .2 STBI3**

Stbl3™ E. coli strain was designed for cloning direct repeats found in lentiviral expression vectors. These cells reduce the frequency of unwanted homologous recombinations of long terminal repeats. The transformation was carried out in a similar

way to the JM109 however the incubation on ice for 30min after DNA addition and the addition of 250µl SOC were different.

### **2.3.3.8 DNA Purification**

#### **2.3.3.8.1 Quick plasmid isolation**

The quick plasmid isolation protocol was used as a fast and easy way to obtain plasmid DNA for screening. The purity of the sample was low, but adequate for a simple digest to confirm the identity of clones.

The evening before 3 to 5ml of LB was inoculated with a clone from an agar plate or a frozen stock. The next morning 2ml of overnight culture was spun down for 1 min at 13000rpm and the supernatant carefully discarded. The pellet was resuspended in 100µl P1 buffer and lysed with 100µl of P2 buffer for 5min. Lysis was stopped with 100µl of P3 buffer and incubated on ice for 5min. The forming precipitates were spun down for 10 min at full speed and the supernatant transferred to a new tube. Into this 750µl absolute ethanol was added. The precipitate was then centrifuged for 30min at 14000rpm at 4°C and the supernatant discarded. The resulting pellet was washed with 500µl ice-cold 70% ethanol and spun for 10 min at 14000rpm at 4°C. Finally the supernatant was discarded, the pellet air dried and resuspended in 50µl EB buffer.

#### **2.3.3.8.2 Mini kit, midi kit and maxi kit**

Mini, midi and maxi-kits were used according to the guidelines of the manufactures in the corresponding handbooks. Likewise the quick plasmid isolation protocol a single

colony from a selective plate was picked and a starter culture of 2–5 ml LB medium inoculated which contained the appropriate selective antibiotic. This starter culture was incubated for approximately 8 h at 37°C with vigorous shaking (approx. 300 rpm). In the evening a main overnight culture was inoculated diluting the starter culture 1/50 - 1/100. The next morning the bacteria were spun down, the pellet resuspended, the cells lysed and neutralised with the buffer system in the kits. The DNA was then purified by spinning down the membrane-protein-genomic DNA aggregates and the plasmid DNA washed. The DNA has then been finally concentrated by a column or by precipitation and the dried pellets resuspended in the appropriate buffer.

### **2.3.3.9 Lentivirus Production**

For the lentivirus production the cell line 293T was used. Viable 293T cells were seeded at  $2 \times 10^6$  cells / 10ml DMEM medium, supplemented with 10%FCS and 2mM L-Glutamine, into a 10cm Tissue culture dish one day before transfection and cultured overnight in an incubator (5% CO<sub>2</sub>, 37°C, 95% air humidity). The cells reached approximately 30% confluence the next day. For the transfection by calcium precipitation, a mix of 5µg pMD2. G envelope plasmid, 15µg pCMVdeltaR8.91 packaging plasmid and 20µg of the 2nd generation lentivirus transfer plasmid were prepared in 0.5M CaCl<sub>2</sub> and filled up to 500µl with special water. Then 500µl 2xHeBS was added slowly and dropwise by gently producing air bubbles from the bottom of the Eppendorf tube with a 1ml pipette. The mix was incubated for 30min at RT to allow the precipitates to form. Prepared 293T cells were infected by slowly dropping the precipitates over the plate. The precipitates were further distributed by carefully shaking the plate. Then the cells were put back in the incubator overnight (see Figure 25). A



coarse precipitation was distributed over the plate the following day, but not adjacent to the cells due to their precipitate uptake. The medium was changed carefully and the cells were incubated for three more days. Four days after transfection, all medium was collected and spun down to remove cells. Additionally the medium was filtered through a 0.45µm filter.

The virus in the medium was concentrated ultracentrifugation in a Beckman ultracentrifuge. To keep to virus sterile the buckets from a swinging bucket rotor, the Beckman Instruments Inc thickwall-style (open-top) polyallomer conical tubes and the Derlin PKGED'1 adapters were filled with 70% ethanol, poured out and left to dry under a flow. The medium containing the virus was filled into the tubes which were then topped up leaving no rim. The buckets were closed, hanged into the rotor and the rotor mounted into the centrifuge. The virus was concentrated for 2h at 26,000rpm, 4°C and negative pressure. After completion the buckets were carefully transported and the supernatant very carefully poured off. The pellets were usually resuspended in 3ml medium, which could then be directly used, kept at 4°C for a week or frozen at -80°C. The protocol for the lentiviral production is a modification by Vasily Grinev from the University of Minsk (Department of Genetics, Biology Faculty, Belarusian State University, Minsk, Belarus) based on a previous protocol from D. Trono's Laboratory of Virology and Genetics (EPFL, Lausanne, Switzerland).

Figure 25 gives an overview over the process.

### **2.3.3.10 Lentivirus Transduction**

The day prior to transduction the leukaemic target cells were seeded in 6-well plates at a concentration dependent on the cell line, for SEM  $2 \times 10^6$  cells per lentiviral transduction were used. The next day 1ml per well of the concentrated lentivirus was mixed with the cell suspension in each well. To prevent leakage of lentiviral medium the plates were sealed with parafilm. The centrifuge was pre-warmed to  $32^{\circ}\text{C}$ , and the plates were spun at 1500g for 2h. Following the spinoculation the plates were located in an incubator for lentiviral work until the next morning. Then to remove free lentiviruses the cells were washed with PBS and resuspended in 3ml of new medium. The cells were further cultured in their incubator and monitored for marker gene expression such as GFP, mCherry or DsRed.

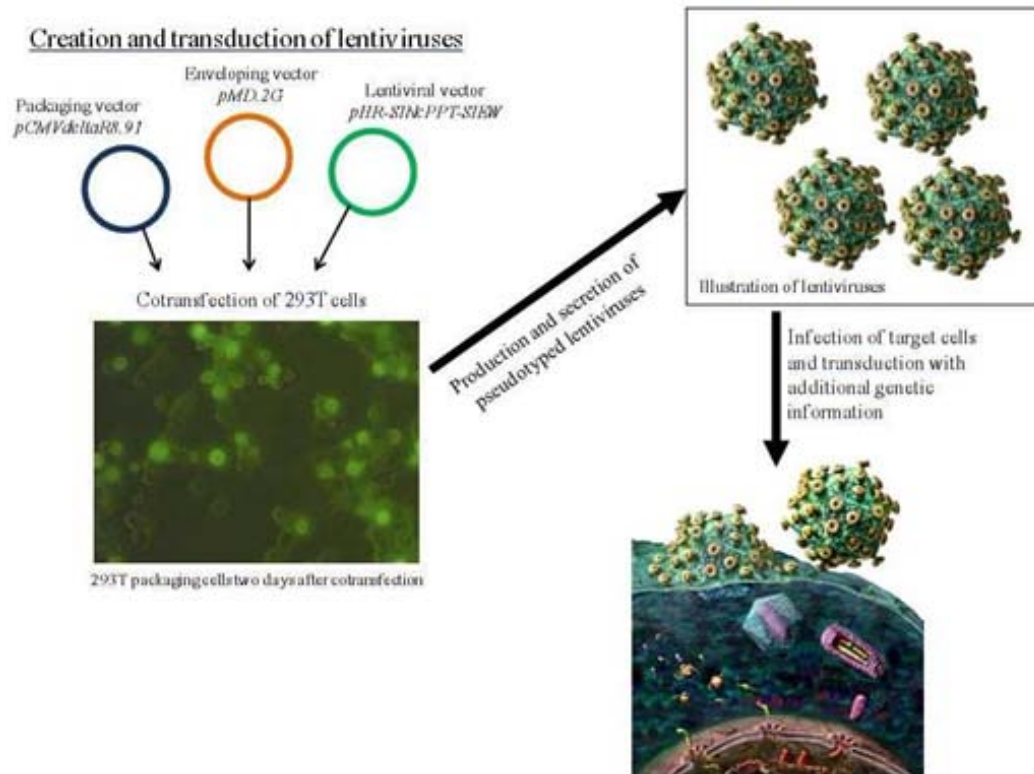


Figure 25 Schematic of Lentivirus generation and transduction

293T cells are transfected with 3 plasmid types comprising a packaging, an enveloping and a lentiviral vector. Transfected 293T cells produce lentiviruses and show reporter gene expression (here GFP). After purification and concentration the lentivirus is used to transduce target cells, integrating a sequence from the lentiviral vector into the genome of the host cell. communication Vasily Grinev

### **2.3.3.11 Measurement of Transduction rate**

If the virus contained a reporter gene such as GFP the transduction was monitored using fluorescent microscopy which gave an approximation of the proportion of cells transduced. Often the signal was not strong enough to be visible by fluorescent microscopy.

For the determination of the transduction rate a more accurate and sensitive method was used, detecting the fluorescent signals of the reporter genes by flow cytometric analysis. For this an aliquot of cells was taken and cells were washed and resuspended in PBS. As a control non transduced cells of the same cell-line corresponding to the transduced samples were used to set the normal, basic fluorescence of each cell type. Then the shift in the fluorescent signal could be detected. By determining the cell numbers in the control gate and the fluorescence positive gate the percentage of transduced cells were retrieved.

### **2.3.3.12 Sort**

On the day before sorting the sorter was sterilized with bleach.

The next morning the sorter was sterilized with ethanol, washed with sterile water and with medium. About  $1 \times 10^6$  cells were prepared in 3ml medium in a FACS-tube. The cells were used to set and calibrate the sorter. When set a pre-sort flow cytometric analysis was performed on the sorter and the gates set at which size or signal intensity cells should be sorted. The sorted cells were collected in a FACS-tube recording the number of sorted cells of the desired parameters. After each sort a flow cytometric analysis was recorded as well, checking the purity of the cells. Often cells were spun

down after sorting to concentrate them in a higher density and the cells were left usually a week or two to recover from the physical stress of sorting.

### **2.3.3.13 Test of Function**

To test the functionality of the Teton vector, 293T cells were co-transduced with the Teton and a tetO  $\beta$ -Gal virus. The tetO  $\beta$ -Gal plasmid contained a tetoperator sequence to which the tet activator, after induction by doxycycline could bind. This drove the expression of  $\beta$ -Galactosidase which converts X-Gal as a substrate into a blue dye. By this the amount of blue cells in the double transduction compared to controls gave an impression if the tet activator was expressed by the Teton vector.

This experiment was performed by Vasily Grinev, Minsk.

## **2.3.4 Methods Chapter 6 - Mouse work**

### **2.3.4.1 Handling**

Mice were handled according to the animal project license, number PPL60/3846. Animals were regularly checked for food and drink supply and any signs of distress or pain. If handled or procedures were carried out they were kept under a laminar flow hood using aseptic techniques to avoid infections in these immune deficient mice. Painful procedures were accompanied by anaesthesia, Carprofen injection and suffering animals were euthanatized.

## **2.3.4.2 Injections**

### **2.3.4.2.1 Intraperitoneal injection, i.p.**

The mouse was fixed by scruffing the loose skin at the nape of the neck and also the tail and the legs were restrained by holding them down with the small finger of the same hand. A needle with up to  $2 \times 10^7$  cells in  $400 \mu\text{l}$  was injected into one of the lower quadrants of the abdomen. The first resistance was overcome and the needle pushed deeper. Up to  $200 \mu\text{l}$  were injected slowly, ensuring that no sample backflow occurred after the needle was removed.

### **2.3.4.2.2 Intrafemoral injection, i.f.**

For intrafemoral injection mice were anaesthetized with isoflurane and the knee to be injected shaved. Through the knee, parallel to the femur and towards the hip an incision hole was made with a bigger needle by turning it slightly and then a thinner needle with the suspension was used to inject a small volume into the bone marrow. Mice were marked by ear clipping and were given Carprofen subcutaneously as an analgesic.

### **2.3.4.2.3 Intrahepatic injection, i.h.**

$5 \times 10^5$  SEM in  $30 \mu\text{l}$  PBS were prepared and kept on ice. Before use a Hamilton syringe was filled and kept bubble free. Two day old Newborn R2G mice were tightly scruffed. The Hamilton needle was injection in the middle of the body below the sternum and parallel to the body surface and moved under the skin above the liver. When the needle

was at the position of the liver, the needle was turned towards oneself so that the tip of the needle incised into the liver. 10µl were carefully and slowly injected. Animals were marked by ear marking and returned to their cage. Before and between each injection the Hamilton needle was flushed with PBS and ethanol.

### **2.3.4.3 Section of mice**

To harvest bone marrow, tumours and organs the mouse was sacrificed by cervical dislocation and weighed. The abdomen was opened with a vertical incision and the organs or tumour isolated and cut out and weighed and size measured. Tissues were washed with PBS and then either used for a cell harvest or fixed in formalin, stained and analysed by microscopy.

To retrieve the bone marrow the femurs and tibiae were removed from skin and muscles, the tips of the bones cut on each side and the bone marrow was flushed out by a needle with PBS. The bone marrow was then used for flow cytometric analysis.

Blood was taken either by the tail vein or by cardiac puncture of an anaesthetized mouse before sectioning it.

### **2.3.4.4 Cell harvest**

Tissues from organs were cut into small pieces and a shredder (BD, Medicon, sterile, 35µm) filled with it. The shredder was also filled with 1ml of medium and put into the Medimachine (Becton Dickinson). After some seconds of shredding the container was removed and opened to check if the tissue pieces were thoroughly homogenised. If so

medium with single cells was sucked out while carefully pipetting up and down. Usually cells retrieved from live organs were kept in 2% Pen/Strep, initially kept at a high concentration and monitored over a time or directly used for analysis.

### **2.3.4.5 Imaging**

For developing the imaging techniques culled mice were used. Several degrees of preparation were necessary. From furry, to shaved (hair clipper), to removed fur (Veet), to skinned and finally to muscles above bones removed.

Veet treatment allowed removing hairs with follicles, which also blocked light from going into the body and out of it. In principle this technique could also be applied to live animals, only regions with sensitive mucosa should be spared. Mice were shaved (hair clipper) and Veet was applied over the desired region with a gloved hand. After 5-10min the Veet and the hairs were washed off and the mice put into the imaging device. For mice injected with SEMcami cells (dsRed + GFP) white light for absorption and a green or a dual green, red filter for capturing were chosen.



## **Chapter 3**

### **Array analysis and validation**

# Chapter 3 Array analysis and validation

## 3.1 Introduction

The investigation of the transcriptional expression of a gene can elucidate its regulation. But how to identify such genes, which could be differentially expressed due to genetic events, such as mutations, translocations, deletions or amplifications?

Expression array analysis is a powerful tool to screen the global transcriptome expression which is differentially regulated due to a certain factor. It makes use of the hybridisation of nucleic acids, e.g. mRNA, to probes which have been synthesized complementary to sequences of any already sequenced mRNA and located at a certain spot representing a gene locus. Fluorescent labelling, for example of to be analysed transcripts, allows detection and quantification.

After identification of interesting genes, these can then be validated in more detail by analyses such as Western Blot, qRT-PCR or functional studies.

In 2005 a micro array platform enriched for leukaemic cDNA (cDNAs retrieved from leukaemic bone marrow) was developed to screen for differentially expressed transcripts with relevance to paediatric ALL. This analysis showed distinct gene expression patterns of several ALL subtypes, i.e. T-ALL, B-ALL and B-ALL with the *MLL/AF4* fusion. They stated that microarray analysis allows the identification of new genes involved in leukaemogenesis (De Pitta, Tombolan et al. 2005).

## 3.2 Aims

The aim of this section of my work was to identify possible target genes of MLL/AF4. The knockdown of a gene, in particular this fusion gene, is a convenient way of investigating its functions by detecting associated changes in global transcript expression. This was accomplished by cDNA - and oligo-Array analysis. Further validation of interesting and strongly affected genes substantiated these generated data. This validation relied on the knockdown of MLL/AF4 by RNAi and subsequent validation of the induced transcript level alterations by quantitative Real Time PCR analysis.

Specific aims:

1. To interrogate cDNA and oligo-array data from MLL/AF4 knockdown cells in order to identify putative direct and indirect transcriptional targets.
2. To validate changes in gene expression of putative MLL/AF4 targets using real-time PCR.

## 3.3 Results Array Analysis and validation

### 3.3.1 Array analysis

#### 3.3.1.1 Oligo array (Affimetrix U133 Plus 2.0) Ingenuity analysis

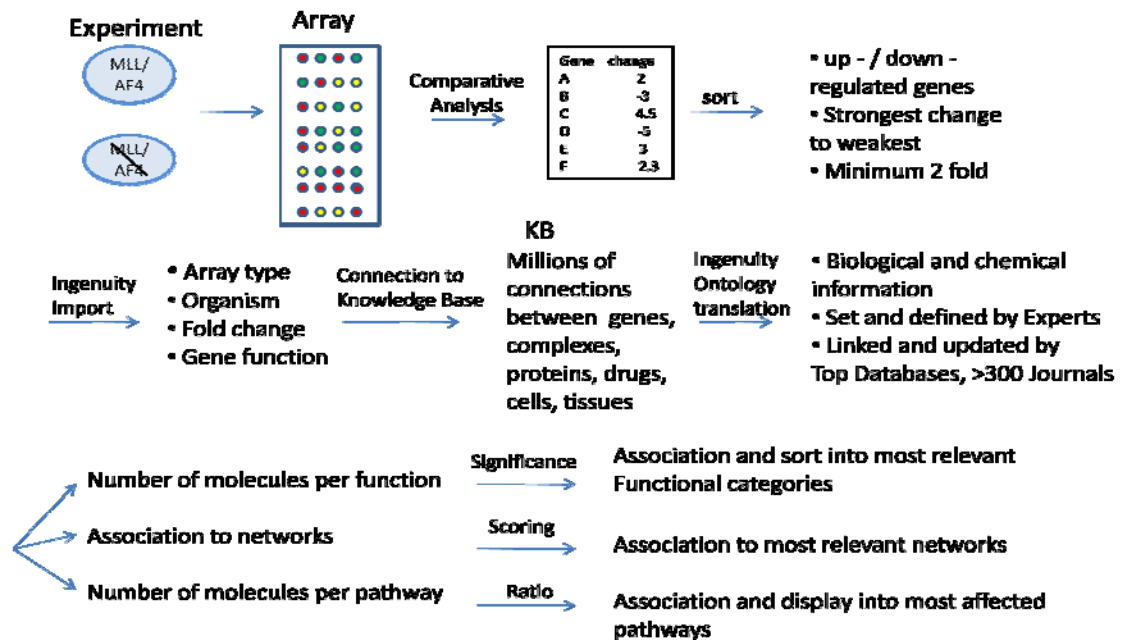


Figure 26 Flow chart of using Ingenuity Pathway Analysis for array data analysis

Flowchart how data have been handled from the experiment to the array, the array output and the processing in Ingenuity Pathway Analysis (IPA)

For the Affimetrix U133 Plus 2.0 Array SEM cells had been depleted of *MLL/AF4* for 2 days and isolated mRNA was used to perform the analysis. This experiment was performed by my predecessor Maria Thomas (Thomas, Gessner et al. 2005). To introduce the generated data into the Ingenuity Pathway analysis the array data were sorted for strongest change and a minimum fold change of 2.

The Ingenuity Knowledge Base (KB) is the basis of all Ingenuity Pathway analyses and it is the largest knowledge base of its kind. It comprises millions of connections between genes, complexes, proteins, drugs, cells, tissues and diseases. These data are further translated into correlated functions by Ingenuity Ontology also integrating biological and chemical information. Several parameters such as species, tissue context and direction of change can be selected. The type of connection can be specified such as molecular, cellular and organism specific. Ingenuity is most up to date by weekly input from experts including experimentally demonstrated findings from full text journals covering more than 300 top journals. The sources of databases include Entrez gene, RefSeq, OMIM, GWAS Database, Gene ontology, KEEG and many more.

The Ingenuity Pathway analysis connected the MLL/AF4 depletion responsive genes (transcripts) to functions, diseases, physiological systems, networks and canonical pathways (see Figure 26).

The functional analysis of an expression dataset shows biologically most important functions connected to those data. The 500 top functions are displayed if they have a p-value smaller than 0.05. Functional Analysis comprises 3 main categories: “*Molecular and Cellular Function*”, “*Physiological System Development and Function*” and “*Diseases and Disorders*”. These 3 categories are subdivided hierarchically into more than 85 subcategories, defined as “*high level functional categories*”, of which each has several specified subgroups, termed “*low level functions*” and “*lowest level functions*”. One such hierarchy would be cancer – haematological disease – leukaemia.

The statistical probability that altered transcription levels from the array analysis have a connection to a function, process or physiological pathway is calculated with the right tailed Fisher exact test. The bigger the p-value is, the greater is the chance that this

connection is due to random chance. Here, p-values smaller than 0.05 are considered as statistically significant and the association as non random. The right tailed Fisher exact test uses the number of molecules participating in that function and the total number of molecules associated in that function to calculate this p-value. In the case that a high level function comprises for two or more specific functions a range of significances is generated. The top 5 high level functions of the several main categories are those with the lowest p-value or p-value range, representing the top 5 categories with the highest significance.

The following tables show these sorted results.

<b>Diseases and Disorders</b>	<b>p-value</b>	<b># Molecules</b>
Cancer	2.02E-19 - 5.11E-03	456
Skeletal and Muscular Disorders	1.35E-13 - 3.95E-03	440
Reproductive System Disease	8.03E-10 - 5.11E-03	282
Inflammatory Disease	1.11E-09 - 4.64E-03	412
Genetic Disorder	1.99E-09 - 4.83E-03	899

Table 2 Oligo-array Ingenuity analysis: The top 5 subcategories of Diseases and Disorders sorted on p-value, generated using Ingenuity Pathway Analysis; Ingenuity Systems Inc.

In the category “*Diseases and Disorders*” (Table 2) “*Cancer*” was the most significant disease; connected to 456 affected molecules on the array. “*Diseases and Disorders*” is one of the 3 main functional categories. The high level function “*Cancer*” is defined as a cancer associated function, such as transformation or metastasis. It could also show a connection to tumours, cancer cells or cancer tissue. This function is a very sensible and expectable finding.

With 440 involved molecules the second top high level function is “*Skeletal and Muscular Disorders*” which includes diseases and abnormalities in the skeletal and muscular system. It may not be very obvious how a leukaemic fusion protein contributes to genes involved in those diseases, but as several cell types involved in skeletal diseases such as osteoblasts and fibroblasts, are important in the interactions with both haematopoietic and leukaemic stem cells, this category may show an influence of those cell types. Additionally, the cytoskeleton could contribute to these categories, which is required for functions as migration and homing.

The third high level function “*Diseases and Disorders*” is “*Reproductive System Disease*” with 282 affected molecules, and categorizes diseases and abnormalities of the reproductive system. Again the link to leukaemia is not clear; possibly stemness and self-renewal capacity genes associated with reproductive cell types (De Felici, Farini et al. 2009; Golestaneh, Beauchamp et al. 2009) might provide a link to leukemia.

Furthermore, 412 molecules comprise the forth category “*Inflammatory Disease*”. The association with inflammatory diseases may contribute to the involvement of immune defence cells in inflammatory responses (Luster, Alon et al. 2005) as well as an interferon response to the siRNA treatment (Reynolds, Anderson et al. 2006) which will be discussed later.

Finally, the 5<sup>th</sup> of 5 top categories is “*Genetic Disorder*” with 899 related molecules, including diseases and disorders resulting from genetic defects. As *MLL/AF4* is a genetic lesion itself and as several leukaemia types are caused or promoted by genetic disorders, such as trisomy 21(Pui, Robison et al. 2008), the depletion of *MLL/AF4* probably generates the gene pattern comprised by this category.

The 5 most significant molecular and cellular functions connected to this array were cellular growth and proliferation, followed by cell death, cellular movement, cell to cell signalling and interaction and finally cell morphology (see Table 3).

<b>Molecular and Cellular Functions</b>	<b>p-value</b>	<b># Molecules</b>
Cellular Growth and Proliferation	3.72E-15 - 5.11E-03	325
Cell Death	5.34E-11 - 5.11E-03	271
Cellular Movement	8.03E-11 - 4.50E-03	182
Cell-To-Cell Signalling and Interaction	2.32E-10 - 5.11E-03	232
Cell Morphology	7.24E-08 - 4.68E-03	87

Table 3 Oligo-array Ingenuity analysis: The top 5 of Molecular and Cellular Functions sorted on p-value generated using Ingenuity Pathway Analysis; Ingenuity Systems Inc.

With 325 affected molecules i.e. *IGFBP5*, “*Cellular Growth and Proliferation*” is the most significant “*Molecular and Cellular Function*” describing functions associated with the growth and the proliferation of cells. As this is one of the main properties of cancer in general it links nicely to leukaemia (Table 3).

“*Cell Death*” as the the second category is also coherent with leukaemia, as modulation of cell death factors helps leukaemic cells to resist apoptotic stimuli. 271 molecules associated with this category i.e. *MAP2K5*, were found to be affected on the array.

On the 3<sup>rd</sup> place is “*Cellular Movement*”, with 182 affected molecules i.e. *KITLG*. It associates to movement and localization of cells. Amongst affiliated processes are immune cell connected processes such as chemotaxis, rearrangement, transmigration of cells but also cancer associated infiltration.

“*Cell-To-Cell Signalling and Interaction*”, the fourth of five top functions comprises 232 affected molecules, i.e. *IL8*, linked to intercellular interactions like communication,



stimulation, binding detachment and more specifically intercellular junction components. These processes are also most important for immune cells and for interactions of haematopoietic cells with niche environments.

Finally the fifth group “*Cell Morphology*” with 87 involved molecules, i.e. TNC, includes associated processes such as cell size, transformation of cells, enlargement and fluidity, i.e. remodelling of the cytoskeleton. Again this is linked to immune cell processes and niche interactions.

Table 4 shows the last main function category top 5 summary

<b>Physiological System Development and Function</b>	<b>p-value</b>	<b># Molecules</b>
Tissue Development	1.13E-08 – 5.11E-03	131
Hematological System Development and Function	1.85E-07 – 5.11E-03	140
Lymphoid Tissue Structure and Development	6.80E-07 – 1.93E-03	14
Immune Cell Trafficking	1.46E-06 – 4.31E-03	60
Haematopoiesis	5.46E-06 – 5.11E-03	59

Table 4 Oligo-array Ingenuity analysis: The top 5 of Physiological System Development and Function sorted on p-value, generated using Ingenuity Pathway Analysis; Ingenuity Systems Inc.

Above it is shown that amongst the 5 top “*Physiological Systemic Developments and Function*” categories “*Tissue Development*” is followed by “*Haematological System Development and Function*”, “*Lymphoid Structure and Development*” and “*Immune Cell Trafficking and Haematopoiesis*” (see Table 4).

With 131 involved molecules “*Tissue Development*” comprises functions associated to normal development and differentiation of tissues as well as the formation of tissue

through the association of cells. These include survival of tissue, accumulation and adhesion of cells.

Secondly, “*Hematological System Development*” and Function with 140 affected molecules, associates functions to “normal development and function of cells, tissues and organs that make up the hematological system as well as functions specific to the hematological system”.

The 3<sup>rd</sup> top “*Physiological Systemic Development and Function*” category is “*Lymphoid Tissue Structure and Development*”, with 14 involved molecules. It describes links to “physical structure of immune organs including vasculature and sub-organ tissue organization and the processes of their formation”.

“*Immune Cell Trafficking*” ranks forth and includes 60 altered molecules describing movement-associated functions for all cell types. Some examples are accumulation, activation, adhesion, cell-cell adhesion, cell movement, chemoattraction, chemokinesis, delay in infiltration, delay in migration, homing, localization, migration, mobilization, and transdifferentiation.

Finally, there is “*Haematopoiesis*” with 59 altered molecules. It is restricted to lymphocytes, myeloid and mesenchymal cell types and their subclasses linked to processes associated with haematopoiesis.

The next type of analysis is the IPA network generation (see Figure 27). A set of molecules, defined by the array analysis that interacts with other molecules in the Ingenuity Knowledge base, is identified as “*Network Eligible Molecules*”. These are combined into networks to maximize the interconnectedness of each molecule to all. Smaller networks are connected to larger ones by using additional molecules from the

Ingenuity Knowledge base with maximally 35 molecules per network. The scoring uses the number of network eligible molecules” in the network and ranks networks according to their degree of relevance. Besides the number of network eligible molecules in the network, it uses its size, the total number of Network Eligible molecules analyzed and the total number of molecules in the Knowledge Base which could be included in the network. For calculation of the hypergeometric distributed score the Fisher’s right tailed Exact test is used.

To exemplify the scoring, a network of 35 molecules is supposed with a Fisher’s exact test result of  $p=1 \times 10^{-6}$ . By calculating the negative logarithm of this value the network score of 6 is generated. This score shows how each network fits to the network eligible molecules (descriptions of IPA computational processes are based on quotations of the IPA manual) (Figure 27).

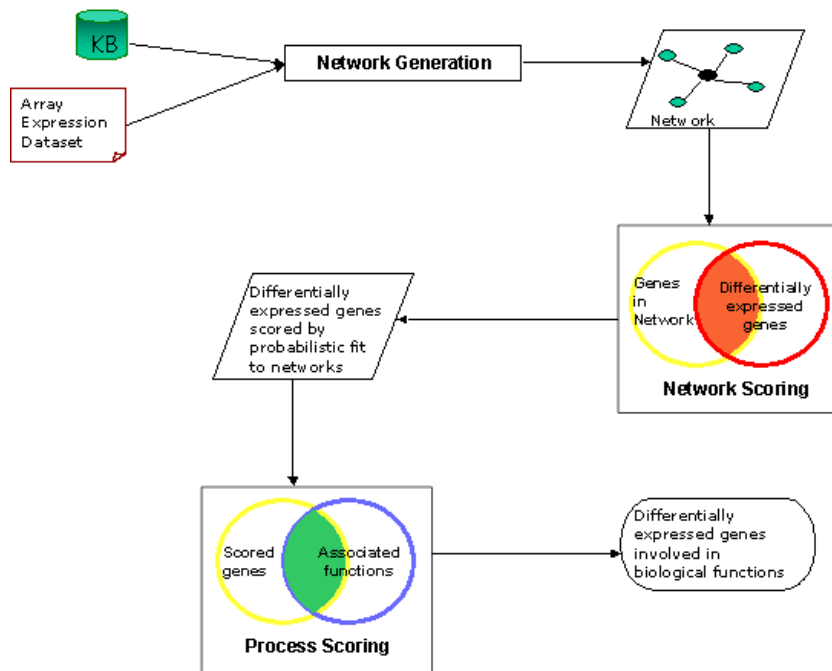


Figure 27 IPA Network Generation, Ingenuity Feature descriptions generated using Ingenuity Pathway Analysis; Ingenuity Systems Inc.

The next table (Table 5) lists associated network functions that are linked to altered genes on the oligo array. Interestingly the highest score is found for “*Cancer, Endocrine System Development and Function, Small Molecule Biochemistry*”, and the second highest for “*Cellular Movement, Skeletal and Muscular System Development and Function, Cellular Growth and Proliferation*”.

But also the other network functions give interesting information about the connection of the affected genes.

	<b>Associated Network Functions</b>	<b>Score</b>
1	Cancer, Endocrine System Development and Function, Small Molecule Biochemistry	26
2	Cellular Movement, Skeletal and Muscular System Development and Function, Cellular Growth and Proliferation	24
3	Behaviour, Reproductive System Development and Function, Infection Mechanism	22
4	Cellular Movement, Inflammatory Response, Cell-To-Cell Signalling and Interaction	21
5	Cell-To-Cell Signalling and Interaction, Cellular Growth and Proliferation, Hematological System Development and Function	18

Table 5 Oligo-array Ingenuity analysis: The top 5 of Associated Network Functions sorted on scoring, generated using Ingenuity Pathway Analysis; Ingenuity Systems Inc.

Each of the networks is called after the 3 top high level functions it is containing. The network scored at the highest, 26, is “*Cancer, Endocrine System development and Function, Small Molecule Biochemistry*”. This network seems to comprise cancer signalling functions, which is clearly relevant in leukaemia (Table 5).

The second network with a score of 24 is “*Cellular Movement, Skeletal and Muscular System Development and Function, Cellular growth and Proliferation*”. The probable link to leukaemia is the niche context.

Thirdly, with a score of 22, the network “*Behaviour, Reproductive System Development and Function, Infection Mechanism*” is found. Behaviour in this context means functions of multi-cellular organisms associated with behaviour such as feeding. Infection mechanism includes processes associated with organismic response to virus infections. This network may contribute to the stemness, developmental and B-cell related genes affected by MLL/AF4.

“*Cellular Movement, Inflammatory Response, Cell-To-Cell Signalling and Interaction*” is the next network, scoring with 21. It shows some functions associated with immune cell behaviour.

The last network category is “*Cell-To-Cell Signalling and Interaction, Cellular Growth and Proliferation, Hematological System Development and Function*” and links strongly to leukemic cell functions.

In the pathway analysis the dataset of altered genes on the array is linked to canonical pathways by the ratio which is the number of genes affected per total number of genes in that pathway, and the significance via the p-value, which describes if the association between a specific pathway and the altered array genes is likely.

The smaller the p-value, the more significant the association. The ratio mainly tells which pathways were most affected i.e. illustrated by percentage of altered genes in that pathway.

However, the judgment how a pathway is modulated has to be made by considering the effect of the altered gene in that pathway. For example, if inhibitors are up-regulated and activating parts are down-regulated then a pathway would be considered as down-regulated.

In the following table, (Table 6) a list of the 16 most significant canonical pathways correlated to the oligo array data is displayed.

<b>Ingenuity Canonical Pathways</b>	<b>-log (p-value)</b>	<b>Ratio</b>	<b>altered genes / total</b>
Hepatic Fibrosis / Hepatic Stellate Cell Activation	4.44	0.23	30/ 128
G-Protein Coupled Receptor Signalling	3.11	0.18	38/ 210
Coagulation System	2.97	0.30	11/ 37
cAMP-mediated Signalling	2.57	0.19	29/ 157
Macrophages, Fibroblasts and Endothelial Cells in Rheumatoid Arthritis	2.41	0.15	48/ 313
Metabolism/ Xenobiotics by Cytochrome P450	2.38	0.19	18/ 97
Complement System	2.17	0.27	9/ 34
Role/ Cytokines in Mediating Communication between Immune Cells	2.04	0.23	12/ 52
LPS/IL-1 Mediated Inhibition/ RXR Function	2.03	0.16	31/ 197
Acute Phase Response Signalling	2.02	0.17	29/ 173
Wnt/ $\beta$ -catenin Signalling	2.01	0.17	28/ 166
VDR/RXR Activation	2.00	0.21	16/ 78
Communication between Innate and Adaptive Immune Cells	1.94	0.19	14/ 75
Pathogenesis/ Multiple Sclerosis	1.91	0.44	4/ 9
Serotonin Receptor Signalling	1.83	0.24	8/ 33
LXR/RXR Activation	1.83	0.18	14/ 76

Table 6 Oligo-array Ingenuity analysis: The 16 most significant Canonical pathways sorted on p-value, generated using Ingenuity Pathway Analysis; Ingenuity Systems Inc.

The top canonical pathway sorted by significance is “*Hepatic Fibrosis / Hepatic Stellate Cell Activation*” (Table 6). Of 128 genes associated to that pathway, 30 are affected by MLL/AF4. In the pathway array related genes like *FGF1*, *FGF2*, *FGFR1*, *FGFR2*, *IGF1*, *EGF* and *IL-6R* are found. These genes probably explain why this pathway was scored despite hepatic cells not being related to leukaemia.

The pathways “*G-Protein Coupled Receptor Signalling*” (2<sup>nd</sup>), “*cAMP-mediated Signalling*” (4<sup>th</sup>) are generally important pathways in a huge number of signalling events. “*Coagulation System*” (3<sup>rd</sup>) and “*Complement System*” (7<sup>th</sup>) pathways are mostly linked to leukaemia by their haematological functions.

The “*Macrophages, Fibroblasts and Endothelial Cells in Rheumatoid Arthritis*” pathway may show stromal and inflammatory gene patterns.

“*Role/ Cytokines in Mediating Communication between Immune Cells*” (8<sup>th</sup>), “*Communication between Innate and Adaptive Immune Cells*” (9<sup>th</sup>) and “*LPS/IL-1 Mediated Inhibition/ RXR Function*” (13<sup>th</sup>) pathways are mainly describing immune system functions and those may contribute to leukaemia.

The “*Metabolism/ Xenobiotics by Cytochrome P450*” pathway (6<sup>th</sup>) could help MLL/AF4 positive cells to survive chemotherapy by metabolizing these agents.

“*Wnt/β-catenin Signalling*” (11<sup>th</sup>), “*VDR/RXR Activation*” (12<sup>th</sup>) and “*LXR/RXR Activation*” (16<sup>th</sup>) are very important signalling pathways which can be leukaemogenic processes like growth, survival and niche interactions.

In summary there are many signalling pathways affected that regulate cellular processes, but also pathology-associated pathways such as inflammation related pathways linked to fibrosis, arthritis, sclerosis, acute phase signalling. As previously mentioned, it is possible that this is due to siRNA mediated interferon response or an effect of MLL/AF4 knockdown affected genes. This issue will be discussed more thoroughly in the discussion.

A different way of displaying this data was chosen for the next pie chart. The pathways were sorted on the ratios (the number of genes affected per total number of genes in that pathway, Figure 28).

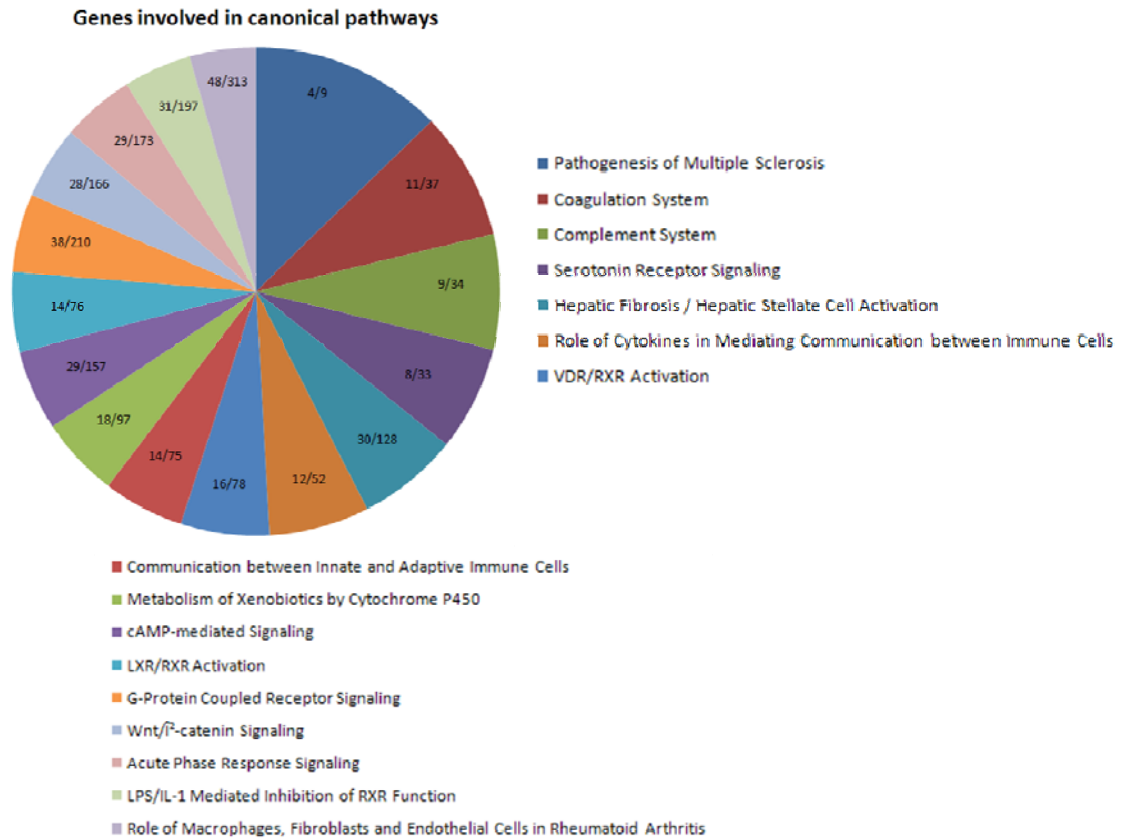


Figure 28 Pie chart of canonical pathways

sorted on ratios of altered genes from the array to total number of genes per pathway, generated using Ingenuity Pathway Analysis; Ingenuity Systems Inc.

The sort by ratio slightly changes the order of the top pathways (Figure 28). Two of the strongest affected pathways are Coagulation System and Complement System with 11 of 37 and 9 of 34 genes involved, respectively. Both pathways link to the innate immune system functions such as chemotaxis and vascular permeability. Here, the signalling pathways and the inflammatory pathways dominate.

Both ways of sorting the pathways use relatively high ratios and high significances informative and are equally.



The following schemes illustrate altered genes on the oligo-array in the most significant canonical pathways from the Table 6.

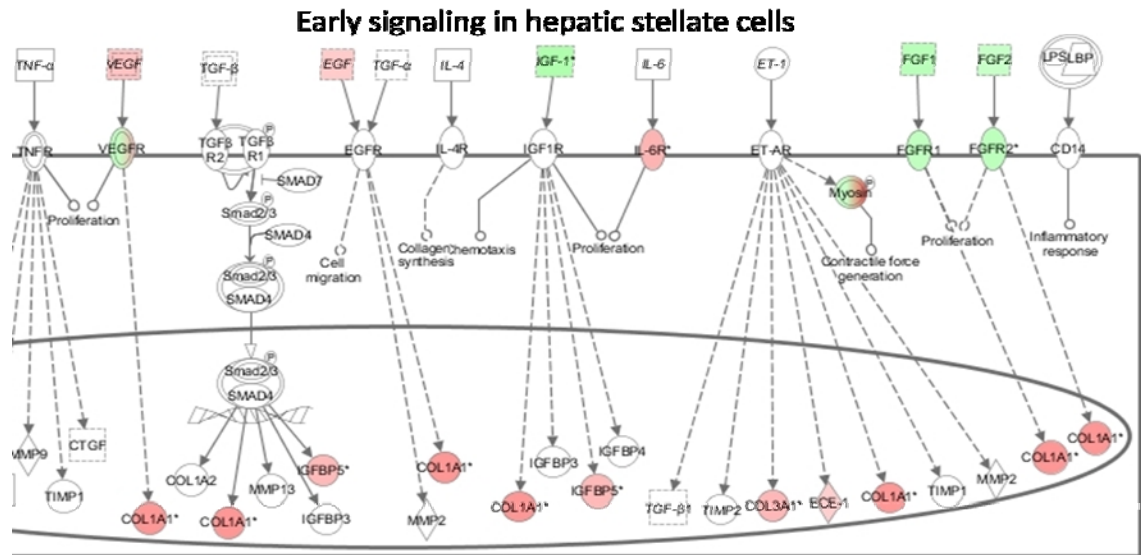


Figure 29 Early signalling in hepatic stellate cells

Oligo-array Ingenuity canonical pathway analysis, scheme of pathway: Early signalling in hepatic stellate cells, colours indicate gene up/down-regulated on array: Red: strongly up-regulated, light red: up-regulated, green: down-regulated, green-red: various family members differentially expressed, generated using Ingenuity Pathway Analysis; Ingenuity Systems Inc.

The scheme above (Figure 29) shows the illustration of the canonical pathway “*Early signalling events in hepatic stellate cells*”. Here it is shown that the knockdown of MLL/AF4 had an influence on VEGF receptor which is regulating proliferation, the EGF / EGFR pathway which is involved in cell migration, on the IGF1 receptor via IGF1 and in FGFR1/2 and its ligands FGF1/2 and its ligands FGF1/2 as well which are involved in proliferation amongst others.

The next 2 pathways the “G-protein signalling” (Figure 30) and “cAMP mediated signalling” (Figure 31) both show the involvement of MKP1/2/3/4 (MAP Kinase Phosphatase). One example of those found on the array is *DUSP6*. Both pathways also show the involvement of CREB. and comprise very important cell regulation systems

like MAPK and ERK which signalling regulate manifold processes in a cell. But also important regulators like NF- $\kappa$ B and I $\kappa$ B are affected. “*G-protein coupled signalling*” and (Figure 30) “*cAMP mediated signalling*” (Figure 31) are connected to diverse pathways and regulative systems in the cell.

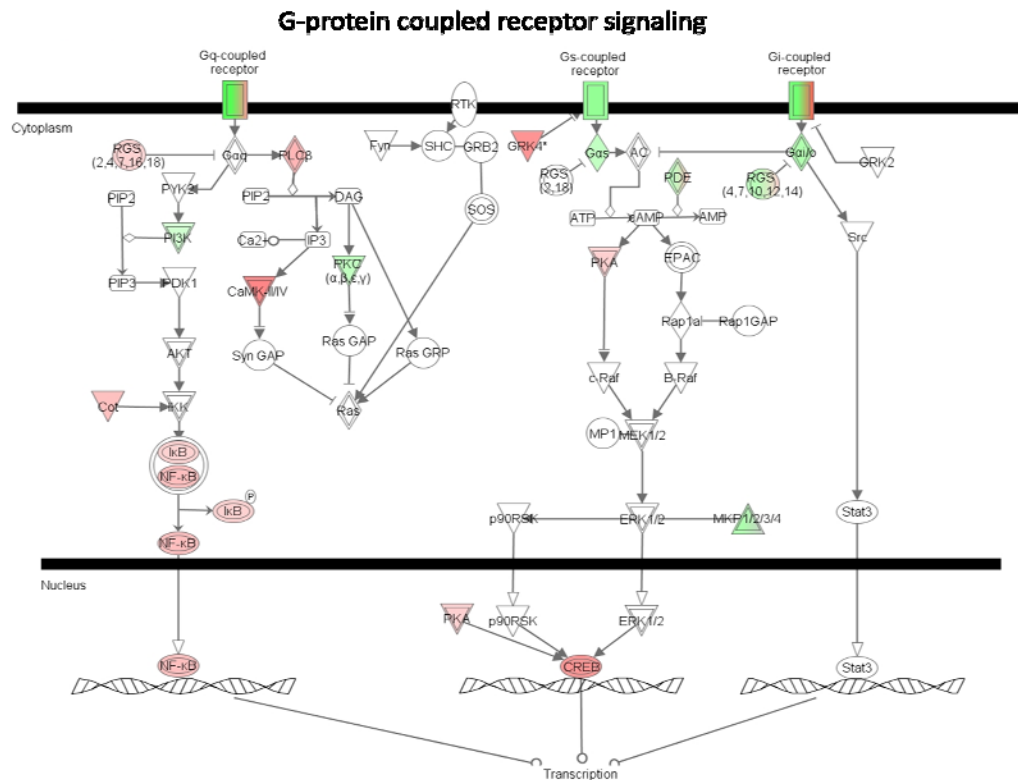


Figure 30 G-protein coupled receptor signalling

Oligo-array Ingenuity canonical pathway analysis, scheme of pathway: G-protein coupled receptor signalling; colours indicate gene up/down-regulated on array: Red: strongly up-regulated, light red: up-regulated, green down-regulated, green-red: various family members differentially expressed, generated using Ingenuity Pathway Analysis; Ingenuity Systems Inc.





LEF/TCF transcription factor is additionally affected by the TGF $\beta$ R family member *ACVR1B*, which is also altered on the array.

### Role of Oct4 in mammalian embryonic stem cell pluripotency

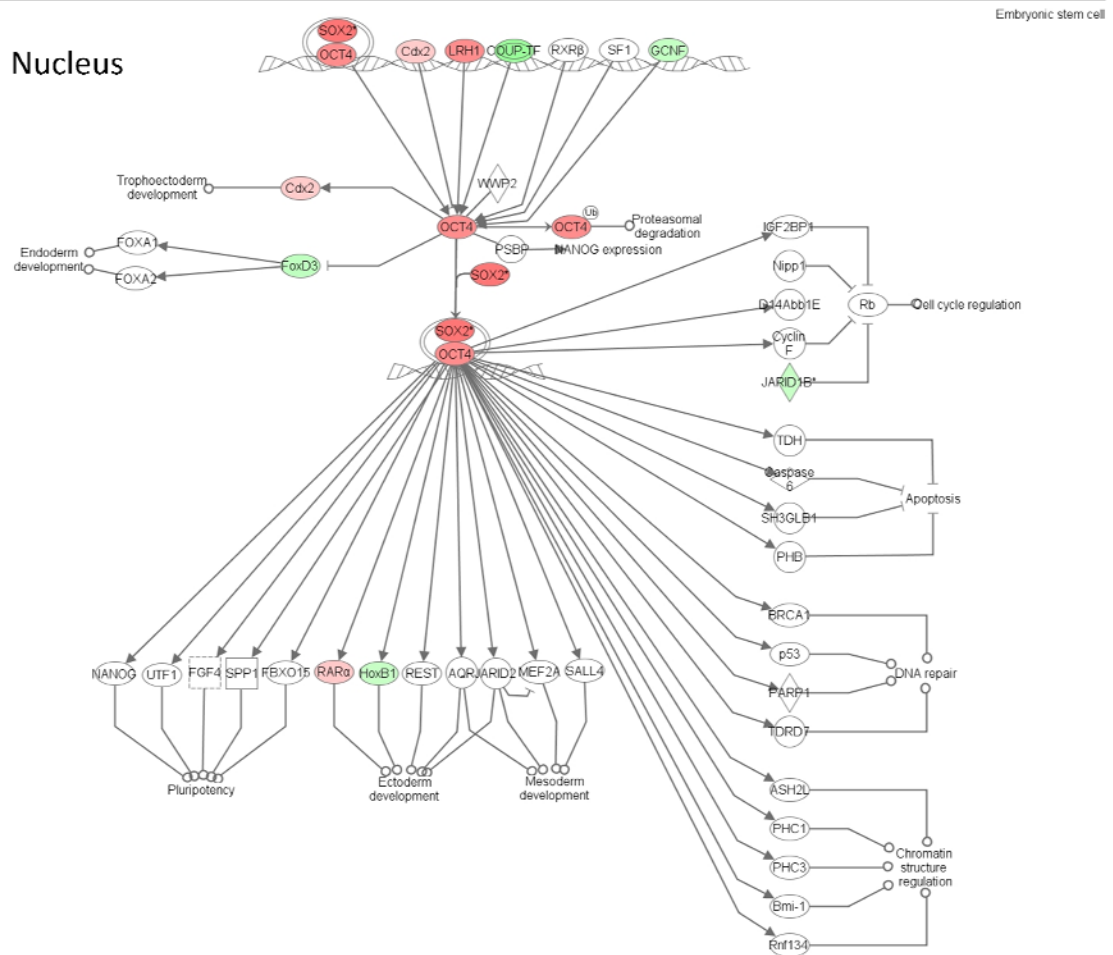


Figure 33 Role of Oct4 in Mammalian embryonic stem cell pluripotency

Oligo-array Ingenuity canonical pathway analysis. scheme of pathway: Role of Oct4 in Mammalian embryonic stem cell pluripotency, colours indicate gene up/down-regulated on array: Red: strongly up-regulated, light red: up-regulated, green down-regulated, green-red: various family members differentially expressed, generated using Ingenuity Pathway Analysis; Ingenuity Systems Inc.

The pathway “Role of OCT4 in mammalian embryonic stem cell pluripotency” (Figure 33) shows genes influencing OCT4. OCT4 is also known to play a role in the haematopoietic stem cell regulation. Amongst the influenced genes are *OCT4*, *SOX2*,

*RAR $\alpha$*  and *HOXB1*. OCT4 signalling regulates processes such as cell cycle, apoptosis, DNA repair, chromatin structure regulation and pluripotency.

Already in the previous pathways RXR was mentioned. RXR is very important in the vitamin D induced regulation. The following pathway “*VDR/ RXR activation*” (Figure 34) shows MLL/AF4 depletion sensitive genes such as *PKC*, *RXR* and *VDR* which regulate processes such as calcium homeostasis, cell differentiation, growth regulation, bone metabolism and cell proliferation.

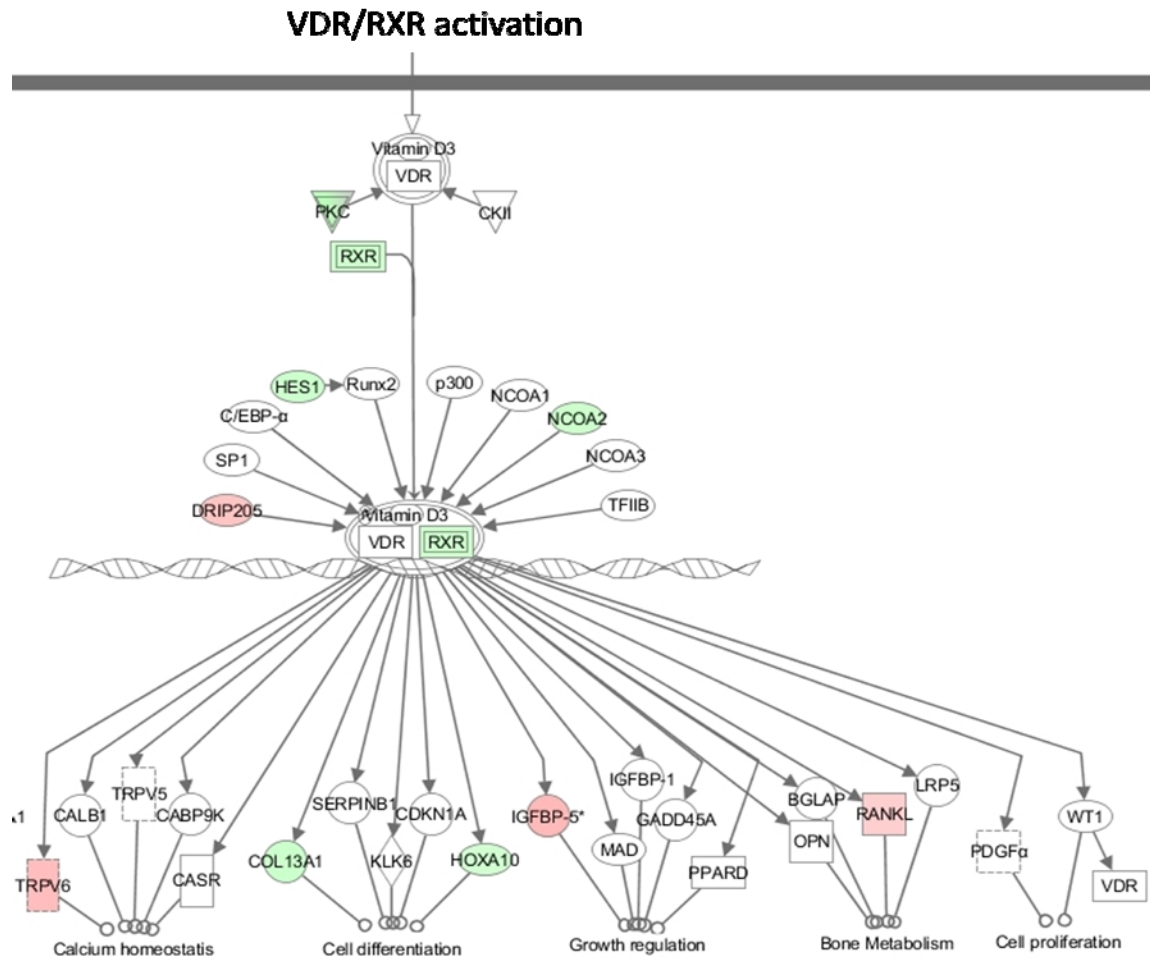


Figure 34 VDR / RXR activation

Oligo-array Ingenuity canonical pathway analysis. scheme of pathway: VDR / RXR activation, colours indicate gene up/down-regulated on array: Red: strongly up-regulated, light red: up-regulated, green down-regulated, green-red: various family members differentially expressed, generated using Ingenuity Pathway Analysis; Ingenuity Systems Inc.

### 3.3.1.2 Array comparison and validation of possible target genes

The depletion of the target fusion gene *MLL/AF4*, used in both array analyses was confirmed by Real Time-PCR and the conformation of *MLL/AF4* depletion was a prerequisite for all experiments relying on the depletion of the fusion gene.

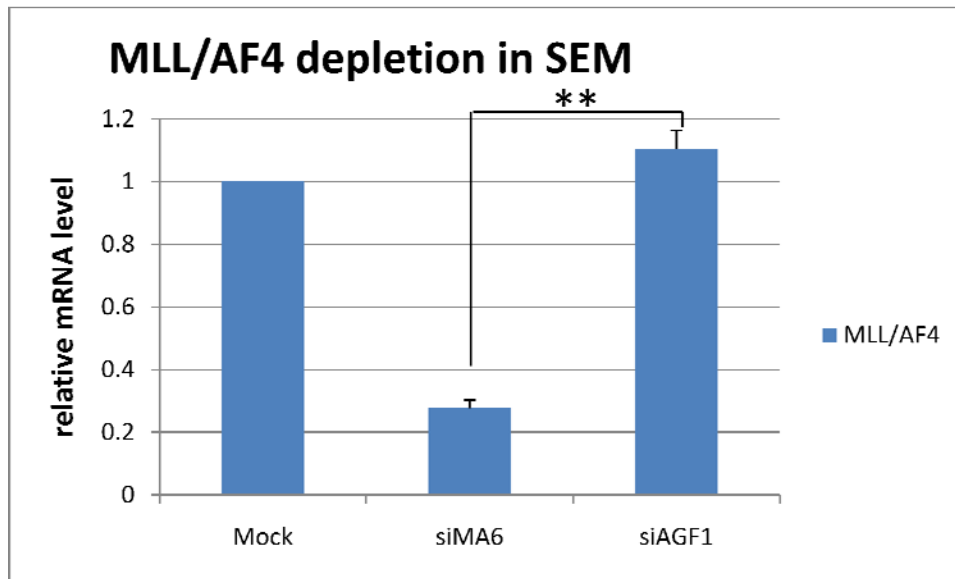


Figure 35 *MLL/AF4* depletion in SEM

*MLL/AF4* transcript qRT-PCR analysis after *MLL/AF4* knockdown in SEM for 96h. Mock: electroporated without siRNA, siMA6: anti *MLL/AF4* siRNA siAGF1: active siRNA control. Shown are relative mRNA expression levels and averages of 3 independent experiments. Error bars show SD values. The knockdown of *MLL/AF4* transcript was highly statistically significant with  $p = 0.003$  (Students t-test).

The 70% knockdown of *MLL/AF4* in SEM was found to be highly statistically significant with a p-value of 0.003 as determined by Students t-test (Figure 35). The siRNA targeting the fusion transcript in SEM was siMA6. Due to several breakpoints in the fusion region *MLL/AF4* transcripts differ between the t(4;11) positive cell lines SEM, RS4;11 and MV4;11. The electroporation control was Mock, which was performed in parallel to the other samples but without siRNA and which was usually set to 1. Conversely, the siAGF1 control is an active siRNA against the fusion gene *AML/MTG8*, a fusion gene not present in the cell line SEM. This was found to be a suitable siRNA control for *MLL/AF4* knockdown and due to its proven activity in cell lines carrying *AML/MTG8* to be superior to scrambled siRNA controls.

The two array data sets from the oligo- and the cDNA array sorted for genes with more than 2 fold change and a p-value higher than 0.05 were compared for concordance (Table 7). The tables of the genes found in cDNA and oligo array analysis are shown in



the appendix. The following list of genes validated by qRT-PCR summarizes these candidates.

Gene	Function	Direction
ATP2B3	Ca <sup>2+</sup> Homeostasis	down
BNIP3	pro-apoptotic, regulation of apoptosis	down
CD69	proliferation, signal transmitting receptor in lymphocytes	down
DAAM1	regulation of cytoskeleton structure	up
DCT	regulates neural progenitor cell proliferation	down
DUSP6	negative regulate members of (MAP) kinase superfamily	down
ECE1	procession of endothelin1	down
FGFR1	regulation of mitogenesis and differentiation	down
FLJ13639	metabolism resulting in cell growth	down
GLEIL	RNA nuclear export	down
NAP1L4	histone chaperone	down
PLAT	cell migration and tissue remodeling	down
PRDM2	tumour suppressor, methylates H3K9	down
SCD	regulation of cell growth and differentiation	down
SLC16A3	monocyclic acid transporter	down
TRIM31	unknown function	down

Table 7 Genes overlapping in cDNA- and oligo array analysis of MLL/AF4 depleted leukaemic SEM cells

As mentioned also data from a cDNA array were available. Here, *MLL/AF4* was depleted in SEM cells for a period of 144h. The most significantly changed genes from the cDNA array were validated by qRT-PCR for which primers were designed. The generated amplicons were checked by DNA-PAGE analysis. All 3 data sets, from the oligo array, the cDNA array and qRT-PCR were compared for concordance of their effects, meaning up or down regulation. Only a restricted number of genes were analyzed by all 3: oligo, cDNA array and qRT-PCR.

Following diagrams show the fold changes of these (Figure 36 A, B and C).

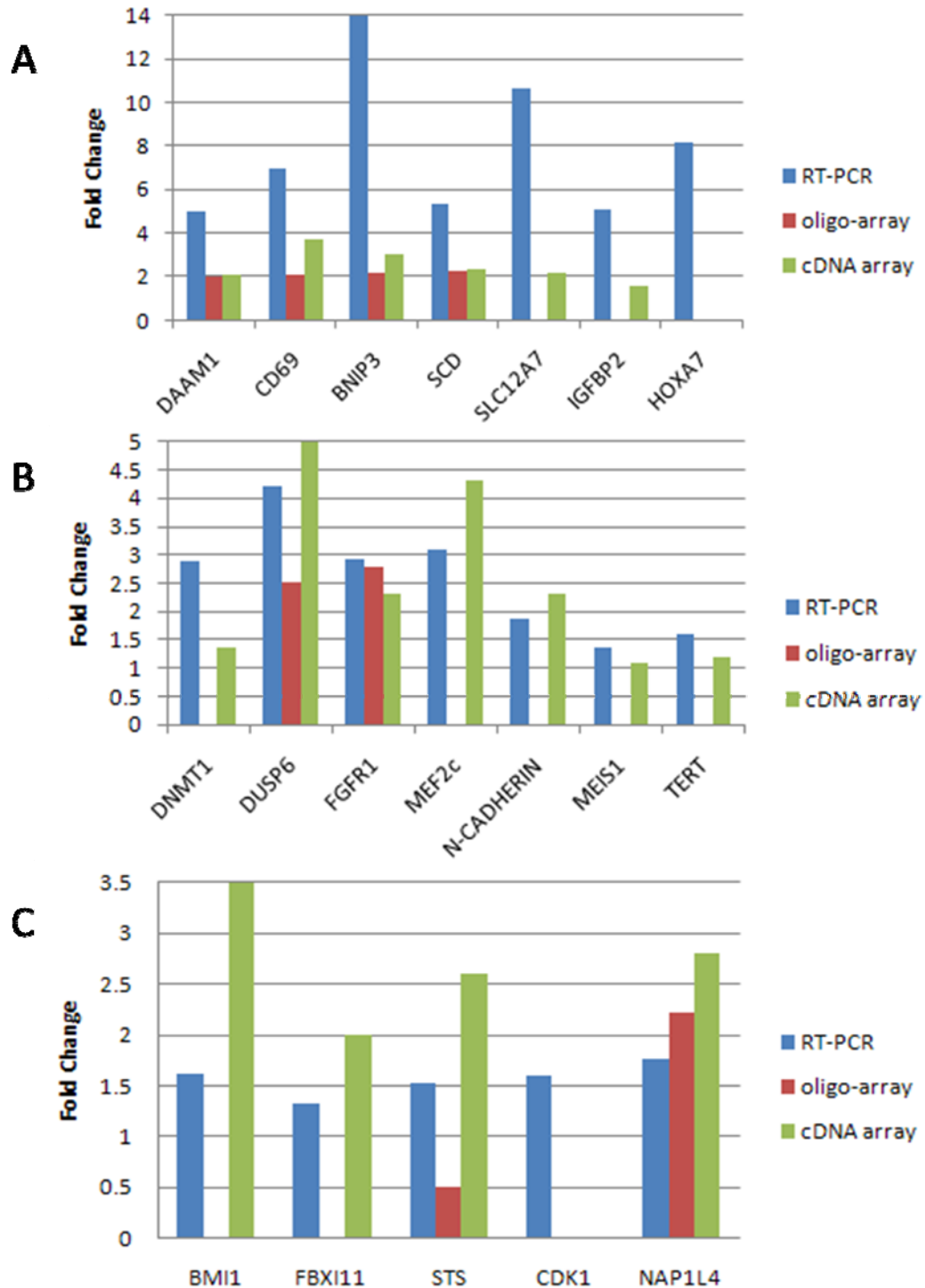


Figure 36 Genes affected by MLL/AF4 Knockdown

Comparison of fold change of genes in oligo-array, cDNA-array and qRT-PCR (A) Panel of genes with high fold changes in expression up to 14 times, *DAAMI* was upregulated, all other transcripts were downregulated upon MLL/AF4 depletion (B) Panel of genes with intermediate fold changes up to 5 times (C) Panel of genes with lower fold change up to 3.5 times Blue: qRT-PCR, Red: fold change on oligo-array and Green: cDNA array; missing columns represent genes not covered by all 3, qRT-PCR, cDNA - and oligo array.

This comparison shows a good concordance of the compared genes. Genes down-regulated (all of the shown except *DAAMI* which was upregulated) were found down-regulated in all 3 assays if included. The data from the qRT-PCR tended to have a stronger fold change than the array data.

Two of those genes which were strongly altered in qRT-PCR are shown below (Figure 37). *DAAMI*, which is involved in the cytoskeleton amongst other functions, was strongly up-regulated. *BNIP3* involved in processes such as apoptosis, was found strongly down-regulated.

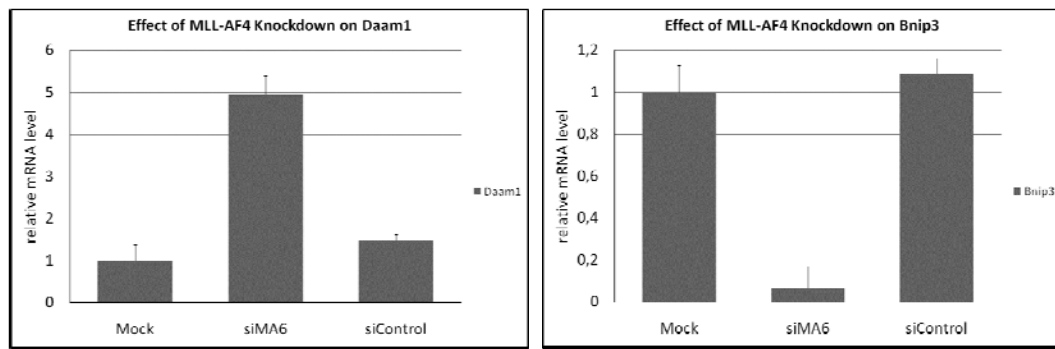


Figure 37 qRT-PCR validation of *DAAMI* and *BNIP3*

qRT-PCR transcript analysis after MLL/AF4 knockdown in SEM for 48h. (Left diagram) relative expression levels of *DAAMI* (Right diagram) relative expression levels of *BNIP3*. Shown are triplicates of one single representative experiment. Mock: electroporated without siRNA, siMA6: anti *MLL/AF4* siRNA siControl: control siRNA

Next, possible target genes of MLL/AF4 were investigated by determining their mRNA levels in comparison to the controls. This was based on the thought that if other transcripts levels change consistently due to the depletion of MLL/AF4, they may be influenced directly or indirectly by MLL/AF4. Because MLL/AF4 contains transcript factor properties it can be assumed that genes downstream of *MLL/AF4* underlie its regulation.

One of this proposed target genes already found on both arrays is *DUSP6*.

DUSP6 is a dual specificity protein phosphatase which inactivates its target kinases by dephosphorylation. These cytoplasmic kinases are involved in pathways such as MEK/ERK. Thus DUSP6 is known to regulate proliferation and differentiation.

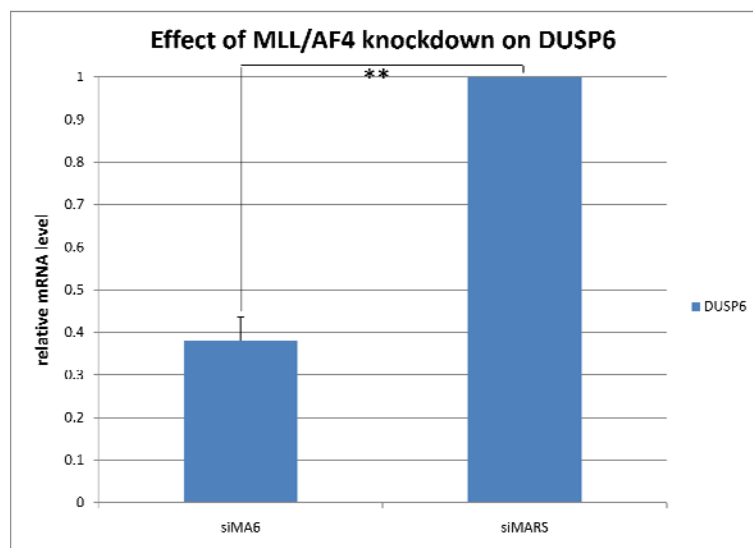


Figure 38 *DUSP6* expression analysis

*DUSP6* transcript qRT-PCR analysis after MLL/AF4 knockdown in SEM for 96h. siMA6: anti *MLL/AF4* siRNA, siMARS: siRNA control. Shown are relative mRNA expression levels of *DUSP6* and averages of 3 independent experiments. Error bars show SD values. The knockdown of *DUSP6* transcript was highly statistically significant with  $p = 0.0026$  (paired student's t-test).

Following depletion of MLL/AF4, qRT-PCR analysis showed more than 50% depletion of *DUSP6* with  $p = 0.0026$  (Figure 38). The data were normalised to the siRNA control siMARS. Like siAGF1, siMARS is also an active siRNA control targeted to a fusion transcript. In case of siMARS, the target transcript is MLL/AF4 but with a different MLL/AF4 breakpoint.

As mentioned previously *MLL/AF4* genes can have different breakpoints. The fusion gene in SEM cells contains *MLL* exons 1 to 9 and *AF4* exons 4 to 20 (e9-e4). siMA6 targets this fusion gene. The fusion gene in RS4;11 cells contains *MLL* exons 1 to 10 and *AF4* exons 4 to 20 (e10-e4). The breakpoint in RS4;11 cells is targeted by

siMARS which is not specific to the SEM fusion transcript. The MV4;11 fusion gene contains *MLL* exons 1-9 and *AF4* exons 5-20 (e9-e5).

Another target gene of MLL/AF4 was *HOXA7*. *HOXA7* belongs to the homeobox gene cluster A. These transcription factors play an important role in regulating definitive hematopoiesis. *HOXA7* is especially known to be dysregulated in MLL-rearranged acute leukaemias and AML.

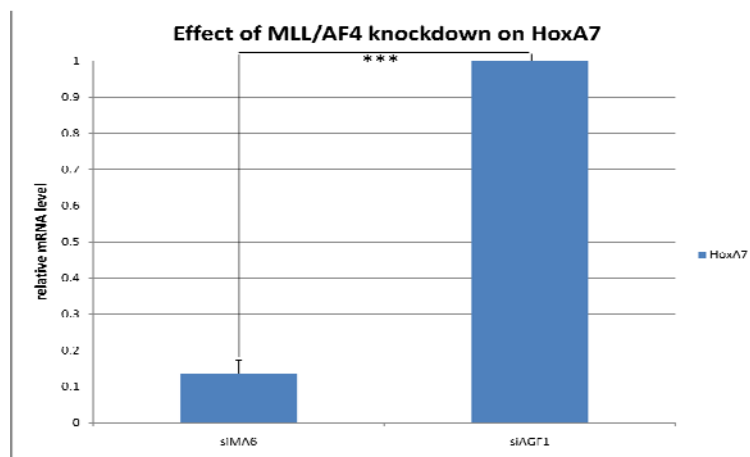


Figure 39 *HOXA7* expression analysis

*HOXA7* transcript qRT-PCR analysis after MLL/AF4 knockdown in SEM for 96h. siMARS6: anti *MLL/AF4* siRNA, siAGF1: active siRNA control. Shown are relative mRNA expression levels of *HOXA7* and averages of 3 independent experiments. Error bars show SD values. The knockdown of *HOXA7* transcript showed highest statistical significance with  $p = 0.0006$  (paired student's t-test).

Figure 39 shows the roughly 90% depletion of *HOXA7* mRNA ( $p = 0.0006$ ) in response to MLL/AF4 depletion. The data are normalised to the active siRNA control siAGF1.

Next, (Figure 40) analysis of *FGFR1* transcript levels subsequent to MLL/AF4 depletion are shown. *FGFR1* was found to be down-regulated on both arrays, which was confirmed by qRT-PCR. Knockdown of *FGFR1* by more than 60% normalised to siAGF1 was found to be highly statistically significant with  $p = 0.0022$ . FGFR1 is the Fibroblast Growth Factor Receptor 1 and is known to be involved in important cell

functions such as proliferation. Moreover it is thought to be a regulator in the haematopoietic stem cell niche.

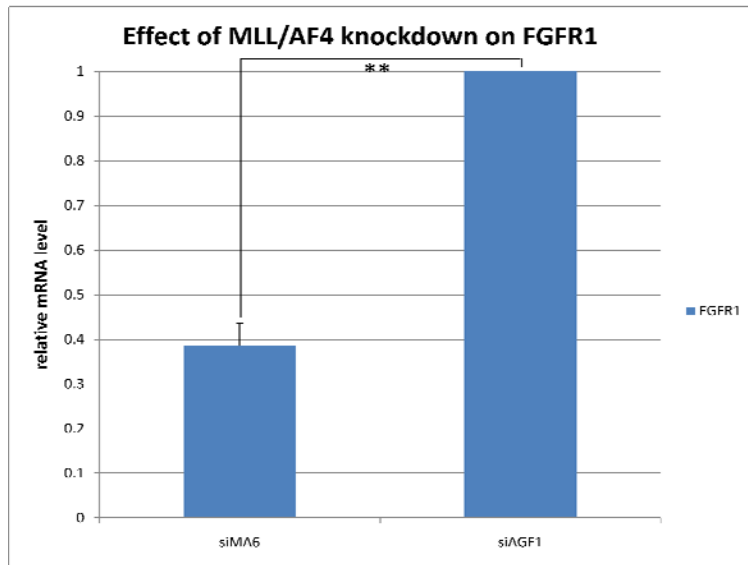


Figure 40 *FGFR1* expression analysis

*FGFR1* transcript qRT-PCR analysis after MLL/AF4 knockdown in SEM for 96h. siMA6: anti MLL/AF4 siRNA, siAGF1: active siRNA control. Shown are relative mRNA expression levels of *FGFR1* and averages of 3 independent experiments. Error bars show SD values. The knockdown of *FGFR1* transcript was highly statistically significant with  $p = 0.0022$  (paired student's t-test).

Finally the reduction of N-cadherin (*CDH2*) transcript levels by 40% is shown, normalised to control siRNA (Figure 41). This reduction is also highly statistically significant with  $p = 0.0039$ . N-cadherin protein is calcium-dependent and expressed on the surface. But it also involved in signalling and adhesion. Together with *FGFR1*, N-cadherin can form heterodimers and is thought to be implicated in the regulation of the haematopoietic stem cell niche as well.

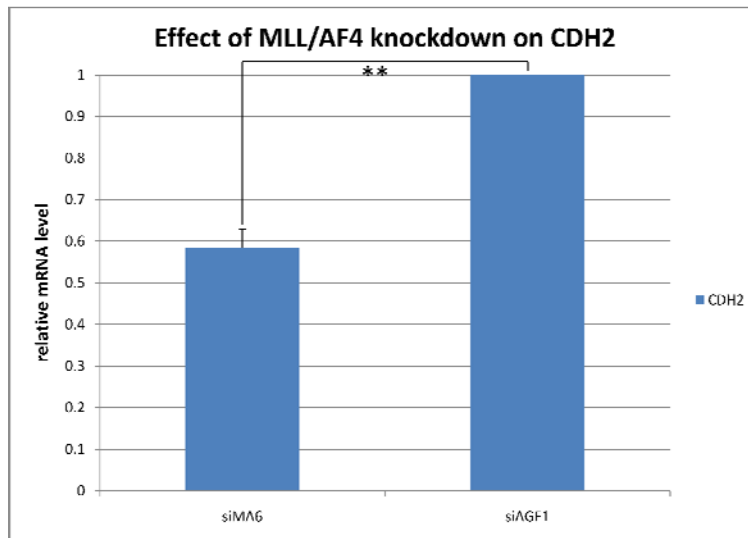


Figure 41 N-cadherin expression analysis

*CDH2* (N-cadherin) transcript qRT-PCR analysis after MLL/AF4 knockdown in SEM for 96h. siMA6: anti *MLL/AF4* siRNA, siAGF1: active siRNA control. Shown are relative mRNA expression levels of N-cadherin and averages of 3 independent experiments. Error bars show SD values. The knockdown of N-cadherin transcript was highly statistically significant with  $p = 0.0039$  (paired student's t-test).

### 3.3.1.3 Evaluation of N-cadherin Surface expression

As mentioned before, N-cadherin is expressed on the cell surface. Additional to transcript level changes in SEM following MLL/AF4 depletion its surface expression was investigated.

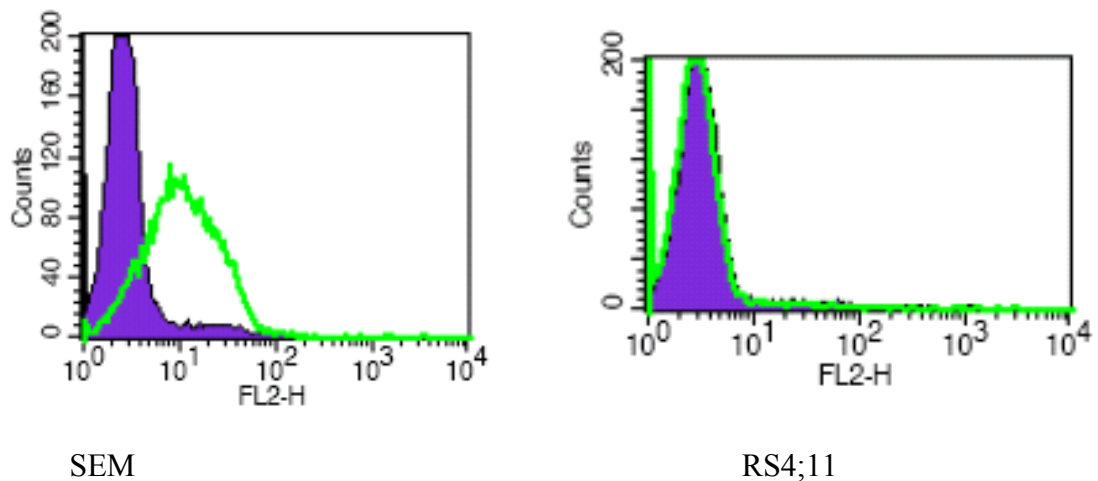


Figure 42 N-CADHERIN surface expression analysis

Flow cytometric analysis of N-cadherin expression levels. (Left histogram) SEM (Right histogram) RS4;11 N-cadherin-PE antibody signal is shown in the FL2-H channel. Lilac: control cells not stained with anti N-cadherin, green curve: N-cadherin stained cells

SEM and RS4;11 cells were analysed for the surface expression of N-cadherin by flow cytometric analysis (Figure 42). Several controls like unstained cells and isotype controls were run to solidify the data. SEM showed N-cadherin surface expression, RS4;11 did not.



## 3.4 Discussion Array Chapter

The aim of this chapter was to identify target genes of MLL/AF4. RNAi mediated knockdown of *MLL/AF4* transcripts in t(4;11) positive SEM cells subsequently reduces encoded fusion protein levels, as shown by the Heidenreich group (Thomas, Gessner et al. 2005). In principle, a target gene of MLL/AF4 should be affected by its depletion; but MLL/AF4 activity can regulate gene expression at different levels, either as direct target genes, or indirectly via other affected pathways. The further downstream genes are, the greater the potential number of genes affected. Therefore gene expression patterns associated with MLL/AF4 depletion reflect several levels of MLL/AF4 dependent regulation. Differential gene expression in result of MLL/AF4 depletion was accessed using transcriptome profiling. SEM cells transfected with si*MLL/AF4* were analysed by cDNA and oligo-arrays.

The functional analysis of expression data sets from the oligo arrays comparing control SEM cells with si*MLL/AF4* transfected SEM cells was performed using the Ingenuity Pathway Analysis software. MAS software pre-analysed oligo array data were filtered for a minimum fold change of 2 and sorted for strength of fold change of expression.

Differentially expressed genes were categorised in following main functions: “*Diseases and Disorders*”, “*Molecular and Cellular Functions and Physiological System Development and Function*”, “*Associated Network Functions*” and “*Canonical Pathways*”.

Independent from the Ingenuity Pathway Analysis MLL/AF4 depletion responsive gene expression found on the oligo and cDNA arrays were sorted for their significance. A comparison of overlapping genes from both arrays showed a set of genes with the same

direction of fold change. These and other and functionally interesting candidates were validated by qRT-PCR (Figures 35-41).

For the comparison of oligo-, cDNA-array and qRT-PCR transcript analysis the different time points after MLL/AF4 depletion have to be considered. The oligo array shows transcript level responses after two days, the cDNA array after 4 days and qRT-PCR up to 6 days of MLL/AF4 depletion. Therefore oligo array analysis mostly shows early responses to MLL/AF4 depletion, this could be transcripts with a high turnover, a low stability or direct targets.

In order to interpret these data retrieved from array and qRT-PCR analysis in the context of MLL/AF4 and the leukaemogenesis, the different features of a cancer cell in general have to be considered.

A cancer cell has the ability of increased proliferation; for that restrictions to unlimited growth have to be overcome. These are cell cycle checkpoints, growth inhibition by cell to cell contact in tissues and dependence on growth factors. Cancer cell must be also able to resist to apoptosis signals. Cancer cells often have mutations or other genetic lesions which would normally induce apoptosis if not repaired. Additionally, chemotherapeutic agents often generate apoptotic stimuli, providing advantage for cancer cells with apoptosis resistance. Cancer cells must be able to self renew, at least a fraction, to provide maintained proliferation in the cancer cell population. Somatic, differentiated cells have restricted numbers of divisions e.g. by telomere shortening which can lead to senescent cells - cancer cells show increased proliferation, therefore this restriction has to be overcome by cancer cells.

Migration, invasion and homing are further important properties associated to cancer cells allowing them to spread over the whole organism to settle and form new tumours.

The process of homing into a niche and becoming quiescent like a haematopoietic stem cell may additionally give a cancer cell the chance to survive chemotherapeutic treatment, which mainly affects proliferating cells, and moreover start proliferation again leading to a relapse.

In agreement with these considerations the Ingenuity Pathways Analysis (Figures 28–34) showed a link of MLL/AF4 responsive genes to leukaemia and cancer in general as affected genes were sorted in the categories “*Diseases and Disorders*”, amongst which “*Cancer*” most significantly; “*Molecular and Cellular Functions*” and “*Associated Network Functions*”.

The *MLL/AF4* fusion gene is a genetic event causing acute mixed lineage leukaemias (Domer, Fakharzadeh et al. 1993). The correlation to “*Genetic Disorder*” by Ingenuity shows several pathways frequently altered in genetic events, which are presumably important for the malignant biology of the cancer cell.

The mentioned required ability of cancer cells to proliferate was correlated to MLL/AF4 responsive genes in “*Cellular Growth and Proliferation*”, in “*Associated Network Functions*” such as “*Cell-to-Cell Signalling and Interaction, Cellular Growth and Proliferation, Haematological System Development and Function*” and in “*Canonical Pathways*” such as “*G-Protein Coupled Receptor Signalling*”, “*cAMP-mediated Signalling*” and “*WNT/ $\beta$ -Catenin Signalling*”. Signalling by G-proteins such as Ras GTPases and NF-kB are known to be important for proliferation and cancer relevant (Nadella, Blumer et al. 2010). cAMP signalling has an influence on proliferation and is linked to cancer in general (Abramovitch, Tavor et al. 2004). The WNT/ $\beta$ -Catenin pathway has a critical role in regulating proliferation and is also linked to cancer (Jiang, Yu et al. 2010). Moreover it was found to be required for MLL/AF9 fusion gene

positive AML (Wang, Krivtsov et al. 2010). These growth related findings agree with published work where MLL/AF4 depletion reduces proliferation of t(4;11) positive cells (Thomas, Gessner et al. 2005).

Another important property of cancer cells mentioned is the ability to overcome cell cycle checkpoints and progress in the cell cycle. This was correlated to the array data by Ingenuity Pathway Analysis in the already mentioned “*WNT/β-Catenin Signalling*” which influences the cell cycle and differentiation (Williams, Oh et al. 2010). The “*VDR/RXR*” canonical pathway was also connected to MLL/AF4 functions by Ingenuity with affected and correlated genes such as *RXRG* (retinoid X receptor gamma), *PTH* (parathyroid hormone) and *CSF2* (colony stimulating factor 2). *VDR/RXR* (vitamin D receptor / retinoid X receptor) polymorphisms are relevant to leukaemia; e.g AML derived translocations products block the vitamin D receptor induced differentiation by impairing the VDR localisation into the nucleus (Puccetti, Obradovic et al. 2002). The importance of cell cycle regulation by MLL/AF4 was published; MLL/AF4 depletion caused cell cycle arrest (Thomas, Gessner et al. 2005) and targets cell cycle genes.

Furthermore it was stated that cancer cells must be able to resist to apoptotic signals. These can originate from the cell itself, e.g. due to genetic events, from immune cells such as killer cells or be caused by chemotherapeutic agents. Ingenuity correlated MLL/AF4 depletion to apoptosis relevant functions such as “*Cell Death*” and “*Cell-to-Cell Signalling and Interaction*”, which could be the mentioned interaction with a killer cell. The resistance to chemotherapeutic induced apoptosis could be facilitated by inducing the metabolism of such; the canonical pathway assignment “*Metabolism / Xenobiotics by Cytochrome*” by Ingenuity agrees with this. Thomas et al. and others (Gaussmann, Wenger et al. 2007; Palermo, Bennett et al. 2008) have shown that

MLL/AF4 effectively suppresses apoptosis e.g. by up-regulating anti-apoptotic proteins and down-regulating pro-apoptotic proteins. Additionally, Ronald Stams group found that prednisolone resistance in MLL-rearranged infant ALLs is associated with high-level MCL-1 expression (Stam, Den Boer et al. 2010). MCL-1 is known to enhance cell survival by inhibiting apoptosis and inhibition of MCL-1 was found to be effective in overcoming steroid resistance (Liedtke and Cleary 2009).

A second group of functions connected to MLL/AF4 responsive genes can be drawn for the haematopoietic / niche context. This was another of the requirements for a cancer cell stated before. The haematopoietic niche is based on interactions between haematopoietic cells and stromal cells such as osteoblasts, in the bone environment. Several Ingenuity Pathway Analysis categories such as “*Skeletal and muscular Disorders*”, “*Cell Morphology*”, which could be inter cellular cyto-skeletal structures required to anchor surface adhesion molecules; and “*Associated Network Functions*” showed a correlation in this context. The latter function involved here was “*Cellular Movement, Skeletal and Muscular System Development and Function, Cellular Growth and Proliferation*” which shows properties required in the niche. Ingenuity also assigned canonical pathways such as “*WNT/ $\beta$ -Catenin Signalling*” known to be a regulative pathway in the bone marrow and endothelial niche; and “*VDR/RXR*” controlling functions such as cell differentiation, bone metabolism, growth and Wnt signalling regulation (Cianferotti, Cox et al. 2007).

In the niche, interactions between stromal cells such as osteoblasts, fibroblasts and endothelial cells with haematopoietic cells occur by surface proteins and secreted factors. Both are important regulators of this process (Shiozawa, Havens et al. 2008). Ingenuity Pathway Analysis links “*Cell-To-Cell Signalling and Interaction*” and “*Cell-*

*To-Cell Signalling and Interaction, Cellular Growth and Proliferation, Haematological System Development and Function*” to MLL/AF4 depletion in this context. Haematopoiesis, which is taking place in the niche, is linked by “*Tissue development*”, “*Haematological System Development and Function*”, “*Lymphoid Tissue Structure and Development*” and especially by “*Haematopoiesis*”. The regulation in the niche could also be supported by canonical pathways such as “*Role/Cytokines in Mediating Communication between Immune Cells*” found to be correlated here. Furthermore “*Lymphoid Tissue Structure and Development*” generates a strong correlation between MLL/AF4 functions and haematopoiesis. In this context also the homing of a haematopoietic cell is important. As previously discussed, it could give a cancer cell the possibility to reside in the niche. Ingenuity analysis functions such as “*Cellular Movement*” and “*Immune Cell Trafficking*” agree with this.

Finally, the cancer cell was stated to require self renewal potential. The correlation of MLL/AF4 depletion to “*Reproductive System Disease*” is presumably based on the fact that reproductive cells have stem cell properties and activate similar pathways (Lee, Jung et al. 2010). In the array data Oct4 (*Pou5F1*) is upregulated more than 5fold. The importance of Oct4 in t(4,11) ALL has recently been emphasized (Eberle, Pless et al. 2010). This pathway was not amongst the top 16 pathways (Table 6), but still judged as significant. It is known to be an important pathway in haematopoiesis. Controlling processes such as cell cycle, apoptosis, and pluripotency.

The last group of functions connected by Ingenuity Pathway Analysis to the expression changes upon MLL/AF4 depletion is inflammation. Recently inflammation signalling in cancer has been more and more in discussion. In order to maintain the ability to self renew and maintain a cancer cell population, cancer cells block differentiation.

However, that can lead to an arrest in cell cycle progression. One possible explanation for the importance of inflammatory pathways could be that they provide stimuli for cell cycle progression, thereby enabling cancer cells to be both rather immature and highly proliferative (Hamsa and Kuttan 2010). For the fusion gene *TEL-AML1* it was shown that sensitivity for TGF-beta induced proliferation inhibition was reduced by binding to SMAD3 (Ford, Palmi et al. 2009).

Ingenuity Pathway analysis generated a correlation of MLL/AF4 responsive genes and inflammation by functions such as “*Inflammatory Disease*”, “*Cellular Movement, Inflammatory Response, Cell-To-Cell Signalling and Interaction*” and “*Cellular Movement, Inflammatory Response, Cell-To-Cell Signalling and Interaction*”. Also several canonical pathway assignments such “*Hepatic Fibrosis/Hepatic Stellate Cell Activation*”, “*Macrophages, Fibroblast and Endothelial Cells in Rheumatoid Arthritis*”, “*LPS/IL-1 Mediated Inhibition /RXR Function; Acute Phase Response Signalling*” and “*Communication between Innate and Adaptive Immune cells and Pathogenesis / Multiple Sclerosis*”, which can be connected to inflammatory processes, support this.

However, the Heidenreich group has previously shown that MLL/AF4 depletion by siRNAs like siMA6 induces no interferon response (Thomas, Gessner et al. 2005). Interestingly, amongst the MLL/AF4 depletion responsive genes on the array is also NF- $\kappa$ B. A very recent publication links MLL/AF4 to Interferon (IFN) response, showing that the two tested MLL/AF4 cell lines SEM and RS4;11 were not IFN resistant, despite many other ALLs. The proposed required transcription factor in this pathway was NF- $\kappa$ B (Tracey, Streck et al. 2010).

The gene comparison brought up genes such as BNIP3, an apoptosis related gene; CD69, a proliferation and lymphocyte signalling linked gene; DAAM1, important in regulating the cytoskeleton and WNT; DUSP6, a MAP kinase phosphatase; *FGFR1*, an mitogenesis and differentiation regulation gene and PLAT, involved in cell migration and tissue remodelling. Interestingly, DAAM1 leads to inhibition of endothelial cell proliferation, migration, and angiogenesis (Ju, Cirone et al. 2010). PLAT is also related to endothelial cells, found in tumour cells and involved in angiogenesis and cell migration (McMahon and Kwaan 2008).

The gene array comparison (Figure 36) and qRT-PCR validation (Figures 36-41) brought up genes which could be contributing to leukaemia by increasing proliferation (*CD69*, *DUSP6*, *FGFR1*, *N-CADHERIN*, *SCD*, *BMI1*), regulating the HSC niche (*N-CADHERIN*, *FGFR1*, *DAAMI*, *MEF2C*, *NAP1L4*), regulating differentiation (*SCD*, *CD69*, *DUSP6*, *FGFR1*, *HOXA7*), self-renewal (*MEF2C*, *BMI1*), immortality (*TERT*, *HOXA7*), cell cycle regulation (*CDK1*, *MEIS1*) and migration (*IGFBP2*, *NAP1L4*).

depleted mRNA	by depletion affected gene	selected functions	involved pathways
M	<i>CDH2</i>	cell adhesion, niche regulation	WNT/beta, cellular signalling
L	<i>FGFR1</i>	niche regulation, differentiation	MAPK, PI3-K/AKT, NOTCH
L	<i>DAAMI</i>	cytoskeleton, motility, adhesion	PCP(cell polarity), WNT
/	<i>DUSP6</i>	proliferation, differentiation	MEK/ERK, SAPK/JNK, p38
A	<i>MEF2C</i>	self renewal, angiogenesis, apoptosis	MAPK, p38
F	<i>CD69</i>	proliferation, lymphocyte activation	CD69-pathway, ERK
4	<i>SCD</i>	cell growth, differentiation	PPAR, AMPK
	<i>NAP1L4</i>	cell migration, nucleosome assembly	BCR, CTLA4

Table 8 Selected genes affected by MLL/AF4 depletion  
orange reduced transcript levels, green increased levels

Among the genes significantly reduced in the qRT-PCR validation was *DUSP6* (Figure 38), which is a member of the dual specificity protein phosphatase subfamily



inactivating target kinases by dephosphorylation. *DUSP6* regulates members of the MAP kinase family (ERKs) which is a pathway highly important in proliferation. It was linked to *FGFR1*, another growth related gene, in many papers. For example *DUSP6*<sup>-/-</sup> mice represented a phenotype usually found with *FGFR1* and *FGFR2* constitutive activation (Bermudez, Pages et al. 2010). The down regulation of *DUSP6* in MLL/AF4 depleted cells might indicate that *DUSP6* has to be precisely regulated and that *DUSP6* may have different effects if strongly up regulated. Another highly significant altered gene was *HOXA7* (Figure 39) a member of the Homeobox gene family Cluster A which is important in development, gene expression, morphogenesis and differentiation. Also significantly altered is *FGFR1* (Figure 40), the fibroblast growth factor receptor 1, it has both signalling and adhesion function. FGFR1 was reported to be required for the regulation of HSCs (Weinreich, Lintmaer et al. 2006).

Finally, a significant reduction upon depletion in MLL/AF4 was found in N-cadherin mRNA levels (Figure 41). Neuronal cadherin belongs to the family of cadherins. It is dedicated to roles such as regulation of the of HSC niche interaction, in particular in retaining haematopoietic stem cells in the niche. Recently, it has also been reported to play a role in chemotherapy resistance (Zhi, Wang et al. 2010) and engraftment of HSCs (Hosokawa, Arai et al. 2010).

Surprisingly, the cell line SEM expressed N-cadherin on the surface, while RS4;11 did not (Figure 42). A possible explanation could be that RS4;11 cells are more mature than SEM cells and therefore N-cadherin could not be required anymore. This is supported by the finding that SEM express CD133; indicating an immature cell (Thomas, Gessner et al. 2005). However, controversially some authors doubt that N-cadherin is required for the HSC (Kiel, Radice et al. 2007)

## **Chapter 4**

# **Bone marrow feeder interactions**

# **Chapter 4 Bone marrow feeder interaction**

## **4.1 Introduction and Theory**

### **4.1.1 Stem cells**

Hallmarks of stem cells are their ability to self-renew and to differentiate into two and more different lineages. Self-renewal is the ability to produce progeny identical to the parental cell. The capability to differentiate into numerous types of cells defines the potency of a stem cell, which can be toti- (e.g. zygote), pluri- (ES cells) or multipotent (adult stem cells). Stem cells can principally be classified either as embryonic stem cells found in blastocytes or adult stem cell found in adult tissues. Adult stem cells provide cells for tissue to either replace normally dying cells or to repair damaged tissue.

### **4.1.2 The haematopoietic niche**

In 1978 Schofield (Schofield 1978) developed the niche hypothesis defining the microenvironment which supports haematopoietic stem cells. In human adults HSCs are located in the bone marrow which is present in the trabecular cavities of large bones (Fig. 45 a+b). The bone marrow niche is formed by stromal cells including fibroblasts, osteoblasts, endothelial cells and adipocytes (Taichman 2005). These stromal cells in the bone marrow are derived from mesenchymal stem cells and probably form the niche physically (Shiozawa, Havens et al. 2008). In addition, they also regulate HSC by cell-

cell adhesive interactions as well as by cytokines thereby affecting proliferation, differentiation and self-renewal (Miura, Gao et al. 2006).

The following model (Figure 43) comprises hypotheses regarding the niche. In this model special osteoblasts form the endosteal niche adjacent to trabecular bone, while endothelial form the vascular niche cells in adjacent vessels (c). The entrance and the exit of HSC in the endosteal niche is regulated by the vascular niche. In this model HSCs can enter the endosteal niche, interact with osteoblast and become quiescent. The process of localising back into the bone marrow is called homing. A quiescent HSC can also be mobilized, locate to the vascular niche, proliferate and differentiate (d). The osteoblast is regulating the HSC by surface molecules such as adherence factors, receptors and by soluble factors (e) (Shiozawa, Havens et al. 2008).

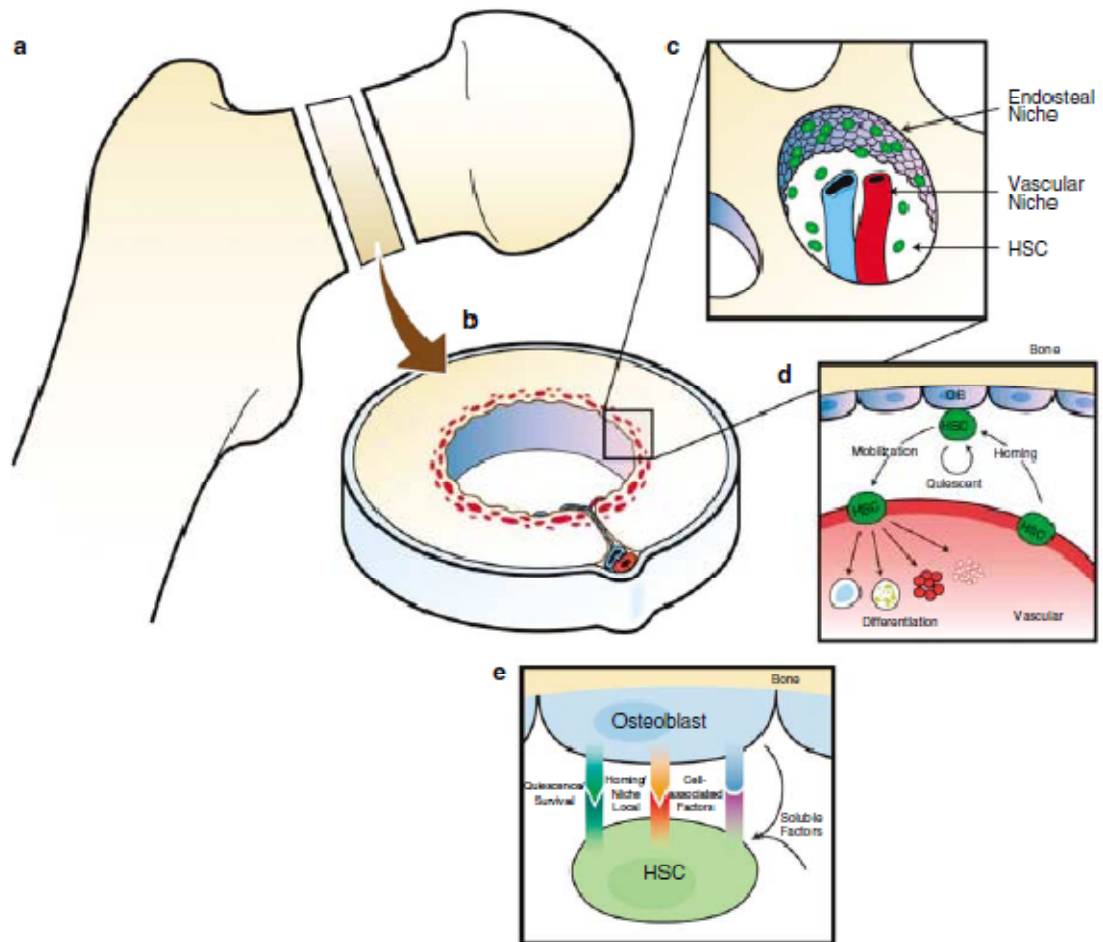


Figure 43 Model of the haematopoietic stem cell niche

The HSC niche is located in large bones (a) within the trabecular structure (b) which provides osteoblast surfaces and high vascularisation (c). HSC can reside at their osteoblast niche or migrate to adjacent vessels differentiate and proliferate into blood cells (d). The osteoblast HSC interaction involves adherence factors, receptors and soluble factors (e) from (Shiozawa, Havens et al. 2008)

Haematopoiesis as described before originates from haematopoietic stem cells differentiating into committed progenitors (CPs) whilst increasing proliferation. If all HSC ultimately differentiated into CPs the stem cell niche would be finally exhausted stopping the further supply for blood cells. However, if HSCs did not differentiate into CPs HSC numbers in the niche would increase but the supply for blood cells would stop as well. In the normal healthy steady state an asymmetric division is required providing CPs and maintaining the HSC pool. After asymmetric division one daughter cell remains undifferentiated maintaining and retaining HSCs in the niche while the second daughter cell differentiates into CPs and finally blood cells leaving the niche (Wilson,

Murphy et al. 2004). For the regulation of the asymmetric division of a HSC the *c-MYC* levels are important. Low *c-MYC* levels induce HSC quiescence in the niche by interaction with spindle-shaped, N-cadherin-positive osteoblasts (SNO) (Zhang, Niu et al. 2003). In the HSC niche model of Wilson, Murphy et al. (Wilson, Murphy et al. 2004) high *c-MYC* levels reduce cell adhesion molecules which promotes the cell to leave the niche environment and differentiate into committed progenitors (CP) (Figure 44). If after division *c-MYC* levels are low in one HSC and high in the future CP, this will lead to the result of asymmetric division leaving one HSC bound to the niche while the other differentiates and leaves the niche.

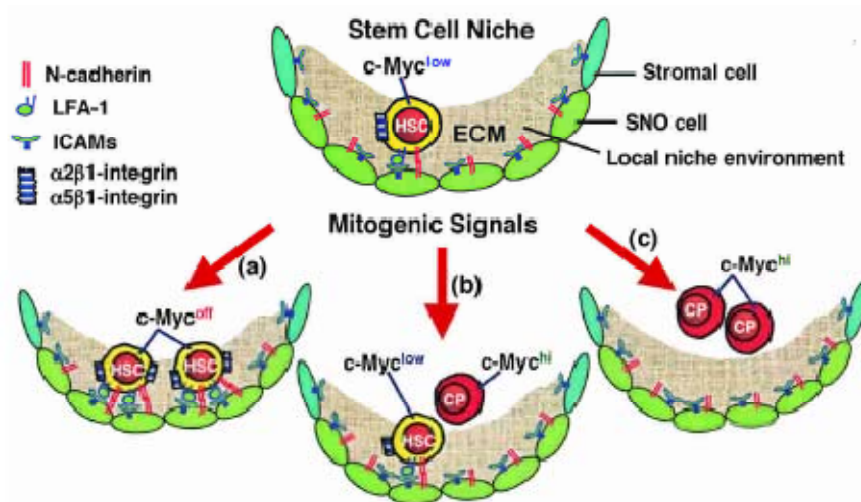


Figure 44 Regulation of a HSC in the bone marrow niche

(a) symmetric division of a HSC (b) asymmetric division of a HSC and (c) symmetric division into two progenitor cells. N-cadherin, LFA-1, ICAMs and Integrins are cell adhesion factors and receptors, SNO spindle shaped N-cadherin positive osteoblasts from (Wilson, Murphy et al. 2004)

As described in Figure 44 there are several adhesion factors which retain the HSC in the niche by interacting with factors such as α2β1 / α5β1 integrins, ICAMs, LFA-1 and N-cadherin. In addition to N-cadherin, integrins are involved in homing and mobilization

of HSCs in the bone marrow (Whetton and Graham 1999) by providing cell adhesion, thus retaining a HSC in the niche environment.

### **4.1.3 Surface molecules regulating the niche**

#### **4.1.3.1 Neuronal cadherin**

Neuronal cadherin (*CDH2*) is known to be upregulated in invasive cancer cell lines (Hazan, Kang et al. 1997) and to promote migration and invasion (Nieman, Prudoff et al. 1999; Hazan, Phillips et al. 2000). N-cadherin is an intercellular cell adhesion molecule which is calcium dependant and interacts in a homophilic manner. It is a member of the cadherin family which regulate tissue morphogenesis, cell recognition and are required in solid tissue maintenance (Takeichi 1991; Gumbiner 1996).

The *CDH2* gene translates into a 135kDA transmembrane glycoprotein with 5 extracellular repeats, a transmembrane domain and a cytoplasmic tail which interacts with  $\beta$ -catenin and the cytoskeleton via  $\beta$ -catenin. Extracellular cleavage of N-cadherin by the metalloprotease ADAM10 influences cell-cell adhesion and  $\beta$ -catenin signalling by liberating it and thus increasing the cytoplasmic pool. This cleavage represents a signalling switch from external N-cadherin to lymphocyte enhancer binding factor-1 (LEF-1) driven gene expression of  $\beta$ -catenin target genes (Reiss, Maretzky et al. 2005). WNT/ $\beta$ -catenin signalling is crucial for regulating self-renewal in HSCs (Staal and Luis 2010) in particular the decision self-renewal versus differentiation.

N-cadherin was also found to be interacting with platelet derived growth factor receptor  $\beta$  (PDGFR $\beta$ ) in a complex with  $\beta$ -catenin and the scaffold protein NHERF whilst

modulating the actin cytoskeleton and regulating cell motility (Theisen, Wahl et al. 2007).

#### **4.1.3.2 Fibroblast growth factor**

Fibroblast growth factor 2 (FGF-2) was reported to amplify N-cadherin derived effects, therefore N-cadherin and the FGF receptor (FGFR1), were suggested to act synergistically especially in inducing invasiveness (Hazan, Phillips et al. 2000). Furthermore FGFR1 and N-cadherin were proposed to interact via the HAV (cell adhesion recognition sequence) motif on FGFR1 and the EC4 on N-cadherin (Williams, Williams et al. 2001). This interaction also increased FGFR1, stability and MAPK-ERK signalling (Suyama, Shapiro et al. 2002).

Fibroblast growth factors are heparin binding proteins and comprise more than 20 ligands that can induce signalling. The FGF family is involved in differentiation, migration, proliferation morphogenesis and angiogenesis (Ornitz and Itoh 2001; Coumoul and Deng 2003). One of the 4 receptors FGFR1, a tyrosine kinase, is involved in haematopoietic differentiation (Faloon, Arentson et al. 2000); constitutive activation by translocation was found in myeloproliferative and T-cell lymphoma syndromes (Roumiantsev, Krause et al. 2004).

Weinreich et al (Weinreich, Lintmaer et al. 2006) claimed that receptors such as FGFR1 are a new class of haematopoietic regulators with activities exceeding effects of growth factors such as G-CSF and GM-CSF (Granulocyte and Granulocyte –Macrophage colony stimulating factor) .



Finally the FGF pathway with its intermediates FGFR1, GRB2, SOS, RAS and MAP-kinases is required in haematopoiesis and thus niche regulation. FGF receptor is a marker of HSCs and critical for HSC proliferation (de Haan, Weersing et al. 2003).

#### **4.1.3.3 $\beta$ -catenin**

The regulation of the HSC by surface receptor-ligand signalling has already been mentioned for  $\beta$ -catenin, FGFR1 and N-cadherin.  $\beta$ -catenin is an essential part of the classical Wnt pathway which is started by the binding of Wnt to the Frizzled/LRP receptor complex outside the cell, activates dishevelled which then inhibits a complex of axin, GSK-3 and APC. This complex would normally induce  $\beta$ -catenin degradation by ubiquitylation; therefore, its inhibition leads to  $\beta$ -catenin accumulation which drives target gene expression in the nucleus via LEF/TCF. Haematopoietic tissues express Wnt ligands and frizzled and activation induces HSC proliferation and expansion (Austin, Solar et al. 1997; Reya, Duncan et al. 2003).  $\beta$ -catenin was found to be up regulated in human and mouse HSCs (Bug, Gul et al. 2005). However, other pathways such as Notch, might replace  $\beta$ -catenins' role (Ross and Li 2006); results obtained by conditional inactivation of  $\beta$ -catenin suggested that haematopoiesis is not necessarily dependent on it (Cobas, Wilson et al. 2004).

#### **4.1.3.4 Notch**

Such a pathway complementing WNT signalling is Notch. Wnt3 influences Notch target genes. But without Notch WNT signalling cannot affect self-renewal (Duncan,

Rattis et al. 2005). Notch signalling is initiated by binding of the Jagged ligand to the Notch receptor resulting in cleavage induced liberation of NICD (Notch intracellular domain) which translocates to the nucleus to regulate its target genes. Calvi et al (Calvi, Adams et al. 2003) have shown that HSC expansion is supported by high titers of jagged produced by osteoblasts. This might reflect two different results of niche regulation; either quiescence where the cells adhere or differentiation where the cells start to proliferate. However the role of Notch signalling as an important actor of the HSC compartment has recently been challenged as HSC-generated reconstitution of haematopoiesis in mice was not affected by conditional inactivation of Notch1 and Jagged1 (Mancini, Mantei et al. 2005). The following figure (Figure 45) summarizes some of the already mentioned pathways in the regulation of a HSC.

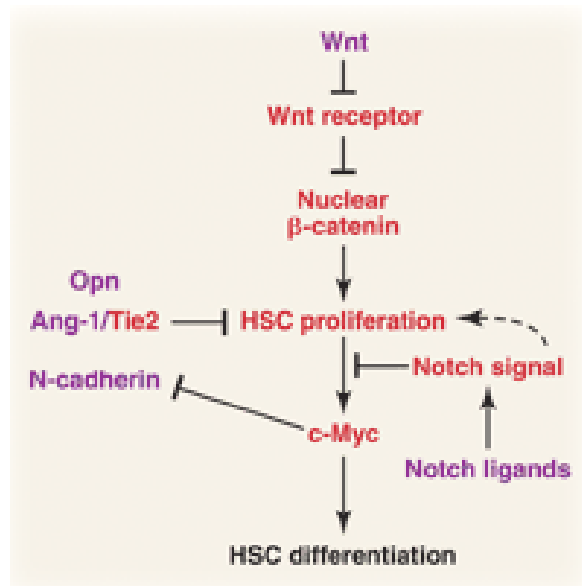


Figure 45 Schematic of the regulation of a HSC

The proliferation and differentiation of a HSC is regulated by several pathways including Wnt/ $\beta$ -catenin signalling where beta catenin increases HSC proliferation, Ang-1/Tie2 signalling inhibits HSC proliferation, Notch signalling inhibits c-myc level up regulation and thereby differentiation and N-cadherin is downregulated by high c-myc levels which reduces adhesion. Ang-1 Angiopoietin-1, Tie2 Angiopoietin receptor from (Moore and Lemischka 2006)

### 4.1.3.5 BMP

Bone morphogenic protein (BMP) signalling negatively controls the endosteal niche size negatively and thus maintains HSCs in mice (Zhang, Niu et al. 2003). BMP binds to its receptor BMPR inducing several Smads to complex and regulate gene transcription in the nucleus. BMP belongs to the TGF- $\beta$  super-family and TGF- $\beta$  signalling is involved in the regulation of haematopoiesis including precursors and adult HSCs (Larsson and Karlsson 2005).

There is also evidence for a connection between BMP and Sonic hedgehog (SHH) signalling in mammalian HSCs (Bhardwaj, Murdoch et al. 2001). SHH binds to its receptor Patched (PTC) thus releasing Ptc inhibition on Smo; the latter transcription is regulated by GLI proteins which are transcription factors determining cell fate. SHH signalling is necessary for the generation of HSCs which also depends on intact Notch signalling as shown in zebrafish (Gering and Patient 2005).

The following diagram (Figure 46) comprises these pathways with the allocation to, if possible, the endosteal or the vascular niche. This separation has previously been described.

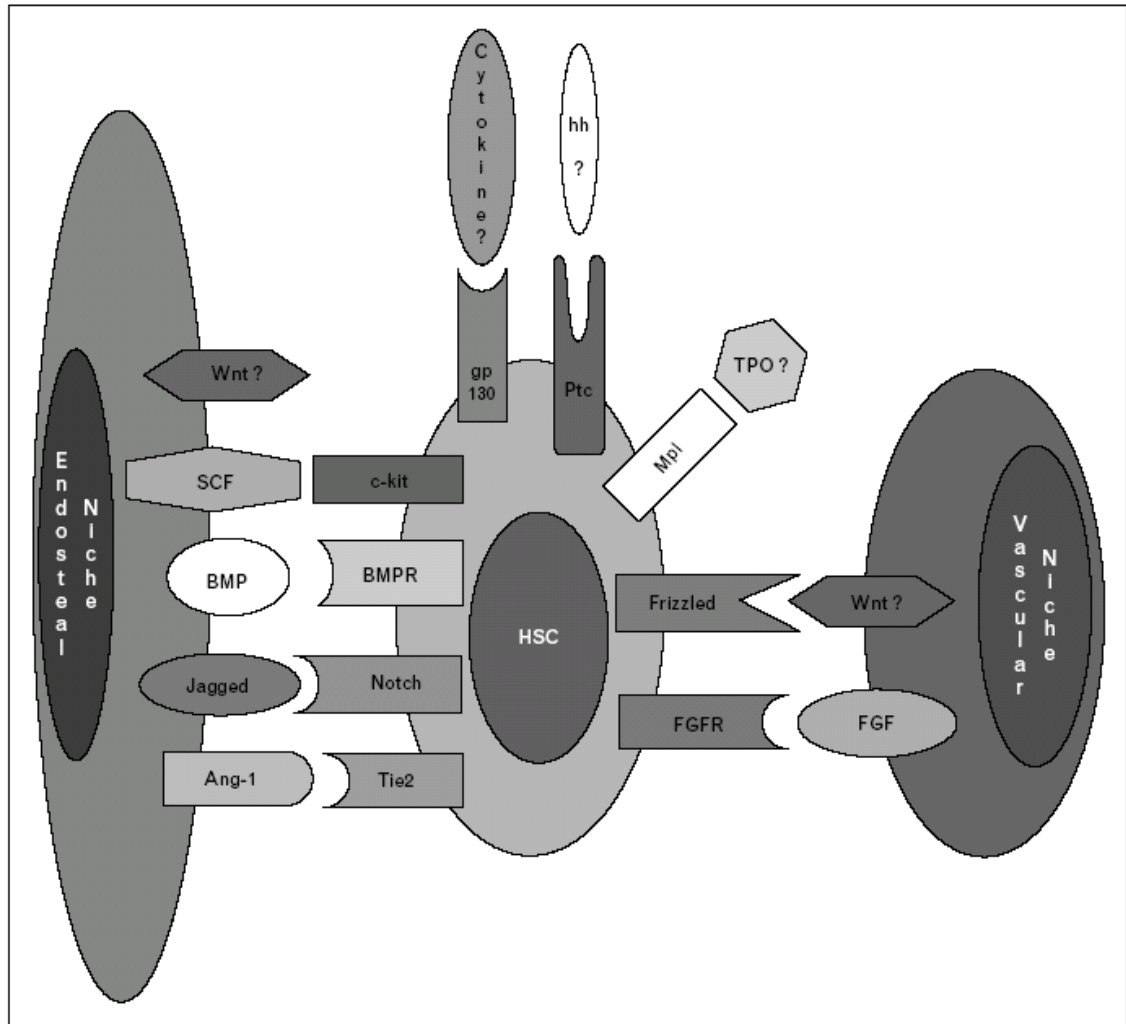


Figure 46 Pathways regulating the HSC in the endosteal and vascular niche

Shown are receptors and ligands of pathways SCF stem cell factor, BMP(R) bone morphogenic protein(receptor), Ang-1 Angiopoietin-1, gp130 glycoprotein 130, Ptc Patched, hh hedgehog, mpl myeloproliferative leukaemia, TPO thrombopoietin, FGF(R) Fibroblast growth factor (receptor) from (Ross and Li 2006)

An interesting view on the niche was made by Y Shiozawa (Shiozawa, Havens et al. 2008) by suggesting that the microenvironment and the mechanisms in maintaining HSCs could be used by neoplastic cells, functioning as “molecular parasites of the niche”. One such example is prostate cancer which preferably metastasizes into bone and form tumours there but also remodel the bone. This migration is thought to be induced by factors provided by the bone, while the bone remodelling is thought to be caused by factors such as VEGF secreted by the prostate cells. The authors propose a general mechanism where cancer stem cells could interact with a type of niche and start

dormancy programs. Like LSCs (leukaemic stem cells) which exhibit many HSC similarities they are expected to interact with the niche environment (Figure 47). By residing in the niche metastatic cells could escape chemotherapy and radiotherapy.

## Niche Interactions For Metastases

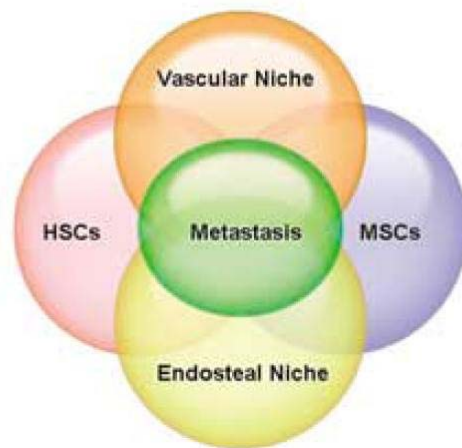


Figure 47 Summary of niche interactions

The vascular and the endosteal niche which interact with HSCs and MSCs could also provide a niche for metastasis. Mesenchymal stem cells (MSC) provide for niche relevant cells such as osteoblast and endothel . MSCs and HSCs which provide for all cells in the niche are thought to be generally regulated. Metastatic cells could use both niches and act as “molecular parasites of the niche” MSC Mesenchymal stem cell, HSC Haematopoietic stem cell from (Shiozawa, Havens et al. 2008)

Haematopoietic stem cells are quiescent when they reside in the niche. If a cancer cell activates quiescence while settling in the niche likewise a HSC, it could provide an enormous advantage to it, as most chemotherapeutic agents mainly affect proliferating cells. The involvement in tumorigenesis could define a neoplastic or leukaemic niche.

## 4.2 Aims

The finding that several validated genes are involved in the bone marrow haematopoietic stem cell niche, resulted in the endeavour of establishing an artificial niche model to examine stem cell - niche interactions and the effect of this interaction on the stem cells. As many of the leukaemic cells with which we work have stem cell properties, this promised to be relevant to other types of leukaemia.

Specific Aims:

1. To establish an artificial model with bone marrow fibroblasts to test niche interactions
2. To relate the Array data to the stem cell niche hypothesis proposed in this thesis

## **4.3 Results Bone marrow feeder interactions**

### **4.3.1 Establishment of Feeder layer**

To be able to co-culture leukaemic cells on a bone marrow fibroblast layer it is important that the feeder layer does not grow and shed off the co-cultured cells. This is especially true if the co-culture has to be maintained over several weeks.

### **4.3.2 Examination of HS-5 for feeder layer properties**

HS-5 is a human bone marrow stromal cell line transformed by amphotropic retrovirus HPV (human papilloma virus) virus. HS-5 expresses E6E7 genes, which are known to affect tumor-suppressor proteins such as p53 and Rb, which suppress cell cycle arrest (Roecklein and Torok-Storb 1995). HS-5 were originally isolated from a male Caucasian donor and show fibroblast morphology. HS-5 cells secrete several factors such as granulocyte -, granulocyte-macrophage - and macrophage colony stimulation factors (G-CSF, GM-CSF and M-CSF), Kit ligand (KL), macrophage-inhibitory protein-1 alpha, interleukin-1 alpha (IL-1alpha), IL-1beta, IL-1RA, IL-6, IL-8, IL-11, and leukaemia inhibitory factor (LIF). HS-5 is known to support proliferation of haematopoietic progenitor cells, removing the need for serum supplementation for *in vitro* culture.

For this reason HS-5 was chosen as the feeder cell-line for co-cultures to test effects similar to the leukaemic stem cell – bone marrow fibroblast interaction. According to protocol HS-5 were irradiated at 15, 20, 40, 60 and 80 Gy of  $\gamma$ -radiation and monitored.

Unfortunately, the treatment seemed to kill a fraction of the HS5 cells, proportional to the radiation dose used. Cells which did not receive a lethal dose started to proliferate again after a maximum interval of two weeks. According to protocols for other fibroblast cells-lines, Actinomycin D and Mitomycin C (MMC) treatment at various concentrations and incubation times were used to induce growth arrest. The effect was in principle similar, depending on the dose the toxicity was increased but parameters where all cells were arrested could not be found, the output was apoptosis versus proliferation. The following images of HS-5 (Figure 48) show an example of those experiments. Starting from a homogeneous fibroblast layer, cells were treated with MMC at two concentrations and various incubation times. After one week there were areas where cells had undergone apoptosis, leaving gaps. In other areas cells were quite dense, even forming foci where they were growing over each other.



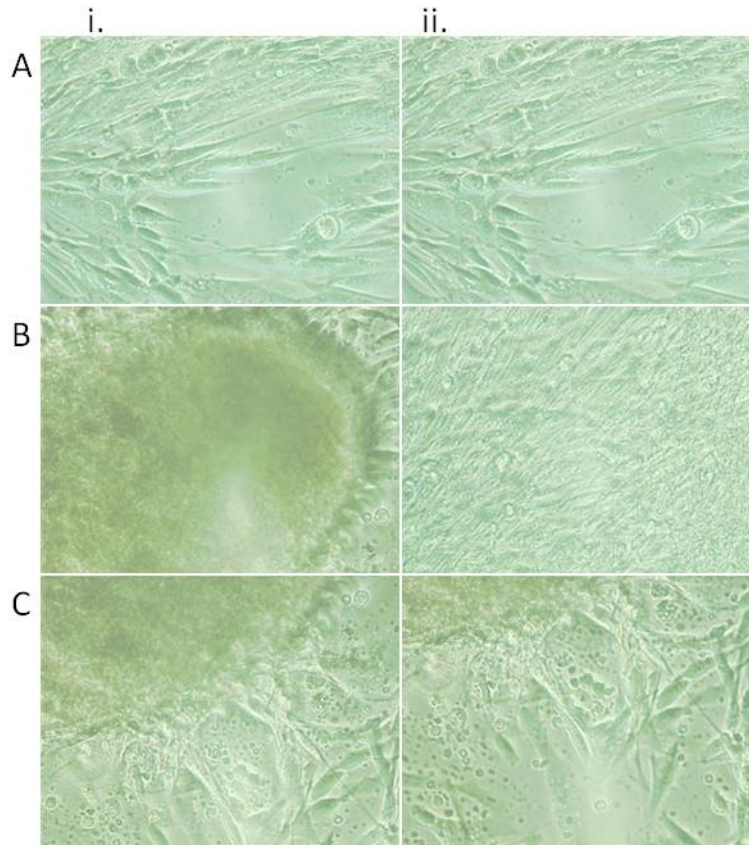


Figure 48 HS-5 feeder layers treated with Mitomycin C

(A i. and ii.) HS-5 fibroblast layer with gaps due to cell death (B i.) foci of HS-5 growing on top of each other (B ii.) dense layer of re-growing HS-5 (C i. and ii.) edges of foci, gaps in close proximity to foci, magnification 200x

To investigate why the HS-5 could not be arrested under conditions successfully applied to other cell lines, a genotype analysis was made.

The resulting karyotype was:

- 42~45, XY, -2[3], -7[3], del(7), (q2?), der (10) t(2;10)q1?;q26[7], -13[4], -16[3], -19[5], -19[3], -20[6], -21[3], -22[4], -22[3], 1-5mar[4], inc[cp6]/70~86, idem

The HS-5 showed a complex abnormal genotype, inter cell variation, unbalanced translocations, hyperdiploidy and polyploidy. (Dr N P Brown, Northern Genetics Service Cytogenetics Laboratory, Newcastle)

Parallel to this a cell cycle analysis was performed. Shown is the DMSO control for a range of MMC concentrations tested (see Figure 49 and Figure 50).

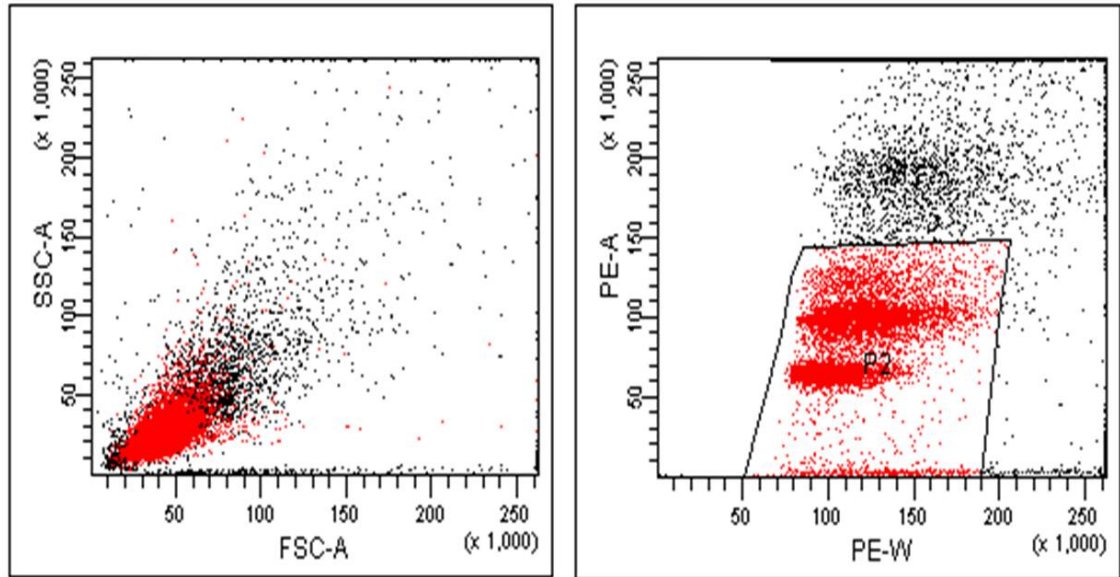


Figure 49 Cell cycle analysis dot plots of HS-5

Untreated HS-5 were subjected to PI (propidium iodide) cell cycle analysis (Left) SSC-FSC Dot plot of PI stained HS-5 cells (Right) PE-A/PE-W Dotplot of PI stained HS-5 Red: cells gated in P2 (right), these cells were inserted into histogram analysis below

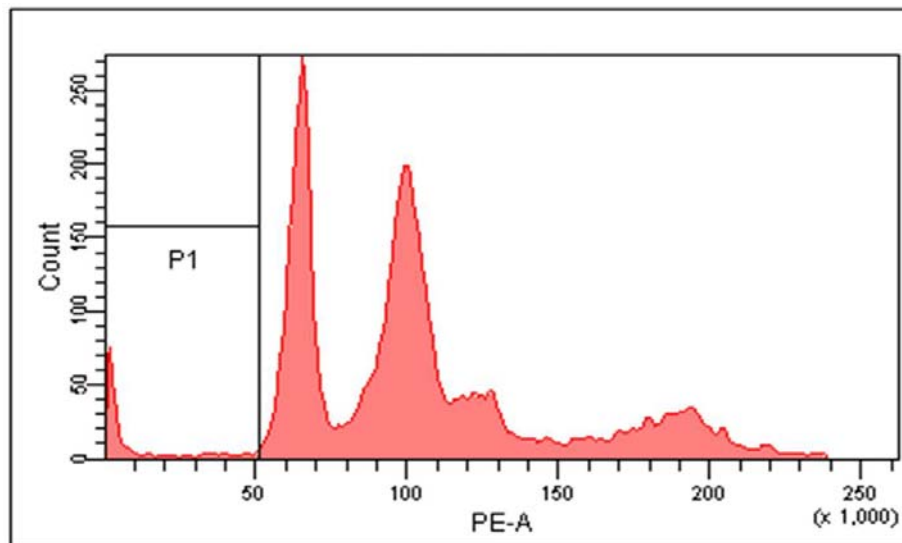


Figure 50 Cell cycle analysis Histogram of HS-5

HS-5 were stained with PI and the PI signal detected in the PE-A channel P1 represents apoptotic cells, particles

The cell-cycle showed an abnormal pattern (Figure 50). Usually a high G1/G0 peak is present followed by a flat, stretched S phase and then a G2/M peak. The HS-5 showed, probably due to their polyploidy, two big G1 peaks of different ploidy. The second G1

peak was at the position where the flat S-phase should be located. These results suggest two cell-cycles, of different ploidy, were superimposed onto one another.

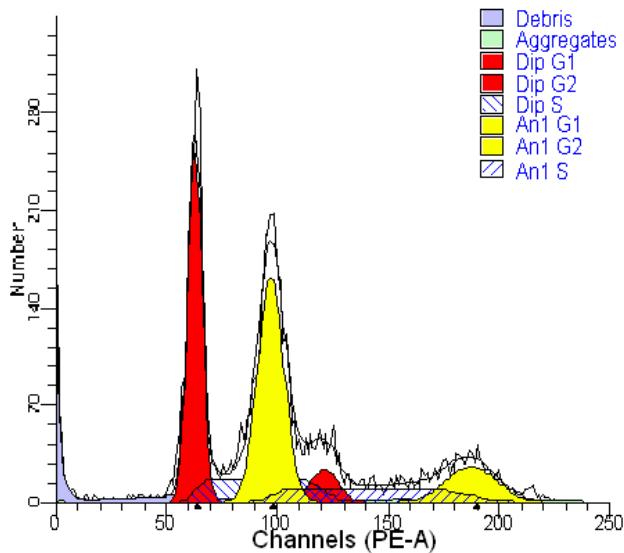


Figure 51 HS-5 cell cycle Modfit Analysis using Aneuploid and Diploid mode  
PI stained HS-5 cells analysed for cellcycle distribution, DIP G1, G2, S: diploid cell cycle phases, AN1 G1, G2, S: aneuploid cell cycle phases.

In the diagram above (Figure 51) a ModFit analysis of HS-5 cell cycle was performed. A special mode which can fit the cell phases to cells with diploidy and aneuploidy was used. However this was not sufficient to determine exact cell cycle phase distribution and so cell cycle arrest could not be demonstrated.

The heterogeneity of this cell-line and the presence of E6E7- HPV gene functions mentioned before, were probably the reasons why it could not be arrested. If one subgroup was arrested, the others were going into apoptosis or were proliferating.

Nevertheless, for a limited period of time until HS-5 layers reached confluence, it was possible to co-culture HS-5 and MV4;11 (Figure 52).

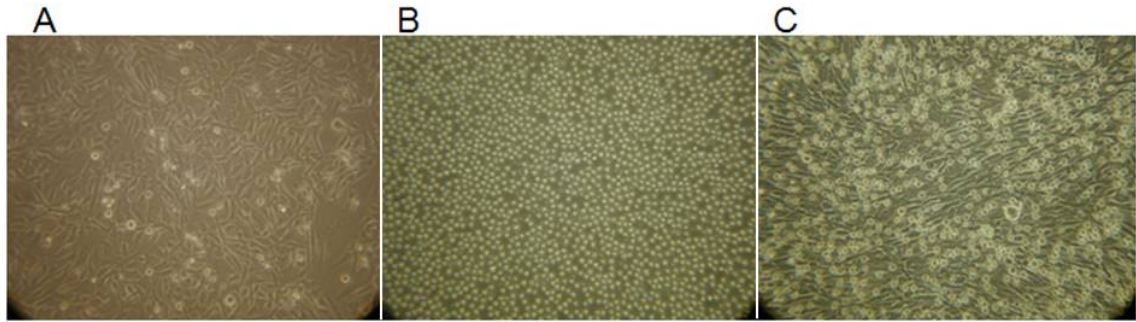


Figure 52 HS-5, MV4;11 and co-culture

Images of HS-5 monoculture, MV4;11 monoculture and HS-5 MV4;11 (A) HS-5 half confluent layer (B) MV4,11 culture (C) HS-5 - MV4;11 co-culture, magnification 200x

MV4;11 cells, which have no tendency to adhere to surfaces, seemed to be attached to HS-5 co-cultures as shaking under the microscope did not move MV4,11 on top of the HS-5 feeders (Figure 52).

### 4.3.3 Test of M210B4

The M210B4 cell line is derived from mouse bone marrow stromal cells. They show a fibroblast morphology, express laminin and collagen IV and growth factors such as KL (Kit ligand), IL3 (Interleukin 3) and G-CSF (Granulocyte colony stimulating factor) (Lemoine, Humphries et al. 1988). M210B4 are known to support human and murine myelopoiesis as well as several pre-B cell lines (Lemoine, Krystal et al. 1988). In LTC-IC (long term culture initiating cell) assay protocols, the usage and growth arrest of M210B4 by irradiation was described. Therefore, this cell-line was chosen as alternative to the HS5 cell line to produce a feeder layer.

### 4.3.3.1 Growth arrest

M210B4 cells were irradiated at 60 to 80Gy and monitored by microscopy for re-growth and cell death. Additionally, a cell cycle analysis before and after the treatment was performed to validate those observations (Figure 53 and Figure 54).

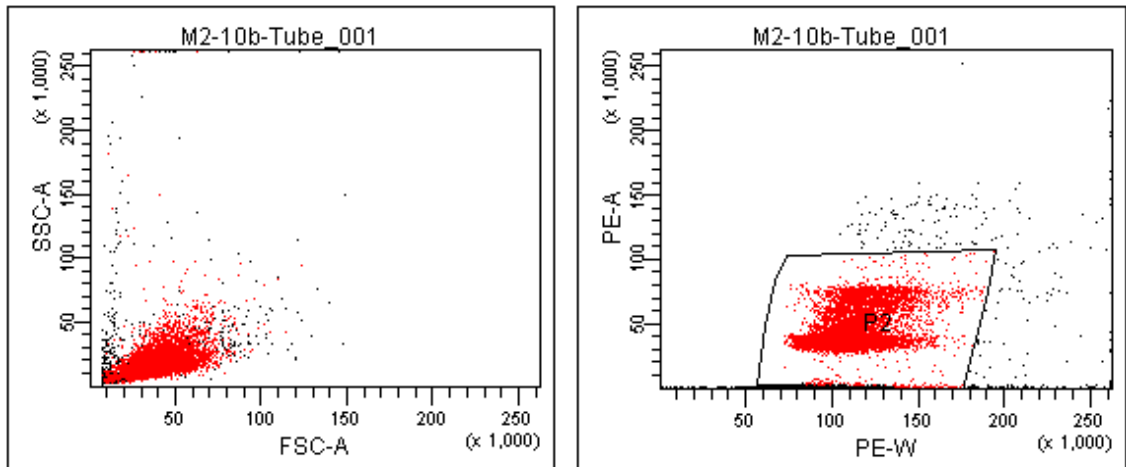


Figure 53 Cellcycle Dotplots of untreated M210B4 cells

Flow cytometric analysis of untreated M210B4 cells in cell cycle analysis (Left) SSC-FSC Dotplot of PI stained M210B4 (Right) PE-A/PE-W PI signal Dotplot of PI stained M210B4

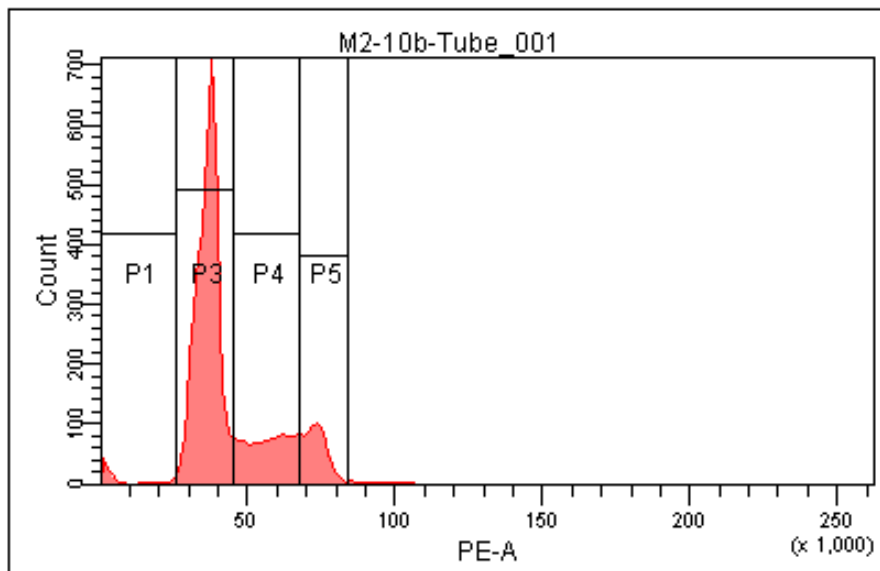


Figure 54 Cellcycle histogram of untreated M210B4

Histogram of P2 gated cells from Figure 53 The PI signal was detected in the PE-A channel P1: Apoptotic fragments, P3: G1/Go, P4: S-Phase, P5: G2/M

This cell-cycle above (Figure 54) showed a normal cell-cycle with a strong G1/G0 peak (P3), a flat S-phase (P4) and a small G2 peak (P5). P1 represented the apoptotic fraction. According to this 66% of M210B4 were in G1/G0 phase, 17% in S phase and 17% in G2 phase.

One week after irradiation the cell cycle of M210B4 showed an increase in the apoptotic fraction P1 compared to the non-irradiated cells (Figure 55 and Figure 56). Apoptotic cells were gated out to better display the cell cycle fractions. The G1/G0 peak (P3) was significantly reduced and the G2 peak (P5) correspondingly bigger.

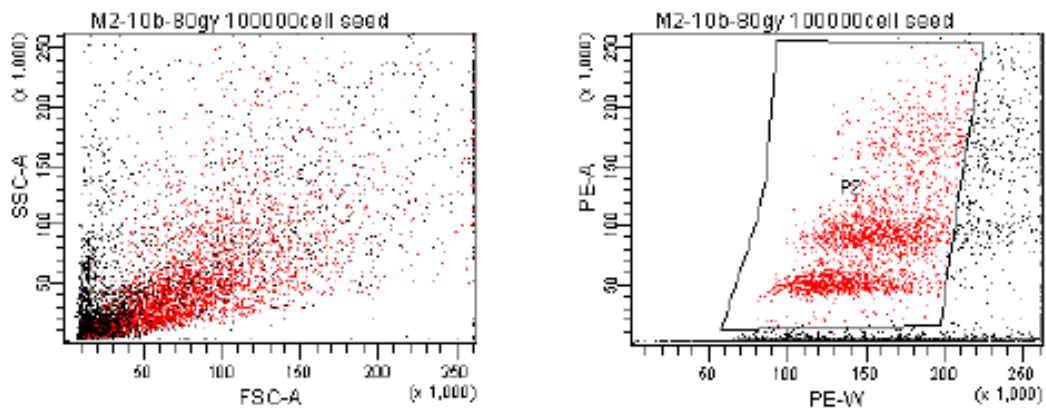


Figure 55 Cell cycle Dotplots of M210B4 cells irradiated at 80 Gy

Irradiated M210B4 were subjected to cell cycle analysis (Left) SSC-FSC Dotplot of PI stained irradiated M210B4 (Right) PE-A/PE-W PI signal Dotplot of PI stained irradiated M210B4

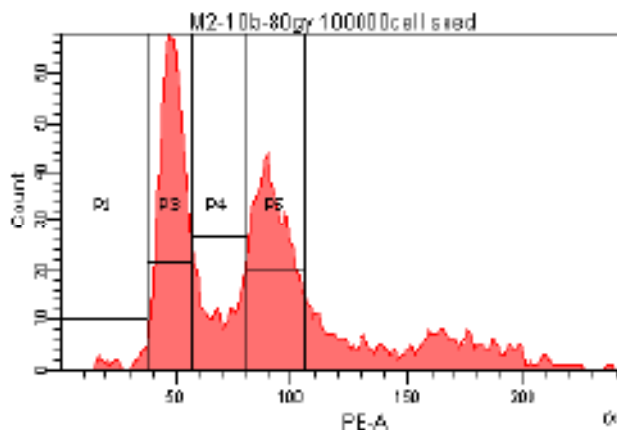


Figure 56 Cell cycle of irradiated M210B4

Cells from the P2 gate of Figure 55 are shown in this histogram. The PI signal was detected in the PE-A channel P1: Apoptotic fragments, P3: G1/Go, P4: S-Phase, P5: G2/M

Right of P5 the histogram shows a basal signal, probably due to background and doublets of fibroblasts (Figure 56). As this was not found in the un-irradiated M210B4 it was probably due to irradiation. According to this analysis 43% of irradiated M210B4 were in G1/0 phase, 16% in S phase and 41% in G2 phase. This showed a strong increase of G2 from 17% to 41% by irradiation representing a pronounced G2 arrest. Growth arrested M210B4 were monitored for over 4 weeks and no proliferation was found. Therefore the arrest of M210B4 proved to be feasible.

#### **4.3.3.2 Incubation of M210B4 feeders with SEMTeton**

Growth arrested M210B4 were seeded on collagen coated wells and left to form a feeder layer for two days. Then different concentrations of fluorescent SEMTeton were seeded on those wells. These were SEM cells which had been transduced with the lentiviral Teton-vector and consequently expressed GFP (see chapter 5). Fluorescent SEM cells were used for a better discrimination of leukaemic from feeder cells. After incubation of 10 days, these feeder - fluorescent cell co-cultures were captured with and without fluorescence imaging using a fluorescent microscope (see Figure 57).



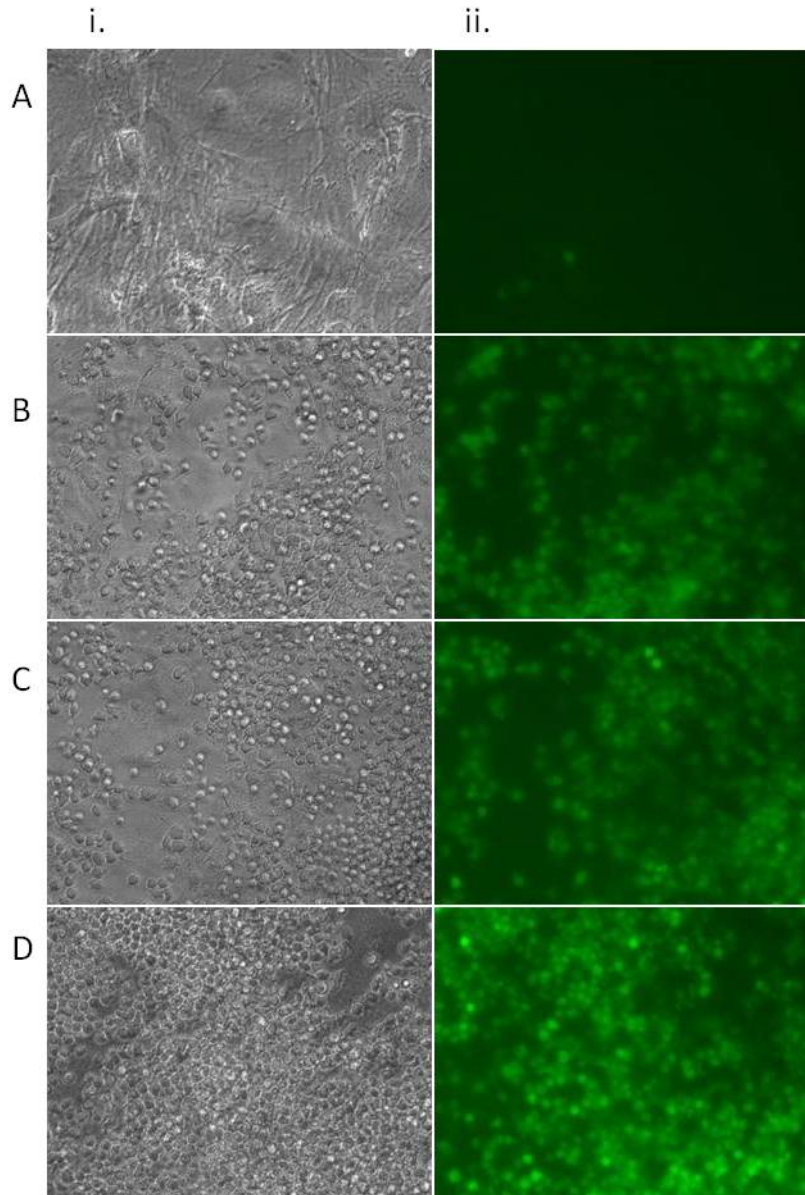


Figure 57 SEMTeton cultured on M210B4 feeder layers

SEMTeton were co-cultured on M210B4 feeders in several dilutions for 10 days (i.) Light-microscopic photographs (ii.) Fluorescence filtered photographs (A)  $0.2 \times 10^6$ , (B)  $1 \times 10^6$ , (C)  $4 \times 10^6$ , (D)  $10 \times 10^6$  cells / ml, magnification 200x

Fluorescent SEM were seeded on homogeneous feeder layers in concentrations of  $0.2 \times 10^6$  (top),  $1 \times 10^6$  (2<sup>nd</sup> from top),  $4 \times 10^6$  (3<sup>rd</sup> from top),  $10 \times 10^6$  (lowest) cells / ml (Figure 57). Cells on the left were captured using normal light microscopy, while cells on the right were captured in the GFP-channel. These images showed that the GFP signal provides an effective way to distinguish between feeder and leukaemic cells.

Furthermore, both these methods demonstrate a strong correlation between the seeding concentration and imaging results.

To get a more accurate analysis of cell numbers and to determine how distinguishable co-cultured cells are in a flow cytometric analysis, cells were trypsinized to remove SEMTeton bound to M210B4. Cell suspensions were analysed by flow cytometry, using SEM, SEM Teton and M210B4 cells as controls (Figure 58 and Figure 59). The number of M210B4 cells was kept constant with approximately  $10^5$  cells per 48 well plate. Consequently, the number of fluorescent leukaemic cells should always correspond to the ratio of detected M210B4 and leukaemic cells.

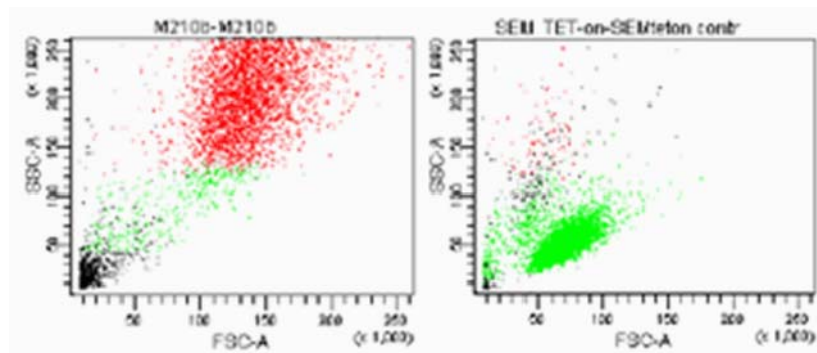


Figure 58 SSC – FSC Dot-Plots for M210B4 and SEMTeton

Flow cytometric analysis of M210B4 and SEM control cells. SSC – FSC Dot-Plots for M210B4 (Left) and SEMTeton (Right), red P1 (gated for M210B4), green P2 (gated for SEM), black (ungated cells).

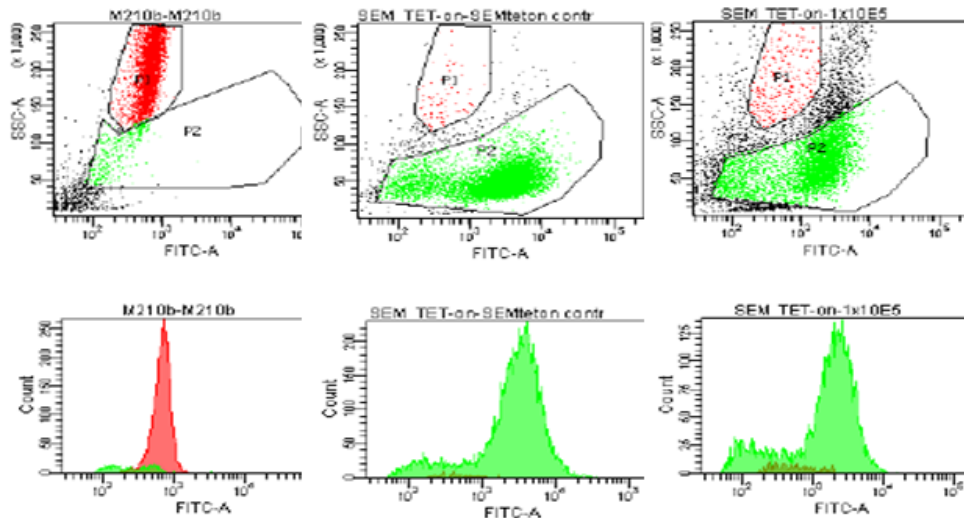


Figure 59 Flow cytometric analysis of M210B4, SEMTetron and co-cultures

A dilution of SEMTetron grown on feeders for 10 days (Right) and controls (M210B4, SEMTetron alone) were analysed by flow cytometry (TOP) Dot-plots SSC vs. green fluorescence (FITC), (Bottom) Histograms counts vs. Green fluorescence (Left) solely M210B4 (Middle) solely SEMTetron (Right) co-culture of M210B4 and  $1 \times 10^5$  SEMTetron, red P1 (gated for M210B4), green P2 (gated for SEM), black (ungated cells). Shown is one single experiment.

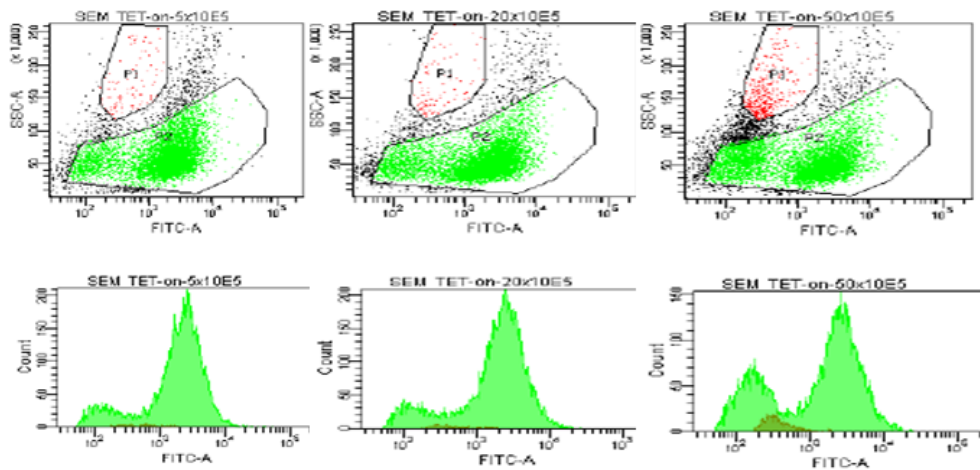


Figure 60 Flow cytometric analysis of M210B4 - SEMTetron co-cultures

Several dilutions of SEMTetron cells co-cultured on M210B4 for 10 days were analysed by flow cytometry (TOP) Dot-plots SSC vs. green fluorescence (FITC) (Bottom) Histograms counts vs. Green fluorescence co-cultures with (Left)  $5 \times 10^5$ , Middle:  $20 \times 10^5$  (Right)  $50 \times 10^5$  SEMTetron, red P1 (gated for M210B4), green P2 (gated for SEM), black (ungated cells). Shown is one single experiment.

The flow cytometric analysis plots and graphs above show the gating of the M210B4 fraction and the SEMTeton according to their size and fluorescence (Figure 58, Figure 59 and Figure 60). Since M210B4 showed strong auto-fluorescence itself, an intentional gap was left between the two gates to reduce the overspill of one cell-line into another gate. This unusual gate setting was necessary to distinguish between the two cell lines. The histograms show SEMTeton in green and M210B4 in red. The corresponding statistics are shown in table 9. They show how, using this analysis, it was possible to distinguish feeders from fluorescent cells using the numbers seeded to form the ratio, Fluorescent gate : M210B4 (p2/p1) gate. This relied on the fact that in a mix of these co-cultured cells and 10000 cells counted in the flow cytometric analysis, the ratio should have got bigger the more SEMTeton cells were present in the sample.

Although the ratio of numbers in the fluorescent gate were concentration dependant to the seeded amounts between  $0.2 \times 10^6$  and  $4 \times 10^6$  cells per ml, the range of concentrations showing proportionality between seeded and measured SEMTeton numbers were limited (see Table 9 and Figure 61).

Events	M210B4	SEMTeton	$1 \times 10^5$	$5 \times 10^5$	$20 \times 10^5$	$50 \times 10^5$
p1	4182	82	325	102	98	399
p2	422	9570	5862	8600	8962	7811
p2/p1	0.1	116.71	18.04	84.31	91.45	19.58

Table 9 Cells counts of M210B4, SEMTeton and co-cultures

Several dilutions of SEMTeton grown on M210B4 for 10 days and single cellline controls (M210B4, SEMTeton) were analysed by flow cytometry P1 M210B4 gate, P2 SEM Teton gate, p2/p1: part of SEMTeton to M210B4

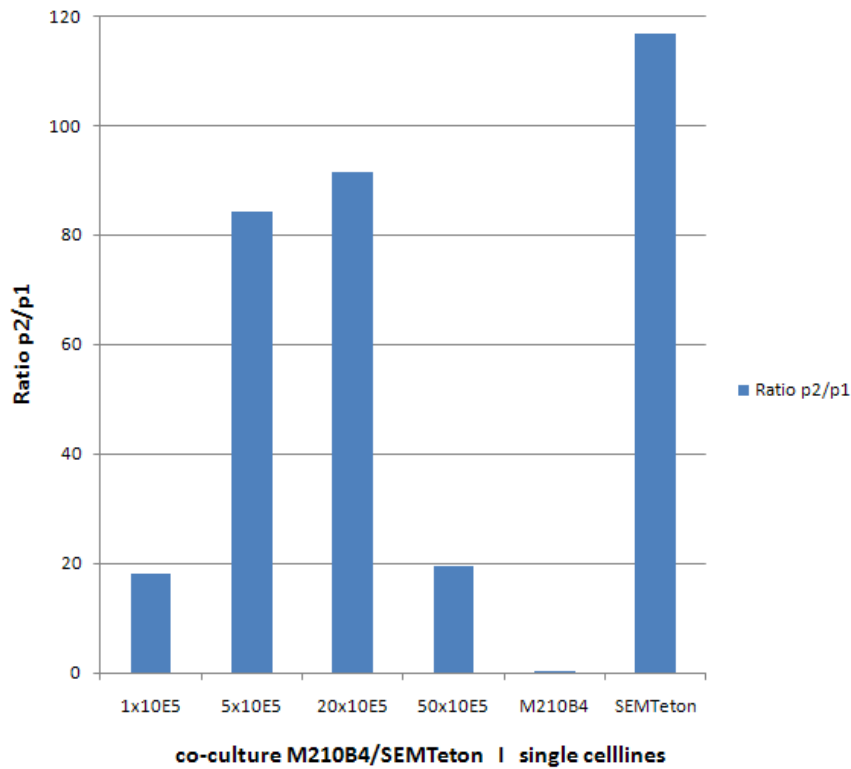


Figure 61 Cell counts of M210B4 and SEMTetron and co-cultures

Several dilutions of SEMTetron grown on M210B4 for 10 days and single cellline controls (M210B4, SEMTetron) were analysed by flow cytometry. Ratios of p2 (SEMTetron gate) against p1 (M210B4 gate) were related to seeded concentrations p2/p1: part of SEMTetron to M210B4 (p1 M210B4-, p2 SEMTetron gate). Shown is one single experiment.

The same analysis was performed for MV4;11Tetron co-cultured on M210B4 feeder layers. These are MV4;11 cells transduced with the lentiviral Tetron vector, as with SEMTetron (see Figure 62, Figure 63 and Figure 64).

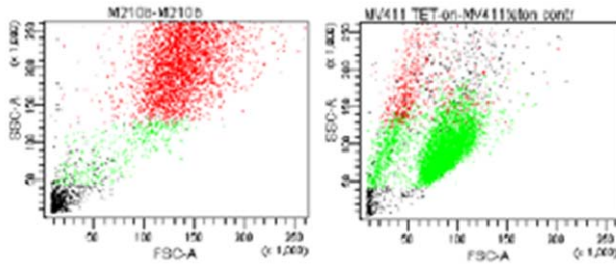


Figure 62 M210B4 and MV4;11Teton controls

M210B4 and MV4;11Teton controls were analysed by flow cytometry (Left) M210B4 (Right) MV4;11Teton. Shown are SSC – FSC Dotplots. The colours refer to the gates shown in Figure 64. Shown is one single experiment.

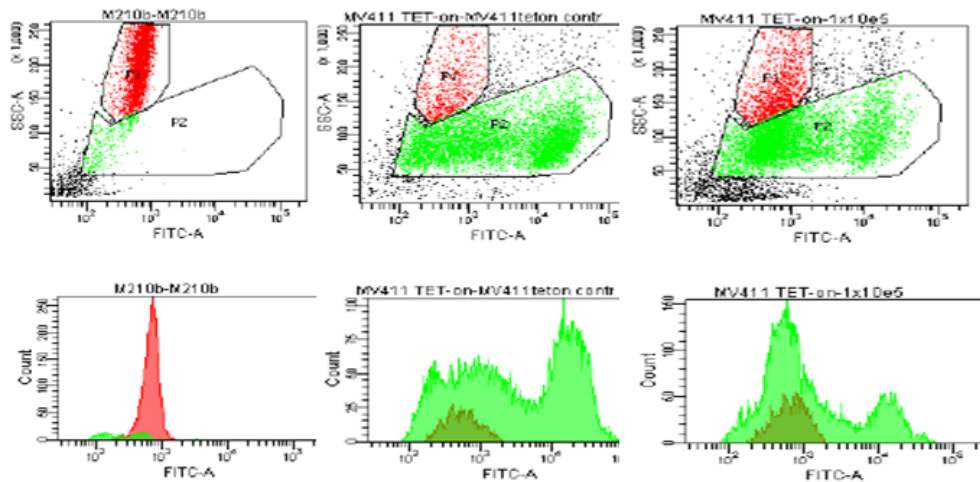


Figure 63 M210B4, MV4;11Teton and co-cultures analysed by flow cytometry

A dilution of M210B4 - MV4;11Teton co-cultured for 10 days and two controls (M210B4, MV4;11 alone) were analysed by flow cytometry (TOP) Dot-plots SSC vs. green fluorescence (FITC) (Bottom) Histograms counts vs. green fluorescence (Left) solely M210B4 (Middle) solely MV4;11Teton (Right) co-culture of M210B4 and  $1 \times 10^5$  MV4;11Teton. Shown is one single experiment.

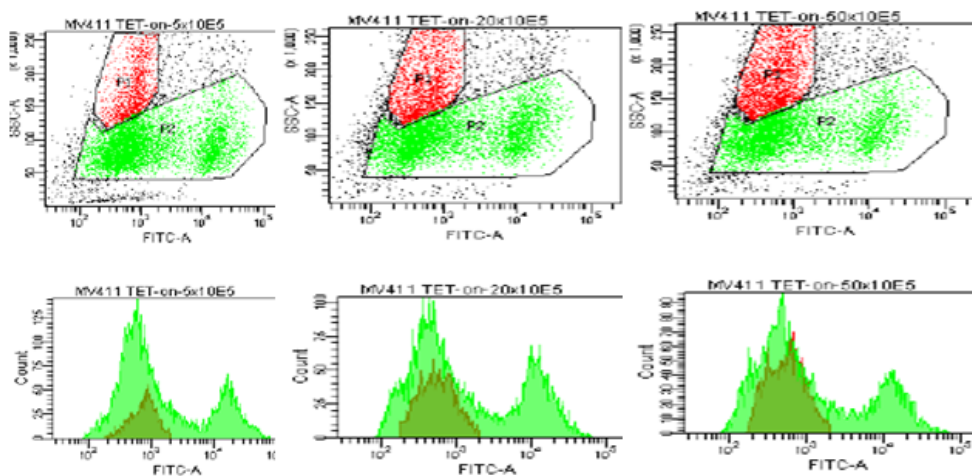


Figure 64 Flow cytometric analysis of M210B4 - MV4;11Teton co-cultures

M210B4 - MV4;11Teton co-cultured for 10 days in several dilutions were analysed by flow cytometry

(TOP) Dot-plots SSC vs. green fluorescence (FITC) (Bottom) Histograms counts vs. Green fluorescence co-cultures with (Left)  $5 \times 10^5$  (Middle)  $20 \times 10^5$  (Right)  $50 \times 10^5$  MV4;11Teton. Shown is one single experiment.

The flow cytometry plots and graphs above (Figure 62, Figure 63 and Figure 64) show the gating of the M210B4 fraction and the MV4;11Teton according to their size and fluorescence. The histograms show MV4;11Teton in green and M210B4 in red peaks. The corresponding statistics are shown in table 10. They show that this analysis was able to distinguish feeders from fluorescent cells using the numbers seeded and the ratio Fluorescent gate / M210B4 (p2/p1) gate. The range of concentrations showing proportionality between seeded and measured MV4;11Teton numbers was limited (see Table 10 and Figure 65).

Events	M210B4	MV4;11Teton	$1 \times 10^5$	$5 \times 10^5$	$20 \times 10^5$	$50 \times 10^5$
p1	4182	847	1671	1293	1948	2289
p2	422	8209	8009	7242	6246	5393
p2/p1	0.1	9.69	4.79	5.6	3.21	2.36

Table 10 Cells counts of M210B4, MV4;11Teton and co-cultures

Several dilutions of MV4;11Teton grown on M210B4 for 10 days and single cell controls (M210B4, MV4;11Teton) were analysed by flow cytometry. P1 M210B4 gate, P2 MV4;11Teton gate, p2/p1: part of MV4;11Teton to M210B4

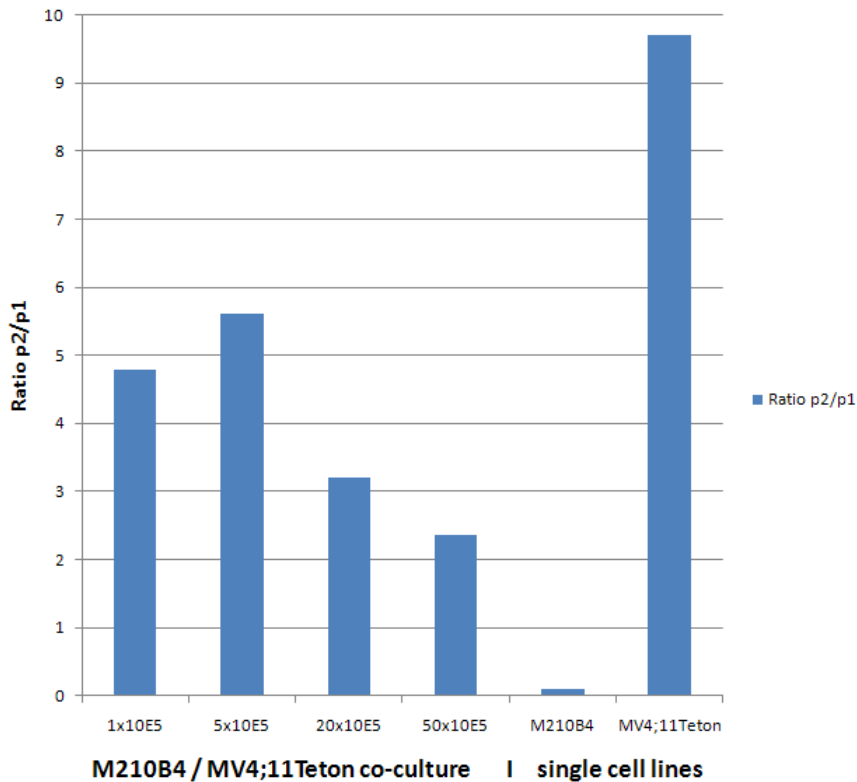


Figure 65 Cell counts of M210B4, MV4;11Teton and co-cultures

M210B4 – MV4;11 co-cultures were cultured for 10 days numbers determined by flow cytometry. Numbers ( $\times 10^5$ ) indicate MV4;11Teton cells per ml and a constant level of  $1 \times 10^5$  M210B4 cells per well, sp2/p1: part of MV4;11Teton to M210B4 (p1 M210B4-, p2 SEMTeton gate). Shown is one single experiment.

#### 4.3.3.3 Establishment of a flow cytometry based cell count assay

The majority of growth data of leukaemic cells on feeder layers in this thesis was generated by visual discrimination of leukaemic cells and M210B4 and by counting in triplicates. To develop a more automated and robust method the fact that, in a dense layer of growth arrested M210B4, the cell number per well was stable was used. For samples analysed by flow cytometry a certain number of cells were counted, here 10000 cells. The more leukemic cells there were in a well with a stable number of M210B4, the bigger the ratio between M210B4 and leukaemic cells was. In this method, the fluorescence of SEMTeton was used to distinguish the SEM from M210B4 as well. The most important differences to the previous flow analysis of M210B4 – SEM co-cultures



was the use of a different Flow cytometer (FACS Calibur) with less automated settings, logarithmic setting of the SSC channel and the use of irradiated M210B4 to set the gates (Figure 66 and Figure 67).

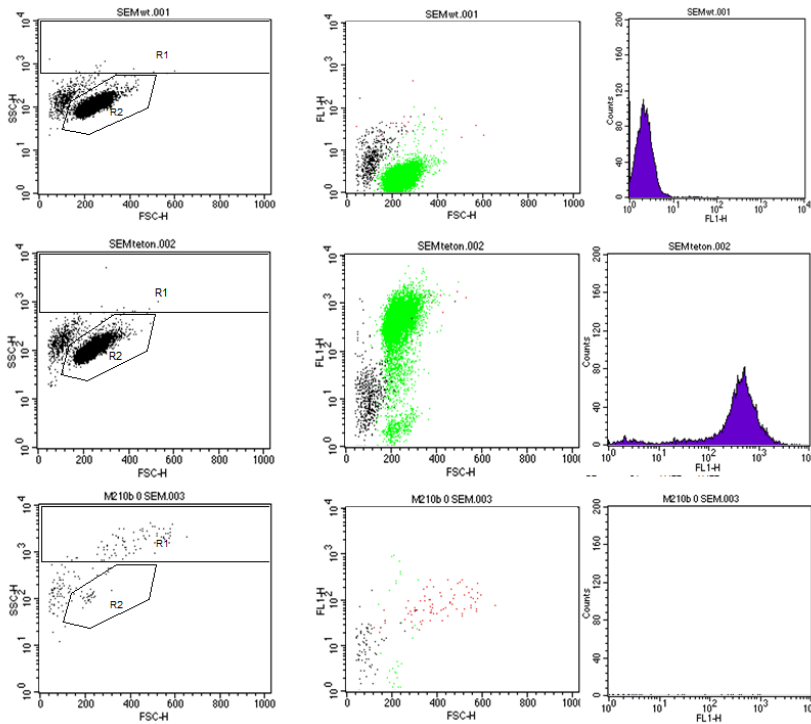


Figure 66 Flow cytometry discrimination of Feeders and SEMTetron

Flow cytometric analysis of SEM (Top row), SEMTetron (2nd row) and irradiated M210B4 (3<sup>rd</sup> row).

The gating for the discrimination of M210B4 was set using SEM, fluorescent SEMTetron and irradiated M210B4. The size and granularity was used to distinguish M210B4 from SEMTetron. M210B4 were gated in R1 and SEM in R2. SEMTetron green shift was recorded in the FL1 channel. (Left) SSC-FSC dot plot (Middle) GFP-FSC dot plot and (Right) counts-GFP histogram. Shown is one single experiment.

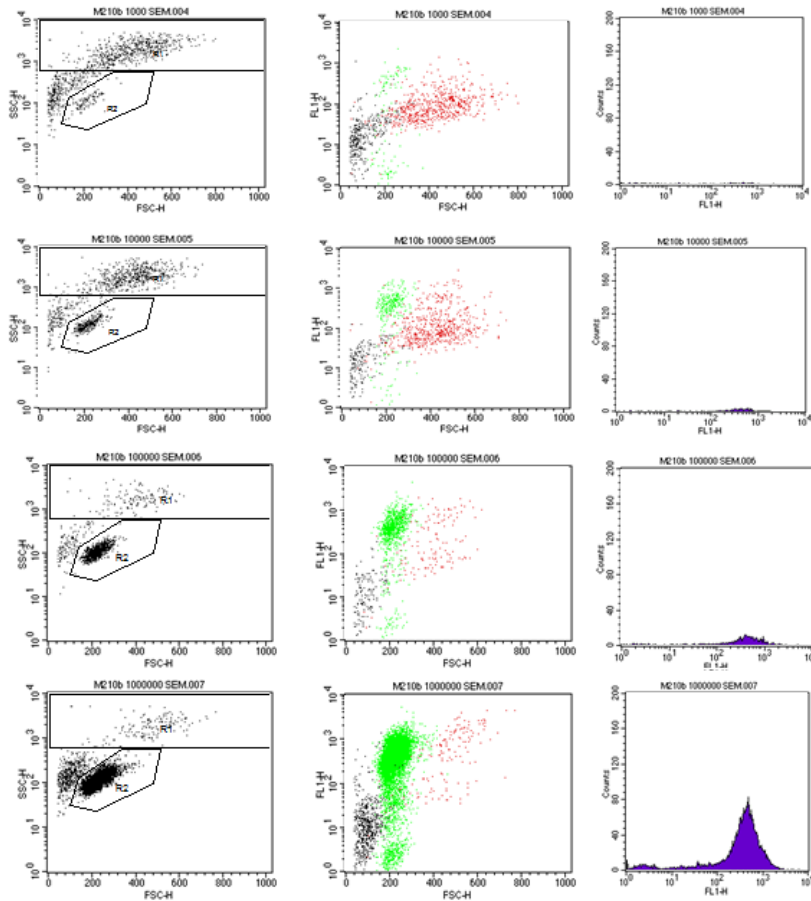


Figure 67 Flow cytometry discrimination of SEMTeton dilutions on feeders

10,000 cells of cell-mixtures from a M210B4 well of a 48 well plate (approx.  $10^5$  cells) and dilutions of SEMTeton were recorded by flow cytometry while the number of cells per M210B4 gate (R1) and SEMTeton gate (R2) was determined. Different numbers of SEMTeton were added per M210B4 well: + 1,000 (1<sup>st</sup> row), + 10,000 (2<sup>nd</sup> row), + 100,000 (3<sup>rd</sup> row), + 1,000,000 (4<sup>th</sup> row) (Left) SSC-FSC dot plot (Middle) GFP-FSC dot plot and (Right) counts-GFP histogram. Shown is one single experiment.

SEMTeton and M210B4 were gated by size and fluorescence (Figure 67 and Figure 66).

Cells were counted in the SEMTeton gate and the M210B4 gate. As controls SEM, SEMTeton and irradiated M210B4 were analysed. Then SEM in increasing numbers were added to wells with feeders.

Sample	M210B4	SEMTeton	SEMTeton/ M210B4	seeded cell number
M210b-SEM E3	598	104	0.173913	1000
M210b-SEM E4	575	289	0.502609	10000
M210b-SEM E5	131	942	7.19084	100000
M210b-SEM E6	88	5933	67.42045	1000000

Table 11 Statistics of Figure 66 and Figure 67

Numbers of M210B4 and SEMTeton detected from co-cultures, according to flow cytometry analysis shown in Figure 67.

The ratio of M210B4/SEMTeton showed a good linearity to the seeded cell numbers (see Table 11 and Figure 68).

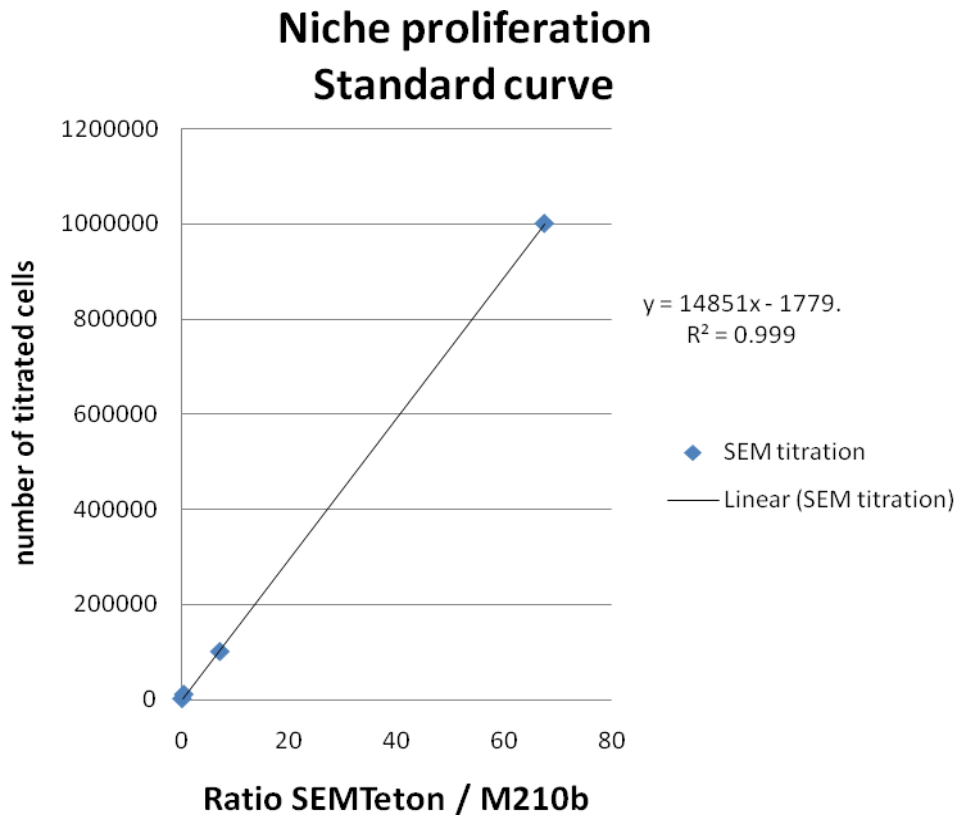


Figure 68 Niche proliferation standard curve

Standard curve of detected SEMTetron/M210B4 ratios against seeded concentrations of SEMTetron. SEMTetron were seeded at  $10^3$ ,  $10^4$ ,  $10^5$  and  $10^6$  cells per M210B4-feeder layer well. Data represent those in Table 11. Flow cytometric analysis was run using controls for greenshift (SEM, irradiated M210B4) and controls for SEMTetron gating and M210B4 (no feeders, SEMTetron and M210B4 irradiated). Shown is one single experiment.

The plot shows (Figure 68) that this method was practicable and proportional to the actual cell numbers throughout a wide range of concentrations. This provides a quick and reliable measure of cell number which is especially useful for large scale experiments, when different parameters are tested.

#### 4.3.3.4 Co-cultures of SEMTeton and MV4;11Teton on M210B4

To further investigate how well leukaemic cell-lines like SEM and MV4;11 can be visually distinguished from the feeder cells by size and shape further co-cultures of SEMTeton or MV4;11Teton with M210B4 feeder layers were incubated and captured by light-microscopy (see Figure 69).

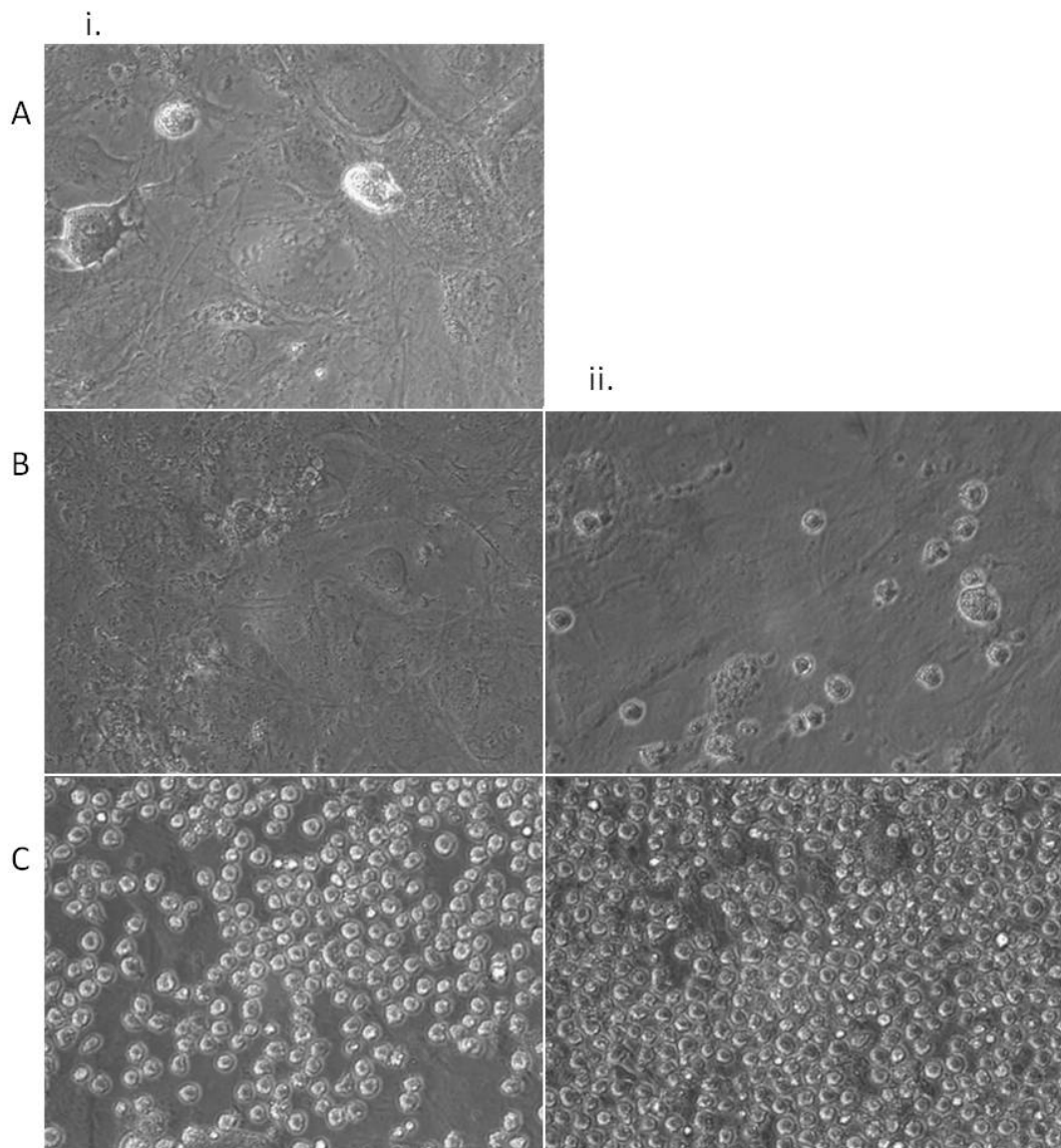


Figure 69 Co-culture images of Mv4;11Teton on M210B4 feeders

Growth arrested M210B4 feeder layers were co-cultured with dilutions of MV4;11Teton numbers (A i.) M210B4 (B i.)  $10^3$ -, (B ii.)  $10^4$  -, (C i.)  $10^5$  - and (C ii.)  $10^6$  -MV4;11TETon, magnification 200x.

The co-culture imaging (Figure 69) shows the basic M210B4 feeder layer (A) and the increasing numbers (from B i. to ii. to C i. and ii.) of small round bodied MV4,11Teton cells.

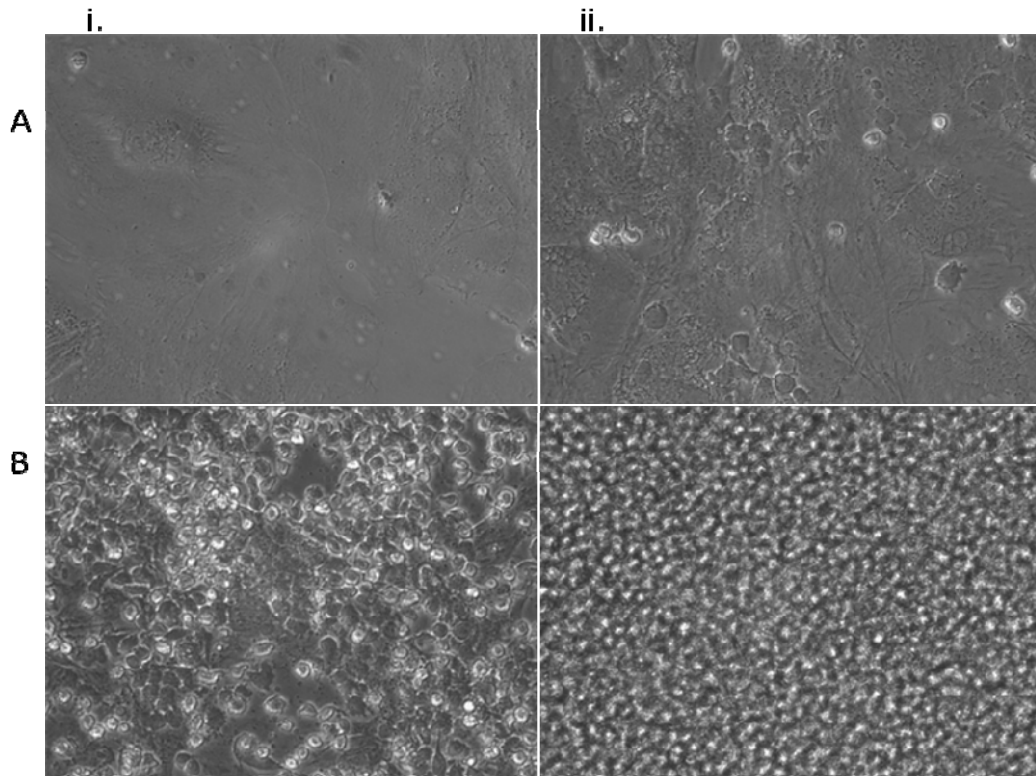


Figure 70 Co-culture images of SEMTeton on M210B4 feeders

Growth arrested M210B4 feeder layers were co-cultured with dilutions of SEMTeton. (A i.)  $10^3$ -, (A ii.)  $10^4$  -, (B i.)  $10^5$  - and (B ii.)  $10^6$  -SEMTETon, magnification 200x

The co-culture imaging above (Figure 70) shows the increasing numbers (from A i. -left, - A ii. to B i. and B ii.) of small round bodied SEMTeton cells. The basic M210B4 feeder layer can be found in the previous image panel (Figure 69 A i).

These two image-panels (Figure 70 and Figure 69) showed that in a wide concentration range the small, round bodied leukaemic cells can be easily distinguished from the fibroblast feeders. Additionally the focal level is different between them, as the leukaemic cells are found on top of the M210B4 cells.

### 4.3.3.5 Inversion test

The next question to be asked of the growth arrested M210B4 layers was if they were able to interact physically with the leukemic co-cultured cells, as bone marrow fibroblast cells would - by homo and hetero dimeric interactions of surface proteins. Visually, cells on top of the M210B4 seemed to adhere to them, because when shaken, leukaemic cells in the supernatant moved but not the ones directly on top of the feeders.

To rule out binding unrelated to feeder layer adherence molecules and to show real physical interaction of the cells, an inversion test was adapted to this system. SEM cells have not been used because they show a slight tendency to adhere to culture surfaces. Therefore, two non-adherent leukaemic cell-lines were chosen to demonstrate that it is the interaction with M210B4 which immobilizes the cells (see Figure 71).

These myeloid leukaemic cells were Kasumi-1 and SKNO-1, which are both t(8;21) positive AML-cell lines.

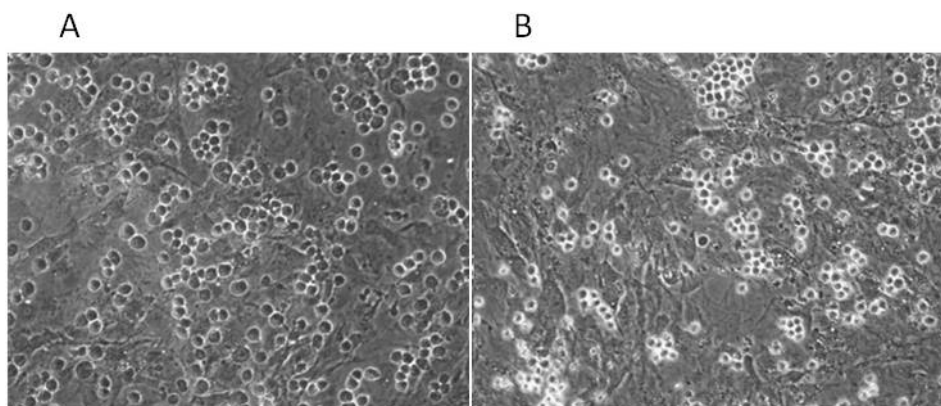


Figure 71 Images of M210B4 co-cultures with Kasumi-1 or SKNO-1  
Growth arrested M210B4 layers co-cultured with Kasumi-1 or SKNO-1 (A) KASUMI-1 on M210B4 (B) SKNO-1 on M210B4, magnification 200x

In the previous images (Figure 71) co-cultures of M210B4 and SKNO-1 or Kasumi-1 are shown. The SKNO-1 cells especially, have a tendency to form clusters. They appeared similar under the microscope and were cultured like ALL-cells.

The principle of this test was that the co-culture was turned upside down; cells not bound by interactions to the feeder layer sunk down, moved away by gravity and were removed after 1-2h incubation by gravity leaving only fibroblasts and cells attached to them (see Figure 72).

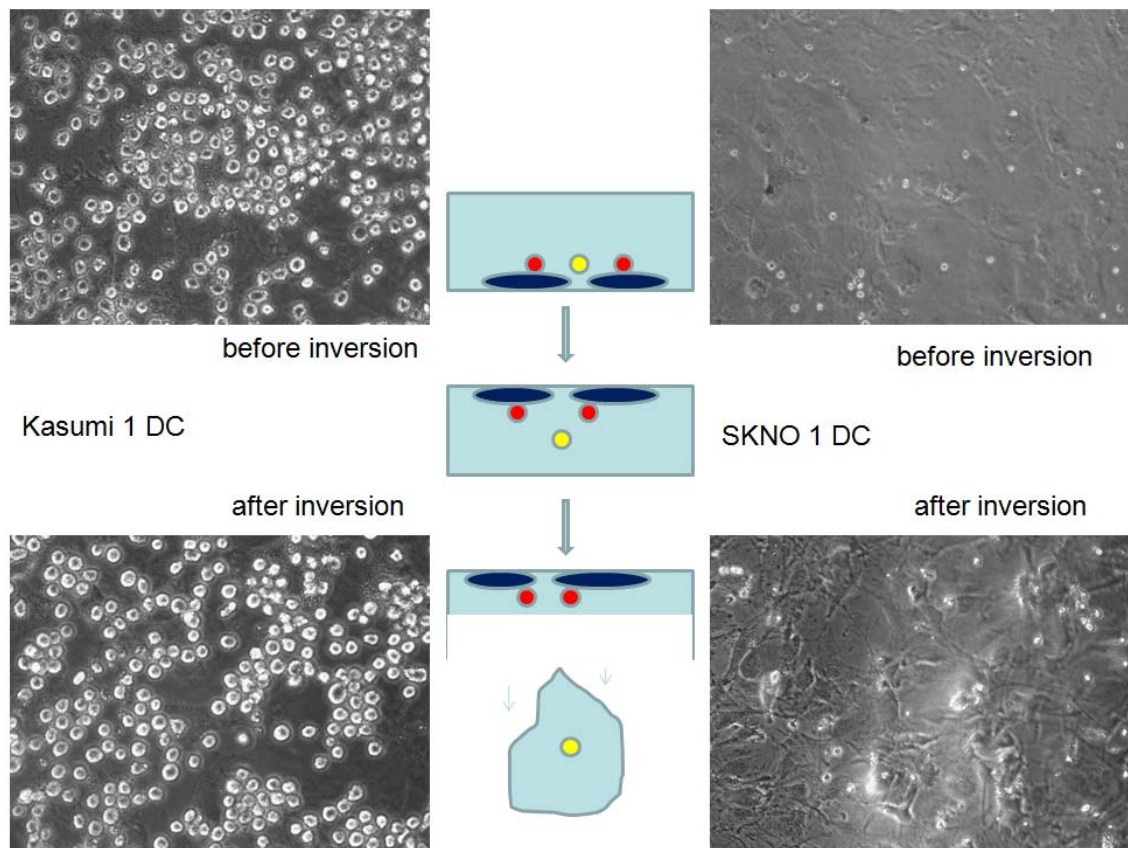


Figure 72 Inversion experiment on M210B4 Feeder

Cells grown on M210B4 feeders were inverted and separated from the feeders by gravity if they were not physically attached to them. The principle is shown in the schematic in the middle. (Top) before inversion (Bottom) after inversion (Right) Kasumi-1 (Left) SKNO-1, magnification 200x



These images (Figure 72) showed that after incubation the cell-numbers on the feeder did not decrease much. This result supported the finding that cells are attached to M210B4 by stronger interactions.

#### **4.3.4 Fusion gene knock down and feeder interaction**

After developing and testing the bone-marrow-fibroblast - leukaemic-cell interaction assay, the effect of those interactions on growth, and hence doubling times, was investigated.

Several questions were addressed in the following experiments:

1. Does co-culture of leukaemic cells on feeders affect the knockdown of the corresponding fusion gene by siRNA?
2. If not, how does the feeder affect the phenotypic consequences of MLL/AF4 or AML1/MTG8 knockdown?

Before siRNA treatment of SEM, SEMTeton and Kasumi-1 DC (lentivirally transduced by Vasily Grinev, expressing Dsred) and feeder co-cultures was performed, it had to be shown that, firstly, successful knockdown of fusion genes could be demonstrated in siRNA treated cells in M210B4 co-culture, and secondly, that the two transduced cell lines SEMTeton and Kasumi-1 DC are still accessible to siRNA mediated fusion gene depletion. This is addressed in the two following diagrams (Figure 73 and Figure 74).

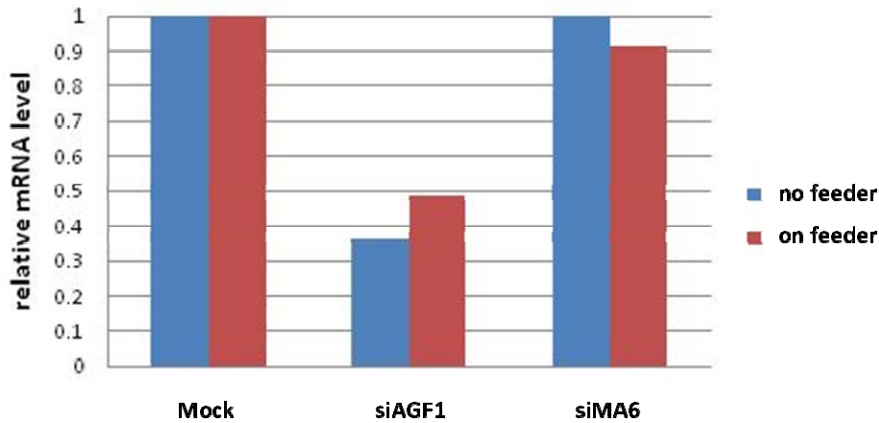


Figure 73 *AML/MTG8* knockdown in Kasumi-1 DC

Electroporation of Kasumi-1 DC with siAGF1 and siMA6, cultured with and without feeders. The relative mRNA level of *AML/MTG8* was detected by qRT-PCR. siAGF1: siRNA against *AML/MTG8*, siMA6: active siRNA control (in Kasumi), Mock: no-siRNA control; red columns: cultured on feeders, blue columns: cultured without feeders. The relative mRNA levels were corrected to Mock. Shown is one representative experiment

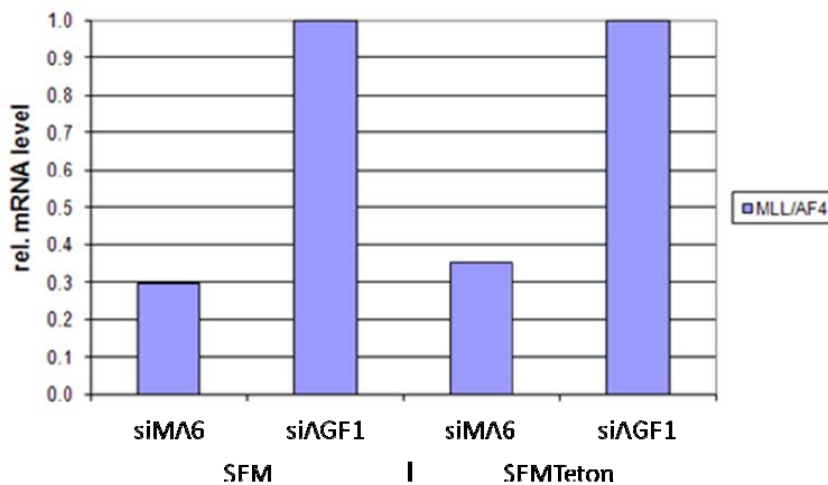


Figure 74 *MLL/AF4* expression in siRNA treated SEM and SEMTetron

SEM and SEMTetron were electroporated with siAGF1 and siMA6. The relative mRNA levels of *MLL/AF4* were detected by qRT-PCR. siAGF1: active siRNA control (in SEM, SEMTetron), siMA6: siRNA against *MLL/AF4*. The relative mRNA levels were corrected to AGF1. Shown is one representative experiment.

The transcript expression data (Figure 73 and Figure 74) show that fusion gene depletion was present not only in control cells, but also in co-cultured cells. Single

control wells with M210B4 did not provide enough mRNA for cDNA synthesis, only if several wells were pooled. The fusion gene transcripts could not be detected even in increased concentrations of RNA input. This showed that the M210B4 did not influence these results.

This answers the first question stated above; incubation on feeder did not substantially affect the degree of knockdown of either fusion gene.

When qRT-PCR was performed with primers for *MLL/AF4* in Kasumi1-DC negative for *MLL/AF4* and primers for *AML/MTG8* in SEMTeton negative for *AML/MTG8*, the Ct-values for *MLL/AF4* and *AML/MTG8* were high. The Cts were detected approximately 15 cycles later than in cell lines expressing the fusion product. This proves that using siMA6 to deplete *MLL/AF4* in SEM and as a control siRNA in Kasumi-1 while using siAGF1 to deplete *AML/MTG8* in Kasumi-1 and as a control in SEM, is a reliable system to investigate transcript levels of those cells on M210B4.

To answer the second question raised before, SEM were electroporated with no siRNA (Mock), *MLL/AF4* siRNA (siMA6) or siControl (siAGF1).

After knockdown the cells were either diluted 1/20 or 1/40 from the standard culture condition of  $0.5 \times 10^6$  cells/ml, which corresponds to 0.25 or  $0.125 \times 10^5$  cells / ml and incubated on feeders for 8 days (see Figure 75 and Figure 76).

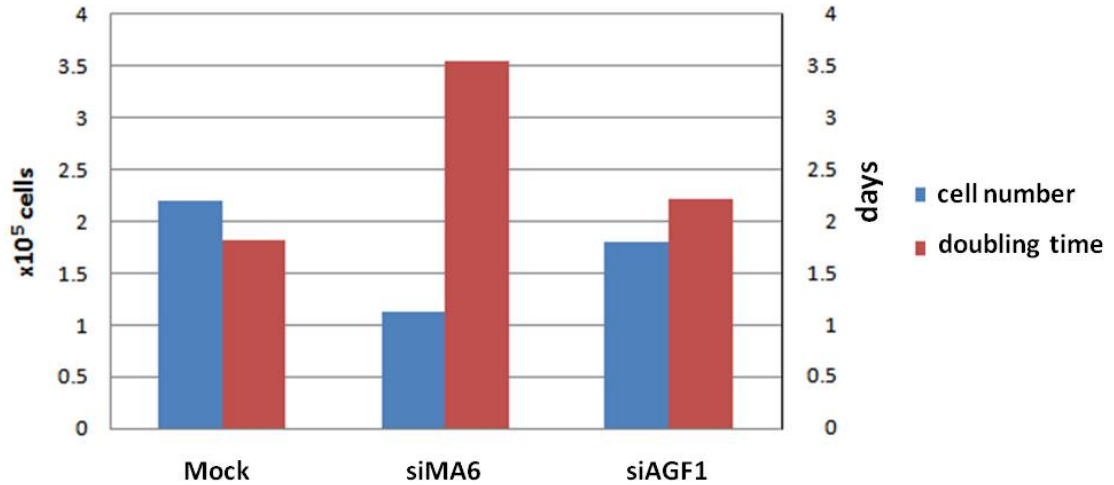


Figure 75 SEM electroporated and co-cultured on feeder in 1/20 dilution

SEM were with siMA6 and siAGF1, diluted to  $0.25 \times 10^5$  cell/ml and cultured on feeders. (Left axis, blue columns) number of SEM counted  $\times 10^5$  (Right axis, red columns) doubling time in days siAGF1: active siRNA control (in SEM), siMA6: siRNA against MLL/AF4, Mock: no siRNA control. Shown is one representative experiment.

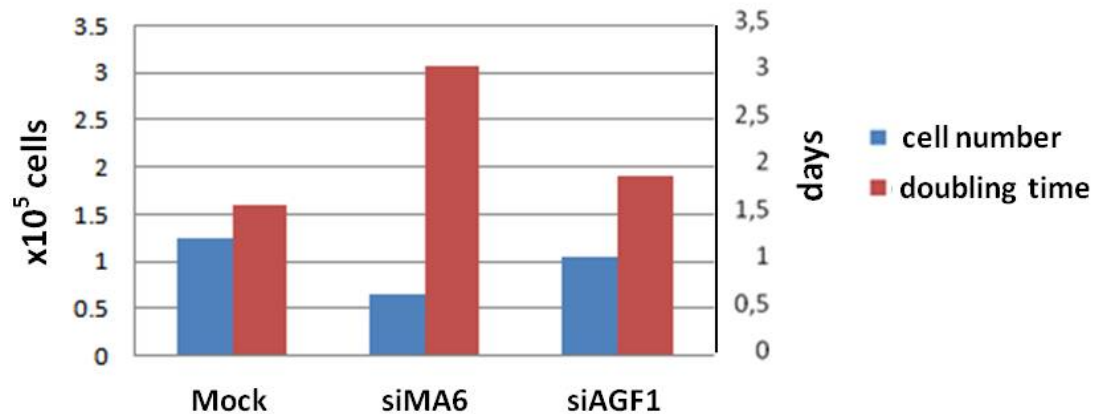


Figure 76 SEM electroporated and co-cultured on feeder in 1/40 dilution

SEM electroporated Mock, with siMA6 and siAGF1 diluted to  $0.125 \times 10^5$  cell/ml and cultured on feeders (Left axis, blue columns) number of SEM counted  $\times 10^5$  (Right axis, red columns) doubling time in days siAGF1: active siRNA control (in SEM), siMA6: siRNA against MLL/AF4, Mock: no siRNA control. Shown is one representative experiment.

The resulting cell counts (Figure 75 and Figure 76) showed decreased numbers in MLL/AF4 depleted cells compared to controls and hence increased doubling times.

To investigate the influence of the feeder co-culture on cell functions such as proliferation, gene expression and apoptosis, two cell-lines; one ALL (SEM) and one AML (Kasumi-1) were compared following fusion gene knockdown and culture with and without a feeder layer.

The fusion-transcript of SEM *MLL/AF4* was depleted with siMA6 and the fusion transcript of Kasumi-1 AML/*MTG8* was depleted with siAGF1. Because the SEM cells transcribe no AML/*MTG8* and Kasumi-1 transcribe no *MLL/AF4*, siAGF1 has also been used as an active siRNA control in SEM and siMA6 in was used in Kasumi-1 vice versa.

Following this validation, SEM and Kasumi-1 were electroporated with siRNA to knockdown their fusion genes and then seeded in different concentrations on feeder and control wells without feeder. The cultures were analysed by counting after trypsinisation and visual discrimination, as explained before (Figure 77 and Figure 78).

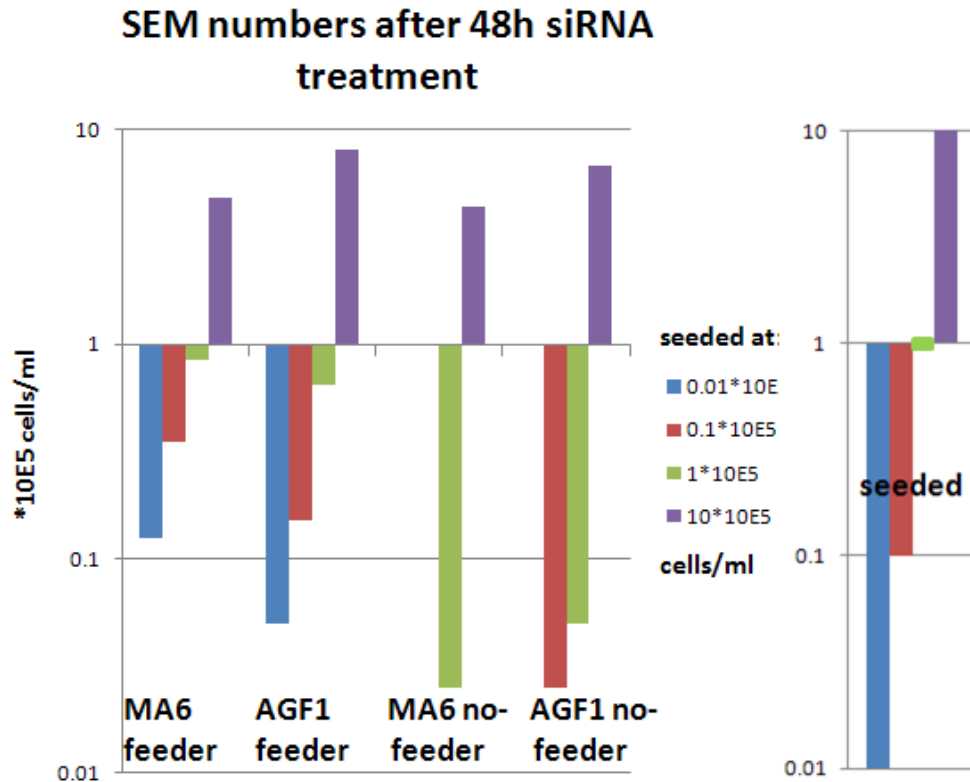


Figure 77 siRNA treated SEM seeded in dilutions with and without feeders

SEM electroporated with siMA6 and siAGF, seeded in a high concentration range (0.01, 0.1, 1 and 10  $\times 10^5$  cells/ml) with or without feeders and cultured for 48h. The y-axis shows counted leukaemic cell numbers displayed as  $\times 10^5$  cells/ml in a logarithmic scale. siMA6 is targeted against *MLL/AF4* while siAGF1 is the siRNA control. right: simulated display at which concentration cells were seeded; violet columns  $10 \times 10^5$  -, green columns  $1 \times 10^5$  -, red columns  $0.1 \times 10^5$  - and blue columns  $0.01 \times 10^5$  - cells/ml. Shown is one single experiment.

The diagram above (Figure 77) shows SEM with anti *MLL/AF4* siRNA (siMA6) treatment and an active siRNA control (siAGF1) either cultured in normal wells (no feeders) or on M210B4 feeders. Cells were seeded in parallel at different concentrations (0.01, 0.1, 1 and 10  $\times 10^5$  cells/ml) and incubated for 2 days. The seeded numbers are shown in the right.

As expected, cells electroporated with the control siRNA, siAGF1, show higher cell numbers with feeders than without feeders. This effect is more pronounced with lower cell numbers seeded considering the logarithmic scale. In the group of the same seeded concentration, SEM cultured on feeders showed higher concentration of cells. The

lowest concentration (AGF1 no feeder) and the two lowest concentrations (MA6 no feeder) were too small to count. Comparing the cells kept on feeders and the ones cultured alone there is a strong tendency towards the following: the lower the concentration of cells, the more their cell number benefit from the feeder interaction. Whether this is due to increased proliferation, decreased apoptosis or both will be addressed later.

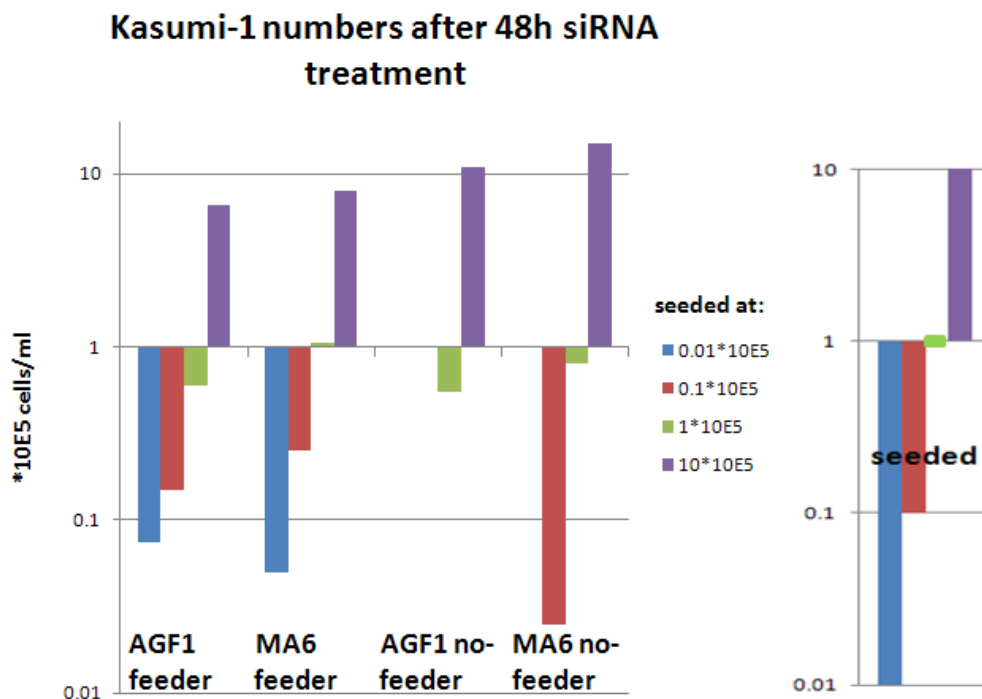


Figure 78 siRNA treated Kasumi-1 seeded in dilutions with and without feeders

Kasumi-1 were electroporated with siMA6 and siAGF, seeded in a high concentration range (0.01, 0.1, 1 and 10  $\times 10^5$  cells/ml) with or without feeders and cultured for 48h. The y-axis shows the cell concentrations as  $\times 10^5$  cells/ml in a logarithmic scale. Here siMA6 is the siRNA control while siAGF1 is the siRNA against the fusion gene *AML/MTG8* right: simulated display at which concentration cells were seeded violet columns  $10 \times 10^5$  -, green columns  $1 \times 10^5$ -, red columns  $0.1 \times 10^5$ - and blue columns  $0.01 \times 10^5$  - cells/ml. Shown is one single experiment.

The Figure 78 shows Kasumi-1 with anti *AML/MTG8* siRNA (siAGF1) treatment and an active siRNA control (siMA6) either cultured in normal wells or on M210B4 feeders. Cells were seeded in parallel at different concentrations (0.01, 0.1, 1 and 10  $\times 10^5$  cells/ml) and incubated for 2 days.

On the very right the seeded numbers are shown. Cells electroporated with the control siRNA siMA6 show slightly higher cell numbers when cultured with feeders than without feeders. With lower seeded cell numbers this effect is more pronounced considering the logarithmic scale. When the same concentration was seeded, Kasumi-1 kept on feeders showed higher concentration of cells. The lowest concentration (MA6 no feeder) and the two lowest concentrations (AGF1 no feeder) were too small to count. Comparing the cells kept on feeders and the ones cultured alone there is a strong tendency towards: the lower concentration at which cells are kept, the more their cell number benefit from the feeder interaction. Again the question of increased proliferation, decreased apoptosis will be addressed for SEM later.

In both cell lines, when grown on feeders, the lowest seeded group showed more cells in the fusion gene depleted samples than the controls. This seems to be contradictory to what is expected and published. However this was usually measured in concentrations almost 1000 fold higher than the lowest concentrations here (blue column). The explanation for higher numbers of fusion gene depleted cells than control siRNA treated ones when grown on feeders, could be inexact counting in low concentrations. The higher concentrations show expected effects (about twice as many cells in control siRNA groups). The most important effects on cell numbers were shown by the comparison with and without feeder culture.

The two cell-lines showed a similar result. At high concentrations of  $1 \times 10^6$  cells/ml there was no difference in cell numbers between co-cultured and non co-cultured cells. At the lower the concentrations, a more substantial difference between co-cultured and control cells was seen.



### 4.3.5 Investigation of feeder influence on fusion gene depletion derived gene expression and viability

SEMTeton and Kasumi-1 DC treated with siRNA to knockdown their fusion genes were seeded in different concentrations on feeder and control wells. The cultures were analysed by counting leukaemic cells and images of feeder co-cultures were captured (Figure 79).

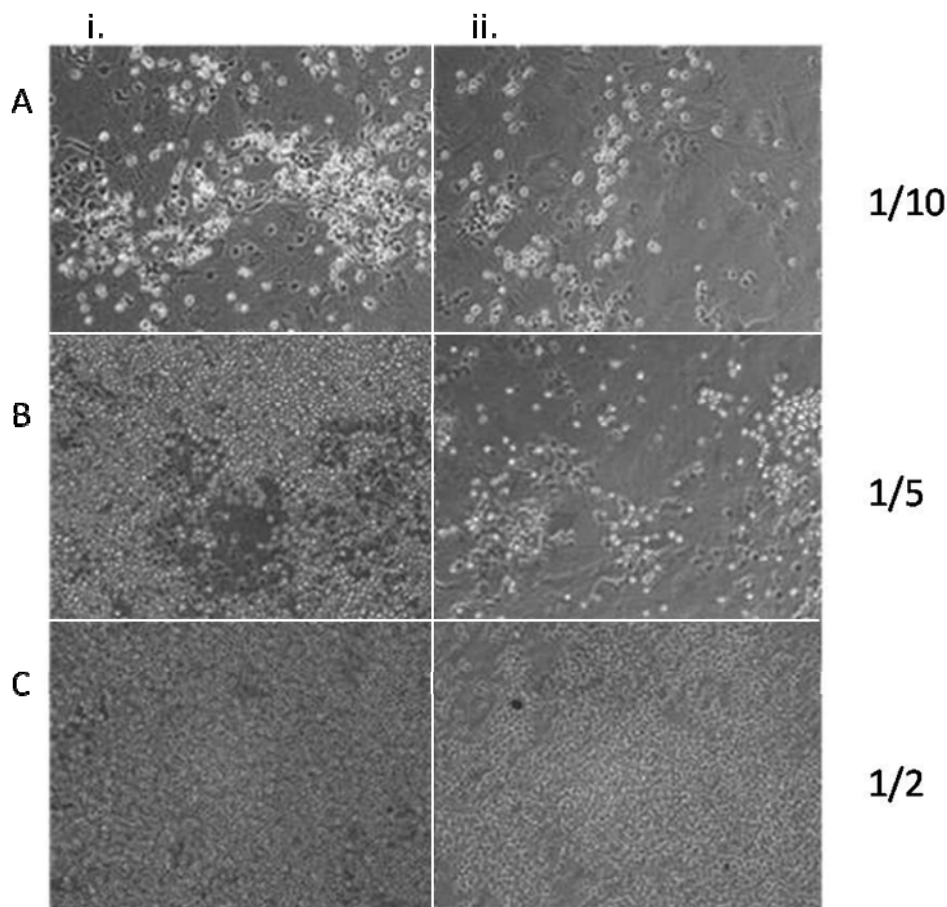


Figure 79 *MLL/AF4* depletion in SEMTeton on feeders

SEMTeton treated with siAGF1 (i.) and siMA6 (ii.) seeded in 3 dilutions on M210B4. (A) 1/10 -  $0.5 \times 10^5$  cells/ml (B) 1/5 -  $1 \times 10^5$  cells/ml and (C) 1/2 -  $2.5 \times 10^5$  cells/ml dilution, magnification 200x

On the left side of Figure 79 (i.), SEMTeton treated with siAGF1 (control siRNA) were seeded in 3 concentrations: lowest ( $0.5 \times 10^5$  cells/ml) (A), double ( $1 \times 10^5$  cells/ml) (B) and 5-fold ( $2.5 \times 10^5$  cells/ml) (C). On the right side (ii.) SEMTeton were treated with the

fusion gene specific siRNA (siMA6). They were seeded as the siAGF1 treated cells had been.

These images showed that the cell number is decreased in the siMA6 group, which is best seen in the density difference at highest concentration. The corresponding cell numbers of co-cultured cells and feeder free cells are shown in the following diagrams (Figure 80 and Figure 81).

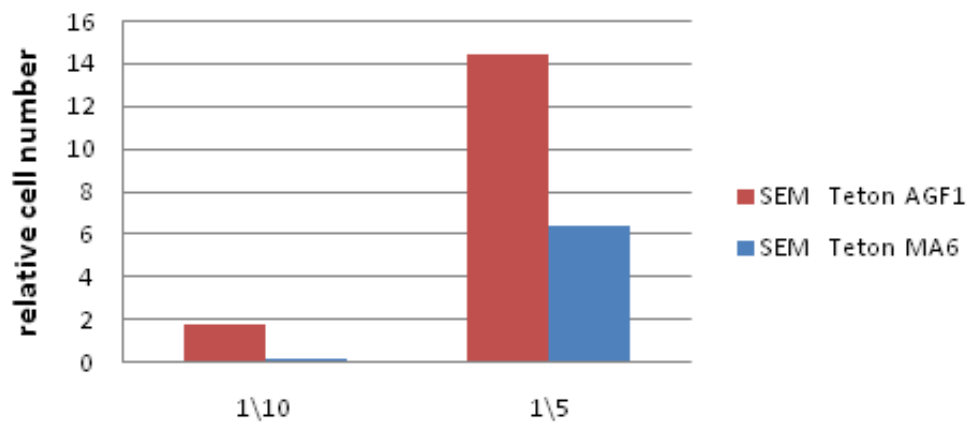


Figure 80 Cell numbers of MLL/AF4 depleted SEMTeton without feeders

Relative cell numbers of SEMTeton treated with siMA6 and siAGF1, cultured without feeders. Cells were diluted after electroporation and cultured without feeders. (Left) 1/10 dilution -  $0.5 \times 10^5$  cells/ml (Right) 1/5 -  $1 \times 10^5$  cells/ml. Blue columns: siMA6 treated, Red columns: siAGF1 treated, siMA6: fusion transcript directed and siAGF1 control siRNA. Shown is one representative experiment.

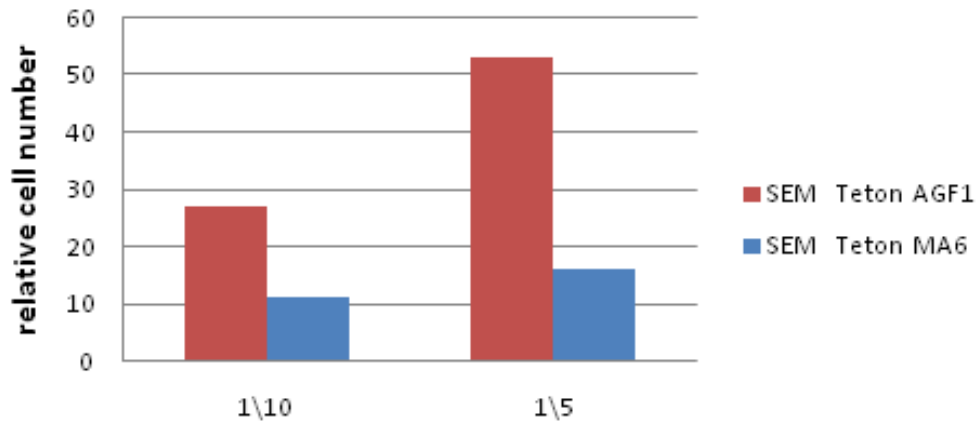


Figure 81 Cell numbers of MLL/AF4 depleted SEMTet on feeders

Relative cell numbers of SEMTet treated with siMA6 and siAGF1; cultured on feeders. (Left) 1/10 -  $0.5 \times 10^5$  cells/ml dilution (Right) 1/5 -  $1 \times 10^5$  cells/ml dilution after electroporation Blue columns: siMA6, Red columns: siAGF1; siMA6: fusion transcript directed siRNA and siAGF1: control siRNA Shown is one representative experiment.

The same experiment was performed with Kasumi-1 DC cells to show a broader relevance of the feeder's interactions with leukaemic cells (see Figure 82).

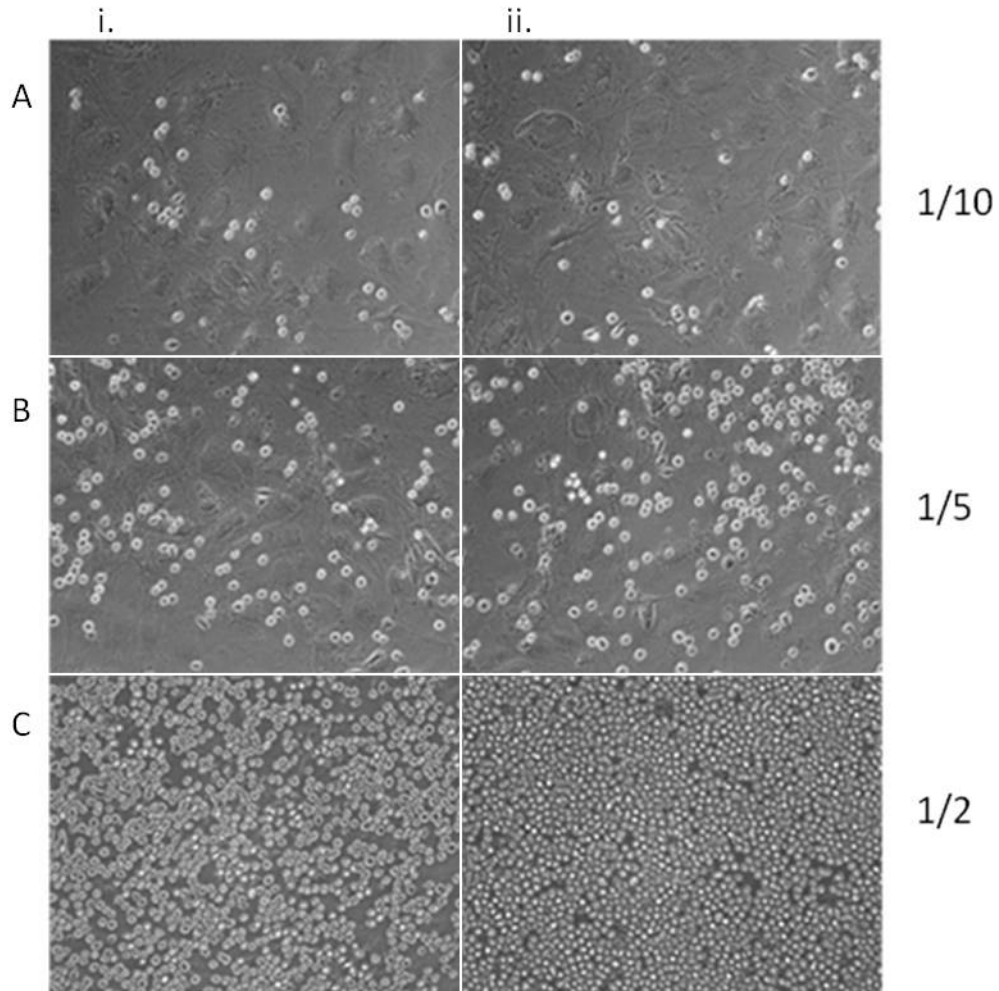


Figure 82 Fusion gene depletion in Kasumi-1 DC on feeders

Kasumi-1 DC were treated with siAGF1 and siMA6 and seeded in 3 dilutions on M210B4. (A) 1/10 -  $0.5 \times 10^5$  cells/ml (B) 1/5 -  $1 \times 10^5$  cells/ml and (C) 1/2 -  $2.5 \times 10^5$  cells/ml dilution. i. siAGF1 and ii. siMA6, magnification 200x

On the left side (i.) of Figure 82, Kasumi-1 DC treated with siAGF1 (Fusion gene specific) were seeded in 3 concentrations: 1/10 ( $0.5 \times 10^5$  cells/ml) (A), 1/5 ( $1 \times 10^5$  cells/ml) (B) and 1/2 ( $2.5 \times 10^5$  cells/ml) (C). On the right side (ii.) Kasumi-1 DC were treated with the control siRNA (siMA6). They were seeded as the siAGF1 treated cells had been.

These images show that the cell number is decreased in the siAGF1 group, which is best seen in the density difference at highest concentration.

The corresponding cell numbers of co-cultured cells and feeder free cells are shown in the following diagrams (Figure 83 and Figure 84).

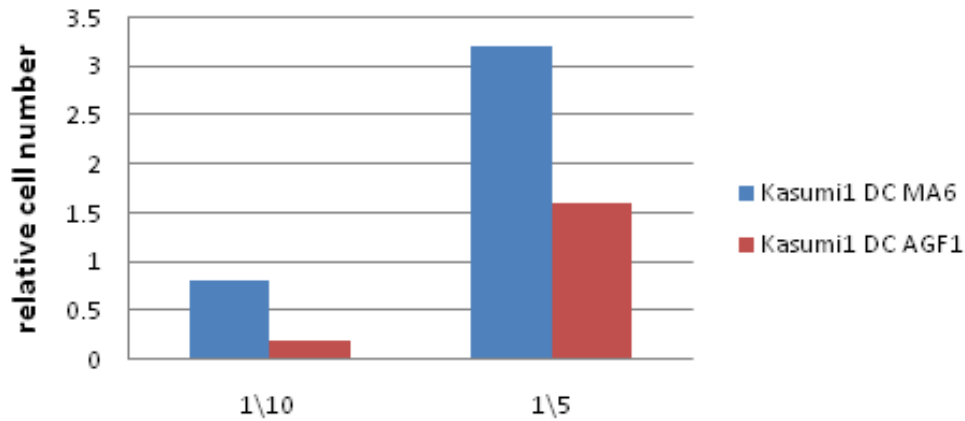


Figure 83 Relative cell numbers of Kasumi-1 DC treated with siMA6 without feeders  
Kasumi-1 DC were treated with siMA6 and siAGF1, diluted after electroporation and cultured without feeders. (Left) 1/10 -  $0.5 \times 10^5$  cells/ml (Right) 1/5 -  $1 \times 10^5$  cells/ml Blue columns: treated with siMA6, Red columns: treated with siAGF1. Shown are averages of triplicates of one single experiment.

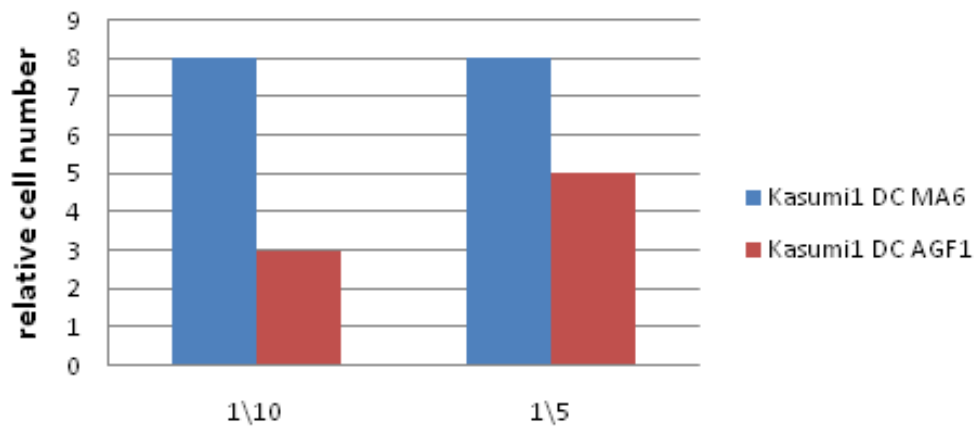


Figure 84 Relative cell numbers of Kasumi-1 DC treated with siMA6 on feeders  
Kasumi-1 DC were treated with siMA6 and siAGF1, diluted after electroporation and cultured on feeders. (Left) 1/10 -  $0.5 \times 10^5$  cells/ml (Right) 1/5 -  $1 \times 10^5$  cells/ml Blue columns: treated with siMA6, Red columns: treated with siAGF1. Shown are averages of triplicates of one single experiment.

From this point, after establishing the feeder –leukaemic cell interaction assay, studies to investigate the role of fusion genes in bone marrow fibroblast - leukaemic interaction used only the MLL/AF4 positive ALL cell line SEM.

In the previous chapter, interesting possible target genes of MLL/AF4 were identified. Several of those genes strongly pointed towards a role in niche biology. The most interesting candidates, like *FGFR1* and *N-CADHERIN* were tested with this established system.

SEM were treated with siMA6 and siAGF1 and then either cultured in normal wells or on M210B4 feeders. After 4 days, these SEM were harvested and an analysis of their transcript-levels was performed (see Figure 85).

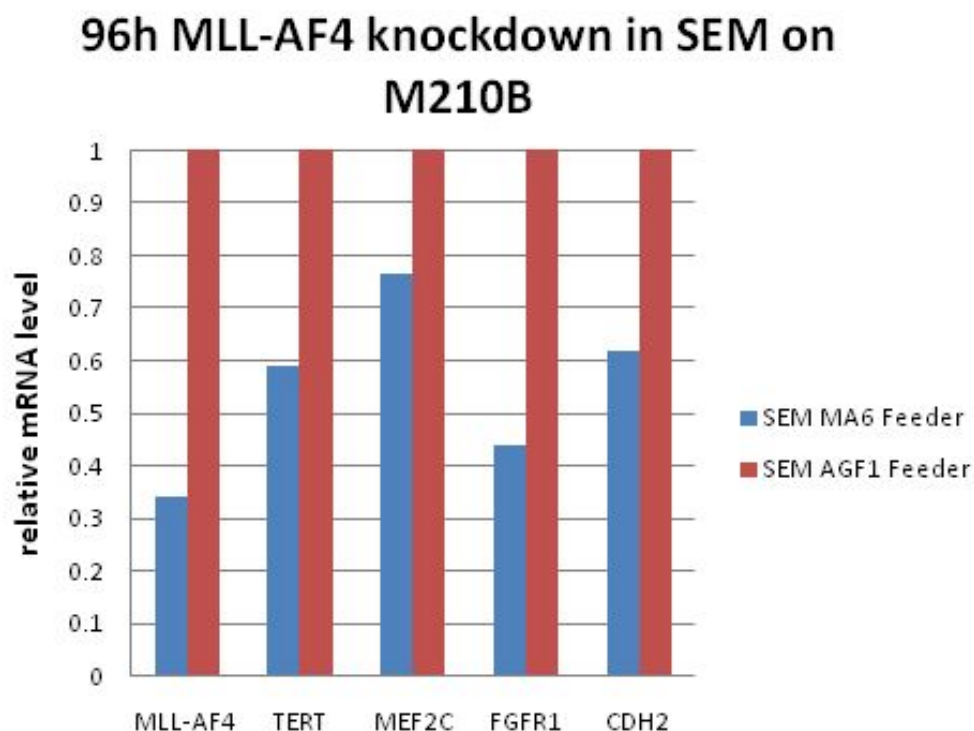


Figure 85 Gene expression changes of MLL/AF4 depleted SEM kept on feeders. Electroporated SEM cells were kept on feeders for 96h. Blue columns: siMA6 treated cells, Red columns: siAGF1 (control) treated cells. The relative mRNA levels were normalised to siAGF1. Shown is one representative experiment.

The diagram above (Figure 85) shows relative transcript levels normalized to GAPDH as a housekeeping gene and to AGF1, the siRNA control, which was set to 1. The blue columns show transcript levels of cells treated with siMA6 while red columns represent siAGF1 treated cells. These cells were kept on M210B4 feeders for 4 days.

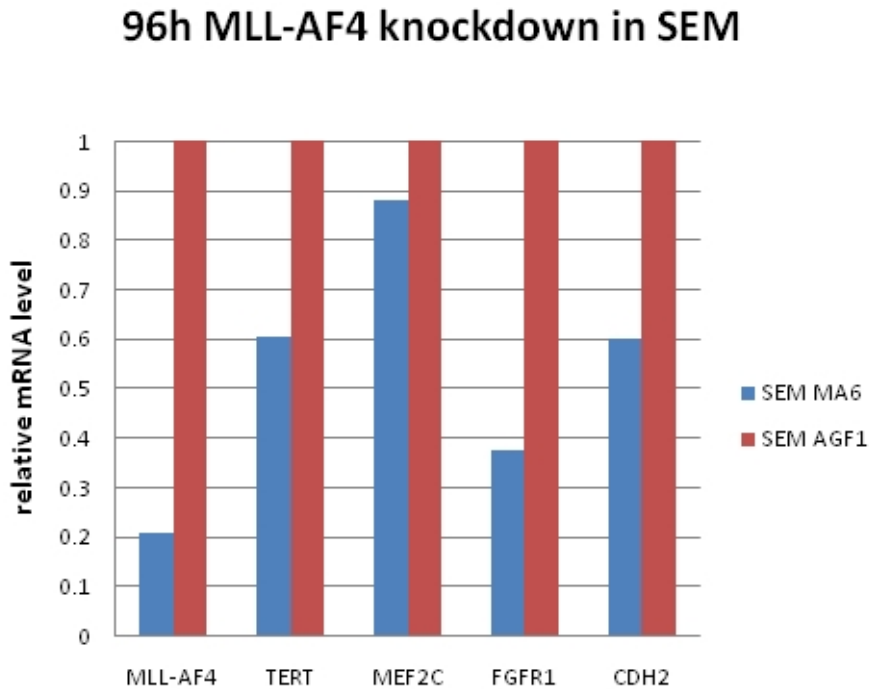


Figure 86 Gene expression changes of MLL/AF4 depleted SEM without feeders  
SEM were electroporated with siMA6 and siAGF1 and cultured for 96h without feeders. Blue columns: siMA6 treated cells, Red columns: siAGF1 treated cells. The relative mRNA levels were normalised to siAGF1. Shown is one representative experiment.

The diagram above (Figure 86) shows relative transcript levels normalized to GAPDH as a housekeeping gene and to AGF1, the siRNA control, which is set to 1. The blue columns show transcript levels of cells treated with siMA6 while red columns represent siAGF1 treated cells. These cells were cultured without feeders for 4 days as a control.

Both of these results demonstrate a greater reduction in transcript levels in the cells cultured without feeder cells.

As the bone marrow fibroblast – leukaemic cell interaction affected the cell numbers of leukaemic cells in a wide concentration range the question was if this effect was due to decreased apoptosis, to increased proliferation or to both. This promised also to give information about the function and type of interaction taking place between bone marrow fibroblasts and leukaemic cells.

To further determine the effect on apoptosis of the feeder contact, SEM were depleted of MLL/AF4 and cultured on or without M210B4. The proportion of viable cells was measured using the Annexin-V – PI assay (Figure 87, Figure 88 and Figure 89 ).

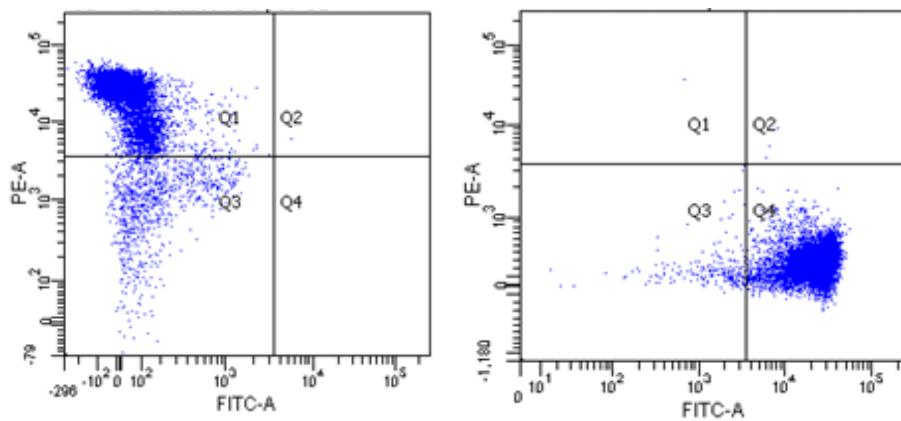


Figure 87 SEM controls for PI and Annexin-V staining

SEM were heated and stained with either PI or Annexin-V and subsequently analysed by flow cytometry as positive controls. (Left) SEM heated at 65C for 5min, stained with PI, used to set necrotic Q1 quadrant (Right) SEM heated at 65C for 5min, stained with Annexin-V to set apoptotic Q4 quadrant. PE-A channel: used to record PI fluorescence, FITC-A channel: used to record Annexin-V FITC. Quadrants: Q1 necrosis, Q3 viable cells, Q2 late apoptosis, Q4 early apoptosis. Shown is one representative experiment.



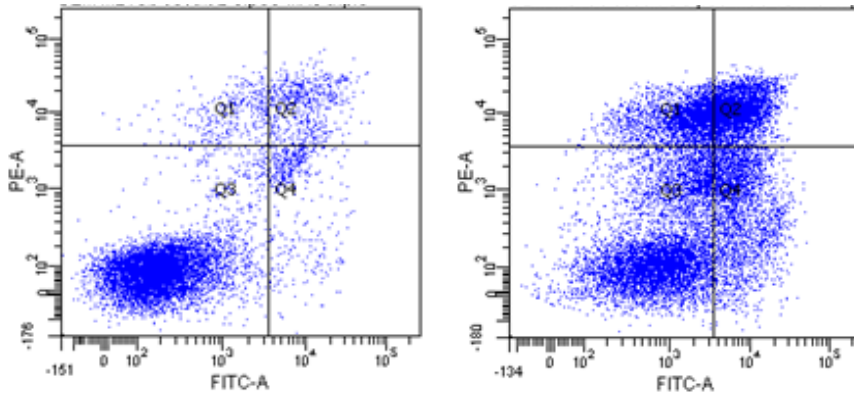


Figure 88 Apoptosis in siMA6 treated SEM

SEM were treated with siMA6, cultured for 5 days with and without feeders and then stained with PI and Annexin-V. They were also subjected to CD19 staining (B-cell marker) and gated on this. (Left) grown on feeders (Right) grown without feeders. PE-A channel: used to record PI fluorescence, FITC-A channel: used to record Annexin-V FITC, Quadrants: Q1 necrosis, Q2 late apoptosis, Q3 viable cells and Q4 early apoptosis.

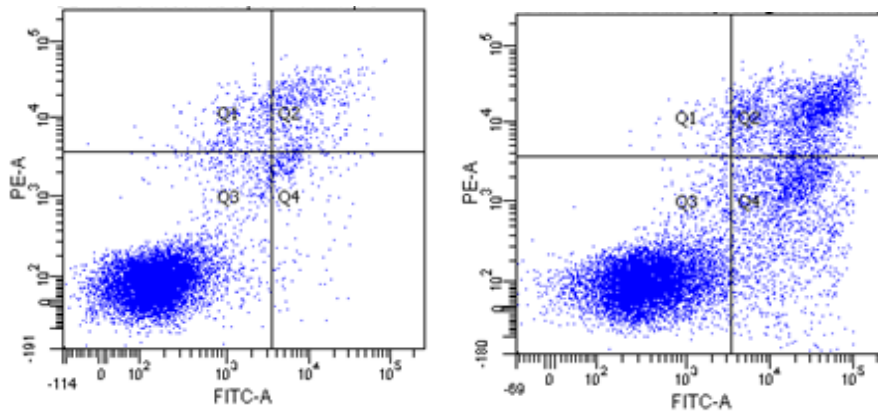


Figure 89 Apoptosis in siAGF1 treated SEM

SEM were treated with siAGF1, cultured for 5 days with and without feeders and then stained with PI and Annexin-V. They were also subjected to CD19 staining (B-cell marker) and gated on this. (Left) grown on feeders (Right) grown without feeders. PE-A channel: used to record PI fluorescence, FITC-A channel: used to record Annexin-V FITC, Quadrants: Q1 necrosis, Q2 late apoptosis, Q3 viable cells and Q4 early apoptosis.

		MA6 coculture	AGF1 coculture	MA6 control	AGF1 control
Q1	necrosis	3.5	2.6	15.6	0.7
Q4	early Apoptosis	5.3	2.3	18.1	15.3
Q2	late Apoptosis	6.7	4.4	24.4	14.9
Q3	viable cells	84.4	90.6	41.8	69.1
Q 1,4,2	compromised cells	15.5	9.3	58.1	30.9

Table 12 Statistics of Figures 88 and 89

Number of SEMs in 4 quadrants according to the Annexin-V – PI assay shown in Figure 88 and Figure 89. SEM were siRNA treated for 5 days cultured under normal conditions or on feeders and then harvested for the determination of viability. Compromised cells: sum of cells in quadrants Q1, 4 and 2 (not fully viable)

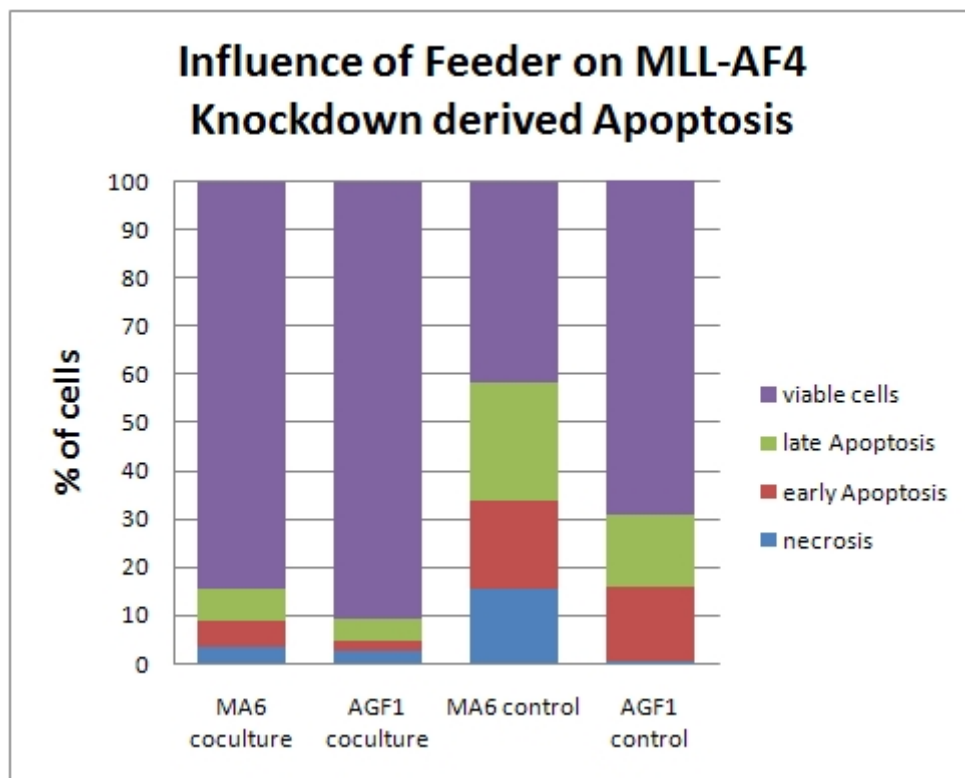


Figure 90 Feeder Influence on MLL/AF4 derived apoptosis

SEM treated with siMA6 and siAGF1 (control) for 5 days, comprising two electroporations on day 1 and day 3. Half of the batch was kept in control wells and the other half were cultured on feeders at the same concentration. CD19 gating was used for the selection of B-cells and selected cells were detected in 4 quadrants according to their Annexin-V and PI staining. This diagram displays the data from Figure 88, Figure 89 and Table 12. Shown is one single experiment.

The diagram (Figure 90) and the table (Table 12) above show that cells kept on M210B4 clearly had a larger fraction of viable cells. Furthermore, co-cultured cells showed a much smaller difference between MLL/AF4 depleted cells and cells treated

with the corresponding siRNA control compared to the cells with no feeder contact. Late apoptosis and necrosis increased in feeder free cultured cells, however especially necrosis seemed to rise in siMA6 treated cells (15.6% necrosis) without M210B4 contact compared to siAGF1 treated cells (0.7% necrosis).

This result showed that feeder contact reduced apoptosis in SEM after siRNA treatment but also reduced the MLL/AF4 depletion derived cell death.

### **4.3.6 Track of daughter populations after MLL/AF4 knockdown**

From previous work within the Heidenreich group it is known that depletion of MLL/AF4 increases apoptosis and leads to cell cycle arrest. M Thomas et al. (Thomas, Gessner et al. 2005) have shown that due to MLL/AF4 knockdown anti-apoptotic markers such as BCLXL decreased while apoptotic markers like cleaved Caspase 3 increased in expression. Moreover a G1 cell-cycle arrest was found in MLL/AF4 depleted cells. Further data on growth curves showed reduced proliferation for MLL/AF4 depleted cells. This raised the question of whether the different cell numbers are due to a bigger proportion of cells being affected by apoptosis or by inhibited proliferation.

To accomplish this, SEM were tracked throughout proliferation while being electroporated on day 1, 3 and 5, introducing the CFSE assay which allowed tracking of the daughter cell populations (see Figure 91).

## CFSE tracking of daughter populations in siRNA treated SEM

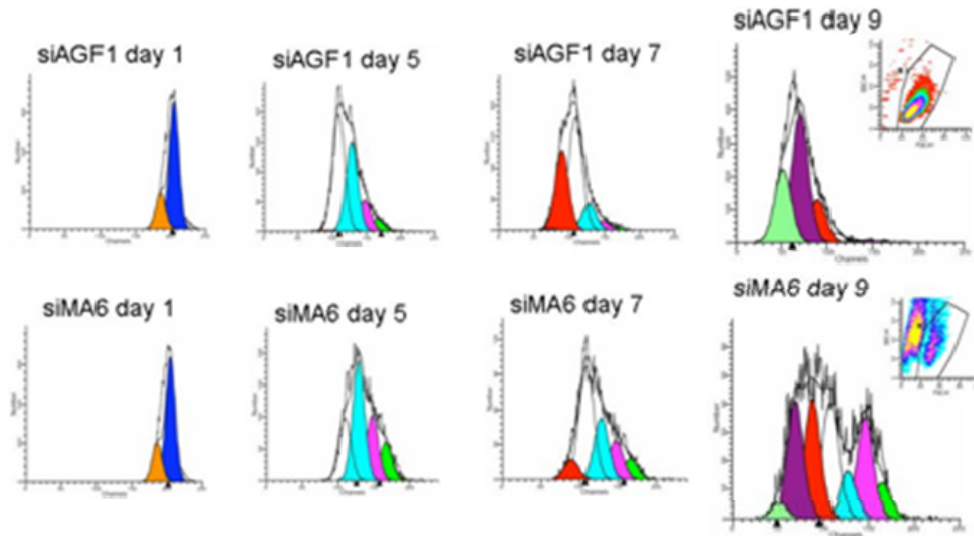


Figure 91 CFSE tracking of daughter populations in siRNA treated SEM

CFSE stained SEM were treated with siRNA on day 1,3 and 5; Daughter populations were tracked by detecting the CFSE signal. The blue peak (Right) represents the parent population, each peak left of it represents a daughter population of the peak before. The x-axis represents the number of cells detected and the y-axis the signal strength (population). On the right also the forward-sideward scatterplots are shown for day 9 and the gating. siAGF1: control siRNA, siMA6: siRNA targeting *MLL/AF4*. Shown is representative experiment.

The schematic above (Figure 91) shows tracked daughter populations from siMA6 (targeted to fusion gene transcript) and siAGF1 (control) treated cells throughout 9 days of *MLL/AF4* depletion and monitoring. The blue peak on the right represents the parent population. All peaks to the left in different colours represent daughter populations.

The data showed that *MLL/AF4* depleted cells were not just proliferating slower than the siRNA control, they seemed to split into different populations, from cells with a low rate of proliferation (siMA6, day 9, intense green peak, most right) to cells with high proliferation (siMA6, day 9, lighter green peak, most left). Compared to the control cells, where the majority of cells were present in 3 populations of highest proliferation, the *MLL/AF4* depleted cells were distributed in 7 detectable populations.

## 4.3.7 The feeder as an assay system for interactions

### 4.3.7.1 MLL/AF4 influence on *HOXA7* and *TERT*

In the Heidenreich group we have found that two genes *TERT* (Telomerase reverse transcriptase) and *HOXA7* (Homeobox gene, cluster A) are not only influenced by the depletion of MLL/AF4 but are also interacting with each other. Upon MLL/AF4 depletion, the telomerase activity was reduced. Furthermore *HOXA7* binds to the promoter of *TERT* (Gessner, Thomas et al. 2010).

Firstly the levels of *TERT* and *HOXA7* transcript were analysed following depletion of MLL/AF4. SEM treated with siAGF1 (control), siMA6 (anti *MLL/AF4*) and si*HOXA7* (anti *HOXA7*) were analysed for their transcript levels of *MLL/AF4*, *TERT* and *HOXA7* two days after the first and two days after the second electroporation (Figure 92).

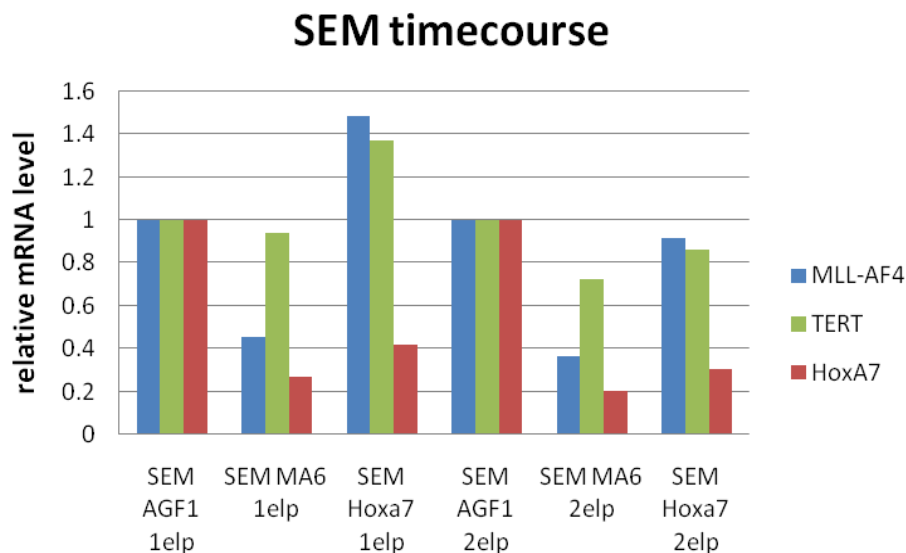


Figure 92 Gene expression levels of a 96h timecourse in siRNA treated SEM without feeders

SEM treated with siAGF1, siMA6 and si*HOXA7* for 2 days (1elp) and for 4 days (2elp). Normalised relative transcript levels (normalised to 1 using AGF1 1elp and AGF1 2elp) of *MLL/AF4* (blue columns), *TERT* (red columns) and *HOXA7* (green columns) are represented by the x-axis showing relative mRNA levels. Shown is one representative experiment.

The diagram (Figure 92) shows that siMA6 reduced levels of *MLL/AF4* two days after the first and two days after the second electroporation. Treatment with siMA6 also reduced *TERT* levels after the second electroporation by 30%, while after the first electroporation *TERT* levels were hardly changed. Finally siMA6 reduced *HOXA7* transcript levels by 70 (1<sup>st</sup> -) to 80 (2<sup>nd</sup> electroporation) percent.

The siRNA si*HOXA7* which is targeted against the *HOXA7* transcript reduced its target mRNA by 60 (1<sup>st</sup> -) to 70 (2<sup>nd</sup> electroporation) percent, however levels of *MLL/AF4* and *TERT* mRNA were not substantially reduced.

That *HOXA7* is substantially reduced by *MLL/AF4* depletion was known already (Gessner, Thomas et al. 2010).

To monitor those transcript levels over an extended period of *MLL/AF4* and *HOXA7* depletion, a timecourse was performed using 3 consecutive electroporations as well as harvesting for analysis every 2<sup>nd</sup> day. To evaluate if the interaction with feeders does change these results for example by keeping cells with low *HOXA7* levels alive, two separate strands of this experiment were performed. One under normal culture conditions, the other on feeders (Figure 93).

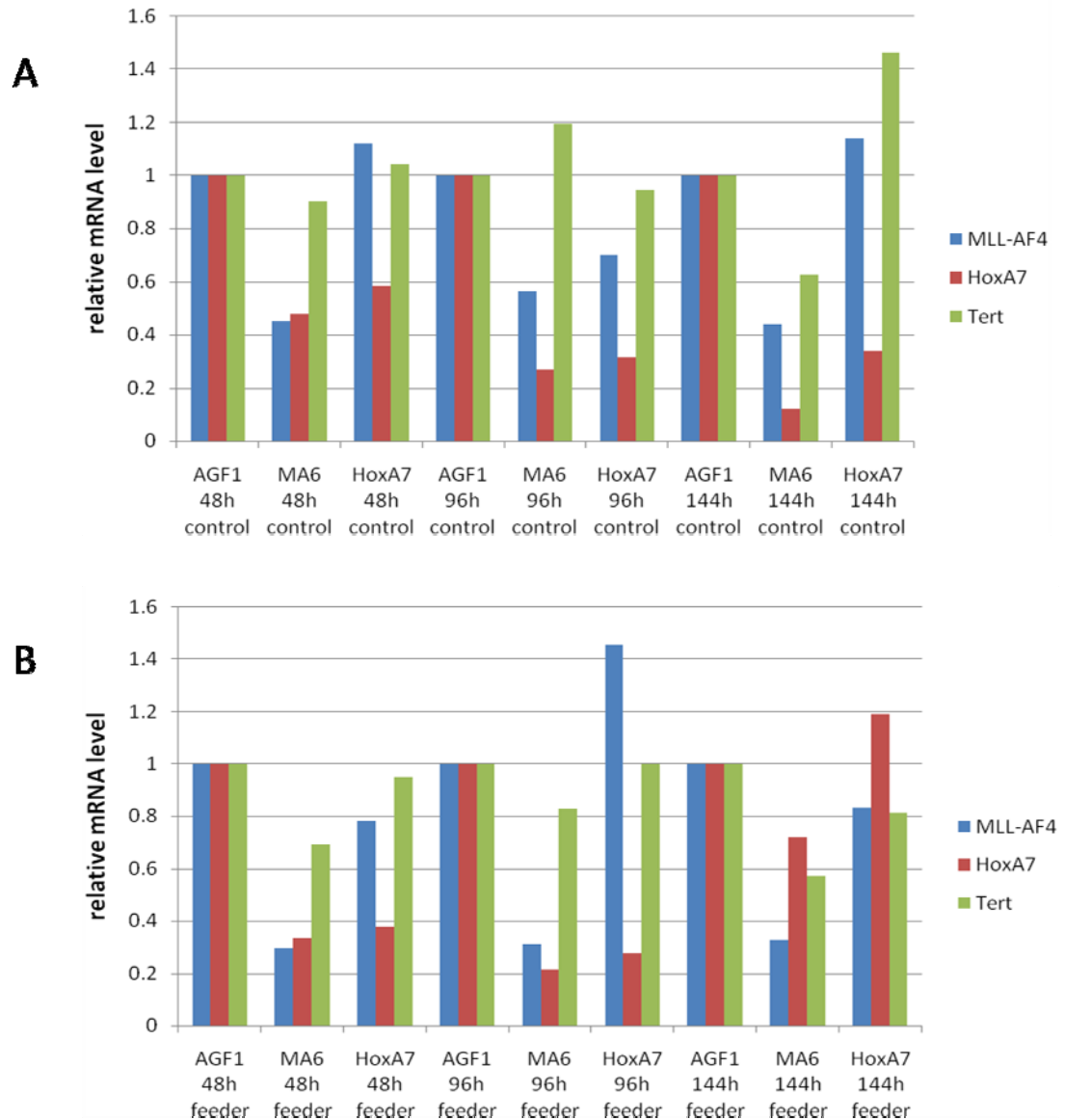


Figure 93 Gene expression levels of a 144h timecourse in siRNA treated SEM

SEM treated with siAGF1, siMA6 and siHOXA7 for 48h, 96h and 144h. Normalised relative transcript levels normalised to 1 using corresponding AGF1 per timepoint. Blue columns: MLL/AF4 transcript, Green columns: TERT and Red columns: HOXA7. The x-axis represents relative mRNA levels of those transcripts (A) cultured without feeders (B) co-cultured on feeders. Shown is one representative experiment.

The diagrams (Figure 93) show depletion of *MLL/AF4* and *HOXA7* for 144h. The control time course where SEMs were cultured under normal culture conditions in between the electroporations resulted in approximately 60% depletion of *MLL/AF4* by siMA6. In parallel, *HOXA7* levels sunk from 50 (48h), to 70 (96h) to almost 90 (144h) percent. *TERT* levels were mainly reduced after 144h siMA6 treatment by 40%.

Furthermore treatment with si*HOXA7* reduced *HOXA7* mRNA levels by 40 (48h), 70 (96h) and 65 (144h) percent. Levels of *MLL/AF4* showed no consistent reduction as expected but also transcript levels of *TERT* showed no consistent effect.

Finally, the data from the time course experiment of SEM cells cultured on feeders showed slightly different results. Anti *MLL/AF4* treatment (siMA6) reduced the corresponding mRNA levels by roughly 70 percent throughout the time course while the transcript levels of *HOXA7* were reduced by 65 (48h), 80 (96h) and 30 (144h) percent. By the same treatment *TERT* levels were reduced by 30 (48h), 20 (96h) and 40 (144h) percent. Surprisingly si*HOXA7* altered corresponding transcript levels to 60 (48h) and 70 (96h) percent reduction but then to 20 percent increase. As seen previously, *MLL/AF4* mRNA levels were not consistently changed by si*HOXA7*, while *TERT* levels were not reduced substantially after 48h and 96h but at 144h a 20 percent reduction was seen.

Comparing those two parallel experiments, the interaction with M210B4 seemed to reduce *HOXA7* depletion after 144h to just 30 percent, compared to 90 percent reduction in the non co-cultured cells. Vice versa, the feeder interaction resulted in a 20% reduction of *TERT* by after 144h compared to 45 percent increase in the non co-cultured cells.

#### **4.3.7.2 The feeder and primary patient material**

Unlike cell lines such as SEM, primary material from patients is difficult to culture due to increased cell death. To test the suitability of feeder systems for mid and long-term culture of primary ALLs, cells from *MLL/AF4* patients were used to check if co-



culturing on M210B4 increases the time they can be cultured. This is important due to limited availability of primary patient material. In our experience these cells hardly grow under normal cell culture conditions. To determine how long primary cells remained viable in feeder layer co-culture, cells were analysed with the Annexin-V PI assay. Frozen white blood cell aliquots from an infant MLL/AF4 positive patient were thawed and cultured on M210B4 feeders for two weeks. Using several controls such as viable SEM cells, SEM incubated at 65°C for 15min and either stained for PI or Annexin-V, for setting the necrotic and the early apoptotic quadrant infant MLL/AF4 cells were analysed for their viable fraction compared to fibroblasts alone (Figure 94, Figure 95 and Table 13).

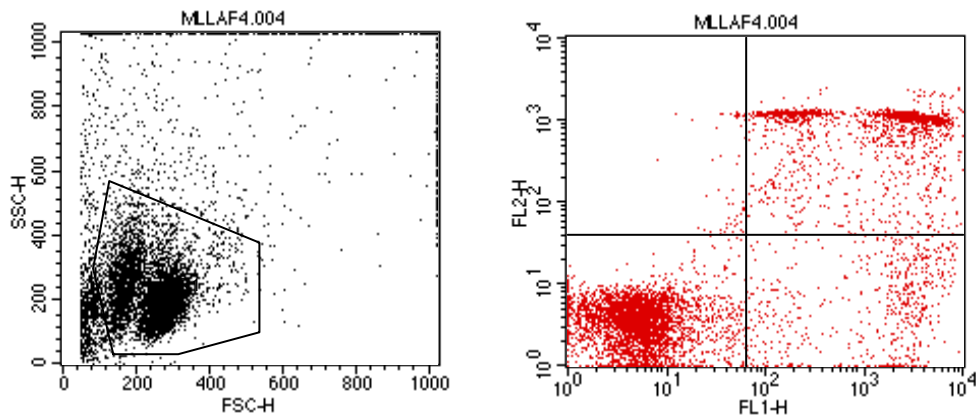


Figure 94 Infant –MLL/AF4 patient viability

Infant-Patient MLL/AF4 positive cells grown on M210B4 for 2 weeks were gated for B-lymphocytes and stained with PI and Annexin-V. (Left) dot-plot: SSC against FSC with lymphoblast gate (Right) dot-plot: PI (FL2-H, necrosis) against Annexin-V (FL1, apoptosis). The quadrants were set using positive controls for necrosis and early apoptosis. The Upper left quadrant (UL) shows necrotic cells, the lower right quadrant (LR) shows early apoptotic cells, the upper right quadrant (UR) shows late apoptotic cells and the lower left quadrant (LF) shows viable cells. Shown is one single experiment.

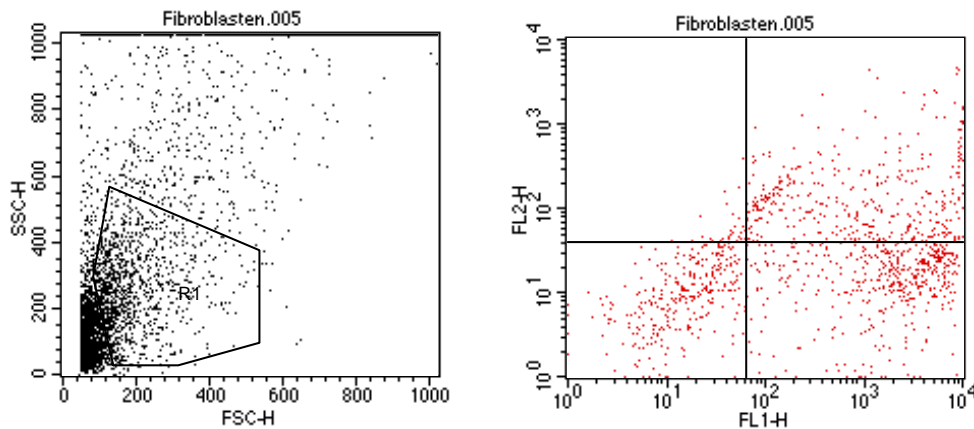


Figure 95 Cell viability fibroblast control

Irradiated M210B4 were gated with the lymphophocyte gate and stained with PI and Annexin-V. (Left) dot-plot: SSC against FSC with B-lymphocyte gate (Right) dot-plot: diagram PI (FL2-H, necrosis) against Annexin-V (FL1, apoptosis). The quadrants were set using positive controls for necrosis and early apoptosis. The Upper left quadrant (UL) shows necrotic cells, the lower right quadrant (LR) shows early apoptotic cells, the upper right quadrant (UR) shows late apoptotic cells and the lower left quadrant (LF) shows viable cells. Shown is one single experiment.

Quadrant	%	MLL/AF4 Infant	Fibroblasts
UL	Necrosis	0.97	3.01
LR	early Apoptosis	9.36	37.88
UR	late Apoptosis	27.08	32.83
UL+LR+UR	damaged cells	37.41	73.72
LL	viable cells	62.59	26.28

Table 13 Summary of quadrant cell numbers from Figures 94 and 95

This data (Table 13) showed that the majority of MLL/AF4 cells were alive after 2 weeks on M210B4 layer. Unfortunately, M210B4 gave the same pattern of Annexin-V - PI staining, making them indistinguishable from leukaemic cells. Nevertheless, in this experiment there was an excess of MLL/AF4 cells to M210B4, so that their influence on the quadrant numbers could be disregarded.

However to overcome this problem the Annexin-V - PI assay was further developed by gating off leukaemic cells using CD19 staining as a B-cell marker previous to the distribution over the 4 quadrants.

Firstly it was tested how sensitive to CD19 this pre-gating is. For this, two concentrations of MLL/AF4 patient cells were seeded on feeder layer wells and analysed for the CD19 shift (Figure 96).

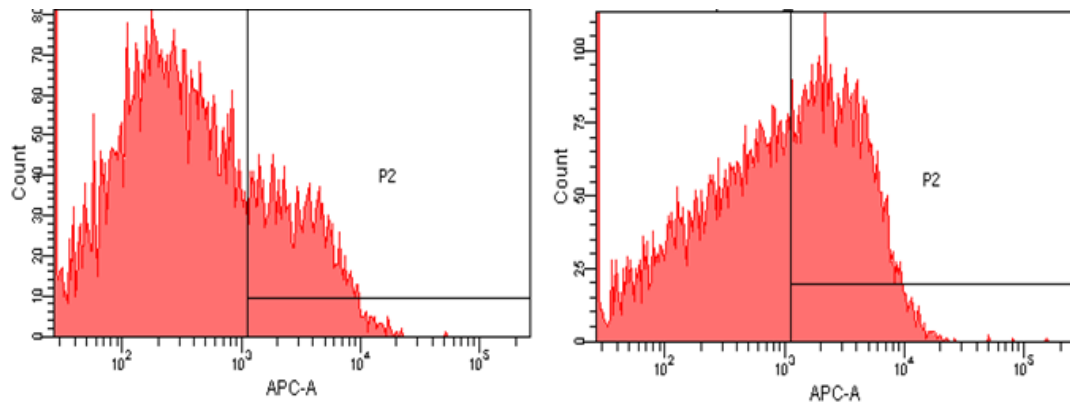


Figure 96 MLL/AF4 patient cells CD19 shifts

MLL/AF4 patient cells co-cultured in two dilutions on feeders, stained with CD19; the APC channel shows CD19 positivity (B-cell marker); P2 gate: cells with CD19 shift compared to control cells, P1: cells with no CD19 shift. (Left)  $10^5$  MLL/AF4 patient cells per well (Right)  $10^6$  MLL/AF4 patient cells per well. Shown is one representative experiment.

The ratio P2/P1 gave an indication of how concentration dependent the CD19 shift was (Figure 96). The ratio means MLL/AF4 leukaemic cells divided by fibroblasts. The higher the ratio the more MLL/AF4 cells were present. For  $10^6$  seeded cells per well the ratio was 0.47 and for  $10^5$  cells per well 0.24.

In addition to the controls used for Annexin-V – PI analysis, additional controls were introduced for CD19 staining. Cells positive for CD19 were used to display the 4 quadrants. The MLL/AF4 cells were incubated for three weeks on M210B4. Because of restrictions in patient material, only co-cultures and irradiated M210B4 cells were used for flow cytometric analysis (Figure 97).

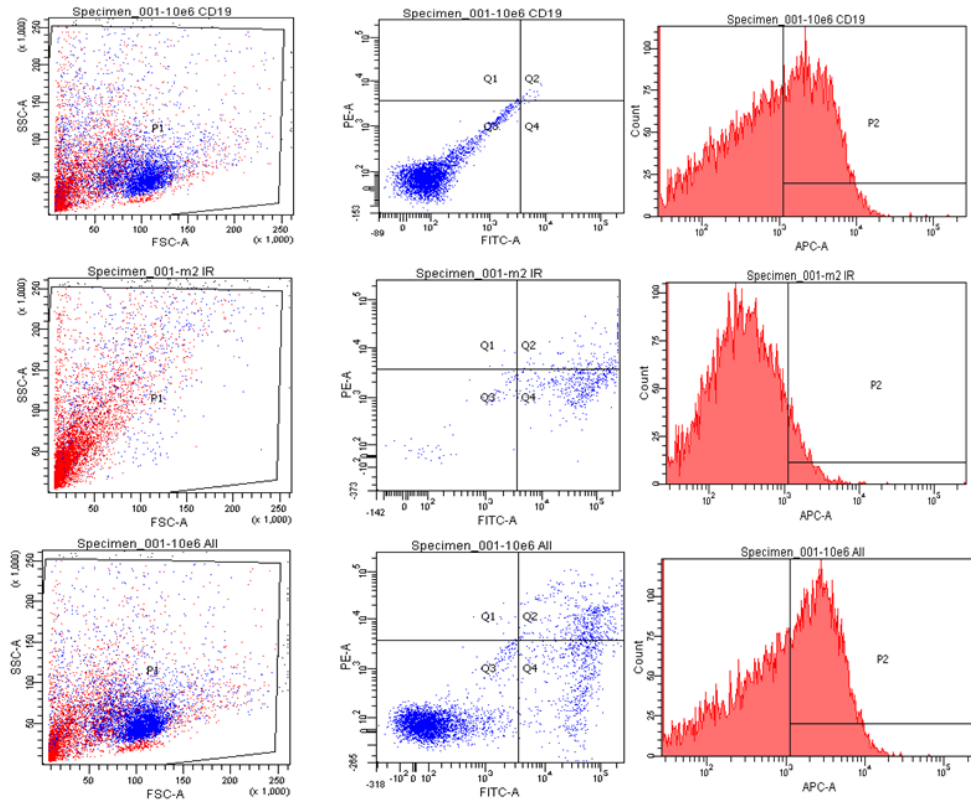


Figure 97 MLL/AF4 patient cells after 3 weeks on M210B4 feeders

MLL/AF4 patient cells ( $1 \times 10^6$  cells /well) kept on M210B4 feeders for 3 weeks, stained and pre-gated with CD19(B-cell marker), stained with PI and Annexin-V for cell viability determination (Top row) MLL/AF4 – M210B4 co-culture CD19 staining only (10e6 CD19) (2nd row) irradiated M210B4 only (m2 IR) (Bottom row) MLL/AF4 – M210B4 co-culture CD19, PI and Annexin-V staining ( 10e6 All) (Left) SSC-FSC plot (Middle) PI - Annexin-V plot + quadrants (Right) count-APC (CD19) histogram; Q1 necrosis, Q2 late apoptosis, Q3 viable cells and Q4 early apoptosis, 10e6:  $1 \times 10^6$ . Shown is one single experiment.

The result (Figure 97) confirmed that 77% of infant MLL/AF4 cells were still viable after 3 weeks on M210B4 feeders.

## 4.4 Discussion Feeder Chapter

The aim of this chapter was to investigate the strong references from the previous chapter towards the HSC – niche context. Therefore the endeavour to establish a model to investigate the bone marrow – HSC, or leukaemic (stem) cell interactions was made.

In a first attempt HS-5, (Roecklein and Torok-Storb 1995) a human bone marrow fibroblast line immortalised by human papilloma virus HPV, was examined for this interaction. HS-5 cells were used to increase survival of human B-CLL patient cells (Seiffert, Stilgenbauer et al. 2007) and also shown to support B-Lymphoma by expression of B cell-activating factor (BAFF) (Lwin, Crespo et al. 2009). Another group showed increased proliferation of the leukaemic cell line K562 if co-cultured with HS-5 (Lee, Chiou et al. 2008).

In contrast to co-cultures in the literature where the main objective was to keep haematopoietic cells alive by co-culturing them with feeders, the interaction system to be developed had to provide a stable environment. This should ensure that interactions between feeders and haematopoietic cells can be monitored without disturbing influences. Therefore feeder layers had to be growth arrested, which had not been published for HS-5.

HS-5 feeders could not be growth arrested by irradiation, Actinomycin D or Mitomycin C treatment (Figure 48), tested at several doses. Actinomycin is known to induce cell cycle and subsequential growth arrest (Kim, Kong et al. 2005). Mitomycin C had been described as an alternative to irradiation for feeders (Ponchio, Duma et al. 2000). The microscope observation always showed an increased toxicity with dose, and cells were either surviving and growing again or dying. Cell cycle (Figure 50) and genotype analysis showed that HS-5 were quite heterogeneous with inter cell variation such as

unbalanced translocations, hyperdiploidy and polyploidy. This observation raised the question if these were really pure, non contaminated HS-5. Considering the handling procedures and that only one fibroblast cell line was cultured that time, contamination is very unlikely. If a mixed culture of HS-5 and another cell line had been used as “HS-5”, then most likely it would have to be in the original HS-5 vials. However, considering how HS-5 were immortalised using HPV, which transduced cells with its genes E6 and E7 known to interfere with p53 and Rb and thereby preventing cell cycle arrest, it is quite feasible that these genes generated genetic instability and subsequently heterogeneity. This could be seen quite nicely in the images of MMC treated HS-5 (Figure 48). They showed foci of HS-5, resulting from strong proliferation, surrounded by gaps which had been generated by died HS-5.

As an alternative the murine bone marrow fibroblast cell line M210B4 (Lemoine, Humphries et al. 1988) was chosen. For over 10 years it was used for LTC-IC (long term culture initiating cell) assays and is accessible to growth arrest by irradiation (Prosper, Vanoverbeke et al. 1997). Growth arrest of M210B4 by 80Gy irradiation could be shown by cell cycle analysis, showing a G2 arrest (Figure 56). Although 80Gy is mortal to many cell types, a substantial fraction of M210B4 is viable after treatment. However increased apoptosis levels the first 2-3 days after irradiation requires seeding of high numbers of M210B4 to form nearly confluent layers that can be maintained for more than 4 weeks.

For initial tests of M210B4 growth arrested feeders, fluorescent SEMTeton (GFP) were used. Apart from the morphological and size differences, fluorescence of co-cultured cells provided an additional marker for the distinction from feeders (Figure 57). This provided the advantage that the distinction of feeders and leukaemic cells not only relied on morphological and size differences. The pre test of co-cultures showed that the

feeders and leukaemic cells can be distinguished under the microscope, as fluorescent signals matched the light microscopic images. The initial assumption that these fluorescent SEM and the feeders should be easily distinguishable in Flow Cytometry analysis proved to be wrong. For this co-cultures of M210B4 and SEMTeton or MV4;11Teton had been used (Figure 59, Figure 60 Figure 61). As it was shown later, leukaemic cells tested adhered on feeder layers (Figure 72). A simple shake of cells or washing, as it was published in M210B4 (Burger, Spoo et al. 2003), does not remove those cells directly attached to the feeder, only cells in suspension. This is sufficient for maintaining and analysing cells in higher concentrations, but as leukaemic cells in lower concentrations seem to be mainly located on the feeders, shaking off is not suitable in retrieving those cells. Therefore co-cultures had to be trypsinized in total, resulting in suspension of M210B4 and leukaemic cells.

The distinction of those M210B4 SEMTeton or MV4;11Teton co-cultures by Flow Cytometry analysis using size and granularity left a remaining fraction of cells over spilling into each M210B4 and leukaemic cells gate. Although M210B2 are bigger, fibroblast shaped with a certain granularity, they show a certain distribution of sizes and granularity and not a strongly defined population. This could be due to irradiation, where cells are arrested in different stages of growth and additionally due to different genetic mutations induced by the irradiation which might lead to different morphological phenotypes. This could be seen by comparing FSC-SSC Dot plots of normal and irradiated M210B4, showing that irradiation results in a different pattern. Additionally these irradiated cells show a high auto-fluorescence.

Several dilutions of SEM- or MV4;11Teton cells on M210B4 feeders showed a limited range of concentration dependence of flow cytometry feeder or leukaemic cell gating (Figure 60 and Figure 64).



This approach was further improved by establishing a Flow Cytometry based cell count assay to determine fluorescent SEM on M210B4 feeders. Instead of counting numerous wells by hand in triplicates per sample, which relied on the visual discrimination of M210B4 and SEMTeton cells, flow cytometric statistics of two gates was used. Due to the constant number of M210B4 per well, the more leukaemic cells are grown per M210B4 well, the higher the ratio of leukaemic cell numbers to M210B4 numbers per 10000 events should be (Figure 68).

The successful development of this method was also based on changes to the previous flow cytometric analysis. The most important changes were the use of a different Flow Cytometry machine (FACS Calibur) with less automated settings, a logarithmic SSC channel and irradiated M210B4 to set the gates to allow this. A standard curve showed that this approach was highly correlative and linear from  $10^3$  to  $10^6$  cells per well.

This method provides easier and more extended experiments on feeders. However the majority of the feeder leukaemic interaction was assessed using visual discrimination and used non fluorescent leukaemic cells which cannot be counted with this assay.

The discrimination of M210B4 from leukaemic cells in an counting chamber had been trained by using trypsinised M210B4 and fluorescent cells separately. Normal light microscope images distinguished both SEMTeton and MV4;11Teton from M210B4.

It was mentioned previously that leukaemic cells adhere to feeders. To demonstrate this, an inversion test was implemented with this feeder assay (Figure 72). The principle is that co-cultured cells adhered to feeders, which were grown on a glass slide based chamber. If there is adhesion to the feeders these co-cultured cells stay connected even when the chamber is converted, while not bound and loosely bound cells are separated by gravity. A similar inversion test had already been described but had to be adapted for

these cells and the glass slide chambers used. SEM cells could not be used for this assay as they show adherence to surfaces. Consequently it could not be ruled out that adherence to M210B4 was unspecific adherence and not specific interaction.

As a replacement the two AML cell lines Kasumi-1 and SKNO-1, which express *AML/MTG8* fusion gene, were used. The test revealed that no substantial decrease in leukaemic cells on feeders was found after 2h of inversion and suspension cell removal. This finding could also be confirmed by hitting against the side of co-cultures wells. Cells in suspension moved, whilst cells on top of the M210B4 feeders did not. These results show that there is a physical interaction between these leukaemic cells and the M210B4 feeders.

Next, the question was addressed if co-culture on feeders affect siRNA mediated knockdown and its consequences for cell growth was addressed.

Several publications from the Heidenreich group have used electroporation mediated delivery of siRNA to knock down fusion genes. It was shown that this affects proliferation, clonogenicity and apoptosis (Thomas, Gessner et al. 2005).

It was shown that the fusion gene depletion *MLL/AF4* and *AML/MTG8* can be detected in cells grown on feeders (Figure 79 and Figure 82), showing depletion to a similar extent. The accessibility for *MLL/AF4* depletion has also been shown for SEMTeton (Figure 79).

The qRT-PCR analysis of fusion gene expression levels of leukaemic cells grown on feeders was validated showing that M210B4 RNA did not influence housekeeping gene GAPDH expression used to normalise gene expression levels, because M210B4 genes have a mouse background and the genes tested are not recognised by human primers.

Secondly primers for *MLL/AF4* in Kasumi-1 and primers for *AML/MTG8* amplified product more than 10 cycles later than in the cells bearing those fusions, and the melting curves indicated primer-dimer peaks. Together this shows the high specificity of this qRT-PCR analysis. Another factor contributing to this was the excess of leukaemic cells used in co-culture in comparison to M210B4 numbers also reducing an effect of M210B4 RNA traces on the analyses.

Normal SEM were treated for *MLL/AF4* depletion and seeded in dilutions below normal culture concentrations on feeders. Determination of SEM numbers showed, that upon *MLL/AF4* depletion cell numbers reduced 2 fold on average, while doubling times increased (Figure 76).

To investigate the influence of feeder contact and leukaemic cell concentration on leukaemic cell numbers, a large scale experiment was performed using SEM and the *AML* fusion cell line Kasumi-1, as a leukaemic control.

Cells depleted for *MLL/AF4* (siMA6) together with controls (siAGF1) were seeded in a wide concentration range from  $1 \times 10^3$  to  $1 \times 10^6$  cells / ml in wells with and without feeders (Figure 83). The most profound effect was that the lower the concentration the cells were seeded out at, the more these cells benefited from the interaction with the feeders. In the lowest concentrations SEM showed substantial increase of numbers while without feeders cells numbers diminished. Depletion of *MLL/AF4* reduced cell numbers to a lesser extent in co-culture than in single culture. The results in Kasumi-1 which were depleted for their fusion gene *AML/MTG8* were quite comparable (Figure 84). This raises the question if this effect is dependent on these bone marrow feeders or if it is due to the proximity of other cells. With the knowledge of physical interactions already shown, a range of growth supporting factors secreted and later findings

regarding apoptosis it seems unlikely that these effects are just caused by the close proximity of other cells. The second question to be answered was if these differences from an increase of cell numbers on the feeder and a strong decrease without feeders were mainly caused by induced proliferation or also due to reduced apoptosis. This question was addressed and will be discussed later on.

In addition to the determination of cell number changes in relation to fusion gene depletion, fusion gene depleted SEM and Kasumi-1 with their controls were seeded in several densities on feeders and the reduction of cell numbers due to fusion gene depletion could be shown in co-culture images (Figure 77 and Figure 78). Parallel to this, the reduction of cell numbers by fusion gene depletion had been confirmed by cell number determination.

Following these pre-validations MLL/AF4 depletion sensitive niche / stemness associated gene expression was investigated comparing non feeder with feeder cultures. These genes had been validated in the previous chapter. The comparison of gene expression levels of *MLL/AF4*, *TERT*, *MEF2C*, *FGFR1* and *CDH2* (N-CADHERIN) showed no significant difference between non feeder and feeder interaction cultures (Figure 92). This result confirmed the feasibility of qRT-PCR analysis in co-cultured samples. It remains unknown if the feeder interaction had an influence on the genes as these cells had only been cultured for 96h after siRNA treatment.

A simple experiment could address the role of MLL/AF4 in N-cadherin adhesion. This would be to knock down MLL/AF4 and to use the inversion assay already mentioned. If the number of cells attached to the M210B4 layers would decrease after inversion compared to a siRNA control, a direct influence of MLL/AF4 on N-cadherin adhesion would be indicated.

To address the question of the viability of the cells, an Annexin-V - PI assay to determine the viability of cells depending MLL/AF4 depletion and feeder contact was performed. To exclude basal levels of feeders from this analysis a pre CD19 gating, selecting for B-lymphocytes was performed. However, CD19 staining could to be stronger in dead cells due to the enrichment of antibody staining dead cells often show, but as M210B4 controls showed, they rarely spill into the CD19 gate .

This analysis revealed that feeder interaction increases the proportion of viable cells especially by reducing late apoptosis but also by reducing necrosis and early apoptosis. Comparing MLL/AF4 knockdown and siRNA controls, feeder contact especially reduced the vast difference in viability found in non feeder cultured samples. In these samples MLL/AF4 depletion especially increases necrosis while in feeder co-cultured samples necrosis levels between MLL/AF4 depletion and control were the same. This analysis showed, that the effect of the feeder on leukaemic cells is not only growth enhancing, but also increasing viability and survival (Figure 90).

Apart from cell cycle analysis and Annexin-V assays the apoptotic effect was shown also by a decrease in BCL-XL, an anti-apoptotic marker, while apoptotic markers such as cleaved Caspase 3 increased in expression. As a consequence of observed growth arrest, growth curves showed reduced proliferation when MLL/AF4 positive cells were depleted for MLL/AF4 (Thomas, Gessner et al. 2005). To answer the question if these effects are more correlated to apoptosis or decreased proliferation a CFSE assay was used. CFSE staining allowed tracking of cell populations for a certain period. Here MLL/AF4 depleted SEM and siRNA control SEM were tracked for 9 days (Figure 91). The analysis of daughter populations showed that the longer cells are incubated, the bigger the difference was between MLL/AF4 depleted cells and the siRNA control. While siRNA control cells were distributed in 3 main populations (furthest, 2<sup>nd</sup> and 3<sup>rd</sup>)

MLL/AF4 depleted cells were distributed in 7 main populations (furthest, to 7<sup>th</sup> furthest). The amount of dead cells was substantially increased for the MLL/AF4 depleted cells and these were gated out in this analysis. This means that from the cells surviving many cells grow slower, divide less often, but some very few proliferate as fast as the control cells. This heterogeneity is an interesting finding which offers some new insight when interpreting effects caused by apoptosis. For example, when determining cell numbers after MLL/AF4 depletion, the conclusion to levels of apoptosis, cell cycle arrest and proliferation should not depend on cell numbers alone.

The influence of the feeders on MLL/AF4 depleted and *HOXA7* depleted cells was further investigated by the determination of *TERT* and *HOXA7* expression pattern changes of up to 144 hours (Figure 93). We have linked MLL/AF4 depletion with reduced *HOXA7* and *TERT* expression levels and as well to reduced telomerase activity (Thomas et al. 2005).

*HOXA7* was found to be dramatically increased in human bone marrow derived mesenchymal stem cells and linked to angiogenesis of those bone marrow cells (Chung, Jee et al. 2009), which is known to be regulated by FGF2, VEGF and TGF- $\beta$ 1.

The role of TERT in the bone marrow context is poorly examined however, a study in a Chinese population connected TERT mutations to bone marrow failure syndrome (Liu, Han et al. 2009) which consisted of symptoms such as damaging of hematopoietic stem cells and their microenvironment. These TERT mutations probably reduce the proliferative potential of haematopoietic stem cells.

Interestingly the expression level reductions of *TERT* and *HOXA7* after 144h of *MLL/AF4* depletion (Figure 93) seemed to be stronger in feeder free cell cultures compared to cells grown of feeders. Also the knockdown of *HOXA7* by siHOXA7 is

more efficient in cells grown without feeders after 144h of culture than in those grown in co-culture. A possible explanation could be, that cells on feeders contain this generation of highly proliferating cells, previously mentioned in the CFSE analysis. This population probably has less depletion of *MLL/AF4* or *HOXA7* and can provide higher survival numbers, whilst the cells cultured without feeders probably contain more cells with less viability. However these results are based on a single experiment. In a previous, similar experiment (Figure 85 and Figure 86) the expression levels of *TERT* after *MLL/AF4* depletion for 96h did not differ. Moreover *HOXA7* mRNA levels had not been analysed. It was shown previously that knockdown of *HOXA7* harms the viability of treated cells (Gessner, Thomas et al. 2010).

For this sustained knockdown of *MLL/AF4* and *HOXA7* for 144h three electroporations with siRNA had to be performed. This required that cells grown on feeders had to be trypsinized, differentially counted and electroporated with the feeders again and seeded onto new feeders repeatedly. Due to this extensive protocol, leukaemic cells had to be kept a higher concentration to provide enough cells for the next electroporation, considering the amount of apoptosis taking place, especially in *MLL/AF4* depleted SEM cells. However the most substantial effects from this feeder culture on leukaemic *MLL/AF4* depleted cells were seen in low concentrations. Such effects may could not be observed in these experiments because of higher concentrations used.

The question if interaction with feeders influences the clonogenicity could be addressed with *MLL/AF4* positive cells growth on feeders and then introduced to a clonogenic assay, as feeder layer cells are growth arrested and can't contribute to this.

Finally the established feeder interaction system was tested in the maintenance of an *MLL/AF4* infant patient sample. As previously described CD19 gating was used to pre

select B-lymphocytes from feeder cells. However CD19 signal seemed to be less strongly expressed, at least in this patient sample, than in ALL cell lines such as SEM. However CD19 signal could be shown to be proportional to the amount of SEM seeded on feeders. The viability analysis showed that the majority (77%) of patient cells were still viable after 3 weeks on feeders (Figure 97). This was not a surprising finding in context with the use of bone marrow feeders in the last 15 years. As already mentioned irradiation has an effect on the state of M210B4, when using irradiated M210B4 as a control in this viability assay, they were detected in the early apoptotic cell quadrant. This probably refers to the amount of damage in these cells by irradiation. The CD19 signal for those M210B4 was mostly determined as negative by the gate set.

Overall this chapter shows the importance of bone marrow interactions with leukaemic cells such as SEM, MV411 and Kasumi-1. Furthermore the established bone marrow feeder interaction assay can be used to investigate functions and interactions of leukaemic cells with those bone marrow feeders in the future. Furthermore this assay could be adapted for testing of therapeutic substances. Finally these data provide evidence for a role of MLL/AF4 in target gene regulated pathways and functions connected to haematopoietic niche interactions which could influence requirements of a leukaemic cell such as survival and growth.



# **Chapter 5**

## **Lentiviral cloning, production and transduction**

# Chapter 5 Lentiviral cloning, production and transduction

## 5.1 Introduction and Theory

In 1892 Dimitry Ivanovsky discovered viruses when he used a filter that removed bacteria to filtrate a solution made from infected tobacco plants. The filtrate could still infect new tobacco plants (Shultz, Schweitzer et al. 1995) and due to the absence of bacteria he assumed it could be due to a poison; in latin virus. Viruses are particles which can infect cells of organisms. There are different opinions if they are forms of life or not. Unlike living forms they cannot multiply themselves, they do not require nutrients or energy. Viruses are dependent on their host cells to be multiplied. But like living forms they do contain a genome meaning genetic information saved in DNA or RNA.

Apart from genetic information viruses contain proteins, which encapsule the genome in a capsid, or other structural proteins, have enzymatic functions or signalling functions. Viruses are classified in 7 groups by the structure of their genome.

The genome can either be single or double stranded and contain DNA, RNA or both. (+) sense RNA has to be transcribed into complementary (-) sense RNA before mRNA can be synthesized (see Figure 98).

The 7 classes are:

- |     |  |                     |
|-----|--|---------------------|
| I   | dsDNA viruses containing double stranded DNA   | e.g. Herpesviruses  |
| II  | ssDNA viruses containing single stranded (+) sense DNA   | e.g. Paroviruses    |
| III | dsRNA viruses containing double stranded RNA   | e.g. Reoviruses     |
| IV  | (+)ssRNA viruses containing (+) sense ss RNA   | e.g. Picornaviruses |
| V   | (-)ssRNA viruses containing (-) sense ssRNA  | e.g. Rhabdoviruses  |
| VI  | ssRNA-RT viruses containing (+) sense RNA with an<br>DNA intermediate in the life cycle using RT | e.g. Retroviruses   |
| VII | dsDNA-RT viruses using Reverse transcriptase (RT)  | e.g. Hepadnaviruses |

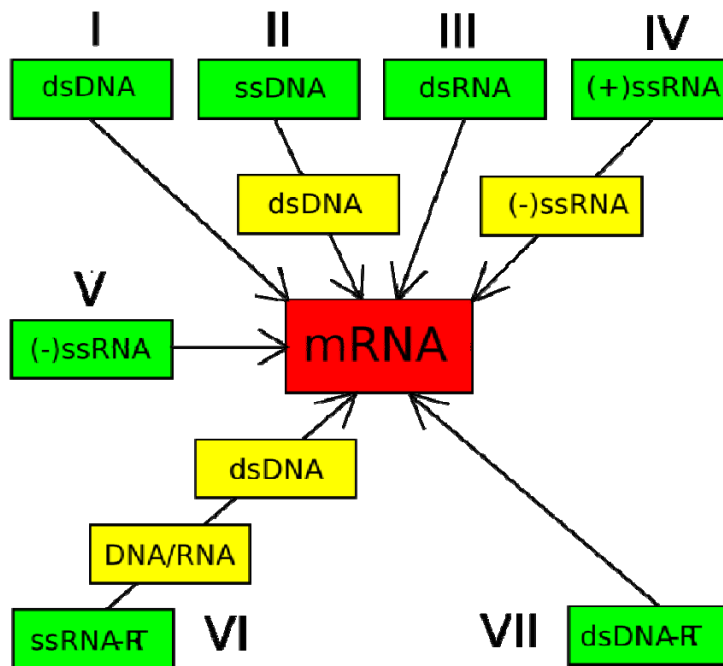


Figure 98 Baltimore Classification of Viruses Classes I-VII  
ds double stranded, ss single stranded, RT Reverse transcriptase free to publish

As previously mentioned (see Figure 98) the best known example of number VI Baltimore classification system are Retroviridae. Amongst the seven retroviridae members the most common are Lentiviruses.

### 5.1.1 Lentiviruses

As lenti means slow this naming stands for the long period it often takes from the infection to the onset of the disease, which can be more than ten years. The pandemic disease AIDS is caused by the lentivirus HIV.

An HIV or lentivirus live cycle starts with the binding of gp120, a viral glycoprotein to the CD4 receptor on the cell surface of certain CD4 positive cells (Landau, Warton et al. 1988). gp120 also binds to a secondary host cell receptor CCR5 forming a stronger complex (Dobrowsky, Zhou et al. 2008) and induces fusion of the virus covering membrane with the cellular membrane and subsequently the release of the virus content into the cell. gp41 complex formation provides the energy for the fusion (Melikyan, Markosyan et al. 2000). Campell et al. (Campbell, Nunez et al. 2004) proposed that nef (negative factor, viral) binding is responsible for the release of the virus core content into the host cell by actin rearrangement, however other reports rather expect virus cellular receptor interactions to be responsible for that (Pizzato, Popova et al. 2008). The viral genome is then reverse transcribed by the reverse transcriptase in a reverse transcription complex (RTC) inside the capsid (Arhel, Souquere-Besse et al. 2007). The resulting provirus DNA is then included in a preintegration complex (PIC) of 56nm (Miller, Farnet et al. 1997) which also contains viral proteins such as Integrase (IN), RT, nucleocapsid protein (NC), viral protein R (Vpr), matrix (MA) and cellular proteins (Bukrinsky, Sharova et al. 1992; Bukrinsky, Sharova et al. 1993). This PIC is then transported through the pore complexes into the nucleus consuming ATP (Bukrinsky, Sharova et al. 1992). Inside the nucleus the provirus DNA is integrated into the hosts genome by IN (this process will be described further later on). The inserted sequence can be transcribed into proviral DNA by RNA polymerase II (RNAP II) which is supported

by viral tat protein. Transcriptional transactivator (TAT) binds to RNAPII generated stem-loop RNA (Feng and Holland 1988) and increases the processivity of RNAPII by interaction of several cofactors. Rev, another viral protein stabilises partially spliced and unspliced mRNA promoting transport to the cytosol (Schmid and Jensen 2008) and viral protein synthesis. New viral particles start to assemble using envelope (env), gag-pol and gag proteins surrounding RNA. Gag binds to viral RNA and host cell membrane by its MA domain (Saad, Miller et al. 2006) and directs the gp120 and gp41 glycoproteins to the cell membrane. By budding virus particles are released from the cell. The virus finally matures by protease driven capsid formation (Pluta and Kacprzak 2009) (see Figure 99).

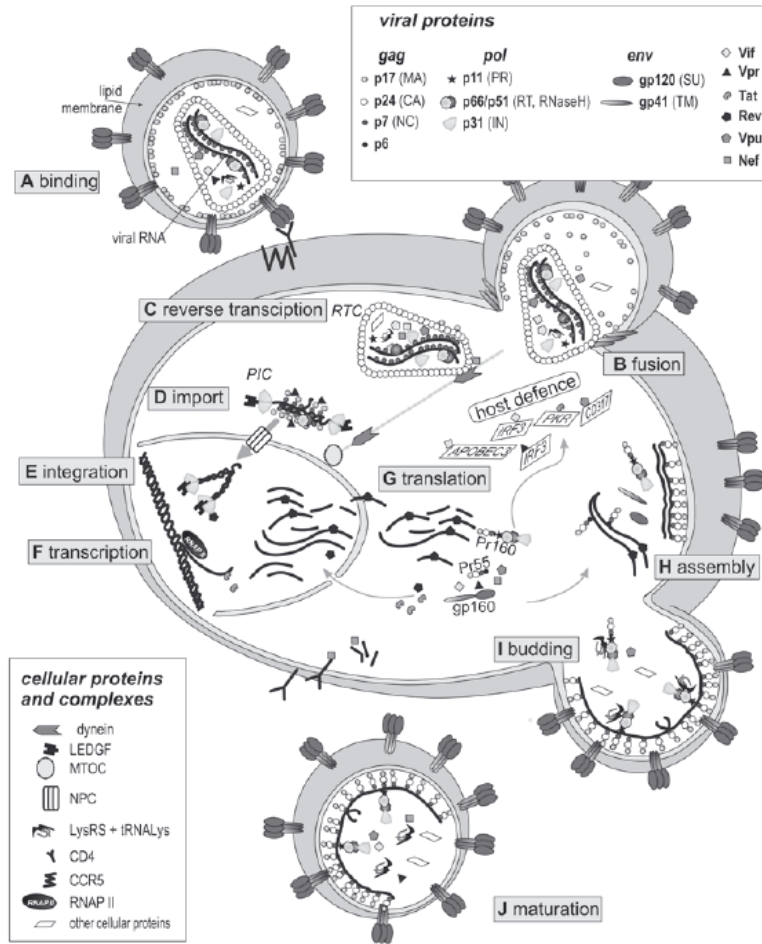


Figure 99 HIV Lifecycle

An HIV virus binds to the membrane of a human cell (A). The viral envelope membrane fuses with the cell membrane and the virus content is released into the cell (B). In the cytosol the virus genome is reverse transcribed and an preintegration complex is formed (PIC) (C). The PIC is imported into the nucleus (D). Inside the nucleus viral DNA is integrated into the genome of the cell (E). Genomic viral sequences can be transcribed into viral RNA and exported into the cytosol (F). Coding viral RNA is translated into viral proteins (G). Viral proteins and the viral ssRNA genome assemble at the cell membrane (H) and viral contents are encapsulated into membrane by budding (I). A fully encapsulated virus is released from the cell (J) and the cell undergoes lysis. from (Pluta and Kacprzak 2009)

## 5.1.2 Reverse Transcription

The discovery of Reverse Transcriptase (RT) in 1970 (Baltimore 1970) has overthrown the former dogma of a one way DNA → RNA → Protein mechanism.

Cytosol located capsid encapsulates the reverse transcription complex (Arhel, Souquere-Besse et al. 2007) where the RT reaction takes place, resulting in a dsDNA copy of the viral RNA. The (-) strand is the ssDNA strand which is complementary to viral RNA while the (+) strand corresponds to the viral RNA sequence. The process is highly complex (see Figure 100).

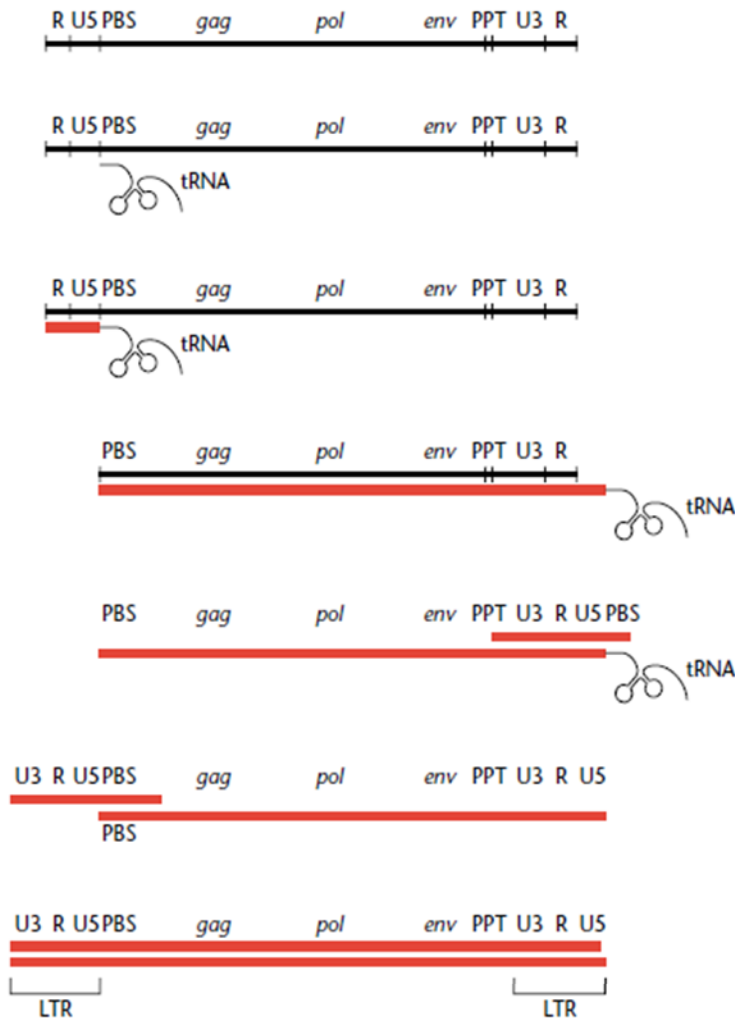


Figure 100 Reverse transcription of lentiviral RNA

A tRNA binds to the primer binding site close to the 5' end of the viral RNA (2<sup>nd</sup> from top). A short complementary DNA is synthesized to the 3' end of the minus strand DNA (3<sup>rd</sup> from top). This cDNA “jumps” to the 3' end synthesis of the (-)DNA strand is started (4<sup>th</sup> from top). RNA upstream of PBS is digested by RT and DNA is synthesized until the new PBS end (5<sup>th</sup> from top). A second jump takes place locating this short sequence to the end of the longer (-) DNA where the complementary PBS sites anneal (6<sup>th</sup> from top). This starts the (+) strand DNA synthesis and the fill in at the end of the minus strand resulting in an double stranded DNA with an 3' and an 5' LTR (7<sup>th</sup> from top). LTR long terminal repeat PBS primer binding site R repeat region U 5/3' unique region 5'/3' ppt polypurine tract gag, pol, env viral genes encoding polymerase (pol), envelope proteins (env) and coat protein (gag) from (Pedersen FS and Duch M 2001)

To start reverse transcription a producer cell tRNA is used as a primer (Figure 100). This tRNA binds to the primer binding site (PBS) close to the 5' end of the viral RNA and a short complementary DNA is synthesized to the 3' end of the minus strand DNA. This tRNA bound DNA serves as a primer at the 3' end of viral RNA after “jumping” to that end and starting synthesis of the (-)DNA strand. For this RNA upstream of PBS including the R and the U5 region are digested by the RNase H function of the RT leading to an initial shortening of the 5' end of viral RNA by the R and U5 region. The (-)strand DNA is then synthesized until the new PBS end while the remaining RNA is digested apart from the polypurinettract (Ppt) sequence which is RNase H resistant and serves as a new primer. The “ppt” primer promotes the synthesis to the tRNA coupled end generating a short sequence complementary to U3 R U5 which is followed by an PBS complementary sequence corresponding to a part of the tRNA. Then the second jump takes place locating this short sequence to the other end where the complementary PBS sites anneal. This starts the (+) strand DNA synthesis and the fill in at the end of the minus strand resulting in an double stranded DNA with an 3' and an 5' LTR (long terminal repeat) (Pedersen and Duch 2001).

### **5.1.3 Integration**

The Integrase (IN) recognizes att sequences in the provirus DNA and coils it into a circular shape. Then both provirus DNA 3' ends are processed removing 2 nucleotides from both 3' ends generating -OH groups there. Genomic DNA is cleaved creating 5' overhangs of host DNA and joining these to the 3'-OH viral DNA groups in a transesterification mechanism. The left gaps are filled and ligated by cellular enzymes. The



resulting genomic DNA bears an integrated provirus sequence. This sequence is stable and retained during cell division (Pedersen and Duch 2001) (see Figure 101).

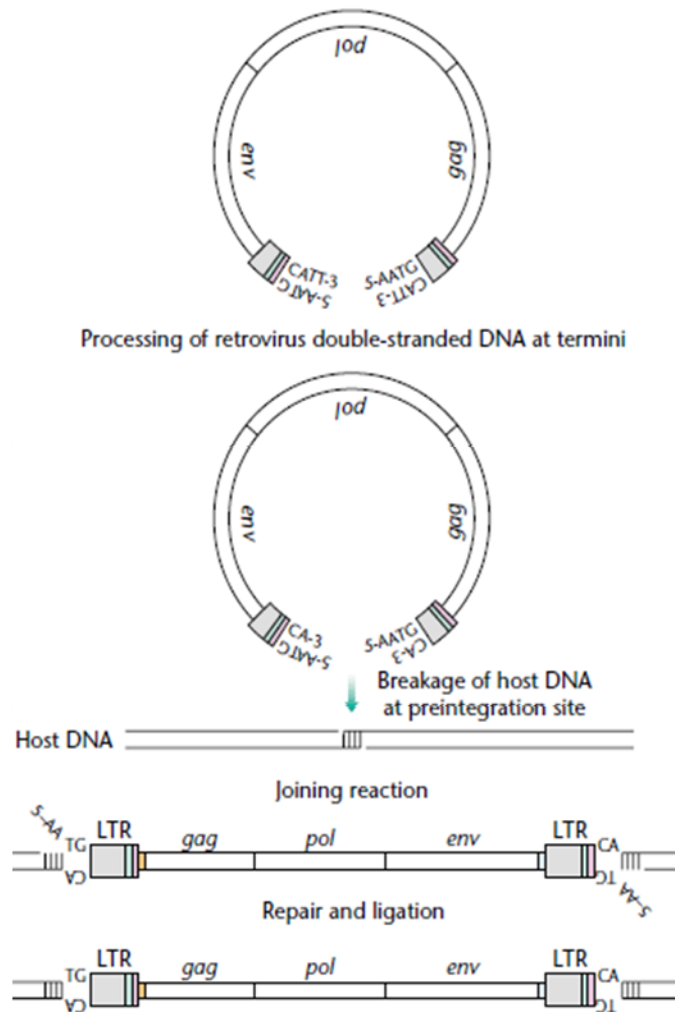


Figure 101 Lentiviral DNA integration

Integrase (IN) recognizes att sequences in the provirus DNA and coils it into a circular shape (Top) and processes both ends generating –OH groups. Genomic DNA is cleaved creating 5' overhangs of host DNA and joining these to the 3'-OH viral DNA groups in a transesterification (2<sup>nd</sup> and 3<sup>rd</sup> from Top). Left gaps are filled and ligated by cellular enzymes (4<sup>th</sup> from top). from (Pedersen and Duch 2001)

LTRs contain vital signals for gene expression such as promoters, enhancers, transcription -initiating, -terminating and polyadenylation signals. LTR signals direct expression by host cell enzymes such as RNA polymerase II, poly A synthetase and guanyl transferase. The U3 region in the 5' LTR encodes enhancer and other

transcription regulators. The promoter TATA box is located closely to the 5'LTR R sequence. The 5'LTR is a promoter for RNA polymerase II, the transcript starts at the 5' R region and is terminated by the poly A tract after the 3' R region (Nolan GP, LAB tutorials).

### **5.1.4 Genomic structure**

An HIV virus contains two positive sense ssRNA molecules which provide its high genetic variability. Especially RT derived recombination is thought to contribute to this variability (Rhodes, Wargo et al. 2003). The HIV provirus DNA is 9.7kb long including nine open reading frames (ORF) which translate into nineteen proteins. As shown in Figure 102 A the majority of the provirus DNA is protein encoding while both edges, the 5' and the 3' LTRs (long terminal repeats) contain the 3' unique element (U3), the repeat element (R) and the 5' unique element (U5). While the trans elements are encoding proteins the LTRs contain cis elements functioning in integration, like the previously mentioned att repeats, enhancer/promoter sequences, transactivation response element (TAR) and a polyadenylation signal. Cis elements downstream the 5' LTRs are primer binding site (PBS) and viral RNA packaging/dimerisation signals ( $\phi$  and DIS), central cis elements are central polypurine tract (cPPT) and central termination sequence (CTS). Upstream of 3' LTR are rev response element (RRE) responsible for the export of viral mRNA into the cytosol and purine rich region (PPT) important for +strand DNA synthesis (Pluta and Kacprzak 2009) (see Figure 102).

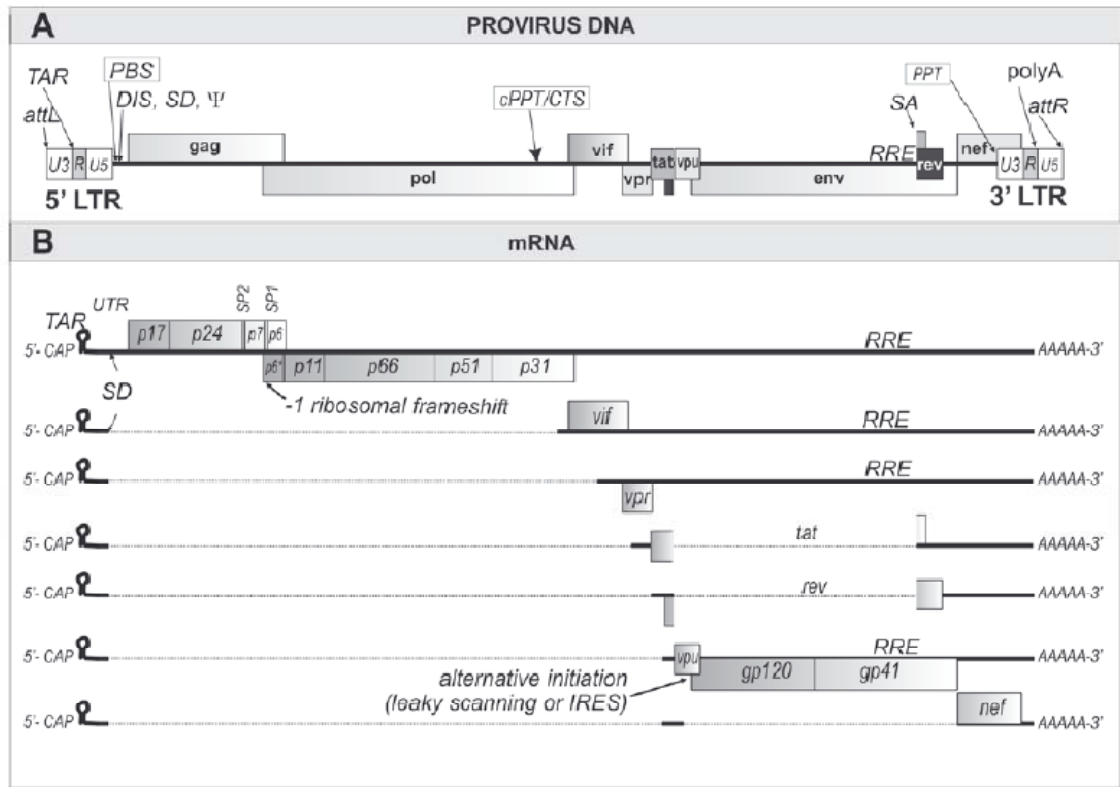


Figure 102 Genomic structure of HIV

(A) Provirus DNA contains the 5' and 3'LTRs (Long terminal repeats) which contain the U3, R and U5 regions. Viral ORFs gag, gag-pol and env encode for proteins. Primer binding site (PBS) is located upstream of gag while the poly A sequence is contained in the R region of the 5' LTR. (B) viral mRNA is alternatively spliced and by this the three open reading frames give rise to several different viral proteins MA matrix, CA capsid, NC nucleocapsid, PR protease, SU gp120, TM gp41, tat transactivator protein, rev regulator of viral protein expression, nef negative factor, vif viral infectivity, vpr viral protein R and vpu viral protein U from (Pluta and Kacprzak 2009)

The 3 longest open reading frames (ORF) gag, gag-pol and env translate into structural proteins and enzymes while the smaller central and 3' ORFs translate into regulatory proteins such as tat and rev genes and accessory proteins encoded by vif, vpr, vpu and nef (Figure 102). The high number of protein driven by one promoter is achieved by alternative splicing of proviral mRNA. By this the HIV virus can reduce the size of its genome. Gag polyprotein cleavage yields 6 structural proteins: matrix (MA) responsible for transport e.g. of PIC, capsid (CA), nucleocapsid (NC) involved virus processing, SP1 and SP2 regulating cleavage rate and p6 a regulative factor. gag-pol polyprotein cleavage mainly produces enzymes like RT, protease (PR) and IN. env gives rise to the

two glycoproteins gp120 (SU) and gp41 (TM) responsible for virus uptake. Purely regulatory are the transactivator protein (tat) which initiates transcription from viral LTRs and regulator of expression of viral proteins (rev). The last group are accessory proteins including negative factor (nef) important in down regulation of CD4 receptor and other receptors, viral infectivity (vif) inactivating host immune response, viral protein R (vpr) connected to processes such as nuclear import of viral PIC and viral protein U (vpu) regulating CD4 receptor, viral particle release and apoptosis (Pluta and Kacprzak 2009).

### **5.1.5 HIV derived Lentiviral vectors**

Lentiviruses are highly efficient gene delivery tools suitable for dividing as well as quiescent cells. Though these vectors are derived from viruses generating lethal diseases they have been refined over the last two decades to provide safe tools. The endeavour to make lentiviral vectors safer started in 1990 with replication defective HIV-1 vectors (Helseth, Kowalski et al. 1990). In the same year work using lentiviruses as a gene delivery tool was published (Page, Landau et al. 1990). Replication defective lentiviruses can transduce, integrate genetic material into the host cell, but do not produce new infectious particles. A well established system of lentiviral transduction is using three vectors a packaging vector, a transfer vector and an envelope vector. The principle is to separate trans elements encoding for structural, accessory and enzymatic proteins from cis elements required for reverse transcription, integration, RNA synthesis and packaging.

Genes encoding for structural proteins for formation of infectious particles as well as viral enzymes are encoded by the packaging vector.

For this several elements were replaced, deleted or added. In the packaging vector the 5' LTR is replaced by another promoter such as CMVie immediate early promoter (ie) from the cytomegalovirus (CMV) (see Figure 103). Additionally the  $\phi$  sequence required for packaging was deleted. Poly A signals can be derived from other viruses e.g. simian virus 40 (SV40). Further modifications such as LTR and PBS abolished the full length viral mRNA to be included into viral particles (Naldini, Blomer et al. 1996). The functioning of mRNA processing was maintained by the RRE sequence. The development of the 2<sup>nd</sup> generation packaging vectors which we currently use in the Heidenreich group, was initiated by the removal of accessory proteins such as vif, vpr, vpu and nef reducing virulence and cytotoxicity while still allowing *in vitro* virus replication (Gibbs, Regier et al. 1994). The final 2<sup>nd</sup> generation packaging vectors were described by several authors 3 to 4 years later (Zufferey, Nagy et al. 1997; Mochizuki, Schwartz et al. 1998) and they contained only gagpol, tat and rev ORFs (Fig. 106 A).

The transfer vector contains the sequence for gene(s) to be expressed and its own promoter, surrounded by elements such as PBS, gag, RRE, cPPT/CTS, PPT and LTRs (modified) (Naldini, Blomer et al. 1996) needed for reverse transcription, nuclear import, integration and packaging. RRE is used to enhance gene transfer efficiency in the presence of gag (Clever, Sasseti et al. 1995). A further step in safety was accomplished by the development of self inactivation (SIN) vectors by deletion of the U3 region in 3'LTR (dull et al. 1998) while the replacement of 5'LTR U3 by CMV promoter was shown to enable tat independent vector cassette expression (Kim, Mitrophanous et al. 1998). SIN vectors express almost no transcripts and strongly reduce generation of new

virus particles in host cells (Bukovsky, Song et al. 1999). As retroviruses preferably integrate near promoter or regulatory proteins (Wu, Li et al. 2003) their LTRs potentially enhance transcription promoting insertional tumours. Hence the SIN vectors provide potentially less harmful viruses and this is supported by the finding that genotoxicity mainly depends on active LTRs (Montini, Cesana et al. 2009). Moreover they show a different integration behaviour (B Moreno-Carranza, M Gentsch, Gene Therapy 2009).

The envelope vector provides glycoprotein missing on the two other vectors providing enhanced specificity towards target cells, reduced sequence homology to wt HIV and increasing particle stability enabling virus concentration and storage. The usage of heterologous glycoproteins such as gp160 in lentivirus production has been known since twenty years (Page, Landau et al. 1990).

Alike the packaging vector the protein encoding sequence is followed by an pA signal and promoted by CMV replacing both LTRs (see Figure 103).

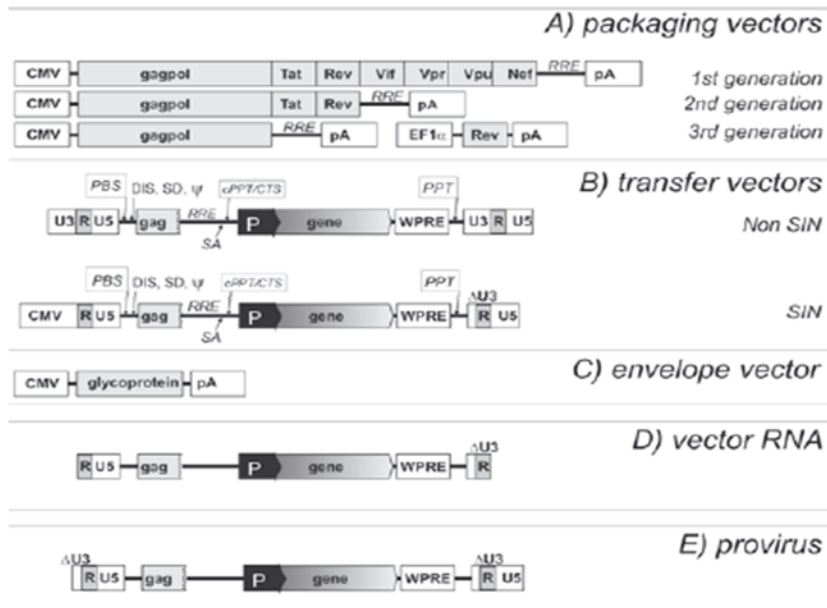


Figure 103 The development of lentiviral vectors

(A) lentiviral packaging vectors. The 2<sup>nd</sup> generation packaging vectors only encode *tat* and *rev* proteins and lack the regulatory and accessory proteins from the 1<sup>st</sup> generation. 3<sup>rd</sup> generation packaging vectors additionally pack the *rev* sequence in another vector. (B) Non-SIN vectors have intact 5' LTR while SIN (self inactivating) vectors have a deletion in U3. (C) Envelope vectors encode for glycoproteins. (D) SIN vector RNA of 2<sup>nd</sup> or 3<sup>rd</sup> generation systems has a deletion in U3 (E) After integration of (D) into host genome the mutated 5'LTR cannot initiate transcription. CMV, cytomegalovirus immediate-early promoter; EF1 $\alpha$ , human elongation factor 1- $\alpha$  promoter; *gag*, 5' portion of *gag* gene containing dimerization /packaging signals; PBS, primer binding site; DIS, dimerization signal; SD, splice donor site; SA, splice acceptor site;  $\psi$ , packaging signal; cPPT, central polypurine tract; CTS, central termination sequence; RRE, Rev response element; PPT, polypurine tract; pA, polyadenylation signal;  $\Delta$ U3, SIN deletion in U3 region of 3' LTR; P, internal promoter for transgene expression; WPRE, woodchuck hepatitis virus (WHV) post-transcriptional regulatory element from (Pluta and Kacprzak 2009)

## 5.1.6 IRES

After viral infection cells often inhibit virus production by a strong reduction in protein synthesis (T. Pe'ery and Mathews 2000). To overcome this inhibition viruses have developed strategies including the use of an internal ribosome entry site (IRES) facilitating initiation of protein synthesis independent of the 5' end. Nowadays IRES sequences are widely used in lentiviral vectors with more than 56 viral and 80 cellular IRES sequences characterised (Baird, Turcotte et al. 2006; Mokrejs, Vopalensky et al. 2006). In SIV it was shown that ribosomes can be recruited to an internal sequence of mRNA by the 5' UTR (Ohlmann, Lopez-Lastra et al. 2000). Experiments have shown

that if two ORFs are linked by an IRES the expression of the second ORF is driven by IRES enabling and enhancing downstream ORF translation. Even if the expression of the upstream ORF is inhibited by interference with an elongation factor (eIF4E) the second ORF is still productive (Balvay, Soto Rifo et al. 2009).

If more than one gene product is to be co-expressed e.g. a marker gene like GFP the ORFs can be linked by an Internal ribosomal entry site (IRES). IRES transcribes for an RNA sequence which form a complex 3 dimensional structure interacting with ribosome units, cellular initiation and elongation factors (Balvay, Soto Rifo et al. 2009).

### **5.1.7 WPRE**

One of the regulative cis activating elements is WPRE. It consist of woodchuck hepatitis virus (WHE) post-transcriptional regulatory element (PRE) (Zufferey *et al.*, 1999). The insertion of this element in the 3' untranslated region of a transcript leads to a more than 6 fold increase in overall transgene expression (Oh *et al.*, 2007).

### **5.1.8 Tet-on**

The need for inducible lentiviral gene expression has lead researchers to develop several systems to inducibly regulate gene of interest expression with the tet-on system. Like tet-on all tet system are derived from prokaryontic components of tet (tetracycline resistance) operon. VP16 a viral transactivation element from herpes simplex virus (HSC) is fused to a mutated version of the bacterial tetrepressor (tetR) rtetR on which the tet system are based. VP16 can strongly activate viral gene transcription (see Figure 104).



A reverse tet-controlled transactivator (rtTA) can bind the tet-responsive element (TRE) when complexed to doxycycline (dox), a synthetic tet-analoga. The binding of Doxycycline, a drug which can easily be distributed to all tissues e.g. by oral intake, induces a conformational change thus inducing gene expression (Gossen, Freundlieb et al. 1995) (see Figure 104). Teton systems have also been developed for HIV based Lentiviral systems however. One major problem were the high background expression levels (Reiser 2000) which would be achieved with the development of SIN Lentiviruses (Koponen, Kankkonen et al. 2003). Work has been done to enhance the rtTA transcativator furthermore by increasing the induction to background level. This was achieved by a different positioning of the tetracycline operator sequences (tetO) such as separating the tetOs by 36bp (Agha-Mohammadi, O'Malley et al. 2004). Such vectors represent now the 2<sup>nd</sup> generation of TREs.

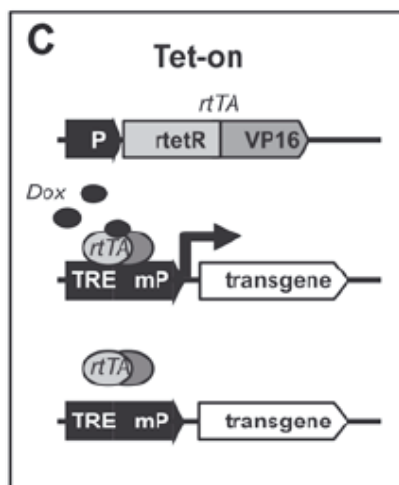


Figure 104 Tet-on system

In the presence of Dox reverse Tet-controlled transactivator (rtTA, mutant version of tTA) binds TRE promoter and activates transcription. P, promoter; TRE, Tet-responsive element; mP, minimal promoter from (Pluta and Kacprzak 2009)

### 5.1.9 Two vector system design

Lentiviral vectors are efficient gene delivery tools which can also transduce non-dividing cells. Since many leukaemic cell lines including the MLL/AF4 positive SEM used here are difficult to transfect, lentiviral gene delivery would be an ideal system for gene (over) expression in target cells. However anti-proliferative and pro-apoptotic genes could counter-select transduced cells before the experiment of interest can be performed. An inducible system would overcome these problems, but as many inducible systems allow basal gene expression before induction a tighter system was needed.

The Heidenreich group is establishing a lentiviral two vector system in cooperation with Christian Berens (Microbiology University Erlangen-Nuernberg). Vector 1 of this system contains a second generation Tet-transactivator stTA2<sup>s</sup>-M2 linked to the reporter gene GFP via IRES. The constitutively active SFFV promoter drives expression of tet activator while marking transduced cells with GFP, which allows for the selection of positive cells (see Figure 105 A).

The second vector contains the gene of interest (GOI). Upstream of GOI seven Tet-operators (tetO) are located. They represent binding sites for the tet transactivator expressed by vector 1. Following rtTA binding sites (tetO7) a minimal CMV promoter is located. If two genes are to be co-expressed their ORF will be linked over an IRES sequence. The positive transduction with vector 2 can be reported by a mCherry sequence, coding for a red fluorescent protein which is constitutively expressed by an upstream PGK promoter. This PGK promoter should not interfere with the CMV promoter (see Figure 105 B).

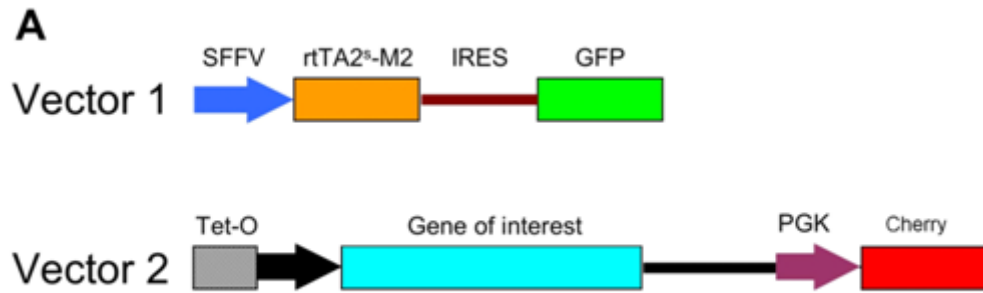


Figure 105 Scheme of Lentiviral two vector system

Vector 1 contains the SFFV promoter followed by the tet activator (rtTA) -, an IRES- and a GFP sequence. Vector 2 contains the tetO promoter followed by the gene of interest, a PKG promoter and a mcherry sequence.

The following schematic (Figure 106) shows how the 2 vector system would be used to provide cells with an inducible GOI expression.

Target cells are transduced by an HIV based Lentivirus containing vector 1. Transduced cells express the rtTA protein constitutively as well as GFP. Positive cells are then selected by their GFP positivity either by clone selection in methylcellulose or by sorting. Cells transduced for rtTA expression are then transduced a second time with vector 2 and selected by the reporter gene, this time mcherry. Doubly transduced cells will be expanded and GOI expression is induced by administration of doxycycline (DOX) (see Figure 106). The administration of doxycycline derived regulation of gene expression can be performed *in vitro* and *in vivo*.

The generation of double transduced highly inducible cells should enable us to investigate leukaemic stem cells (LSC) and apoptosis relevant genes without a selective pressure by these genes during selection. Moreover clonal artefacts can be excluded by further analysis and experimentation.

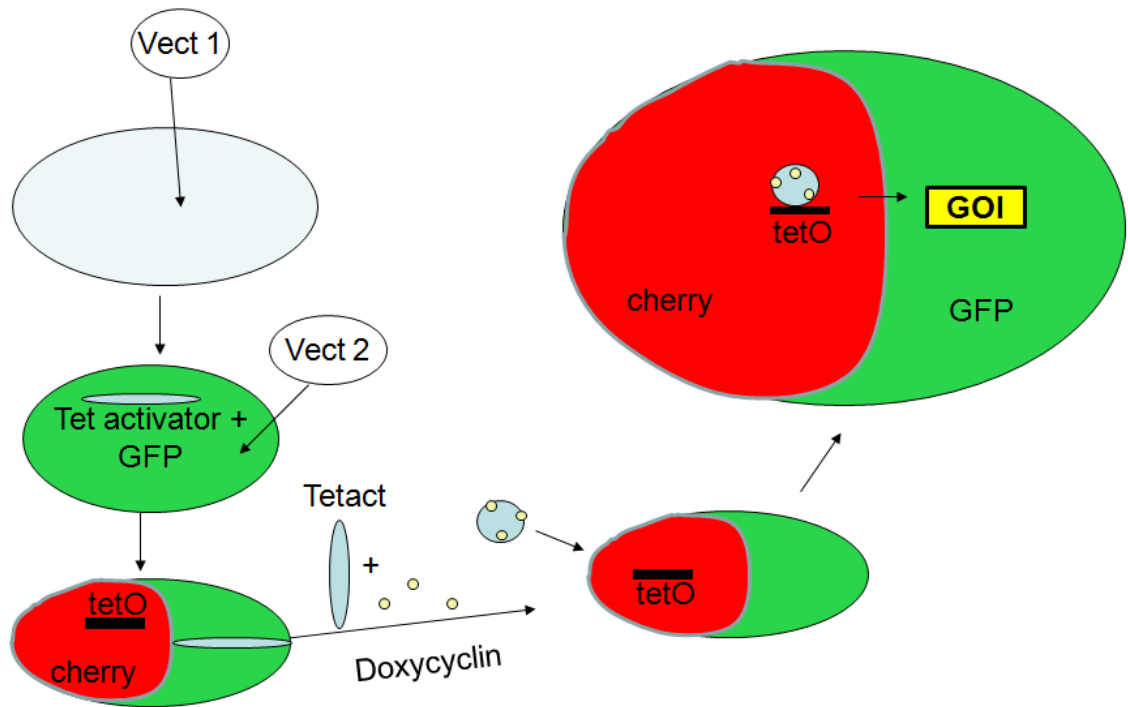


Figure 106 Schematic of the protocol for the lentiviral two vector system

(Top left) A target cell is infected with vector 1. (Below) Transduced cells express tet activator and GFP used for selection. Selected cells will be further transduced by vector 2 and selected by mCherry (Bottom left). By induction with doxycyclin tet activator can bind to tet-operator and induce GOI expression (Right) GOI gene of interest; Tetact tet activator; tetO tet-operator

## 5.2 Aims

As mentioned in the previous chapter gene functions can be investigated by knockdown of the transcript levels which should also affect the corresponding protein levels.

An alternative approach is to over express the target genes and then assay their effect. The most convenient way to achieve this is to transfect cells with an expression vector or even to generate clones with a stable expression of a desired protein. Unfortunately, MLL/AF4 cells lines such as SEM are not accessible to conventional stable transfection. Instead viral expression of target genes is required. Considering that we are also interested in leukaemic stem cells, such an expression system must be able to transduce quiescent cells. Here, lentiviral systems provide the best option. Furthermore, some of the target genes we are interested in may be quite toxic if over-expressed and this would eliminate the selection of a target gene transduced clone. For this reason a novel lentiviral expression system had to be established which allows tight control of the expression of a target gene at a desired time point. Existing systems still allow basal expression levels of target genes. Following aims were to investigate the effect and functions of those target genes for example in the artificial niche assay described above. Furthermore this system is not restricted to analysis of MLL/AF4 target genes, but has potentially wide ranging applications in expression analysis.

Specific aims:

0. To generate such a system, which allows tight control of target gene expression.
  
1. To over express MLL/AF4 target genes using lentiviral transduction methods and a tetracycline-regulated expression system.
  
2. To investigate the downstream effects of target gene over-expression on niche function and clonogenicity.

## 5.3 Results

### 5.3.1 Generation of the TetOn Vector

To produce the Teton vector the pUHrT62-1 vector was used as a source for the Tet activator sequence. A short sequence was removed upstream of the Tet activator element (rtTA2S-M2) and an oligo-linker inserted which provided a novel *Asc*I restriction site in the vector. In parallel, a short sequence between the last 10 bases of the SFFV promoter and the IRES element was removed from the lentiviral vector pSIEW. The Tet activator sequence was cut out of the pUHrT-oligo vector and inserted into SIEW (see Figure 107).

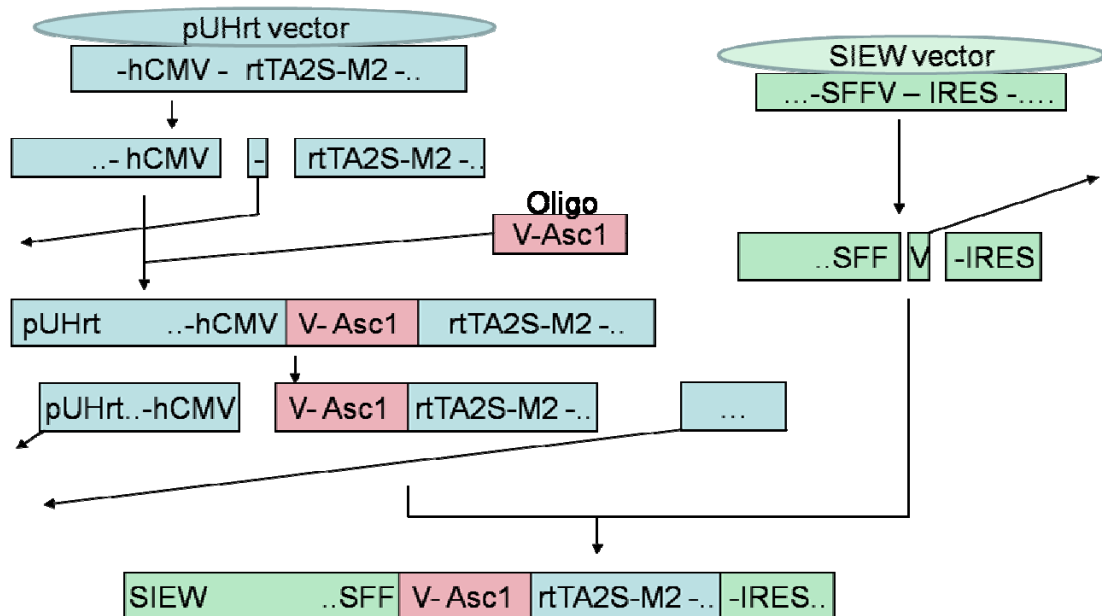


Figure 107 Scheme of Lentivirus 1 (Teton vector) cloning

CMV Cytomegalovirus (promoter), rtTA2S-M2 tet activator, SFFV Spleen focus forming virus (promoter), IRES Internal ribosome entry site, *Asc*I restriction site

### 5.3.2 Cloning of the TetOn vector

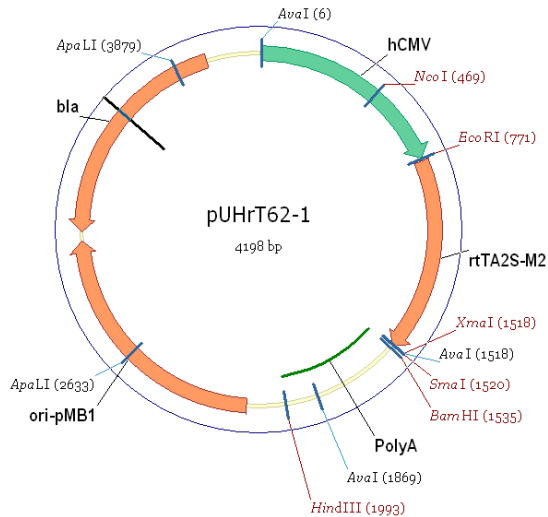


Figure 108 Map of pUHrt62-1

CMV Cytomegalovirus (promoter), rtTA2S-M2 tet activator, bla Blasticidin resistance, ori-pMB1 ori (origin of replication) from pMB1 plasmid

The 4198bp plasmid above (Figure 108) importantly contains an hCMV promoter upstream of the tet activator (rtTA2S-M2), followed by an PolyA tail.

Oligo sequence

```

5'- ggaaggcgcgccagtctccgag -3'
3'- cgcttcgcgcggtcaggaggctcttaa -5'
    SacII AscI SFFV EcoRI
  
```

AscI SFFV  
ggcgcgccagtctccga

The oligo sequence consists of a 3' protruding end, complementary to a 5' end of a cut SacII sequence upstream of EcoRI (771). This is followed by an AscI restriction site, the last 10 base pairs of the SFFV element, which had to be replaced and the 5' protruding end of an EcoRI restriction site. To be able to use the EcoRI restriction site in SIEW (see Figure 109) the last 10 bases of SFFV had to be replaced with the oligo so





The pHR-SINcPPT-SIEW (SIEW) (see Figure 109) lentiviral vector contains an ampicillin resistance gene (Amp), an SFFV promoter, an IRES linker element, an EGFP reporter gene, and several viral elements like GaG, RRE, cPPT, WPRE and the 5' and 3' LTRs (Long terminal repeats, the cassette between 5' and 3' LTR is integrated into the genome of the transfected cell, termed transduction).

The pUHrT62-1 (Figure 108) plasmid was digested with SacII and EcoRI. Oligo 1 was ligated into the open vector. The insertion was confirmed by a restriction digest with BamHI and SgsI. For clones with the oligo insertion, expected bands were 3500bp + 750bp, while the vector without insert was expected at 4200bp of size (see Figure 110).

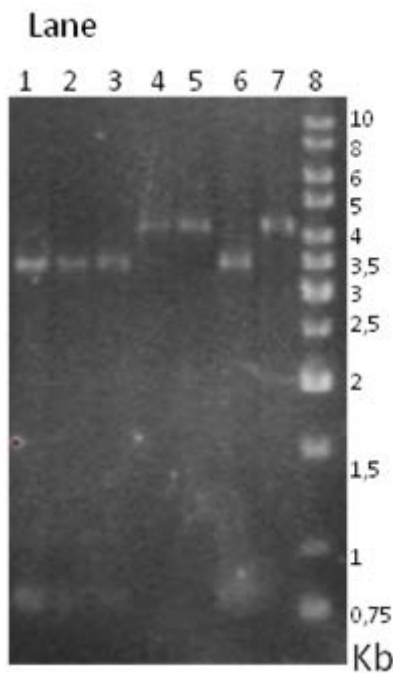


Figure 110 Restriction analysis of pUHrT62-1 oligo ligation  
pUHrt Oligo ligation clones digested with BAMHI and SgsI 1% agarose gel with digests of 7 clones (Lane 1-7) and a 1kb DNA Ladder (Lane 8, Fermentas)

This gel (Figure 110) showed that clones in lane 1, 2, 3 and 6 were positive for the oligo1 insert, while lane 4, 5 and 7 showed clones with no insert.

The tet activator sequence was excised from pUhr1-oligo1 (Figure 107) with BamHI and AscI. The SIEW lentiviral vector (Figure 107) was opened with BamHI and AscI and a short fragment removed. The Tet activator sequence was ligated into SIEW.

To confirm the insertion of this element a control digest was performed using BamHI and AscI. Bands were expected at 750bp and 10000bp if the insertion had worked (see Figure 111).

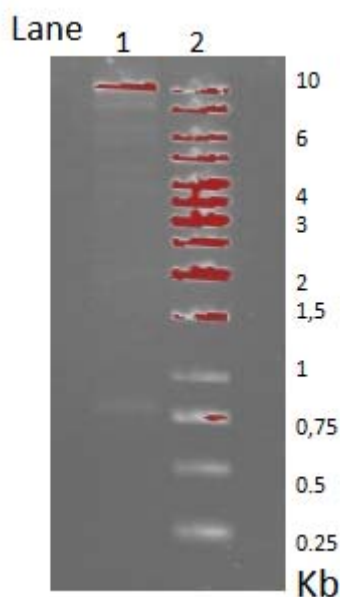


Figure 111 Restriction analysis of Teton vector clone

A Teton-vector clone was digested with BamHI and AscI. 1% agarose gel with digest of 1 clone (Lane 1) and a 1kb DNA Ladder (Lane 2, Fermentas)

The successfully cloned Teton-vector was amplified and stored.

### 5.3.2.1 Test of the TetOn Vector

To test the functionality of the newly cloned Teton vector our collaborator Vasily Grinev has performed an assay using 293T cells. The Teton vector should express the Tet activator when transduced. If cells were transduced with pUHG16-3, a TetO driven beta-galactosidase expression vector in parallel and induced with doxycycline, cells

should have become blue (see Figure 112). The principle is that the induced Tet activator binds to TetO (Tet-operator element) and drives downstream expression of the reporter-gene  $\beta$ -Gal.

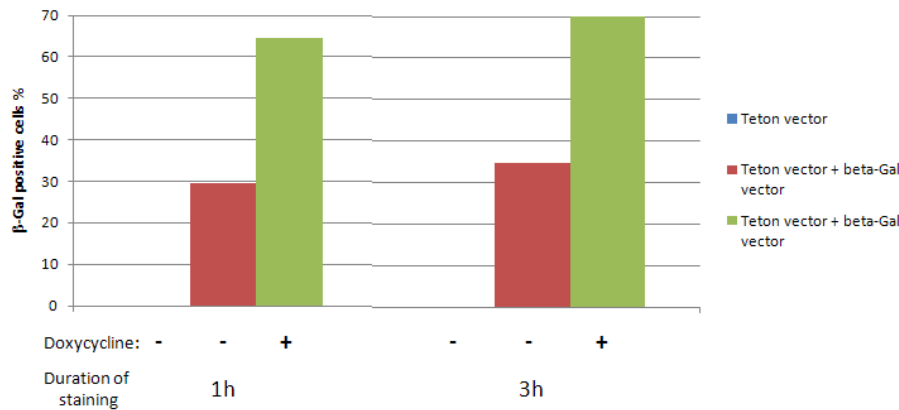


Figure 112 Functionality test of vector 1 (Teton vector)

Performed by Vasily Grinev. 293T cells were transfected with Teton vector (pHR-rtTA, blue columns), additionally transfected with pUHG16-6 reporter plasmid (beta-Gal vector + Teton vector, red columns) and additionally induced with doxycycline (beta-Gal vector + Teton vector + doxycycline) light green columns). Blue cells ( $\beta$ -galactosidase positive) were counted after 1 and after 3 hours of staining. Shown is one single experiment.

The diagram (Figure 112) shows that 293T cells transduced with Teton-vector (pHR-rtTA) alone did not produce any blue cells. Cells additionally transduced with the  $\beta$ -Gal reporter plasmid (pUHG 16-3) produced 29.4% or 34.8 % stained cells after 1 or 3 hours of X-Gal staining respectively. If cells were induced with doxycycline the number of blue cells rose to 64.6% or 70.4% stained cells after 1 or 3 hours of X-Gal staining respectively.

Although this experiment proved that the Teton vector expresses the Tet activator it had some weaknesses. A control with cells only transduced with the  $\beta$ -Gal vector was missing to determine the background levels of  $\beta$ -Gal produced by this vector. Secondly this assay made it hard to judge when cells were positive or negative. Clearly cells were regarded as negative when colourless and positive when deeply blue, but some were

yellow to slightly faint blue. Interestingly, this percentage was higher in the cells with no doxycycline.

In conclusion, it can be said that the doubling of stained cells induced by doxycycline reflects neither the linearity nor the proportionality of the Tet activator induction. Furthermore, doubling of stained cells is not informative with regard to the basal expression levels of Tet activator driven genes.

### **5.3.2.2 Virus generation and transduction of TetOn**

SEM and MV4;11 were transduced with Teton virus, a lentivirus containing the Teton vector (see Chapter 4).

#### **5.3.2.2.1 Validation of Transduction**

The transduction of those cells was checked for the positivity and the intensity of the reporter gene GFP. The green shift compared to normal cells was determined by Flow cytometric analysis (see Figure 113).

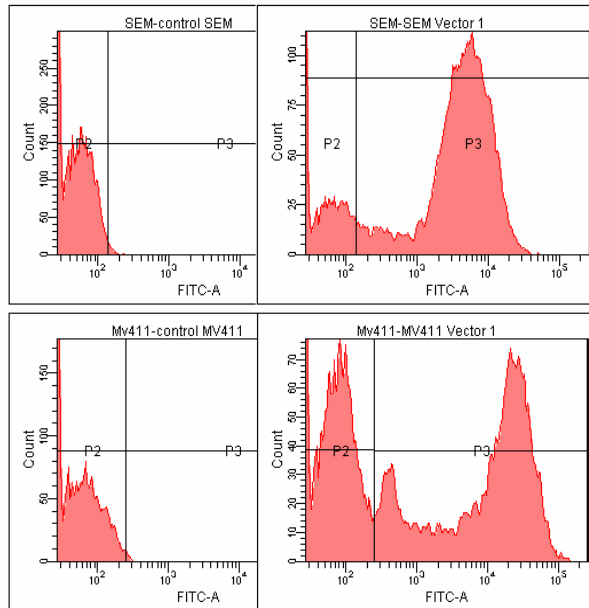


Figure 113 Transduction rates of Vector 1 in SEM and MV4;11

Flow cytometric analysis of SEM (Top row) and MV4;11 (Bottom row) without (Left histograms) and after (Right histograms) Teton vector (vector 1) transduction. The reporter gene GFP was detected in the FITC channel and P3 comprised cells with signal strength above control levels. The efficiencies of the primary inductions were 60% (MV411) to 80% (SEM) from a thawed virus. Sorting purities were 80% (transduced MV4;11) to 90% (transduced SEM).

These new cell lines were further called SEMTeton or MV4;11Teton cells.

### 5.3.2.2.2 Sorting of Transduced cell populations

Surprisingly, after some weeks of culture, flow cytometry showed that less cells were identified as highly GFP positive or GFP positive in total.

To obtain SEM and MV4;11 with a higher percentage of transduction, transduced cells were sorted for GFP expression. Several sorts per cell line were made. After cultivation for two weeks cells were analysed by flow cytometry for their GFP expression.

Sort were termed 73k or 100k for 73 - or 100 - thousand cells sorted and k1,2 or 3 were fractions of those sorts (see Figure 114, Figure 115 and Table 14; Figure 116 and Table 15).

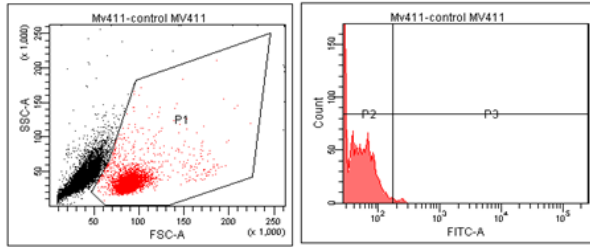


Figure 114 MV4;11 as negative control for transduction

Flow cytometric analysis of normal MV4;11 (Left) SSC-FSC dot-plot with set p1 gate (Right) count-FITC histogram with p2 (GFP negative) and p3 gate.

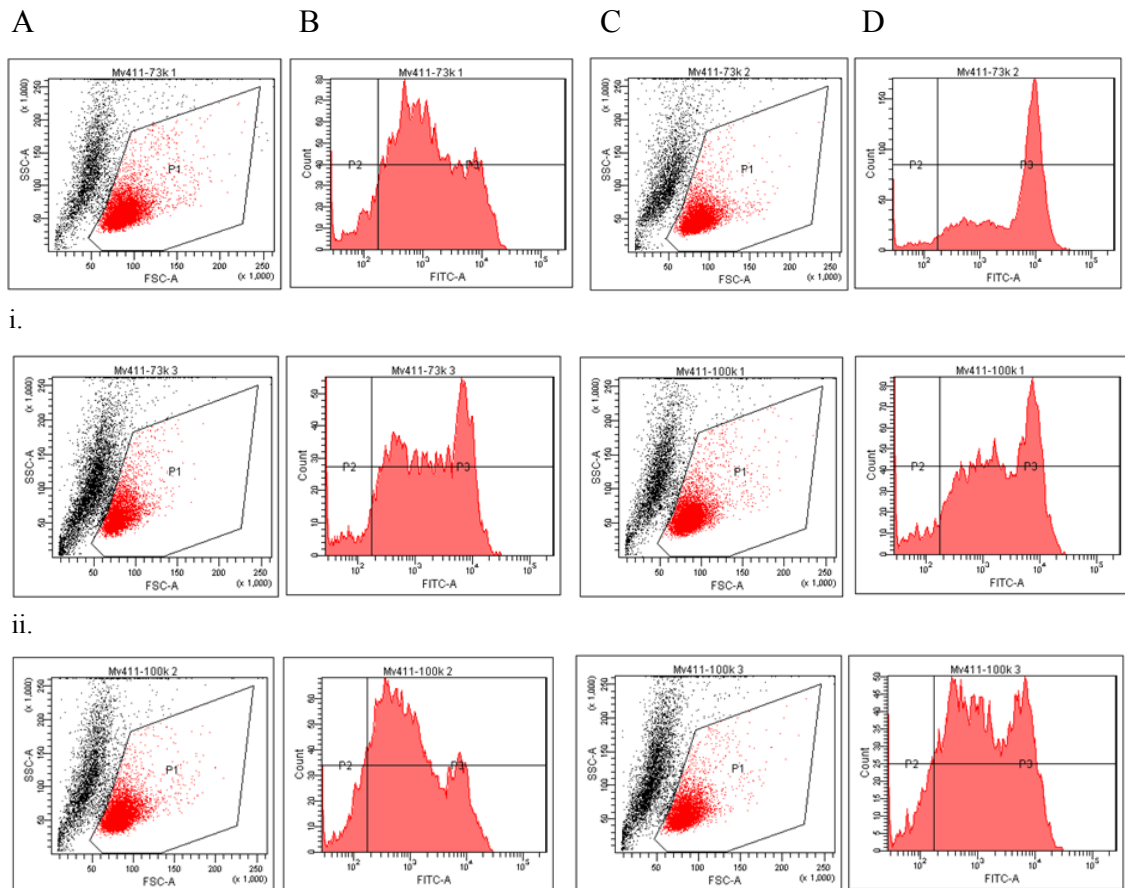


Figure 115 Sorts of Teton transduced MV4;11

Flow cytometric analysis of Teton vector transduced MV4;11 sorted for GFP expression (A and C) SSC-FSC dot-plot with set p1 gate (B and D) count-FITC histogram with p2 (GFP negative) and p3 (GFP positive) gate. (Row i.) sorts 73k1 (A + B) and 73k2 (C + D), (Row ii.) sorts 73k3 (A + B) and 100k1 (C + D) and (Row iii.) sorts 100k2 (A + B) and 100k3 (C + D) 73k/100k 73/100 thousand cells sorted, k1/2/3 fraction of those sorts

Purity %	sort
0.2	MV4;11 control
89.2	73k1
92.4	73k2
89.8	73k3
88.2	100k1
86.8	100k2
87.8	100k3

Table 14 GFP positivity of different MV4;11 sorts  
GFP positivity (purity) of different sorts and control MV4;11

The sorts of MV4;11Teton resulted in different patterns of GFP-intensity distribution but similar purities from 87% to 92 %. Especially the sort 73k2 resulted in a high purity and a distribution with mostly high GFP expression.

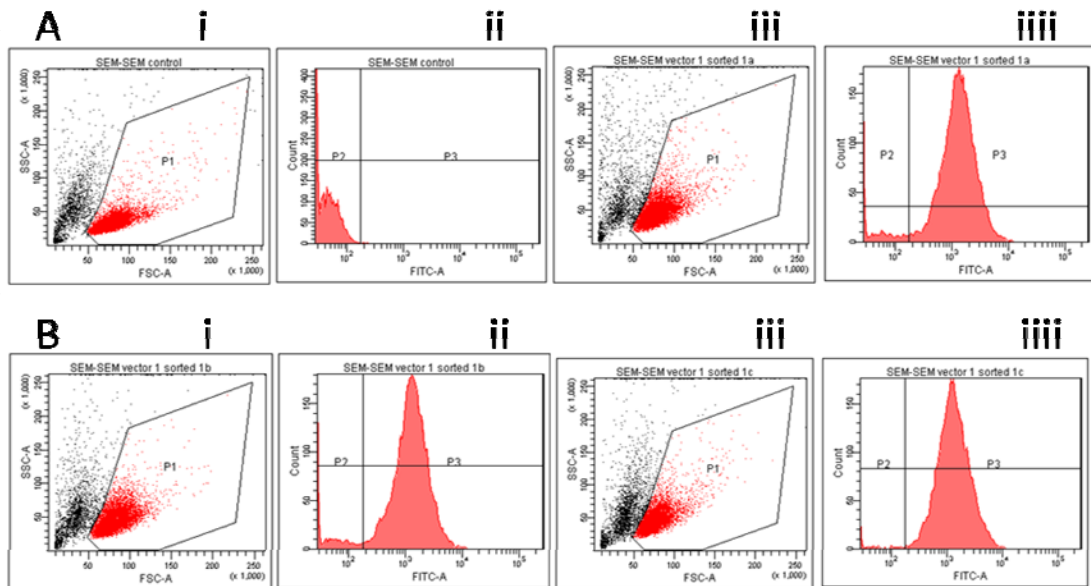


Figure 116 GFP positivity SEM and sorted SEMTeton  
(i and iii) SSC-FSC dot-plot with set p1 gate (ii and ii) count-FITC histogram with p2 (GFP negative) and p3 (GFP positive) gate. (A) Flow cytometric analysis of normal SEM (i + ii) and Teton vector transduced SEMs sort 1a (iii + ii) (B) Flow cytometric analysis of Teton vector transduced SEM, the diagrams show sorts 1b (i + ii) and 1c (iii and ii).



Purity %	sort
0.2	SEM control
91.6	1a
90.9	1b
98.1	1c

Table 15 GFP positivity of SEMTetron  
GFP positivity (purity) of different sorts and control SEM.

The SEMTetron sorts resulted in high purities of nearly 100% (Table 15) but medium levels of GFP expression. Compared to the MV4;11Tetron sorts (Figure 115) the SEMTetron sorts were more homogenous with less distribution in GFP expression.

All sorts were expanded and stored in liquid nitrogen.

### 5.3.2.2.3 Test for accessibility of MLL/AF4 Knockdown

The Tetron cells were of interest for experiments on feeders. To prove that the tet activator or the transduction itself had no influence on the transcript levels or the ability to knock down, native SEM and SEMTetron were treated with siMA6 and siAGF1 and the transcript levels were analysed 2 days after treatment.

The transcript levels of *MLL/AF4* were depleted comparably in the native SEM and the SEMTetron. The Ct values of the *MLL/AF4* amplicons were in a comparable range for SEM (21 to 22.7) and SEMTetron (20.5 to 21.7). This data proved that the transduction did not influence the applicability for such experiments (see Chapter 4).

#### **5.3.2.2.4 Test on bone marrow feeders**

As already shown in chapter 4 (chapter 4.3.3.2) SEMTeton were tested on M210B4. Also transcript-level analysis showed that SEMTeton behaved comparably to native SEM.

#### **5.3.2.2.5 Test of clonogenicity**

SEMTeton and MV4;11Teton were seeded in methylcellulose colony formation assays. Although they showed high proliferation no CFU could be determined due to technical problems, such as colony stability (the cells don't stick together as a normal colony) and time restrictions.

### **5.3.3 Cloning of expression vector**

The cloning of the 2<sup>nd</sup> vector of the bi-vector system relied on a more demanding strategy. It was planned to use the p<sub>tr</sub>e-tight vector which contains the tetO element, insert the PGK promoter from the pWHE vector and downstream of this insert the cherry sequence from pcDNA3 cherry. This cassette would then be inserted into the lentiviral vector SIEW, which had been depleted for GFP beforehand (see Figure 117 and Figure 118). The resulting vector could be used to clone in genes of interest.

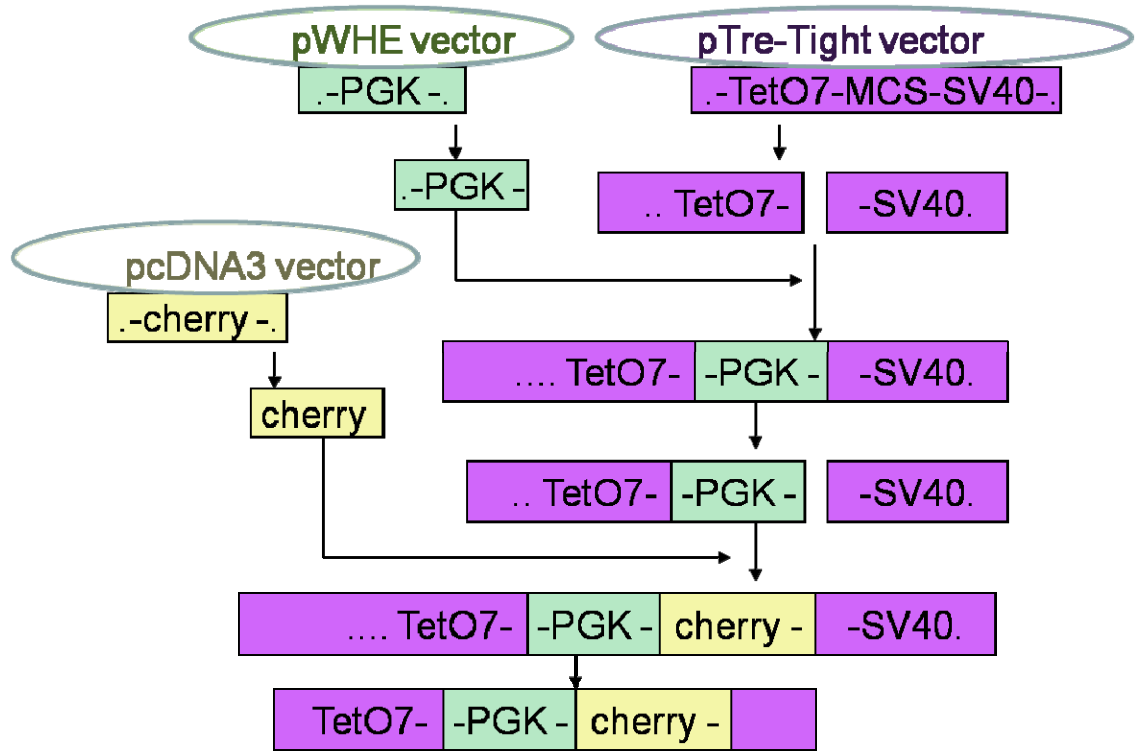


Figure 117 Cloning of the Tet-PGK-cherry cassette

PGK Phospho glycerine kinase (promoter), TetO7 Tet operator (promoter), SV40 Simian virus 40 (poly A), cherry mCherry (red fluorescent protein)

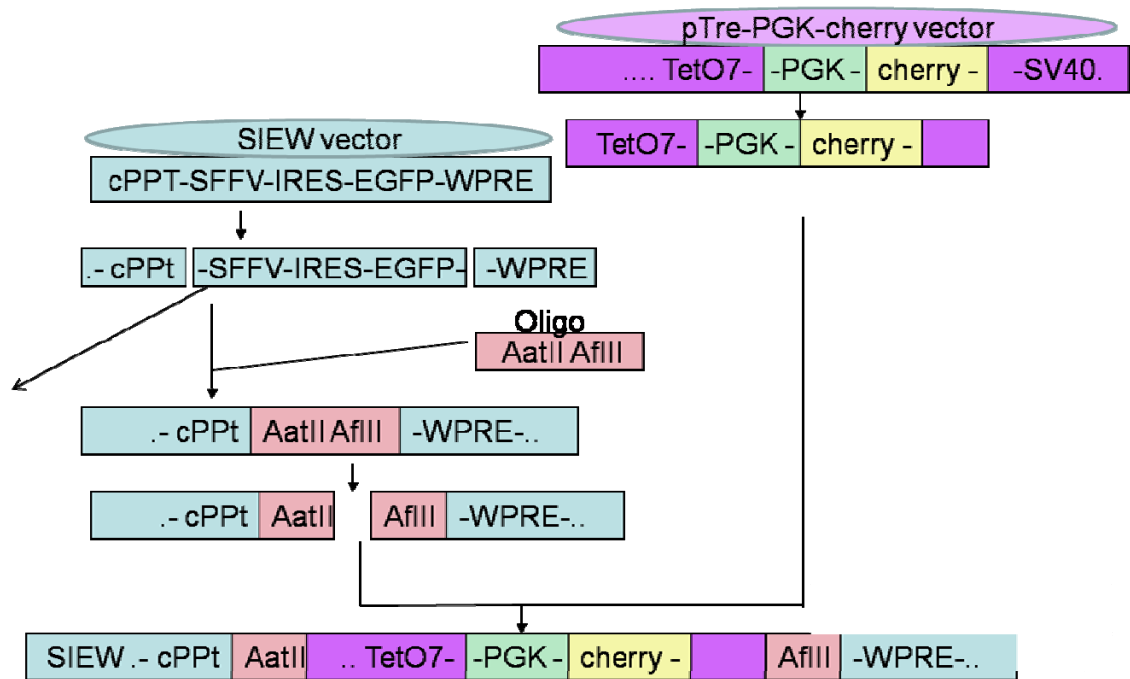


Figure 118 Scheme of SIEW-Tre-PGK-cherry cloning

SFFV Spleen focus forming virus (promoter), IRES Internal ribosome entry site, AatII/AfIII restriction sites, EGFP enhanced Green fluorescent protein, WPRE Woodchuck posttranscriptional regulatory element, PGK Phospho glycerine kinase (promoter), TetO7 Tet operator (promoter), SV40 Simian virus 40 (poly A), cherry mCherry (red fluorescent protein)

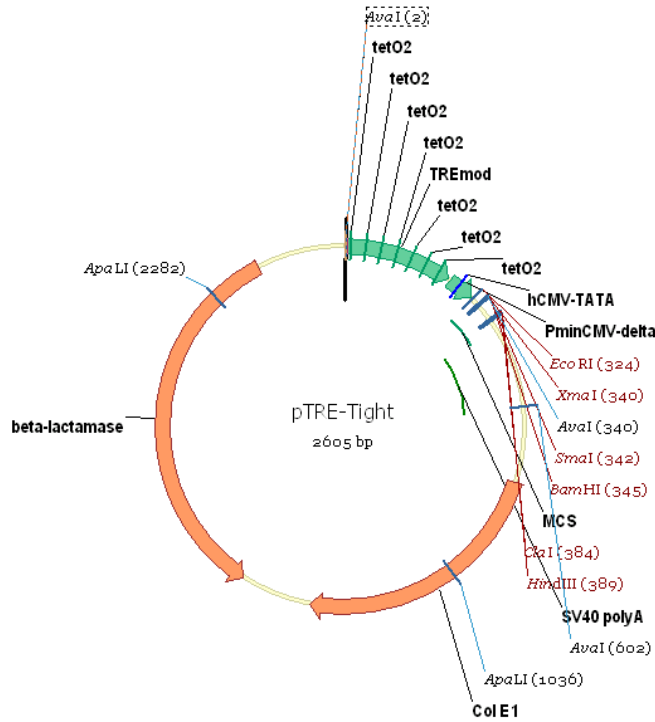


Figure 119 Map of pTRE-Tight vector

tetO2 operator repeats, TRE tet responsive element, CMV Cytomegalovirus (promoter), min minimal, MCS Multiple cloning site, ColE1 C olicinogenic factor EI

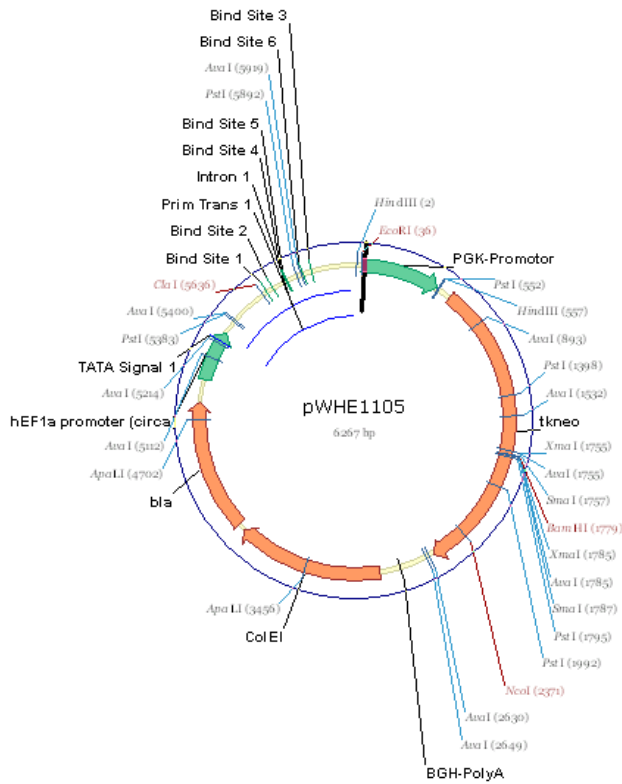


Figure 120 Map of pWHE1105 vector

PGK Phosphoglycerine kinase (promoter), bla Blastocidin resistance, ColE1 C olicinogenic factor EI, tkneo tymidine kinase neomycin resistance gene



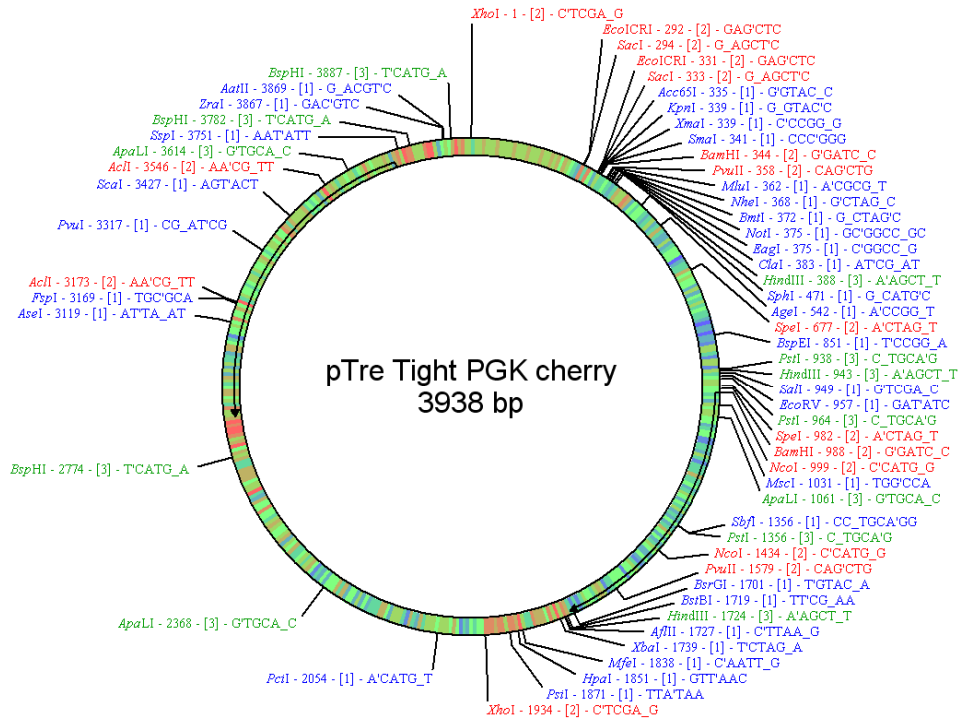


Figure 123 Map of pTre-PGK-cherry vector (PPC)  
 (In colour) restriction sites, (Blue) one cutters, (Red) two cutters, green three cutters tetO 1-388bp, PGK 388- 943bp, mCherry 988-1724bp

To retrieve the PGK element it was cut out from the pWHE plasmid (Figure 120) using HindIII. In parallel, the pTre vector (Figure 119) was opened with HindIII. Next PGK fragment was ligated into the open pTre vector. To check the resultant clones, a control digest using PstI and PvuI was performed. For the correct product, bands were expected at 1600bp, as a double band, while vector without insert should have led to a 2600bp fragment (see Figure 121 and Figure 124).

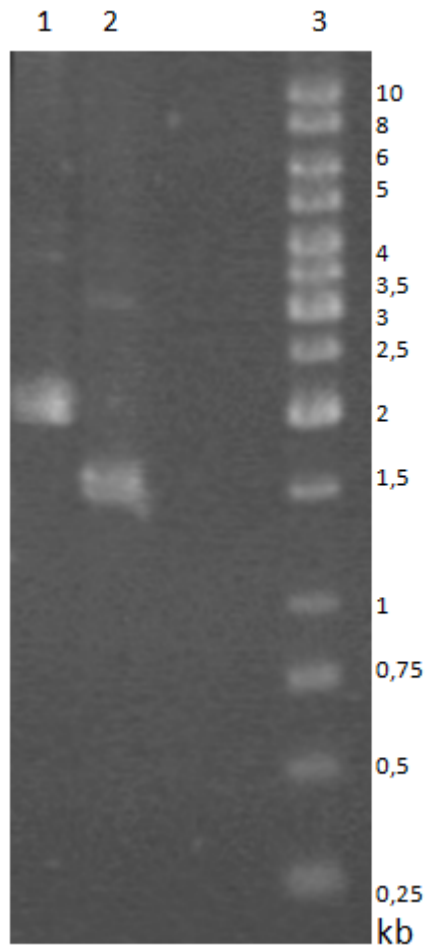


Figure 124 Restriction digest of pTre-PGK clones

The pTre-PGK ligation clones were digested with PstI and PvuI separated and analyzed in an 1% agarose gel. (Lane 1) undigested Plasmid, (Lane 2) digested and (Lane 3) 1-kb Marker Fermentas

The gel (Figure 124) shows a clone with the pTre vector plus the PGK insertion, called pTre-PGK.

Next the Cherry sequence was cut out of the pcDNA3.1-cherry plasmid (see Figure 122) using EcoRV and PmeI. The previously generated pTre-PGK plasmid was opened with EcoRV and the cherry fragment blunt end ligated into it. To confirm the insertion and the right orientation of the cherry sequence generated clones were digested with EcoRV and XbaI, leading to expected bands of 782bp and 3156bp at the right orientation (see Figure 123 and Figure 125).

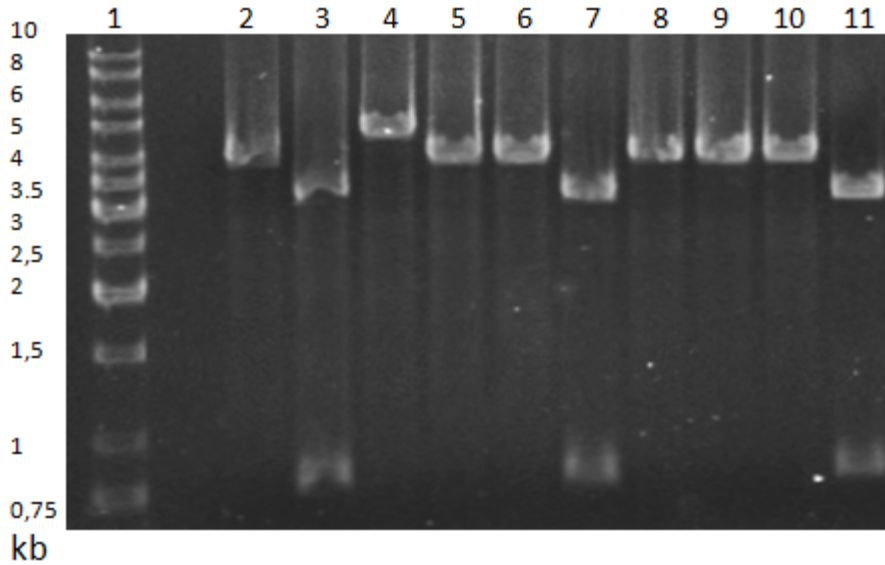


Figure 125 Restriction digest of pTre-PGK cherry clones

pTre-PGK cherry clones were digested with EcoRV and XbaI, run and analyzed in a 1% agarose gel. (Lane 2-11) pTre-PGK-cherry ligation clones and (Lane 1) 1-kb Marker Fermentas

Positive clones were found in Lane 3,7 and 11 (Figure 125).

The digest shown above proved that the pTre-PGK-cherry plasmid with the desired PPC cassette (tetO-PGK-cherry) was successfully cloned.

Unfortunately, despite several strategies using different vector backbones such as p156RRLsinPPTCMV-GFP-PRE/NheI, it was not possible to clone the pTre-PGK-cherry cassette into a lenti-viral vector. The 2 vector system could not be finished in this PhD project due to time restrictions.



## 5.4 Discussion lentiviral results

The aim of this project was to develop and clone a novel tightly regulated lentiviral expression system able to transduce both proliferating and resting cells and allowing tight control led expression of MLL/AF4 target genes in order to investigate their functions. The design is based on a two vector system: a tet activator coding vector (Vector 1, Teton) and an inducible expression vector (Vector 2) (Figure 104).

The cloning of Vector 1 (Teton) used the pSIEW vector backbone, a lentiviral SIN vector with an eGFP reporter following an IRES sequence (Figure 109), and the tet activator coding elements from the pUHrt vector (Figure 108). Before insertion of the tet activator coding sequence into the pSIEW backbone the required restriction sites were cloned into pUHRT via introduction of an oligo-nucleotide sequence. The cloning was confirmed by a control digest showing the insertion of the tet activator sequence (Figure 110 and Figure 111).

The functionality of Vector 1(Teton) was tested in our group by Vasily Grinev. 293T cells were transfected with the teton vector alone or co-transfected with the reporter plasmid pUHG16-6 providing the tetO elements which on binding by the tet activator drive expression of beta-Galactosidase. Beta-Galactosidase is an enzyme which metabolizes the substrate X-Gal into a insoluble blue indigo dye. As expected cells only transduced with the Teton vector did not generate blue cells. Co-transfected cells induced with doxycycline showed approximately 30% of blue cells, increasing to over 60% when doxycycline had been provided to the cells (Figure 112). The proportion of blue cells was slightly higher after 3 hours of staining compared to 1h while singly transfected cells showed no blue staining. Overall these results showed that the cloned Vector 1 is functional and inducible. However two findings were surprising: the high

level of background reporter-gene activity without doxycycline induction and the low fold change (>2fold) by induction. To understand this several parameters have to be considered: the test relied on counting of blue cells by eye, but there is no clear distinction into unstained or blue. Cells are stained from slightly yellow, light turquoise to blue. The experimentator had to decide which cells are counted as positive. So all the cells less than intense blue might have a weak expression of the tet activator, but are still positive for it. Also, from a certain intensity of blue there is no eye discrimination of more intense staining.

In concordance to this, there were more deep blue cells in the group with doxycycline than in the group without. As such the whole range of tet activator driven reporter gene expression is compressed into a small level of response, so that the differences seen between with and without doxycycline induction do not correlate to a linear response. Concerning the high basal levels of X-Gal staining, this experiment lacks a reporter vector control to see the basal level of beta-galactosidase activity of the reporter vector without the presence of the tet activator. Finally, as doxycycline is known to be present in FCS from USA, it is possible that small amounts of doxycycline might result in the basal activity in the doxycycline negative group. In conclusion these results can only state that the vector is functional in tet activator expression and inducibility.

A superior reporter system to quantify the inducibility of the Teton vector would be a tet-operator-driven luciferase system. Luciferase activity quantifiable read out of the signal strength, providing a linear range of doxycycline-mediated tet activator expression of the Teton vector.

The t(4;11) positive cell lines SEM and MV4;11 were transduced with this Teton vector by spinoculation. Analysis by flow cytometry of the reporter gene eGFP showed

transduction rates of 60 to 80% (Figure 113), but as these dropped over several weeks transduced cells were sorted to retrieve cells with high percentage of transduction. The sorting related purities were ~ 90% for MV4;11Teton and up to 98% for SEMTeton (Table 14 and Table 15). However, cells still dropped slightly in eGFP expression over several weeks. To overcome this, aliquots of these highly pure, sorted cells were stocked in liquid nitrogen to provide highly positive Teton cells for experiments. As it seems very unlikely that previously integrated constructs disintegrate in these cells, the most likely cause for this must be a growth advantage of non-transduced cells to transduced ones. This would rise the question if high copy numbers of tet activator could be toxic or disadvantageous for the growth of cells. There were reports that high levels of tet activator can be toxic to mammalian cells (Gossen and Bujard 1992) and this effect was associated to reduced surfactant mRNA accumulation observed in rtTA induced mice and suggested to generate a “synthetic lethality” if other genetic alterations are present (Morimoto and Kopan 2009).

As previously shown (see chapter 4), Teton transduced SEM cells are still accessible to siRNA-mediated MLL/AF4 depletion to the same degree as non transduced SEM cells, making them suitable for any type of RNAi MLL/AF4 studying experiments. As previously shown they are suitable to test and develop the feeder interaction assay.

There has been ongoing work on the functions of tet activators; especially challenging are approaches aiming to regulate several genes simultaneously including tet-repressor. Such a modification of the tet-activator was to express it as a single chain molecule, reducing interference with other tet activation or repression molecules (Krueger, Berens et al. 2003; Zhou, Symons et al. 2007).

The cloning of the second vector of the two vector system, vector 2, consisted of several steps. First, it was required to generate an expression cassette for the cherry reporter gene, consisting of the cherry ORF under the control of a PGK promoter. Upstream of these elements the cassette should contain a MCS, providing an insertion site for ORF of target genes to be expressed. These elements had to be under the regulation of the tet-O promoter (tet responsive promoter) (Figure 117 and Figure 118).

The pTre tight vector was used as a backbone; it contained the tetO element with seven tet activator binding sites and a minimal CMV promoter. The PGK promoter is a relatively weak promoter which was used because it hardly influences the inducibility of the neighbouring tet responsive promoter. The sequence was retrieved from the pWHE-vector and the cherry reporter gene from the pcDNA3-mcherry plasmid. Successful cloning was confirmed by restriction analysis. In order to test the functionality the ORF of the luciferase gene was cloned into the MCS of the generated cassette. However the introduction of this luciferase sequence brought new restriction sites into the cassette such as BsrGI, XhoI and HindIII which handicapped a sub sequential lentiviral vector insertion strategy.

The second finalising part comprised the removal of the SFFV promoter - IRES - eGFP cassette from the SIEW vector and the insertion of the *ptre-pgk-cherry* (ppc) cassette. As the to be inserted cassette contained mCherry and as the sequential transduction of the two vectors relied on two different reporter genes, GFP in Vector 1 and mCherry in Vector 2, GFP had to be removed from the lentiviral host vector. But also the constitutive promoter SFFV and the IRES sequence, which can start translation independent of the SFFV promoter had to be removed. To provide the restriction sites corresponding to the ones flanking the ppc cassette, an oligo-nucleotide sequence was cloned and inserted into the SIEW vector after removal of the SFFV-IRES-eGFP

cassette. Unfortunately the restriction sequences originally planned were already present in the SIEW vector, although not stated as such in the vector map.

Several alternative strategies using different oligo-nucleotides and different restriction enzymes for insertion; finally the use of two other lentiviral vectors as backbones did not succeed in inserting this ppc cassette. Due to time restrictions the final cloning step could not be finished.

One of the possible explanations for this might be the size of the cassette and the final size of the lentiviral vector, which would be exceeding 12000bp. It is known that the cloning of large vectors is difficult. Such a vector could be less stable or produce physical tensions which handicap ligation into such a full size vector.

A new method of cloning, the Gateway technology (Invitrogen), does not require restriction enzymes, ligation, subcloning steps, or screening of colonies thereby accelerating cloning and increasing the likeliness of success. This system makes use of a reversible recombination reaction. It could be use for cloning of such large cassettes.

The two vector lentiviral expression system will be used for the investigation of target genes in the future after being completed by my successors.

The field of inducible gene expression is still progressing. Several tet activator variants were designed over the years, achieving reduced basal expression and increased sensitivity to doxycycline from 1000 ng /ml for the rtTA2S-S2 to only 10 ng /ml; such improved variants are rtTA-V14, -V15 and -V16 (Zhou, Vink et al. 2006).

In conclusion, lentiviral inducible gene expression is a powerful tool in investigating target gene or protein function, but also in a more physiological context. Lentiviral Tet-

On regulated expression was applied to bone marrow MSCs and HSCs. The implantation of those transduced cells into bone marrow was implicated for the treatment of diseases where certain protein over- expression is beneficial (Aguilar, Scotton et al. 2009) this could be used to either over express antagonist of MLL/AF4 and target genes or deplete target genes by shRNA in blood cells. Lentiviral transduction can help to investigate the biology of MLL/AF4 or even be a therapeutic option.

# **Chapter 6**

## **Mouse work**

## Chapter 6 Mouse work

### 6.1 Introduction: mouse models for leukaemia

#### 6.1.1 SCID

In 1976 attempts to establish mouse models for leukaemia by s.c. injection of myeloid or lymphoid cell lines and primary material into nude mice produced myelosarcomas and solid tumours, but no leukaemia (Lozzio, Machado et al. 1976). In 1983 the SCID (severe combined immunodeficient) mouse model with deficient immunity was reported (Bosma and Carroll 1991). SCID mice cannot express rearranged antigen receptors (Lieber, Hesse et al. 1988; Malynn, Blackwell et al. 1988) due to an autosomal recessive mutation on chromosome 16 leading to a lack of functional B and T lymphocytes (Bosma and Carroll 1991). Genetically the recessive mutation on chromosome 16 is responsible for deficient activity of an enzyme involved in DNA repair. The humoral and cellular immune system cannot mature, because V(D)J recombination does not take place. Besides the impaired ability to make T or B lymphocytes they are also impaired in activating components of the complement system. This impaired immune system makes them especially vulnerable to infections but the main advantage is that they cannot reject tumors and transplants. The first successful engraftment of human stem cells in SCID mice was published in 1988 (McCune, Namikawa et al. 1988).



### **6.1.2 NOD SCID**

The NOD/SCID mouse strain was generated by crossing the SCID mouse with the NOD (non obese diabetic) mouse strain. NOD mice were originally used as a model for diabetes 1 which is generated in these mice by T-cell mediated destruction of the pancreas. This defect is generated by a spontaneous mutation. Additionally, NOD mice have defects in natural killer (NK) cells and in the complement system and therefore an impaired immune system (Shultz, Schweitzer et al. 1995). By combining these NOD and SCID backgrounds a mouse strain lacking B- and T-cells and showing reduced NK function was generated and shown to be superior to the SCID strain in the modelling of lymphoid malignancy (Hudson, Li et al. 1998). However NOD mice are sometimes used for xenografts because of the low residual immunity, but to avoid rejection of transplant additional treatment is required such as anti-NK treatment (Taussig, Miraki-Moud et al. 2008). In contrast to these advantages NOD/SCID mice have a high incidence of thymic lymphomas, which are produced by the reactivation of a murine provirus, shortening the lifespan of NOD/SCID mice to an average of 8.5 months. Therefore NOD/SCID mice are not the ideal host for xenografts (Chiu, Ivakine et al. 2002) as the engraftment of leukaemic cells may require more time and events may be missed due to the short life-span of the mice.

### **6.1.3 NSG**

The NOD/SCID mouse strain was further improved by knocking out IL2 receptor gamma chain. This depleted low immunity of NOD/SCID mice even more as NK cells were removed (Shultz, Lyons et al. 2005). The idea for this was based on the finding of

increased engraftment in NOD/SCID mice when treated with antibodies against NK cells (Shultz, Banuelos et al. 2003). So far these NOD/SCID/IL2R mice (NSG) are most widely used to engraft primary human cells with low levels of graft rejection. Moreover NSG mice also do not require irradiation before transplant because they lack lymphocytes (Vormoor, Lapidot et al. 1994). Irradiation of NOD/SCID mice was performed to get rid of mouse lymphoid cells which could compete with transplanted human lymphoid cells.

Finally NSG mice also do not have a predisposition to developing thymic lymphomas, which the NOD/SCID strain does. Viral reactivation causing those lymphomas is prevented by the impaired interleukin signalling. NSG mice therefore have a lifespan of more than 15 months (Ishikawa, Yasukawa et al. 2005).

### **6.1.4 Rag2 knockout mice**

Rag2 knockout mice bear a knock out for the Rag2 gene. Recombination active gene 2 (Rag 2) is a single exon gene (Oettinger, Schatz et al. 1990) that confers V(D)J rearrangement by recombination and was isolated in 1989 (Schatz, Oettinger et al. 1989). In thymus and precursor B-cells a high Rag2 expression was found (Schatz, Oettinger et al. 1989). A mouse model was created with a germline mutation in the rag gene which aimed to block the production of the functional protein. No mature B or T cells were found in homozygous Rag2 knockout mice showing a SCID phenotype (Shinkai, Rathbun et al. 1992). Furthermore Shinkai et al could show that only lymphocyte development is affected by the deletion of the Rag2 gene product (Shinkai, Rathbun et al. 1992).

### **6.1.5 R2G**

Rag2 gamma c double knockout (R2G) mice have reduced peripheral B and T lymphocytes and no NK activity due to gamma c gene (common cytokine receptor gamma chain) deletion (Goldman, Blundell et al. 1998). The development of an adaptive immune system by CD34<sup>+</sup> cord blood cell injection into R2G mice could be shown for the first time by Traggiai et al. (Traggiai, Chicha et al. 2004). This was accomplished by intra hepatic (i.h.) injection of CD34<sup>+</sup> cord blood cells, which are haematopoietic high repopulation active cells, into newborn R2G mice. As the liver facilitates perinatal haematopoiesis it is more suitable to provide an environment for stem and progenitor cells of haematopoiesis. This interaction possibly improves engraftment in the liver, expansion of the precursors and reconstitution of the immune system (Traggiai, Chicha et al. 2004).

### **6.1.6 The use of mouse models for studying leukaemia**

The process of engraftment was thought to be dependent on accessory cells or cytokine treatment early after transplantation besides pluripotent stem cells. This was observed as injection of limited dilutions of special cord blood or AML cells required co-transplantation of accessory cells or cytokine treatment, unlike in higher cell doses (Bonnet, Bhatia et al. 1999).

The importance of CD133 expression in ALL blasts along with a primitive phenotype was found to be important in engrafted NOD/SCID mice as these cells showed long-term *in vivo* proliferation (Cox, Diamanti et al. 2009).

Evidence that gender associated factors could influence self-renewal, proliferation and survival of engrafted cells was provided by injection of human HSCs into NSG mice which showed higher engraftment in female mice (Notta, Doulatov et al. 2010).

Engraftment of flow sorted ALL patient cells to pick populations with certain surface expression profiles, proved to be difficult. To overcome this the Heidenreich group and collaborators have refined the protocol by engrafting directly after sorting, using a non irradiated NSG mice and implementation of intra-femoral injection (see Figure 126) which alone increases the stem cell assay sensitivity by tenfold compared to i.v. injection (Mazurier, Doedens et al. 2003). Mazurier et al. found so called rapid-SCID repopulating cells (R-SRC) in the  $CD34^+CD38^{low}CD36^-$  compartment of human bone marrow (Mazurier, Doedens et al. 2003). Intra femoral injection is often called an orthotopic technique because the cells to be engrafted are transplanted into their natural environment, the bone marrow, which was thought to improve engraftment.

By using limiting dilutions of sorted blast populations of haematopoietic stemness and lymphoid lineage commitment markers the Vormoor / Heidenreich group and collaborators demonstrated that all sorted populations could produce leukaemia in NSG mice, also after secondary and tertiary transplant (le Viseur, Hotfilder et al. 2008).



Figure 126 Intra-femoral injection (i.f.) into a mouse  
Xray image of intra femoral injection position with a mouse leg shown. personal communication from le Viseur, C

A similar finding was reported by Kong et al. who used NOD/SCID/IL2rnull mice for the engraftment of B-cell ALL cells from 3 young patients of whom two had *MLL* rearrangements. They could establish leukaemia with populations of different maturity (CD38 +/- , CD34+,Cd19+) leading them to new conclusions about the LIC hierarchy in ALL (Kong, Yoshida et al. 2008).

As t(4;11) leukaemic cells showed a hemangioblast phenotype expression profile (Armstrong SA, Staunton JE, 2002) and due to the ability of the hemangioblast to contribute to haematopoietic and endothelial lineages, a model suggesting t(4;11) leukaemias could supply cells for angiogenesis was proposed. To verify this model NOD/SCID mice were xeno-transplanted with t(4;11) cells. But tumour supplying vessels only contained murine cells. Together with angiogenesis involved expression profiles such as Tie1, the Ang1 receptor, they concluded that t(4;11) cells promote angiogenesis by cytokines and receptors (Hu, Li et al. 2009).

The NOD/SCID model can also be used for gene expression profiling of ALL infiltrated tissues requiring high engraftment. The transcriptional profiles were species specific and reproducible making it a suitable model for xenotransplant expression profiling (Samuels, Peeva et al. 2010).

Further injection types were described to engraft ALL cells in SCID mice.

In 2009 a test model linking the aggressiveness of nodule growth to the clinical outcome of patients was published. Subcutaneous (s.c.) injections of patient ALL and AML blast cells were used and the growth of s.c. tumours compared to the clinical data, showing that the more aggressive the growth pattern of the s.c. SCID tumours, the poorer the outcome in patients (Yan, Wieman et al. 2009).

A successful engraftment of patient adult ALL using intrahepatic injection into unirradiated newborn NOD/SCID mice was reported in 2009. Cells from 5 of 13 ALL patients engrafted after 6-18 weeks. Interestingly the levels of bone marrow engraftment were linked to those in peripheral blood (Cheung, Fung et al. 2010).

For more than 15 years the SCID mouse models were the standard model for studying leukaemia. Most importantly they proved to be of clinical relevance as for instance relapsed and high risk ALL showed better propagation in them (Kamel-Reid, Letarte et al. 1991).

The R2G model has been used by our own group to investigate *AML/MTG8* translocation derived AML. An *AML/MTG8* positive AML cell line (Kasumi-1) was injected into the liver of irradiated newborn R2G mice inducing human tumour formation in 53 to 55 days. Knockdown of the fusion gene prior to engraftment increased median survival from 50 (controls) to 73 days (fusion gene knockdown) with all controls showing tumours while a part of the knockdown group did not develop tumours. Reducing the number of injected cells and usage of non irradiated newborn mice increased median survival from 64 (controls) to 90 days (fusion gene knockdown). This proved to be a suitable xenotransplantation model (Martinez Soria, Tussiwand et al. 2009).

Later the Vormoor/Heidenreich group compared different injections of ALL cells in R2G mice by i.f. injection resulting in bone marrow engraftment (unpublished work, Klaus Rehe).

By injection of SEM (ALL) intra-hepatically into R2G mice engraftment and tumour formation could be achieved within 2 months (unpublished work, Lars Buechler and Mike Batey).

## 6.1.7 Imaging

Although already isolated in the 60s, GFP, a green fluorescent protein (see Figure 127), was first cloned and sequenced in 1992 by Douglass Prasher (Prasher, Eckenrode et al. 1992). In 2008 the Nobel Prize was dedicated to 3 researchers for the discovery of GFP. Since then several improvements have been achieved such as optimising the spectrum until enhanced GFP (eGFP) was developed (see diagram below).

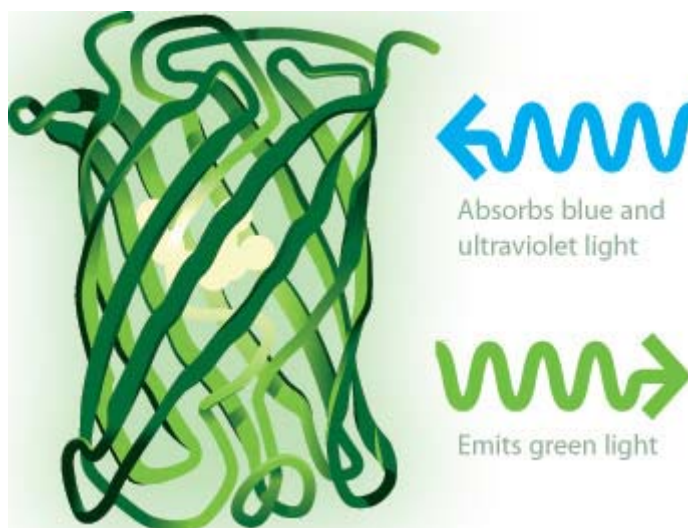


Figure 127 GFP fluorescence  
from [nobelprize.org/.../laureates/2008/illpres.html](http://nobelprize.org/.../laureates/2008/illpres.html)

Several colour mutants such as EBFP (Blue fluorescent protein) and YFP (yellow fluorescent protein) have been generated since. Dsred another fluorescent protein, isolated from corals and emitting a much longer wavelength, was discovered 1999 (Matz, Fradkov et al. 1999). Dsred fluorescence penetrates tissue effectively. Recently lentiviral induction of a dsred involved fluorescent protein was used to track pancreatic cancer cells in in-vivo imaging (Zhou, Yu et al. 2009).

Nowadays fluorescent proteins in general are in wide use to label biological objects from a relatively small protein to tissues or even whole organisms. They serve as



marker or reporter genes for fluorescent microscopy, flow cytometry analysis, sorting, *in vivo* imaging and most recently live recording.

Xie Y et al were tracing GFP labelled HSCs in NOD/SCID engrafted mice, which preferably localised in the trabecular regions of the inner bone, were the bone marrow niche is agreed to be localized. They observed that in well avasculated endosteum vessels tend to be found near N-cadherin positive osteoblasts (Xie, Yin et al. 2009).

An ultimate implementation of *in vivo* imaging in SCID mice was performed by tracking fluorescent labelled pre-B ALL cells homing into the bone marrow niche and perivascular niches. The researchers presented real-time videos of LSCs moving into the cranial bone marrow. This work showed that stem cell factor (SCF) secreted by leukaemic cells is important in the manipulation of niches or creation of malignant niches (Colmone, Amorim et al. 2008).

Overall, using mouse models and live imaging for investigating leukaemia will be an important tool to increase the understanding of the biology of this malignancy.

## 6.2 Aims

In the previous chapters the functions of MLL/AF4 in the establishment and maintenance of acute lymphoblastic leukaemia were investigated. The majority of the work was performed using *in vitro* cell culture. To complement cell culture systems, interactions were investigated in an *in vivo* system including several mouse models. The ability to engraft and the time until the development of clinical disease provide important information about the disease and the relevance to model cell lines. Another aim was to establish a monitoring system for the behaviour of those leukaemic cells in the mouse, to see how those cells distribute in the organism and in which organs or tissues they first start to form tumours.

Specific Aims:

1. To investigate *in vivo* effects of MLL/AF4 in addition to cell line data
2. To establish an *in vivo* monitoring system for engraftment of leukaemic cells

## **6.3 Results mouse work**

### **6.3.1 SCID mice i.f. injections with early SEM**

#### **6.3.1.1 Flow cytometric analysis**

Early or primary SEM are peripheral blood lymphoblasts from a 5 year old female patient with ALL at relapse. These cells were used to establish the cell line SEM (Greil J et al. 1994). Primary SEM are an early passage of patient cells but unlike the cell line SEM, primary SEM are slowly proliferating and more dependent on growth factors.

3 NSG mice and 3 R2G mice had been injected i.f. in 3 cell numbers with primary SEM cells. Two of the NSG mice with the highest doses died before a sample could be taken. 1 NSG mouse (see Figure 131 and Figure 132) and 2 R2G mice (see Figure 128 and Figure 129) were sacrificed one month after injection. Blood was taken by cardiac puncture whilst bone marrow was isolated by dissecting out the femurs and flushing out the bone marrow.

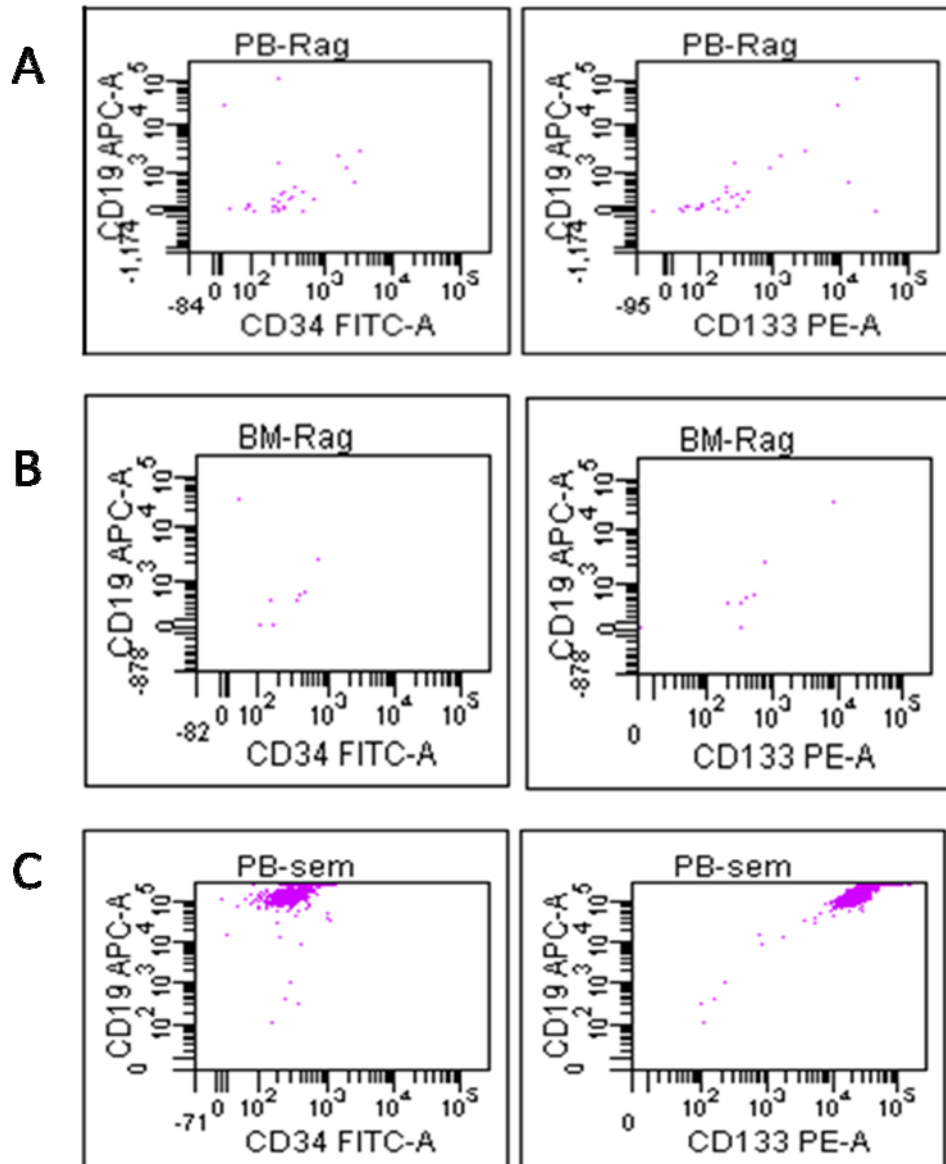


Figure 128 Early SEM and engraftment in R2G mice

Flow cytometry of early SEM (A) Peripheral blood of a R2G mouse transplanted with early SEM, 0.0 % engraftment of early SEM in peripheral blood (B) Bone marrow of a R2G mouse transplanted with early SEM, 0.2 % engraftment of early SEM in bone marrow of an R2G mouse (C) Early SEM control, Early SEM from culture were used as a control for flow cytometry. Shown are dotplots of CD19 expression (y-axis) against CD34(Left) and CD133(Right) expression (x-axis). PB peripheral blood BM Bone marrow

This R2G mouse (Figure 128) showed low engraftment of early SEM in bone marrow and low numbers in peripheral blood. The peripheral blood analysis used many more cells than the bone marrow analysis, resulting in more cells in the dot plot. Despite this, engrafted leukaemic cells made up only a small proportion of all cells analysed. The strategy for distinguishing mouse lymphocytes from human was to gate out mouse cells using two murine specific antibodies. To ensure there was no overlap of mouse cells into the “human” gate, the thresholds for distinguishing these two populations were set quite rigidly. However this leads to a potential loss of human cells. As seen in Figure 134 control early SEM are high in CD19 a B-lymphocyte marker and CD133 a stem cell marker. SEM are usually low in CD34 another stem cell marker. As the engraftment numbers of early SEM were so low, it could be they were harvested too early.

The 2<sup>nd</sup> R2G mouse had an abdominal tumour. The spleen was slightly enlarged to 1.6cm length, but still dark red with 120mg of weight.

The blood and the bone marrow samples, and primary SEMs as a control, were labelled for CD19, CD34, CD133, and anti-mouse antibodies to gate mouse lymphocytes out (Figure 129).

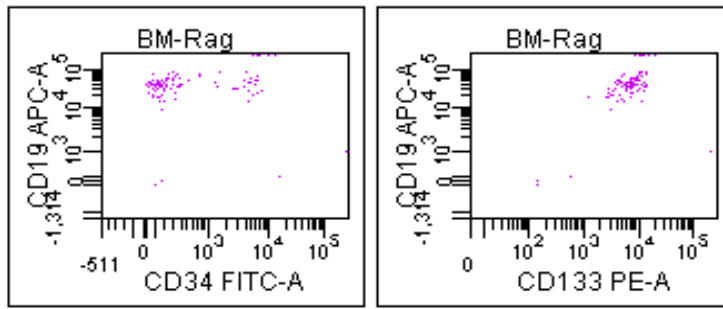


Figure 129 Bone marrow of a 2nd transplanted R2G mouse

An R2G mouse was transplanted with early SEM. The flow cytometric analysis showed 0.1% engraftment of early SEM in bone marrow of an R2G mouse. Shown are dotplots of CD19 expression (y-axis) against CD34 (Left) and CD133 (Right) expression (x-axis). BM bone marrow

Surprisingly the engrafted early SEM showed a second population high in CD34, which was not present in control early SEMs.

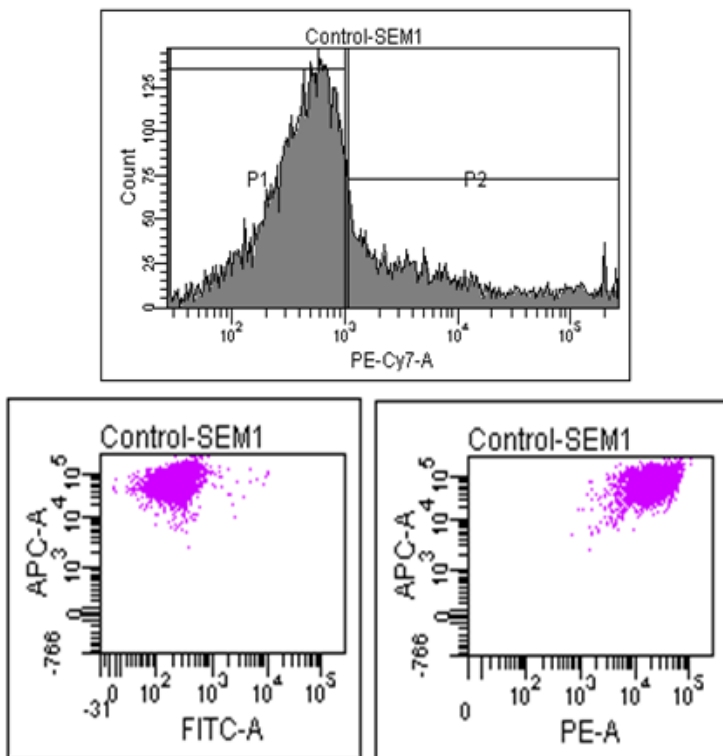


Figure 130 Early SEM control 2

Early SEM were used as a control for setting gates and to control expression patterns. (Top) Histogram showing set of mouse gate (P2, gated out) and human gate (P1, gate in) with the mouse antibodies fluorescence in the PE-Cy7 channel. (Below) Shown are dotplots of CD19 expression (y-axis, APC) against (x-axis) (Left) CD34 (FITC channel) and (Right) CD133 (PE channel) expression.

As seen before, the early SEM control (Figure 130) showed no second CD34 high population.

The engraftment analysis of the 2<sup>nd</sup> R2G mouse (Figure 129) showed low engraftment again, although the SEM profile was clearly visible. A control using early SEM cells, labelled identically to the engrafted cells, showed that 82% of control early SEM were detected in the non-mouse gate (P1). It seems likely that the time allowed for engraftment in this experiment was too short.

The NSG mouse spleen was substantially enlarged measuring approximately 5cm long and 1cm wide (see Figure 133). The mouse also had a large rubbery tumour at the back of the femur and an enlarged unfilled bladder. The spleen and tumour were removed.

White blood cells were isolated from the blood and the bone marrow (Figure 131 and Figure 132).

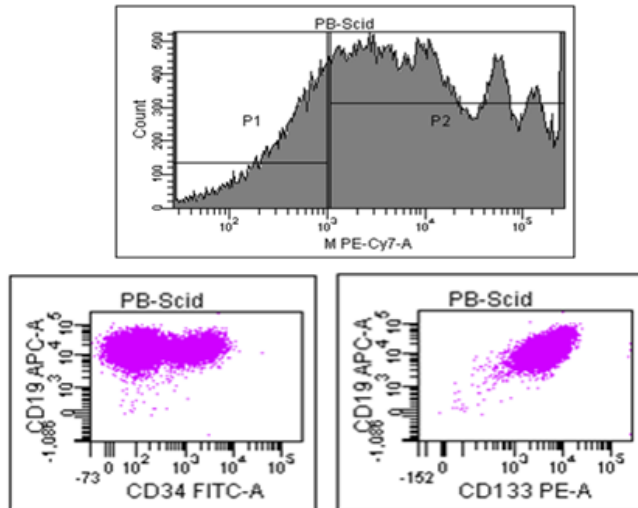


Figure 131 Peripheral blood of a transplanted NSG mouse

An NSG mouse transplanted with early SEM. The analysis showed that at least 36% of peripheral blood cells were early SEM. (Top) Histogram showing set of mouse gate (P2, gated out) and human gate (P1, gate in) with the mouse antibodies fluorescence in the PE-Cy7 channel. (Below) Dotplots of CD19 expression (y-axis) against CD34 (Left) and CD133(Right) expression (x-axis). PB peripheral blood

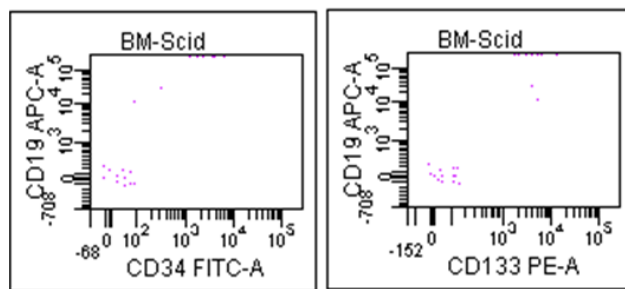


Figure 132 Bone marrow of a NSG mouse

An NSG mouse (from Figure 131) transplanted with early SEM. The flow analysis showed 0.2% engraftment of early SEM in the bone marrow. Dotplots of CD19 expression (y-axis) against CD34 (Left) and CD133 (Right) expression (x-axis).

As Figure 131 shows, 36% of peripheral blood lymphocytes from transplanted NSG mice were early SEM. The histogram on top of Figure 131 shows clearly that the mouse and the human peaks overlap. A more refined gating by plotting using CD19 positivity against PE-Cy7 (mouse antibody signal) and defining the mouse and human populations, can increase that number to 78% early SEM in peripheral blood. However NSG mouse bone marrow showed low engraftment numbers (Figure 132) as did R2G mice before.



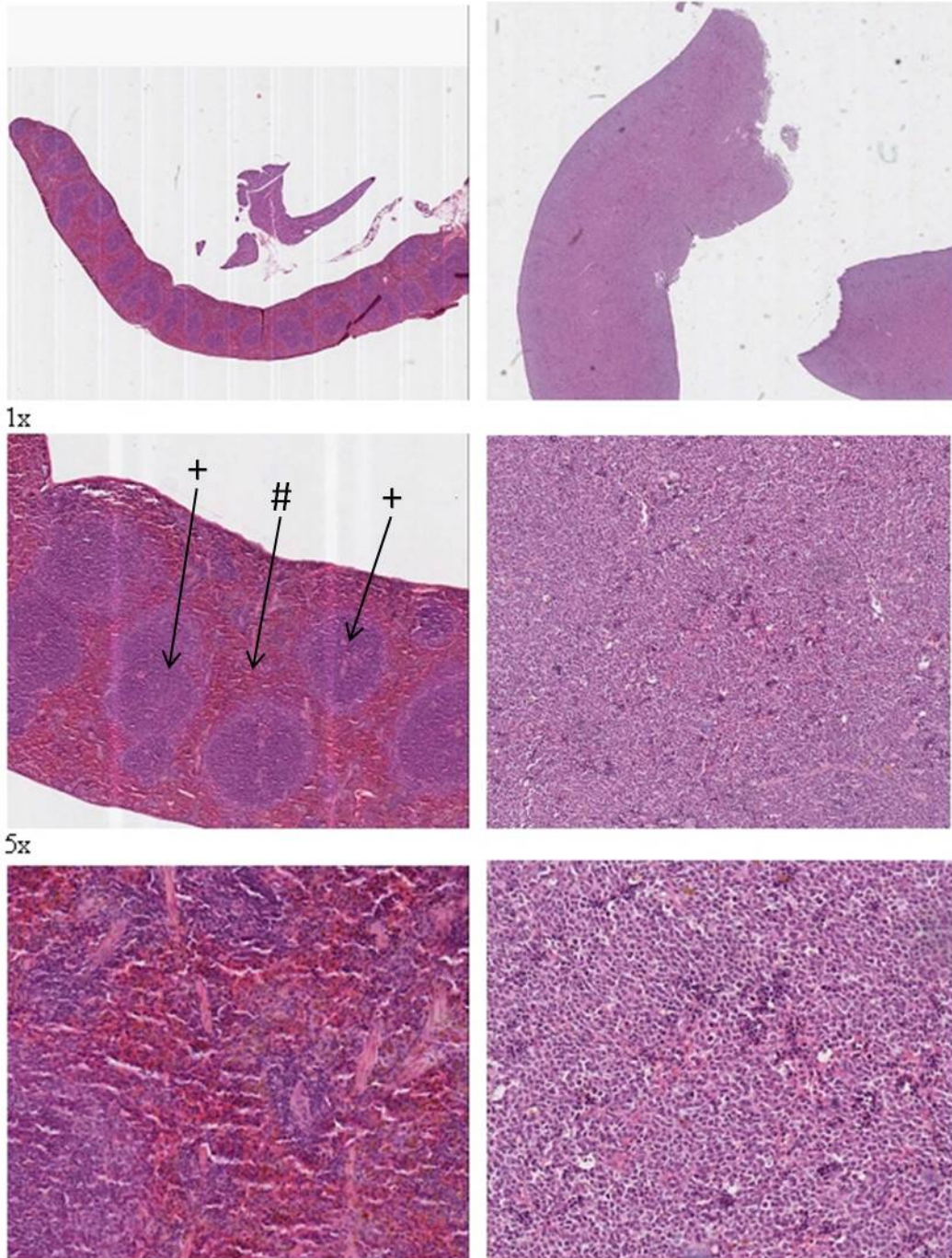
As the gating strategy employed is routinely used in other mouse engraftment experiments within the Heidenreich group, the question arises if these low engraftment numbers show that early SEM are not ideal for this protocol or that early SEM despite forming tumours, do not highly engraft in bone marrow.

### **6.3.1.2 Histological examinations**

One portion of the enlarged spleen from the experiment described above was fixed in formaldehyde. Sections were produced onto glass-slides and HE stained (Kieran O`Toole). As a control, a normal spleen was prepared in the same way (see Figure 133).

Normal mouse spleen

NSG leukaemic mouse spleen



20x

Figure 133 Sections of NSG mouse spleens

NSG mice spleens from a normal mouse and an NSG mouse engrafted with early SEM. The spleens were sectioned and HE stained. (Left) Normal mouse tissue (Right) leukaemic mouse spleen imaged at 1x (Top), 5x (Middle) and 20fold (Bottom) magnification, arrows with + point to nodules (white pulp), arrows with # point to red pulp. Imaged with the Aperio system.

The images of the leukaemic NSG spleen and the normal spleen (Figure 133) showed how massively enlarged the leukaemic spleen was. This was due to leukaemic infiltration. The staining pattern of the control mouse spleen showed normal follicles stained lilac (+ → arrows point to). These correspond to the white pulp which mostly comprises of lymphocytes. The reddish areas around the follicles represent the red pulp (# → arrow points to) which is mainly comprised of red blood cells and macrophages, but also accommodates murine haematopoiesis. In comparison to the normal spleen, this structure was completely wiped out by infiltration in the leukaemic spleen. The majority of cells are now leukaemic lymphocytes, demonstrating advanced disease.

Tumours from all mice were disaggregated to produce a single cell suspension. The single cell suspension was cultured in penicillin and streptomycin containing medium to allow outgrowth of engrafted leukaemic cells. However, leukaemic cells recovered from the mouse did not survive in *in vivo* culture.

## **6.3.2 Establishment of an SEM *in vivo* monitoring in mice**

### **6.3.2.1 SEM cami injections i.f., i.v.**

SEMcami are lentiviral expression vector transduced SEM, which express both GFP and Dsred making it easier to capture signal than with GFP alone. The corresponding vector and transduction was made by Vasily Grinev.

### 6.3.2.1.1 Hair removal

One obstacle for *in vivo* monitoring of fluorescent leukaemic cells is that the fur reflects the excitation light and leads to a high background. Even if shaved (with a hair clipper) the hair follicles are enough to block signals. To overcome this, the skin had been treated with the depilatory cream Veet, which also removes hair follicles. This was done on dead mice but can also be applied to living, anesthetized mice over a restricted area (see Figure 134).

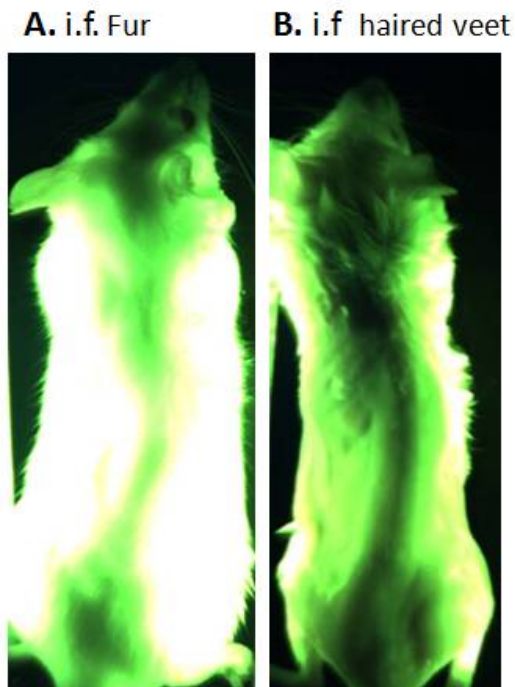


Figure 134 NSG mouse with fur and with Veet hair removal

The fur of a NSG mouse was removed with veet cream. (A) NSG-mouse with fur (B) NSG mouse with Veet hair removal at the lower dorsal side. This mouse was also injected intrafemorally (i.f.). Imaged with an one colour filter.

These images (Figure 134) showed that Veet removed hair-follicles in the lower back skin.

NSG mice which had been injected intra-femorally with SEMcami 1.5 months ago were sacrificed and then images taken with excitation light and filters for fluorescence. Each

mouse was imaged successively with fur and then having been shaved, Veet treated, skinned and then after removal of muscle groups (see Figure 135, Figure 136 and Figure 137). The brain was also dissected out and imaged separately to investigate the origin of signal coming from the head (see Figure 138). Frequently the signal was too weak to image through the skin. Sometimes a faint signal could be seen. Early experiments used an older imaging device (Lightbox) and sub-optimal filters, which only allow passage of either one of the fluorescent colours.

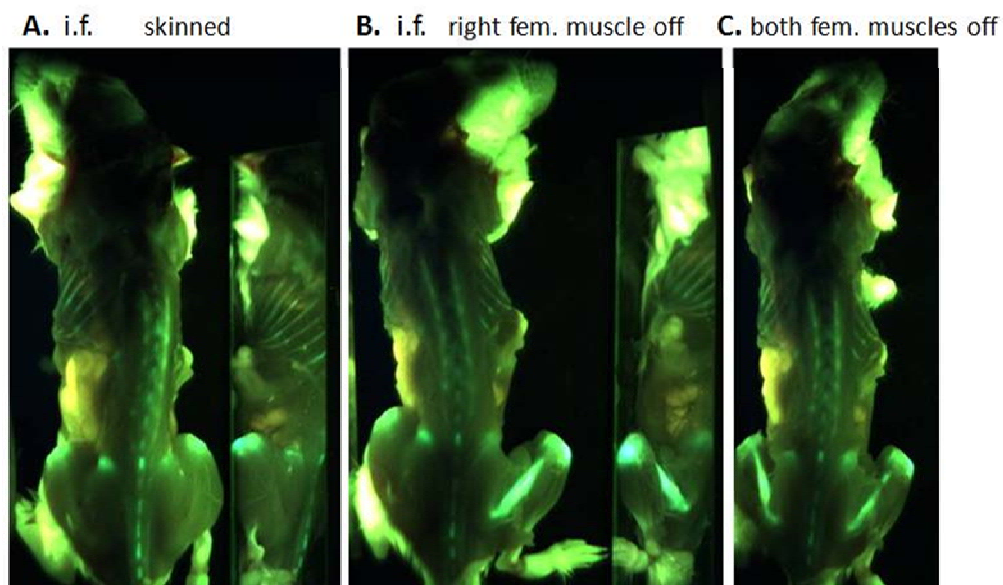


Figure 135 NSG mouse i.f. transplanted with SEMcami

The back of a NSG mouse with i.f. transplanted SEMcami (A) skin removed (B) muscles above the right femur were removed (C) muscles above both femurs removed. Imaged with an one colour filter.

The images of the skinned mouse above (Figure 135) showed that SEMcami infiltrated both knees, the spine (lumbar to chest), the hips and several rib bones. The removal of muscles above the femurs revealed strong signals from both femurs, although the injection site was right. The SEMcami signal appears turquoise, while the green signal from the feet and the head results from reflection from the fur. The yellow signal from the intestines represents auto-fluorescence. At the right side of each picture a mirror is present, showing a right lateral view of the mouse.

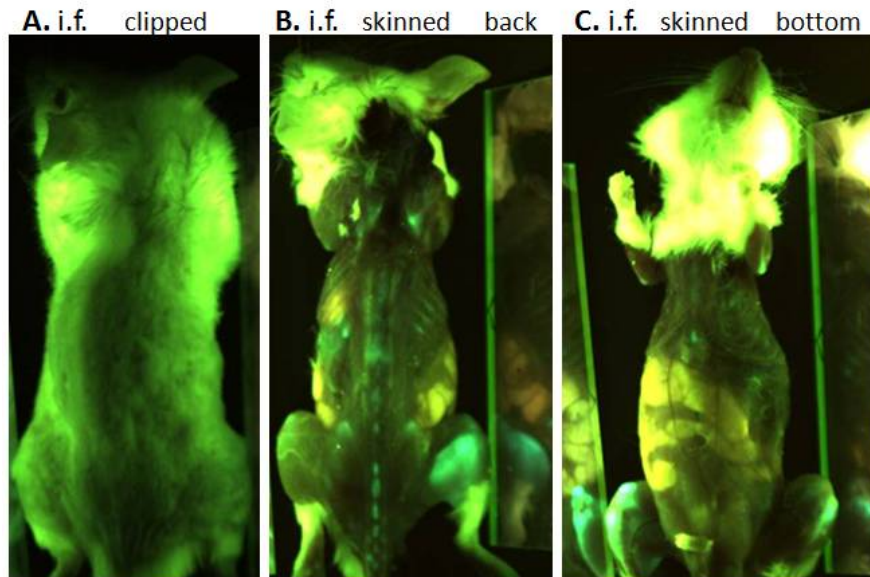


Figure 136 NSG mouse injected i.f with SEMcami

An NSG mouse injected i.f. with SEMcami. (A) Dorsal side, hair removed with a hair clipper, (B) Dorsal side, skin removed (C) Ventral side, skin removed. Imaged with an one colour filter.

Having removed the skin of the mouse shown in Figure 136, a strong signal is revealed from the both knees, the right femur and the lumbar spine. Weak signals were present from the hips and some ribs. As mentioned before, green light represents reflection from the fur shown in Figure 134 A. In Figure 136 B, a mirror at the right side is shown. In Figure 136 C, mirrors are positioned on both sides of the mouse, seen from the ventral aspect. Here the strong intestinal auto-fluorescence in yellow can be seen.



Figure 137 Panel of a control mouse and an i.f. transplanted NSG mouse

(A) control mouse, skinned, backside and not injected (B-D) NSG mouse injected i.f. with SEMcami  
 (A) hairs above right femur removed (hair clipper) (B) mouse skinned and (D) right femur muscles removed. Imaged with an one colour filter.

In this panel (Figure 137) a skinned control mouse is shown alongside an injected mouse with a right leg tumour in showing progressive removal of fur, skin and muscle. This tumour delivered such a strong signal that it could be seen even through hair-clipped fur. Skin and muscle removal showed that the tumour was surrounding the right knee region also involving muscle and other tissues. A weak signal from the spine was suggestive of vertebral infiltration.

The following mice had been injected intravenously and were imaged using the filters and equipment mentioned above.

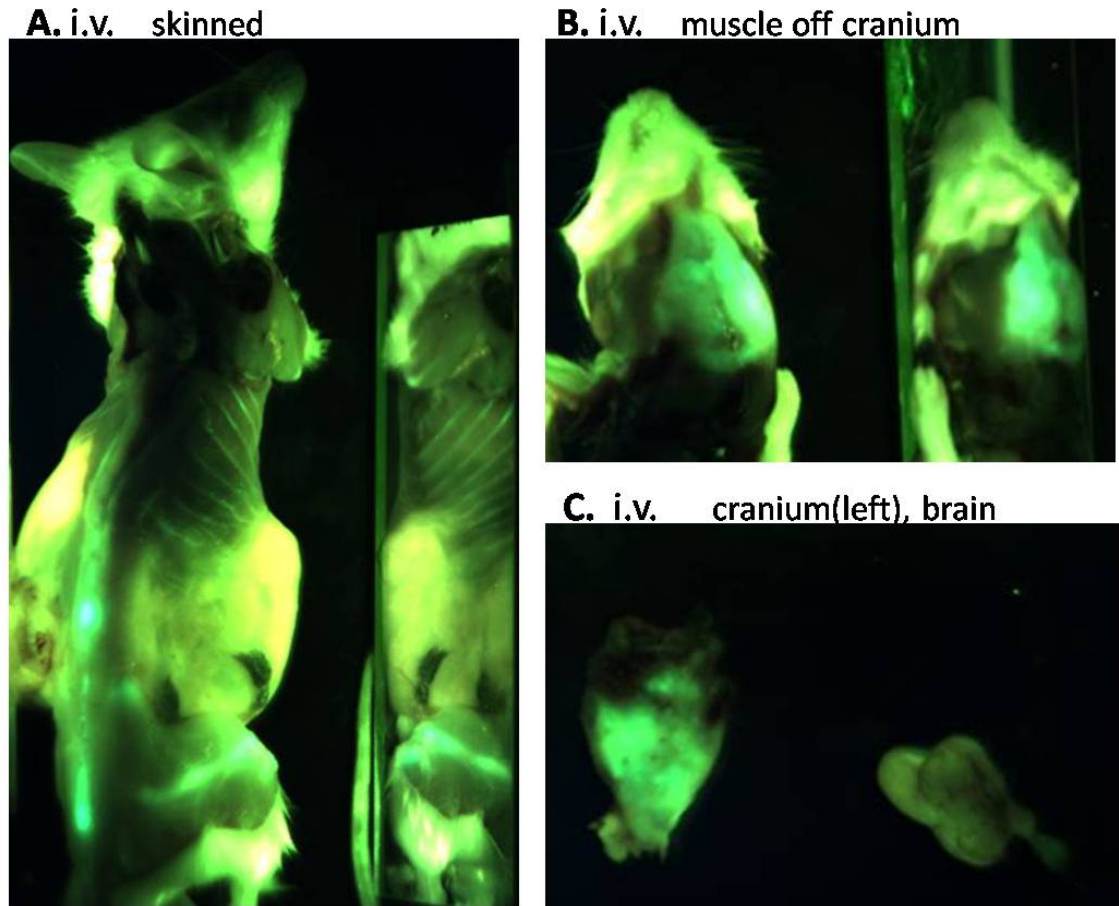


Figure 138 NSG mouse 1 transplanted i.v. with SEMcami

NSG mouse injected i.v. with SEMcami. (A) dorsal side of skinned mouse (B) muscles above cranium removed and (C) isolated cranium, backside (Left); brain (Right). Imaged with an one colour filter.

Here (Figure 138) the i.v. injection of SEMcami led to a signal from the right knee and the lower spine. Following removal of the skin from over the cranium, a signal can be recorded. The isolation of the cranium and the brain showed that the cranium (left) was infiltrated while the brain (right) showed no specific fluorescence. At the right side of A and B a mirror gives a lateral view.

Next, another NSG mouse is shown which had been injected i.v. with SEMcami and monitored for signs of engraftment.



i.v. skinned

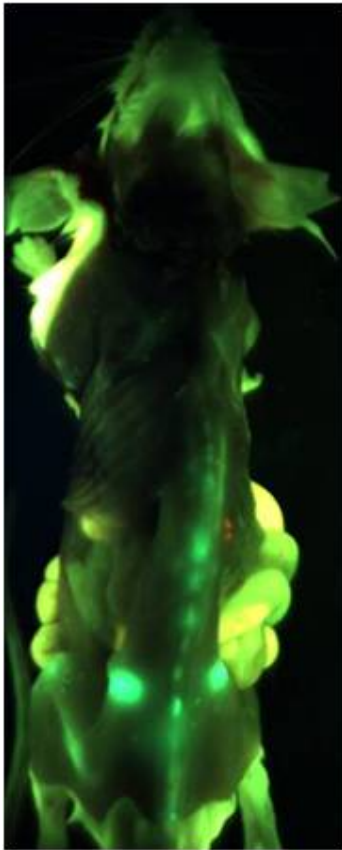


Figure 139 NSG mouse 2 with i.v. transplant of SEMcami  
Dorsal side of a skinned NSG mouse injected i.v. with SEMcami. Imaged with an one colour filter.

In the image above (Figure 139), turquoise signal of SEMcami is present in the lower skeleton while intestines show yellow auto-fluorescence.

This single image from one NSG mouse 2 confirmed again that predominantly the hips and lower spine were infiltrated by SEMcami.

Next a third NSG mouse injected i.v. with SEMcami is shown (see Figure 140).

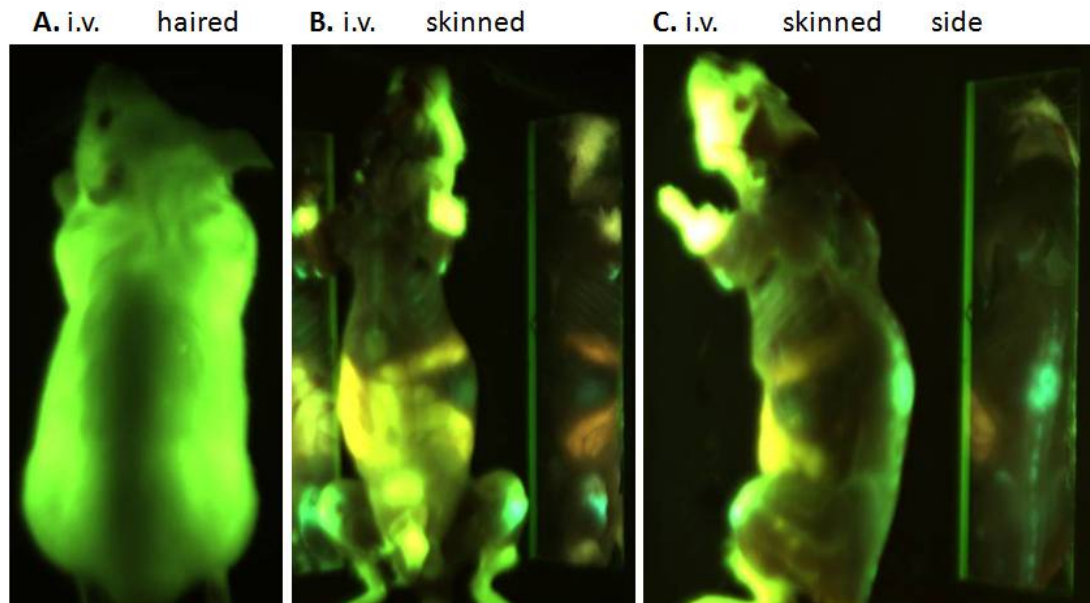


Figure 140 NSG mouse 3 injected i.v. with SEMcami

(A) dorsal side with fur (B) skinned, ventral side and (C) skinned, left side (right: mirror image of back). Imaged with an one colour filter.

In the panel (Figure 140) of this mouse, signals were captured from both knees and the spine. Picture A shows NSG mouse 3 with fur. In picture B the ventral side of this mouse is shown with specific signals from the knees while the feet show green reflections and the abdomen shows yellow auto-fluorescence. Picture C shows SEMcami signal in the left knee and the lower and middle spine, which can be seen in the mirror at the right side of the picture. Here single engrafted vertebrae are shown.

The following images were captured from mice injected i.v., i.f and s.c. with SEMcami.

In contrast to the previous images, these were captured using a dual filter which allowed recording of the green signal from GFP as well as the red signal from Dsred resulting in higher signal strength and a lower background. These two signals (red and green)

generate a composite signal which, depending on the filter used, generate a rather turquoise specific signal, as seen in previous images, or a light blue signal, seen in the following images.

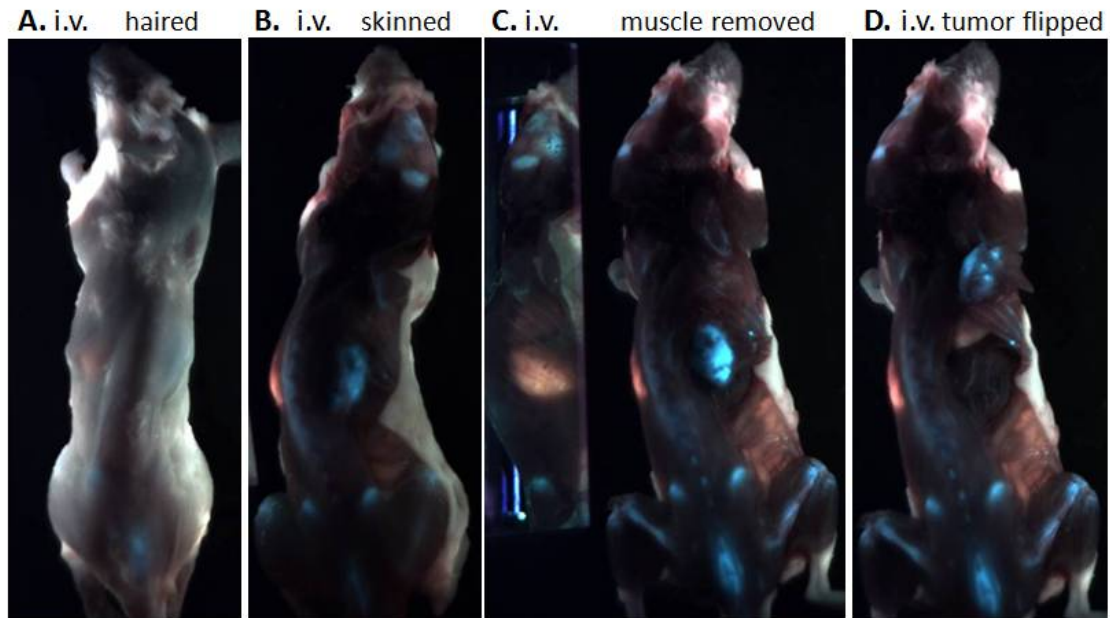


Figure 141 NSG mouse injected i.v. with SEMcami

(A) hair removed with Veet (B) skinned, dorsal side (C) muscles above femurs removed and (D) intercostal tumour cut and turned over. Imaged with a dual filter (GFP + Dsred).

These images (Figure 141) of i.v. injected mice showed a weak signal through the skin in the tail region (injection site), the left hip and the right dorsal thorax/rib region. Skinning also revealed infiltration in the right hip, the knees, the cranium and an intercostal tumour. Under the muscles there was also signal from the femurs. Cutting out and flipping of the inter-costal tumour revealed that the majority of the infiltrated cells had localized above the ribs.

The skull vault and the brain were removed from this mouse also. Imaging confirmed leukaemic infiltration of the cranium and not the brain (Figure 142).

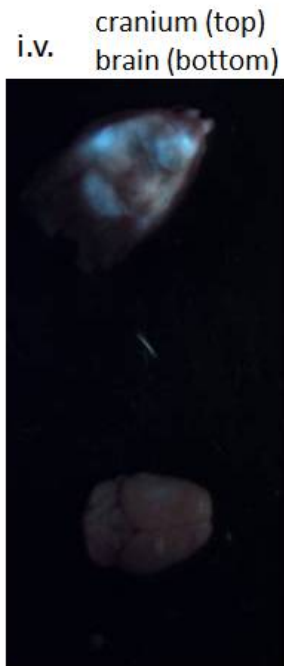


Figure 142 Cranium and brain of NSG mouse

Mouse from Figure 141 (Top) isolated cranium (Bottom) brain. Imaged with a dual filter (GFP + Dsred)

The following mice were injected subcutaneously with SEMcami using a medium with high viscosity which retains the cells where they were injected. This was done to investigate how well signal can be detected through the skin.



Figure 143 NSG mouse injected s.c. with SEMcami

(A) right side, hair cut (B) right side, hair removed by Veet (C) hair removed, dorsal side. Imaged with a dual filter (GFP + Dsred).

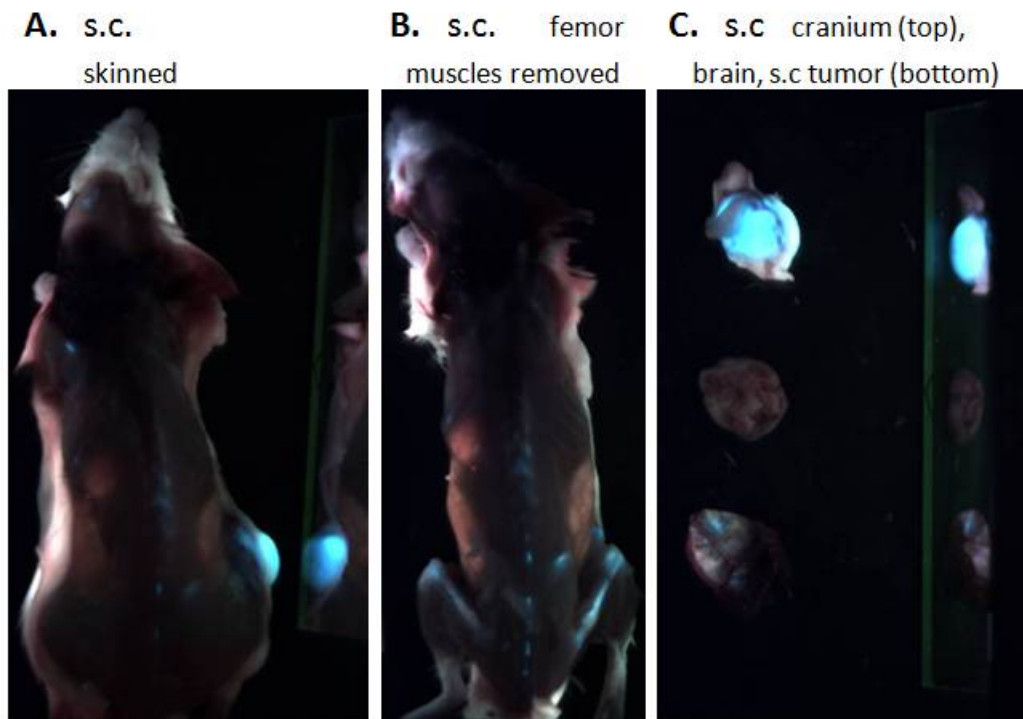


Figure 144 NSG mouse injected s.c. 2nd panel from Figure 143

(A) skinned (B) muscles above femurs removed (C) isolated cranium (Top), brain (Middle) and back of s.c tumor (Bottom). Imaged with a dual filter (GFP + Dsred).

The first panel of this mouse (Figure 143) proved that strong signal can be detected even throughout the fur. A comparably big right s.c. tumour was present. This mouse also showed that if the signal is strong enough, the imaging parameters can be set optimally leading to low background.

The second panel (Figure 144) of this mouse shows spine, femur and strong cranial infiltration from SEMcami which had disseminated from the s.c. injection site. As before the brain showed no infiltration.

Concluding, these results show that primary SEM can engraft in R2G and NSG mice and form tumours, however bone marrow did not seem to be preferred for engraftment. The imaging work with cell line SEM shows the value of hair removal, the double fluorescent cell line SEMcami and double filters. Most importantly SEMcami show good engraftment especially in large bones and especially in this context the imaging in the whole mouse proved to be very useful.

## 6.4 Discussion mouse results

The aim of this chapter was to investigate MLL/AF4 *in vivo* to expand the data gained *in vitro* into a more physiological context. For that, a mouse imaging model had to be established to track engrafted MLL/AF4 positive or leukaemic cells in general, how they distribute and where they form tumours first, in mice.

Intra femoral injection of early SEM, MLL/AF4 positive patient cells, into NSG and R2G mice affected health and survival in those mice. Unfortunately two NSG mice died before a sample could be taken. Most likely the injected early SEM restricted survival. Because other mice were injected with the same batch of cells, it is unlikely that the injection, which took place in a sterile environment, caused the death of the animals by an infection. However two rag mice were sacrificed one month after injection and analysed for engraftment in bone marrow and blood. The first R2dKmouse showed low numbers of cells defined as non-mouse cells (Figure 128). By comparing these transplantation derived cells to the whole number counted, low engraftment was found. Although human cells were present in the blood, the proportion was lower than 0.01%, although the few cells were classified as human. For the bone marrow analysis fewer cells were analysed, therefore even low numbers of cells classified as human generated a proportion of 0.2%. Flow cytometric analysis of control early SEM showed high CD19 expression levels, a B-cell marker, and high CD133 levels, a stem cell marker. The second R2G mouse had an abdominal tumour with a slightly enlarged spleen. A very clear early SEM signature from a distinct population was found (Figure 129). However in comparison to the majority of cells these did only comprise for 0.1%. The blood contained no human cells at all. Recently the involvement of natural killer cells in rejection of engraftment of human hepatocytes in R2G and NOD/SCID mice was shown

(Kawahara, Douglas et al. 2010), however both mouse strains used should have very low levels of natural killer cells. Referring to this, a possible explanation for low engraftment could be a remaining low activity of natural killer cells. Earlier work indicated that unconditioned, e.g. not irradiated, mouse strains have fewer niche space available to engraftment for HSCs (Bhattacharya, Rossi et al. 2006).

The one surviving NSG mouse was sacrificed and harvested. The section showed an enormously enlarged spleen of approximately 5cm length and 1cm thickness. Additionally a huge rubber like tumour at the back of the right femur (injection site) was found, as well as an enlarged unfilled bladder. Bone marrow and blood was analysed as before. The blood showed 36% human cells with clear early SEM signature, a high expression of CD19 and CD133 (Figure 131). However the bone marrow analysis showed only few cells which only comprised 0.2% of all cells (Figure 132). It was reported that enlarged spleens can also be caused by extramedullary haematopoiesis to replace supplanted haematopoiesis (van der Loo, Hanenberg et al. 1998). However, the low bone marrow engraftment makes a displacement of murine HSCs unlikely. More likely these cells are reduced in their ability to migrate and could therefore favour the spleen as an easy accessible niche.

Cells from several organs were isolated and put into culture. Due to the large number of mouse cells present after organ-extraction, which die in culture, a huge amount of debris is crowding the cells intended to culture. The large, almost “white” spleen, compared with the dark red spleen from a normal mouse, was sectioned, PE stained and analysed using a half automated imaging system (Aperio). The histological structure of that spleen was compared to a normal mouse spleen (Figure 133). Several magnifications showed that the normal histological structure was wiped out. The spleen was highly engrafted; normally a sign of advanced leukaemia. In contrast the low engraftment in



the bone marrow does not support this. As a similar finding was made in a R2G mouse with tumour, but no substantial engraftment in the bone marrow, it is unclear if these early SEM preferably engraft non bone marrow murine tissues or if the time given to engraft was enough to form tumours or spleen enlargement, but not for bone marrow engraftment. Additionally the properties of SEM such as the tendency in forming tumours may just out compete tumour growth to bone marrow engraftment. In contrast, bone marrow samples of siRNA treated SEM (cell line) injected into mice, contained substantial numbers of CD45 positive cells (Thomas, Gessner et al. 2005) indicating that human cells (SEM) had engrafted. The established cell line SEM shows high proliferation and less dependence on growth factors compared to primary SEM.

Another possibility is the gating method which gates out cells by mouse antibody staining. The fact that pure early SEM are determined as 82% non-mouse cells shows that there is loss of cells in this analysis. For example if gated by CD19 versus PE-Cy7 mouse specific antibody TER119, the number of human cells in the NSG blood rises from 36 to 78%. However, this different gating approach did not change the ratios in the bone marrow samples. Both methods of gating were established and used successfully for detecting engraftment with many different patient cells (le Viseur, Hotfilder et al. 2008). Maybe the early SEM cells are less accessible to this method or are not preferably engrafting in the bone marrow, at least in these two mouse models.

Most interestingly early SEM cells produced 2 second high CD34+ population after engraftment compared to control early SEM (Figure 130). There were early reports stating that a human CD43+CD38- stem cell fraction has the ability to engraft in NOD/SCID mice and re-establish leukaemia (Lapidot, Sirard et al. 1994).

Additionally, the CD19 signature seemed to drop, sometimes more than 2 decades. In this context, observations in co-cultured patient MLL/AF4 cells showed lower CD19 levels than in cell line SEM. Hotfilder et al. and Castor et al. have found immature CD34<sup>+</sup>CD19<sup>-</sup> cells in two types of high-risk ALL, these were infant ALL with a translocation t(4;11) and Philadelphia chromosome-positive ALL (Castor, Nilsson et al. 2005; Hotfilder, Rottgers et al. 2005). The increase in CD34 expression could indicate that the cells reactivate stem cell programs and also indicate a role in the niche.

The second part of my mouse work dealt with the imaging of fluorescent MLL/AF4 positive cells engrafted in NSG mice. For this, fluorescent SEMcami, which had been generated by Vasily Grinev by transduction of SEM with a lentiviral expression vector, were used. SEMcami express GFP and DsRed, allowing for fluorescent detection. As preliminary experiments show, fur of mice can strongly block a fluorescent signal and reflect excitation light, used to induce fluorescence, which produces a strong background. To be able to detect weak fluorescent signals from small numbers of cells, we worked on hair removal strategies (technical assistance from Mike Batey). Hair clipper cut fur still blocks fluorescent signal strongly, therefore hair follicles were removed using Veet cream (Figure 134). This treatment can be performed on anaesthetised live animals, apart from the head and other sensitive areas. In the following data, sacrificed mice had been used, showing an endpoint analysis.

3 NSG mice transplanted i.f. with SEMcami showed engraftment in femurs knee joints, vertebrae, rib bones, hips and soft tissue (tumours). Some signals from bones could be enhanced or even unveiled by removal of covering muscles. Overall, i.f. injections of SEMcami showed engraftment of SEMcami, tumour formation and preferential localisation to large bones (Figure 135, Figure 136 and Figure 137).

Intravenous injections of SEMcami into 4 NSG mice showed engraftment in femurs, ribs, hips, vertebrae, soft tissue (tumours) and cranium. The brains of those mice with cranium infiltration showed no signal. These data showed that also i.v. injected SEMcami engraft preferably in bone tissue, especially the detection in the cranium is interesting. SEMcami behave like SEM, they are more aggressive and engraft easily in several tissues compared to primary SEM (Figure 138, Figure 139, Figure 140, Figure 141 and Figure 142).

As many of the bone engraftment signals were only retrieved after skin and muscle removal this method was not sensitive enough to monitor living mice, at least not in that stage of the disease. The use of a dual filter, which allows green and red light to pass, increased the signal strength and quality.

The through skin and tissue signal imaging was further tested by injecting SEMcami in the viscous matrigel medium. This medium has a high viscosity and keeps the cells together, enabling the generation of subcutaneous tumours. The accumulation of high numbers of fluorescent cells was thought to produce strong signals for imaging. As expected tumour signals could be detected through the skin and even through clipped fur. Interestingly this s.c. injected mouse also showed engraftment in femur, vertebrae and cranium. No signal was found in the brain as before (Figure 143 and Figure 144).

The Heidenreich group has shown before that SEM with normal levels of *MLL/AF4* transcript engrafted in liver, spleen and bone marrow of intraperitoneal injected NSG. SEM depleted for *MLL/AF4* showed reduced engraftment, especially the spleen was much smaller than the spleens from mice with non depleted *MLL/AF4* expression (Thomas, Gessner et al. 2005). As mentioned before engraftment in the spleen produced an enlarged organ.

All injection methods used in this thesis such as i.f., i.v. and s.c., showed engraftment of SEMcami. In the i.f. injected mice we could detect cranium infiltration. Moreover mice injected i.f. in the right femur also showed engraftment in the left femur. This shows that cells must have left the bone, circulated in the blood stream and settled in the femur and other large bones. Additionally a gradient of signal strength from lumbar to cervical vertebrae was observed in several mice. This gradient cannot have been generated by an intraspinal migration. An explanation would be that circulating cells leave the blood stream and migrate into vertebrae preferably in the lumbar spine because here the cavities are bigger and probably more blood vessels penetrate it.

Large bones contain the spongiosa structure, a trabecular structure with many cavities and blood vessels. The bone marrow niche for haematopoietic and also leukaemic stem cells is thought to be located here. By the high vascularisation blood cells or even tumour cells can access the bones and subsequently the bone marrow. The environment there, formed by stromal cells such as endothelial cells, osteoblasts at the bone site and fibroblasts, is called the endosteal niche. It provides secreted factors such as interleukins 6 and 8, which possibly attract migration through the vessels. This environment also provides adhesion factors which allow the cell to settle. Interactions like this also regulate the “homing” cells in growth and differentiation. Shiozawa proposed that cancer cells could act as “parasites of the niche” (Shiozawa, Havens et al. 2008).

The engraftment of MLL/AF4 positive SEMcami in cranial bone is a very interesting finding, because the first real time imaging of HSC cell - bone marrow niche migration was made in the cranial region of mice (Xie, Yin et al. 2009).

The problem of lacking signal strength for the detection of leukaemic cells was addressed very recently by the purchase of a state of the art mouse imager. Additionally generation of SEM with luciferase expression was used in the Heidenreich group, allowing repeated detection of fewer cells in living mice even through fur. The model established in this thesis provided the rational for this further improvement of an imaging system.

# **Chapter 7**

## **General Discussion**

# Chapter 7 General Discussion

## 7.1 Summary of thesis

MLL/AF4 leukaemia is the most common infant leukaemia. It is a high risk acute lymphoblastic leukemia and associated with a poor treatment outcome. The fusion gene causing this disease, *MLL/AF4*, is generated by the reciprocal translocation between chromosome 4 and chromosome 11. Extensive research and numerous publications over the last 20 years have increased the understanding of how the fusion gene is generated and how it functions. Despite the many advances in understanding, the most recent treatment protocol failed to achieve cure, defined by the 5 year event free survival, in two thirds of cases. Therefore the understanding of MLL/AF4 biology has to be improved.

This thesis investigated several topics. Firstly this work validated gene expression array data of MLL/AF4 depleted t(4;11) ALL cells, identified and investigated several potential target genes of MLL/AF4. Secondly this study aimed to analyse identified target genes of MLL/AF4 in the haematopoietic stem cell niche context. For this an interaction system had to be established to analyse bone marrow feeder - leukaemic cell interactions. Thirdly this work aimed to develop a lentiviral gene expression system to investigate MLL/AF4 target genes by over expression. Finally the biology of MLL/AF4 cells was investigated in an *in vivo* context using immuno deficient mice. An imaging model was developed to track engrafting and migrating MLL/AF4 leukaemic cells

The expression array analysis was carried out in MLL/AF4 positive SEM cells, which had been treated with *MLL/AF4* and control siRNA. Gene pattern changes

corresponding to the comparison of MLL/AF4 control cells and MLL/AF4 depleted cells were analysed for their significance and bio-informatically linked to functions, pathways and diseases by the Ingenuity Pathway Analysis 8.5. Additionally, interesting candidates were validated by qRT-PCR. Ingenuity Pathway analysis showed three main groups of functions, pathways and diseases: cancer / leukaemia, haematopoiesis / niche and inflammation.

MLL/AF4 is clearly related to leukaemia as several publications have indicated its oncogenic potential (Chen, Li et al. 2006; Metzler, Forster et al. 2006) and its restriction to mostly lymphocytic leukaemia (Pui and Campana 2007; Lazic, Tomic et al. 2010; Zuo, Zhang et al. 2010), rarely myelocytic leukaemia (Shih, Liang et al. 2006) but not to cancer of other tissues.

MLL/AF4 was functionally implicated in the haematopoietic niche as mesenchymal stem cells of t(4;11) positive patients expressed the fusion gene MLL/AF4 and thus the authors assumed the bone marrow environment played a role in the disease (Menendez, Catalina et al. 2009). TIE-2, which is known to be involved in the regulation of the vascular niche was reported to be expressed in some t(4;11) cells (Hu, Li et al. 2009). Marschalek speculated that leukaemic cells interact with the niche to support survival and reduce stress caused by oncogenic *MLL* fusions (Marschalek 2010).

The last main group of function, pathways and diseases associated to MLL/AF4 was inflammation. This was the most surprising finding. However MLL/AF4 was linked to interferon (IFN) response recently. Although many ALLs are known to be IFN resistant, the two tested MLL/AF4 cell lines SEM and RS411 were not and NF- $\kappa$ B was found to be an important transcription factor in interferon response (Tracey, Streck et al. 2010). The Heidenreich group found no increase in interferon response due to MLL/AF4



depletion (Thomas, Gessner et al. 2005), however the depletion of MLL/AF4 may increase inflammation pathways i.e. Interferon independent. A possible explanation is that the time interval after siRNA mediated MLL/AF4 depletion was not sufficient. Alternatively, inflammation signalling could be a consequence of the leukaemic biology of the cells rather than a response to siRNA treatment. In a study of children with ALL increased inflammation markers (TNF-alpha and IL-6) were found at diagnosis. After induction of chemotherapy inflammatory chemokines were significantly reduced (Giordano, Molinari et al. 2010). This could suggest that inflammation signalling may help cancer cells to allow proliferation in combination with a differentiation block resulting in the propagation of a leukaemic population. MLL/AF4 could help the cells to survive inflammation related apoptosis due to their apoptotic resistance.

Gene array analysis is a powerful tool in examining MLL/AF4 related gene expression patterns which can provide insights into the biological functions. Other groups experienced in MLL/AF4 research have investigated MLL/AF4 related gene expression by array analysis as well (Gaussmann, Wenger et al. 2007; Guenther, Lawton et al. 2008; Stumpel, Schneider et al. 2009). The effect of MLL/AF4 on epigenetic regulation, which is known to be important in malignant processes, can be addressed by methylation array analysis. Recent work from Ronald Stams group analysed methylation patterns of *MLL* rearranged leukaemias and showed *MLL* fusion specific promoter methylation, particularly MLL/AF4 related hypermethylation. Additionally methylation patterns corresponded to clinical outcomes of patients (Stumpel, Schneider et al. 2009).

MLL/AF4 targets DOT1L a H3K79 (histone 3 lysine 79) methylase. The fusion gene can recruit DOT1L to new methylation sites upregulating genes important for

haematopoietic stem cell function, chromatin regulation such as histone demethylases, cell signalling and cycle progression (Barry, Corry et al. 2010).

The use of MLL/AF4 cell-lines for gene expression arrays has some restrictions, as cell-lines often acquire several mutations which makes it unclear if observed expression patterns are only related to MLL/AF4 depletion or are a consequence of mutations. However, patient material is difficult to manipulate, so far. For the future, the use of more primary material such as early SEM could be beneficial, as knockdown of MLL/AF4 in the latter proved to be feasible (unpublished work).

From the validated genes especially *HOXA7*, *FGFR1*, *MEF2C*, *DUSP6* and N-cadherin were significantly down-regulated upon MLL/AF4 depletion.

*HOXA7* is known to be involved in the regulation of haematopoiesis. Additionally, involvement in leukaemia was reported as research has shown *HOXA7* was dysregulated in AML and mixed lineage leukaemias (Eklund 2007). *FGFR1* is known to be involved in chromosome 8 translocation related fusion genes. As patients with an *FGFR1* fusion gene mostly suffer from myoproliferative neoplasms (Patnaik, Gangat et al. 2010) it could show the influence of *FGFR1* on proliferation and transformation. *MEF2C* was reported to regulate homing and invasiveness in *MLL* fusion, *MLL/ENL* positive, AML patients (Schwieger, Schuler et al. 2009). In a very recent study N-cadherin amongst other adhesion molecules was found to be upregulated in AML leukaemic stem cells (LSC) by chemotherapeutic treatment. The authors stated that interaction of LSCs and the niche environment by adhesion molecules played a role in chemoresistance (Zhi, Wang et al. 2010). Very recent findings strengthen the role of N-cadherin in the endosteal niche. One of such was the work of Nakamura et al., who

showed that the osteoblast fraction of the endosteal niche which most strongly supported long term reconstitution activity of HSCs, were high in cadherin expression and expressed cytokines such as angiopoietin 1 (Nakamura, Arai et al. 2010). The initial finding that N-cadherin expression was altered in our array and in related analyses had focused our attention towards the niche, although the importance of N-cadherin in the HSC niche regulation was doubted by some authors who saw a lack of evidence for the requirement of N-cadherin for HSC (Kiel, Radice et al. 2007). N-cadherin is playing an important role in the haematopoietic niche regulation (Hosokawa, Arai et al. 2010), however due to the complexity of regulation by secreted factors, adherence molecules and numerous involved pathways it is not justified to regard it as an irreplaceable actor in the niche (Li and Zon 2010).

Furthermore MLL/AF4 related functions such as “*Haematopoiesis*” and validated genes such as N-cadherin and *FGFR1* strongly pointed to the HSC niche and this aspect was investigated in more detail. To test such interactions an assay involving bone marrow fibroblasts had to be established. Co-culture of haematopoietic cells with bone marrow feeders such as HS-5 have been used for many years to increase survival of primary patient material (Seiffert, Stilgenbauer et al. 2007; Lwin, Crespo et al. 2009).

Several obstacles had to be overcome to establish the feeder assay and analyse co-cultured leukaemic cells. The separation of leukaemic cells from feeders had to be done in the data analyses of experiments as the harvest of cells by trypsination also caused feeders to be removed. If specific inhibitors of main feeder – leukaemic cells adhesion molecules were identified they could be used for such a separation and the latter would be even more interesting as a therapeutic option. Several such adhesion molecules inhibitors are known. For example matrix adhesion induced by N-CAM could be blocked by inhibitors of FGFR signalling and anti- $\beta_1$ -integrin antibodies (Cavallaro,

Niedermeyer et al. 2001). N-cadherin adhesion could be targeted by a HAV domain mimetic peptide or a N-cadherin specific blocking antibody; both of which were described in the investigation of N-cadherin mediated adhesion (El Sayegh, Arora et al. 2004). Finally small-molecule inhibitors of  $\alpha$ 4-integrins were indicated to interfere with lymphocyte adhesion (Martin, de Moraes et al. 2005) and could be used to reduce leukaemic cell adhesion to feeder cells.

While establishing the feeder assay it could be shown that leukaemic cells adhere to the feeder cells, are easily distinguishable from feeders and can be harvested and analysed for gene expression, apoptosis and proliferation. Feeder co-culture of SEM cells and SEM depleted for MLL/AF4 increased proliferation particularly at low cell concentrations. The M210B4 feeders used in this assay were reported to secrete growth factors and to induce cell expansion of haematopoietic progenitors (Koschmieder, Bug et al. 2001). Additionally SEM cells, SEM depleted for MLL/AF4 and t(4;11) positive patient cells showed increased viability when grown on feeders. In concordance with this M210B4 co-culturing was reported to increase survival of CLL patient cells (Edelmann, Klein-Hitpass et al. 2008).

In a rather recent work a Japanese group presented a “biomimetic osteoblast niche”. They created a “3 D” niche by using bone which was seeded with mesenchymal stem cells (MSC) of CML patients and subsequently the MSCs were induced to differentiate into osteoblasts. This system was used to culture CML patient cells and to analyse the latter by flow cytometry, colony formation assays and long term culture initiating cell LTC-IC assays (Hou, Liu et al. 2009).

In order to examine the influence of feeders on gene expression of MLL/AF4 target genes such as *FGFR1*, N-cadherin, *HOXA7* and *TERT*, SEM cells depleted for

MLL/AF4 were grown with and without feeders and concomitant expression profiles compared. In the future such a system would be useful for detecting gene responses i.e. due to a chemotherapeutic treatment in a bone marrow context.

To investigate target genes of MLL/AF4, such as N-cadherin, in more detail in the leukaemic context, a lentiviral highly regulated expression system was designed. In this system target genes of MLL/AF4 are analysed by over-expression in leukaemic cells and their effect on features of leukaemic cells including proliferation, clonogenicity and viability is measured. The design of this system was based on a two vector system; vector 1 coding for the tet activator and vector 2 coding for the gene to be expressed under the control of an inducible tet-O promoter. The tet activator expression plasmid (vector 1) was cloned and lentivirally transduced in t(4;11) SEM and MV4;11 cells. Although this vector was shown to be functional, transduced cells showed decreased expression of the reporter gene eGFP, which is under the constitutive control of an IRES element. In the literature reports show that high levels of tet activator can be toxic to mammalian cells (Gossen and Bujard 1992). However stable expression of tet activator was successfully performed before in Jurkat cells transduced with a retroviral tTA vector (Jurkat-tTA cell clone 4D9#32) (Chu, Pardo et al. 2003). Very recently a tet on transgenic rat, expressing tet activator, was reported. When transduced with a TetO7/CMV-EGFP lentivirus, fibroblasts from this tTA rat showed doxycycline inducible and dose dependent eGFP reporter gene expression (Sheng, Lin et al. 2010).

The cloning of vector 2 could not be finished in time and stopped at the stage of the ppc (ptre-PGK-mcherry) cassette which only has to be inserted into a suitable lentiviral vector.

Lentiviral (over)expression has already been used to investigate target gene functions. For example, CAV1 function which is known to mediate radioresistance, was tested by over-expression with a lentiviral SIN vector in the lymphoblastic TK6 cell line (Barzan, Maier et al. 2010). More advanced regulated over-expression of target genes was reported using the tet-off system and regulating expression with doxycycline (Kim and Lee 2009). More recently a double transduced teton tet-O system, induced by doxycycline, was used to investigate FGF10 by over-expression (Gupte, Ramasamy et al. 2009). However, the tight (low basal expression) and highly regulated gene expression to investigate functions of genes of interest still remains an important goal. The latter is of interest because genotoxic proteins are difficult to analyse with common expression systems.

In addition to the investigation of MLL/AF4 target genes by lentiviral over expression the biology of MLL/AF4 was also addressed in a more appropriate physiological context. For this xenotransplantation mouse models were used which study human leukaemic cells following engraftment.

Early SEM cells which are an early passage of SEM, derived from patient material, were transplanted intrafemorally into R2G and NSG immuno deficient mice. Early SEM cells are unlike the established cell line SEM, as they grow slowly and are sensitive in culture. Although these t(4;11) cells were able to form tumours in R2G mice and possibly impacted survival if sufficient time was given before sacrificing them, cell numbers of primary SEM were quite low in peripheral blood and bone marrow. However R2G mice are not a common model for xenotransplantation in leukaemia; the majority of ALL xeno-transplantaion models published use NOD/SCID mice (Yu, Yang et al. 2008).

From the three NSG mice transplanted two died before analysis could be performed, possibly due to leukaemic cells restricting survival. The one surviving NSG mouse showed large tumours and a massively enlarged spleen, which was shown to be infiltrated by leukaemic cells by histological analysis. The blood was crowded with leukaemic cells which made up for more than 60%, however only a small number of leukaemic cells were present in bone marrow. No work was published stating bone marrow engraftment of primary SEM cells. The Heidenreich group has shown bone marrow engraftment of cell line SEM cells previously (Thomas, Gessner et al. 2005).

A possible explanation could be that primary SEM are not as aggressive as cells which received additional events to transform into a cell line. Cell line SEM cells were injected intra hepatically into Rag newborn mice which restricted survival and produced tumours (data not shown). However cell line SEM are so aggressive that they formed tumours in i.p. injection directly at the site of injections (data not shown). Additionally the Heidenreich group has shown that beside forming tumours, i.p. injected SEM still produced a leukaemic phenotype in NSG mice (Thomas, Gessner et al. 2005). To retrieve more aggressive primary SEM - organs such as spleen, liver, kidneys and tumour tissues were isolated and cultured from mice with tumours. However even from the highly infiltrated NSG spleen tissue no leukaemic cells could be maintained in culture or amplified (data not shown)

Reducing injected cell numbers and increasing the time until such immune deficient mice are sacrificed could help to develop a more leukaemic phenotype. It was shown that in the mouse model used in this thesis, even 1000 cells could engraft and give rise to bone marrow infiltration (le Viseur, Hotfilder et al. 2008).

As these type of experiments relied on the right time point to sacrifice animals to be able to see engraftment, tumours and a leukaemic phenotype - the development of the disease is difficult to track, apart from taking bone marrow punctures and blood samples at various time points. To be able to monitor location and progression after engraftment, a mouse system using fluorescent SEM cells was developed. For the development and testing, mice were injected i.f., i.v. and s.c. and sacrificed after a timepoint estimated to be sufficient.

Fluorescent, stably GFP expressing ALL cells were used before to track cells *in vivo*; in such a work Nalm-6 cells were investigated for their homing into bone marrow niches, however for the imaging the skin of the back of the skull had to be opened under anaesthesia to allow microscopic imaging (Colmone, Amorim et al. 2008) which is invasive and makes repeated imaging ethically and technically questionable.

As the fur proved to be an effective barrier for fluorescent signal, a method was established to remove areas of fur which would also be suitable with anesthetized living animals. Apart from establishing this system, engraftment in large bones such as spine, cranium and femurs could be shown. The model will be further improved as the Faculty has purchased a state of the art, (IVIS, In Vivo Imaging System) sensitive live imager. Additionally the development of a luciferase SEM cell in the Heidenreich group has succeeded and will increase signal strength and reduce background in mouse imaging. Recently such a system was reported for murine xenograft models using cell lines such as THP1 (acute leukaemia) with an improved red shifted luciferase signal (Mezzanotte, Fazzina et al. 2009).

In the future the Heidenreich group will be able to track small amounts of leukaemic cells in living animals at various time points, further improving the understanding of the



pathology of t(4;11) positive cells. The imaging system developed in this thesis could also be used to investigate therapeutic compound functions in a physiological context.

## 7.2 Overall summary

In summary this work validated target genes of MLL/AF4 and provided evidence for associated biological functions. The feeder assay established during this project showed the influence of bone marrow feeders on MLL/AF4 positive SEM and patient cells, enhancing proliferation and survival. A lentiviral expression system was designed and should allow the functional analysis of MLL/AF4 target genes by over-expression. The more physiological investigation of MLL/AF4 biology in mouse engraftment models and the development of an *in vivo* imaging system in mice can offer more detailed understanding of MLL/AF4 and has already provided evidence for the preferential engraftment of t(4;11) positive SEM into large bones of transplanted mice. Finally this work provided the basis for subsequent live imaging of leukaemic cells in NSG mice.

---

## References

- Abramovitch, R., E. Tavor, et al. (2004). "A pivotal role of cyclic AMP-responsive element binding protein in tumor progression." Cancer Res **64**(4): 1338-1346.
- Adolfsson, J., O. J. Borge, et al. (2001). "Upregulation of Flt3 expression within the bone marrow Lin(-)Sca1(+)c-kit(+) stem cell compartment is accompanied by loss of self-renewal capacity." Immunity **15**(4): 659-669.
- Adolfsson, J., R. Mansson, et al. (2005). "Identification of Flt3+ lympho-myeloid stem cells lacking erythro-megakaryocytic potential a revised road map for adult blood lineage commitment." Cell **121**(2): 295-306.
- Agha-Mohammadi, S., M. O'Malley, et al. (2004). "Second-generation tetracycline-regulatable promoter: repositioned tet operator elements optimize transactivator synergy while shorter minimal promoter offers tight basal leakiness." J Gene Med **6**(7): 817-828.
- Aguilar, S., C. J. Scotton, et al. (2009). "Bone marrow stem cells expressing keratinocyte growth factor via an inducible lentivirus protects against bleomycin-induced pulmonary fibrosis." PLoS One **4**(11): e8013.
- Andersen, A. H., K. Christiansen, et al. (2001). "Uncoupling of topoisomerase-mediated DNA cleavage and religation." Methods Mol Biol **95**: 101-117.
- Arhel, N. J., S. Souquere-Besse, et al. (2007). "HIV-1 DNA Flap formation promotes uncoating of the pre-integration complex at the nuclear pore." Embo J **26**(12): 3025-3037.
- Armstrong, S. A. and A. T. Look (2005). "Molecular genetics of acute lymphoblastic leukemia." J Clin Oncol **23**(26): 6306-6315.

- Asou, H., S. Tashiro, et al. (1991). "Establishment of a human acute myeloid leukemia cell line (Kasumi-1) with 8;21 chromosome translocation." Blood **77**(9): 2031-2036.
- Austin, T. W., G. P. Solar, et al. (1997). "A role for the Wnt gene family in hematopoiesis: expansion of multilineage progenitor cells." Blood **89**(10): 3624-3635.
- Baird, S. D., M. Turcotte, et al. (2006). "Searching for IRES." Rna **12**(10): 1755-1785.
- Baltimore, D. (1970). "RNA-dependent DNA polymerase in virions of RNA tumour viruses." Nature **226**(5252): 1209-1211.
- Balvay, L., R. Soto Rifo, et al. (2009). "Structural and functional diversity of viral IRESes." Biochim Biophys Acta **1789**(9-10): 542-557.
- Barry, E. R., G. N. Corry, et al. (2010). "Targeting DOT1L action and interactions in leukemia: the role of DOT1L in transformation and development." Expert Opin Ther Targets **14**(4): 405-418.
- Barzan, D., P. Maier, et al. (2010). "Overexpression of caveolin-1 in lymphoblastoid TK6 cells enhances proliferation after irradiation with clinically relevant doses." Strahlenther Onkol **186**(2): 99-106.
- Bermudez, O., G. Pages, et al. (2010). "The Dual-Specificity MAP Kinase Phosphatases: critical roles in development and cancer." Am J Physiol Cell Physiol.
- Bhardwaj, G., B. Murdoch, et al. (2001). "Sonic hedgehog induces the proliferation of primitive human hematopoietic cells via BMP regulation." Nat Immunol **2**(2): 172-180.
- Bhattacharya, D., D. J. Rossi, et al. (2006). "Purified hematopoietic stem cell engraftment of rare niches corrects severe lymphoid deficiencies without host conditioning." J Exp Med **203**(1): 73-85.

- Biondi, A., G. Cimino, et al. (2000). "Biological and therapeutic aspects of infant leukemia." Blood **96**(1): 24-33.
- Bonnet, D., M. Bhatia, et al. (1999). "Cytokine treatment or accessory cells are required to initiate engraftment of purified primitive human hematopoietic cells transplanted at limiting doses into NOD/SCID mice." Bone Marrow Transplant **23**(3): 203-209.
- Bosma, M. J. and A. M. Carroll (1991). "The SCID mouse mutant: definition, characterization, and potential uses." Annu Rev Immunol **9**: 323-350.
- Bug, G., H. Gul, et al. (2005). "Valproic acid stimulates proliferation and self-renewal of hematopoietic stem cells." Cancer Res **65**(7): 2537-2541.
- Bukovsky, A. A., J. P. Song, et al. (1999). "Interaction of human immunodeficiency virus-derived vectors with wild-type virus in transduced cells." J Virol **73**(8): 7087-7092.
- Bukrinsky, M. I., N. Sharova, et al. (1992). "Active nuclear import of human immunodeficiency virus type 1 preintegration complexes." Proc Natl Acad Sci U S A **89**(14): 6580-6584.
- Bukrinsky, M. I., N. Sharova, et al. (1993). "Association of integrase, matrix, and reverse transcriptase antigens of human immunodeficiency virus type 1 with viral nucleic acids following acute infection." Proc Natl Acad Sci U S A **90**(13): 6125-6129.
- Burger, J. A., A. Spoo, et al. (2003). "CXCR4 chemokine receptors (CD184) and alpha4beta1 integrins mediate spontaneous migration of human CD34+ progenitors and acute myeloid leukaemia cells beneath marrow stromal cells (pseudoemperipolesis)." Br J Haematol **122**(4): 579-589.

- Bursen, A., S. Moritz, et al. (2004). "Interaction of AF4 wild-type and AF4.MLL fusion protein with SIAH proteins: indication for t(4;11) pathobiology?" Oncogene **23**(37): 6237-6249.
- Bursen, A., K. Schwabe, et al. (2010). "The AF4bulletMLL fusion protein is capable of inducing ALL in mice without requirement of MLLbulletAF4." Blood.
- Calvi, L. M., G. B. Adams, et al. (2003). "Osteoblastic cells regulate the haematopoietic stem cell niche." Nature **425**(6960): 841-846.
- Campbell, E. M., R. Nunez, et al. (2004). "Disruption of the actin cytoskeleton can complement the ability of Nef to enhance human immunodeficiency virus type 1 infectivity." J Virol **78**(11): 5745-5755.
- Castor, A., L. Nilsson, et al. (2005). "Distinct patterns of hematopoietic stem cell involvement in acute lymphoblastic leukemia." Nat Med **11**(6): 630-637.
- Cavallaro, U., J. Niedermeyer, et al. (2001). "N-CAM modulates tumour-cell adhesion to matrix by inducing FGF-receptor signalling." Nat Cell Biol **3**(7): 650-657.
- Chen, W., Q. Li, et al. (2006). "A murine Mll-AF4 knock-in model results in lymphoid and myeloid deregulation and hematologic malignancy." Blood **108**(2): 669-677.
- Cheung, A. M., T. K. Fung, et al. (2010). "Successful engraftment by leukemia initiating cells in adult acute lymphoblastic leukemia after direct intrahepatic injection into unconditioned newborn NOD/SCID mice." Exp Hematol **38**(1): 3-10.
- Chiu, P. P., E. Ivakine, et al. (2002). "Susceptibility to lymphoid neoplasia in immunodeficient strains of nonobese diabetic mice." Cancer Res **62**(20): 5828-5834.
- Chu, P., J. Pardo, et al. (2003). "Systematic identification of regulatory proteins critical for T-cell activation." J Biol **2**(3): 21.

- Chung, N., B. K. Jee, et al. (2009). "HOX gene analysis of endothelial cell differentiation in human bone marrow-derived mesenchymal stem cells." Mol Biol Rep **36**(2): 227-235.
- Cianferotti, L., M. Cox, et al. (2007). "Vitamin D receptor is essential for normal keratinocyte stem cell function." Proc Natl Acad Sci U S A **104**(22): 9428-9433.
- Clever, J., C. Sassetti, et al. (1995). "RNA secondary structure and binding sites for gag gene products in the 5' packaging signal of human immunodeficiency virus type 1." J Virol **69**(4): 2101-2109.
- Cobas, M., A. Wilson, et al. (2004). "Beta-catenin is dispensable for hematopoiesis and lymphopoiesis." J Exp Med **199**(2): 221-229.
- Colmone, A., M. Amorim, et al. (2008). "Leukemic cells create bone marrow niches that disrupt the behavior of normal hematopoietic progenitor cells." Science **322**(5909): 1861-1865.
- Coumoul, X. and C. X. Deng (2003). "Roles of FGF receptors in mammalian development and congenital diseases." Birth Defects Res C Embryo Today **69**(4): 286-304.
- Cox, C. V., P. Diamanti, et al. (2009). "Expression of CD133 on leukemia-initiating cells in childhood ALL." Blood **113**(14): 3287-3296.
- Daser, A. and T. H. Rabbitts (2004). "Extending the repertoire of the mixed-lineage leukemia gene MLL in leukemogenesis." Genes Dev **18**(9): 965-974.
- Davis, M. E., J. E. Zuckerman, et al. (2010). "Evidence of RNAi in humans from systemically administered siRNA via targeted nanoparticles." Nature **464**(7291): 1067-1070.

- De Felici, M., D. Farini, et al. (2009). "In or out stemness: comparing growth factor signalling in mouse embryonic stem cells and primordial germ cells." Curr Stem Cell Res Ther **4**(2): 87-97.
- de Haan, G., E. Weersing, et al. (2003). "In vitro generation of long-term repopulating hematopoietic stem cells by fibroblast growth factor-1." Dev Cell **4**(2): 241-251.
- De Pitta, C., L. Tombolan, et al. (2005). "A leukemia-enriched cDNA microarray platform identifies new transcripts with relevance to the biology of pediatric acute lymphoblastic leukemia." Haematologica **90**(7): 890-898.
- Dobrowsky, T. M., Y. Zhou, et al. (2008). "Monitoring early fusion dynamics of human immunodeficiency virus type 1 at single-molecule resolution." J Virol **82**(14): 7022-7033.
- Domer, P. H., S. S. Fakharzadeh, et al. (1993). "Acute mixed-lineage leukemia t(4;11)(q21;q23) generates an MLL-AF4 fusion product." Proc Natl Acad Sci U S A **90**(16): 7884-7888.
- Duncan, A. W., F. M. Rattis, et al. (2005). "Integration of Notch and Wnt signaling in hematopoietic stem cell maintenance." Nat Immunol **6**(3): 314-322.
- Eberle, I., B. Pless, et al. (2010). "Transcriptional properties of human NANOG1 and NANOG2 in acute leukemic cells." Nucleic Acids Res.
- Edelmann, J., L. Klein-Hitpass, et al. (2008). "Bone marrow fibroblasts induce expression of PI3K/NF-kappaB pathway genes and a pro-angiogenic phenotype in CLL cells." Leuk Res **32**(10): 1565-1572.
- Eklund, E. A. (2007). "The role of HOX genes in malignant myeloid disease." Curr Opin Hematol **14**(2): 85-89.

- El Sayegh, T. Y., P. D. Arora, et al. (2004). "Cortactin associates with N-cadherin adhesions and mediates intercellular adhesion strengthening in fibroblasts." J Cell Sci **117**(Pt 21): 5117-5131.
- Elliott, B., and Jasin, M. (2002). "Double-strand breaks and translocations in cancer." Cell Mol Life Sci **59**: 373-385.
- Faloon, P., E. Arentson, et al. (2000). "Basic fibroblast growth factor positively regulates hematopoietic development." Development **127**(9): 1931-1941.
- Feng, S. and E. C. Holland (1988). "HIV-1 tat trans-activation requires the loop sequence within tar." Nature **334**(6178): 165-167.
- Fire, A., S. Xu, et al. (1998). "Potent and specific genetic interference by double-stranded RNA in *Caenorhabditis elegans*." Nature **391**(6669): 806-811.
- Ford, A. M., C. Palmi, et al. (2009). "The TEL-AML1 leukemia fusion gene dysregulates the TGF-beta pathway in early B lineage progenitor cells." J Clin Invest **119**(4): 826-836.
- Gaussmann, A., T. Wenger, et al. (2007). "Combined effects of the two reciprocal t(4;11) fusion proteins MLL.AF4 and AF4.MLL confer resistance to apoptosis, cell cycling capacity and growth transformation." Oncogene **26**(23): 3352-3363.
- Gering, M. and R. Patient (2005). "Hedgehog signaling is required for adult blood stem cell formation in zebrafish embryos." Dev Cell **8**(3): 389-400.
- Gessner, A., M. Thomas, et al. (2010). "Leukemic fusion genes MLL/AF4 and AML1/MTG8 support leukemic self-renewal by controlling expression of the telomerase subunit TERT." Leukemia **24**(10): 1751-1759.
- Gibbs, J. S., D. A. Regier, et al. (1994). "Construction and in vitro properties of HIV-1 mutants with deletions in "nonessential" genes." AIDS Res Hum Retroviruses **10**(4): 343-350.



- Giordano, P., A. C. Molinari, et al. (2010). "Prospective study of hemostatic alterations in children with acute lymphoblastic leukemia." Am J Hematol **85**(5): 325-330.
- Goldman, J. P., M. P. Blundell, et al. (1998). "Enhanced human cell engraftment in mice deficient in RAG2 and the common cytokine receptor gamma chain." Br J Haematol **103**(2): 335-342.
- Golestaneh, N., E. Beauchamp, et al. (2009). "Wnt signaling promotes proliferation and stemness regulation of spermatogonial stem/progenitor cells." Reproduction **138**(1): 151-162.
- Gossen, M. and H. Bujard (1992). "Tight control of gene expression in mammalian cells by tetracycline-responsive promoters." Proc Natl Acad Sci U S A **89**(12): 5547-5551.
- Gossen, M., S. Freundlieb, et al. (1995). "Transcriptional activation by tetracyclines in mammalian cells." Science **268**(5218): 1766-1769.
- Greaves, M. (2006). "Infection, immune responses and the aetiology of childhood leukaemia." Nat Rev Cancer **6**(3): 193-203.
- Greaves, M. F. and J. Wiemels (2003). "Origins of chromosome translocations in childhood leukaemia." Nat Rev Cancer **3**(9): 639-649.
- Gregory, R. I., T. P. Chendrimada, et al. (2005). "Human RISC couples microRNA biogenesis and posttranscriptional gene silencing." Cell **123**(4): 631-640.
- Gregory, R. I., T. P. Chendrimada, et al. (2006). "MicroRNA biogenesis: isolation and characterization of the microprocessor complex." Methods Mol Biol **342**: 33-47.
- Greil, J., M. Gramatzki, et al. (1994). "The acute lymphoblastic leukaemia cell line SEM with t(4;11) chromosomal rearrangement is biphenotypic and responsive to interleukin-7." Br J Haematol **86**(2): 275-283.

- Guenther, M. G., L. N. Lawton, et al. (2008). "Aberrant chromatin at genes encoding stem cell regulators in human mixed-lineage leukemia." Genes Dev **22**(24): 3403-3408.
- Gumbiner, B. M. (1996). "Cell adhesion: the molecular basis of tissue architecture and morphogenesis." Cell **84**(3): 345-357.
- Gupte, V. V., S. K. Ramasamy, et al. (2009). "Overexpression of fibroblast growth factor-10 during both inflammatory and fibrotic phases attenuates bleomycin-induced pulmonary fibrosis in mice." Am J Respir Crit Care Med **180**(5): 424-436.
- Hamsa, T. P. and G. Kuttan (2010). "Evaluation of the Anti-inflammatory and Anti-tumor Effect of Ipomoea obscura (L) and Its Mode of Action Through the Inhibition of Pro Inflammatory Cytokines, Nitric Oxide and COX-2." Inflammation.
- Hazan, R. B., L. Kang, et al. (1997). "N-cadherin promotes adhesion between invasive breast cancer cells and the stroma." Cell Adhes Commun **4**(6): 399-411.
- Hazan, R. B., G. R. Phillips, et al. (2000). "Exogenous expression of N-cadherin in breast cancer cells induces cell migration, invasion, and metastasis." J Cell Biol **148**(4): 779-790.
- Helseth, E., M. Kowalski, et al. (1990). "Rapid complementation assays measuring replicative potential of human immunodeficiency virus type 1 envelope glycoprotein mutants." J Virol **64**(5): 2416-2420.
- Hilden, J. M., P. A. Dinndorf, et al. (2006). "Analysis of prognostic factors of acute lymphoblastic leukemia in infants: report on CCG 1953 from the Children's Oncology Group." Blood **108**(2): 441-451.

- Hjalgrim, L. L., T. Westergaard, et al. (2003). "Birth weight as a risk factor for childhood leukemia: a meta-analysis of 18 epidemiologic studies." Am J Epidemiol **158**(8): 724-735.
- Hosokawa, K., F. Arai, et al. (2010). "Knockdown of N-cadherin suppresses the long-term engraftment of hematopoietic stem cells." Blood.
- Hotfilder, M., S. Rottgers, et al. (2005). "Leukemic stem cells in childhood high-risk ALL/t(9;22) and t(4;11) are present in primitive lymphoid-restricted CD34+CD19- cells." Cancer Res **65**(4): 1442-1449.
- Hou, L., T. Liu, et al. (2009). "Long-term culture of leukemic bone marrow primary cells in biomimetic osteoblast niche." Int J Hematol **90**(3): 281-291.
- Hsieh, J. J., E. H. Cheng, et al. (2003). "Taspase1: a threonine aspartase required for cleavage of MLL and proper HOX gene expression." Cell **115**(3): 293-303.
- Hsieh, J. J., P. Ernst, et al. (2003). "Proteolytic cleavage of MLL generates a complex of N- and C-terminal fragments that confers protein stability and subnuclear localization." Mol Cell Biol **23**(1): 186-194.
- Hu, Z., X. M. Li, et al. (2009). "MLL/AF-4 leukemic cells recruit new blood vessels but do not incorporate into capillaries in culture or in a NOD/SCID xenograft model." Leukemia **23**(5): 990-993.
- Hudson, W. A., Q. Li, et al. (1998). "Xenotransplantation of human lymphoid malignancies is optimized in mice with multiple immunologic defects." Leukemia **12**(12): 2029-2033.
- Ishikawa, F., M. Yasukawa, et al. (2005). "Development of functional human blood and immune systems in NOD/SCID/IL2 receptor {gamma} chain(null) mice." Blood **106**(5): 1565-1573.

- Isnard, P., N. Core, et al. (2000). "Altered lymphoid development in mice deficient for the mAF4 proto-oncogene." Blood **96**(2): 705-710.
- Jackson, A. L., J. Burchard, et al. (2006). "Widespread siRNA "off-target" transcript silencing mediated by seed region sequence complementarity." Rna **12**(7): 1179-1187.
- Jiang, X., Y. Yu, et al. (2010). "The imprinted gene PEG3 inhibits Wnt signaling and regulates glioma growth." J Biol Chem **285**(11): 8472-8480.
- Ju, R., P. Cirone, et al. (2010). "Activation of the planar cell polarity formin DAAM1 leads to inhibition of endothelial cell proliferation, migration, and angiogenesis." Proc Natl Acad Sci U S A **107**(15): 6906-6911.
- Kamel-Reid, S., M. Letarte, et al. (1991). "Bone marrow from children in relapse with pre-B acute lymphoblastic leukemia proliferates and disseminates rapidly in scid mice." Blood **78**(11): 2973-2981.
- Kawahara, T., D. N. Douglas, et al. (2010). "Critical role of natural killer cells in the rejection of human hepatocytes after xenotransplantation into immunodeficient mice." Transpl Int.
- Ketting, R. F., T. H. Haverkamp, et al. (1999). "Mut-7 of *C. elegans*, required for transposon silencing and RNA interference, is a homolog of Werner syndrome helicase and RNaseD." Cell **99**(2): 133-141.
- Kiel, M. J., G. L. Radice, et al. (2007). "Lack of evidence that hematopoietic stem cells depend on N-cadherin-mediated adhesion to osteoblasts for their maintenance." Cell Stem Cell **1**(2): 204-217.
- Kim, H. K., M. Y. Kong, et al. (2005). "Investigation of cell cycle arrest effects of actinomycin D at G1 phase using proteomic methods in B104-1-1 cells." Int J Biochem Cell Biol **37**(9): 1921-1929.

- Kim, V. N., K. Mitrophanous, et al. (1998). "Minimal requirement for a lentivirus vector based on human immunodeficiency virus type 1." J Virol **72**(1): 811-816.
- Kim, Y. G. and G. M. Lee (2009). "Bcl-xL overexpression does not enhance specific erythropoietin productivity of recombinant CHO cells grown at 33 degrees C and 37 degrees C." Biotechnol Prog **25**(1): 252-256.
- Kong, Y., S. Yoshida, et al. (2008). "CD34+CD38+CD19+ as well as CD34+CD38-CD19+ cells are leukemia-initiating cells with self-renewal capacity in human B-precursor ALL." Leukemia **22**(6): 1207-1213.
- Koponen, J. K., H. Kankkonen, et al. (2003). "Doxycycline-regulated lentiviral vector system with a novel reverse transactivator rtTA2S-M2 shows a tight control of gene expression in vitro and in vivo." Gene Ther **10**(6): 459-466.
- Koschmieder, S., G. Bug, et al. (2001). "Murine M2-10B4 and SL/SL cell lines differentially affect the balance between CD34+ cell expansion and maturation." Int J Hematol **73**(1): 71-77.
- Krueger, C., C. Berens, et al. (2003). "Single-chain Tet transregulators." Nucleic Acids Res **31**(12): 3050-3056.
- Landau, N. R., M. Warton, et al. (1988). "The envelope glycoprotein of the human immunodeficiency virus binds to the immunoglobulin-like domain of CD4." Nature **334**(6178): 159-162.
- Lange, B., M. Valtieri, et al. (1987). "Growth factor requirements of childhood acute leukemia: establishment of GM-CSF-dependent cell lines." Blood **70**(1): 192-199.
- Lapidot, T., C. Sirard, et al. (1994). "A cell initiating human acute myeloid leukaemia after transplantation into SCID mice." Nature **367**(6464): 645-648.

- Larsson, J. and S. Karlsson (2005). "The role of Smad signaling in hematopoiesis." Oncogene **24**(37): 5676-5692.
- Lazic, J., N. Tosic, et al. (2010). "Clinical features of the most common fusion genes in childhood acute lymphoblastic leukemia." Med Oncol **27**(2): 449-453.
- le Viseur, C., M. Hotfilder, et al. (2008). "In childhood acute lymphoblastic leukemia, blasts at different stages of immunophenotypic maturation have stem cell properties." Cancer Cell **14**(1): 47-58.
- Lee, G., L. A. Santat, et al. (2009). "RNAi methodologies for the functional study of signaling molecules." PLoS One **4**(2): e4559.
- Lee, J. H., C. Jung, et al. (2010). "Pathways of proliferation and antiapoptosis driven in breast cancer stem cells by stem cell protein piwil2." Cancer Res **70**(11): 4569-4579.
- Lee, Y. C., T. J. Chiou, et al. (2008). "Macrophage inflammatory protein-3alpha influences growth of K562 leukemia cells in co-culture with anticancer drug-pretreated HS-5 stromal cells." Toxicology **249**(2-3): 116-122.
- Lemoine, F. M., R. K. Humphries, et al. (1988). "Partial characterization of a novel stromal cell-derived pre-B-cell growth factor active on normal and immortalized pre-B cells." Exp Hematol **16**(8): 718-726.
- Lemoine, F. M., G. Krystal, et al. (1988). "Autocrine production of pre-B-cell stimulating activity by a variety of transformed murine pre-B-cell lines." Cancer Res **48**(22): 6438-6443.
- Li, P. and L. I. Zon (2010). "Resolving the controversy about N-cadherin and hematopoietic stem cells." Cell Stem Cell **6**(3): 199-202.

- Li, Q., J. L. Frestedt, et al. (1998). "AF4 encodes a ubiquitous protein that in both native and MLL-AF4 fusion types localizes to subnuclear compartments." Blood **92**(10): 3841-3847.
- Lieber, M. R., J. E. Hesse, et al. (1988). "The defect in murine severe combined immune deficiency: joining of signal sequences but not coding segments in V(D)J recombination." Cell **55**(1): 7-16.
- Liedtke, M. and M. L. Cleary (2009). "Therapeutic targeting of MLL." Blood **113**(24): 6061-6068.
- Lin, X., X. Ruan, et al. (2005). "siRNA-mediated off-target gene silencing triggered by a 7 nt complementation." Nucleic Acids Res **33**(14): 4527-4535.
- Liu, B., B. Han, et al. (2009). "[Study on telomerase gene mutation in northern Chinese patients with acquired bone marrow failure syndromes.]" Zhonghua Xue Ye Xue Za Zhi **30**(12): 808-811.
- Liu, J., M. A. Carmell, et al. (2004). "Argonaute2 is the catalytic engine of mammalian RNAi." Science **305**(5689): 1437-1441.
- Lowe, E. J., C. H. Pui, et al. (2005). "Early complications in children with acute lymphoblastic leukemia presenting with hyperleukocytosis." Pediatr Blood Cancer **45**(1): 10-15.
- Lozzio, B. B., E. A. Machado, et al. (1976). "Hereditary asplenic-athymic mice: transplantation of human myelogenous leukemic cells." J Exp Med **143**(1): 225-231.
- Luster, A. D., R. Alon, et al. (2005). "Immune cell migration in inflammation: present and future therapeutic targets." Nat Immunol **6**(12): 1182-1190.

- Lwin, T., L. A. Crespo, et al. (2009). "Lymphoma cell adhesion-induced expression of B cell-activating factor of the TNF family in bone marrow stromal cells protects non-Hodgkin's B lymphoma cells from apoptosis." *Leukemia* **23**(1): 170-177.
- Ma C, S. L. (1996). "LAF-4 encodes a lymphoid nuclear protein with transactivation potential that is homologous to AF-4, the gene fused to MLL in t(4;11) leukemias." *Blood* **87**: 734-745.
- Malynn, B. A., T. K. Blackwell, et al. (1988). "The scid defect affects the final step of the immunoglobulin VDJ recombinase mechanism." *Cell* **54**(4): 453-460.
- Mancini, M., D. Scappaticci, et al. (2005). "A comprehensive genetic classification of adult acute lymphoblastic leukemia (ALL): analysis of the GIMEMA 0496 protocol." *Blood* **105**(9): 3434-3441.
- Mancini, S. J., N. Mantei, et al. (2005). "Jagged1-dependent Notch signaling is dispensable for hematopoietic stem cell self-renewal and differentiation." *Blood* **105**(6): 2340-2342.
- Marschalek, R. (2010). "Mixed lineage leukemia: roles in human malignancies and potential therapy." *Febs J* **277**(8): 1822-1831.
- Martin, A. P., L. V. de Moraes, et al. (2005). "Administration of a peptide inhibitor of alpha4-integrin inhibits the development of experimental autoimmune uveitis." *Invest Ophthalmol Vis Sci* **46**(6): 2056-2063.
- Martinez Soria, N., R. Tussiwand, et al. (2009). "Transient depletion of RUNX1/RUNX1T1 by RNA interference delays tumour formation in vivo." *Leukemia* **23**(1): 188-190.
- Matozaki, S., T. Nakagawa, et al. (1995). "Establishment of a myeloid leukaemic cell line (SKNO-1) from a patient with t(8;21) who acquired monosomy 17 during disease progression." *Br J Haematol* **89**(4): 805-811.



- Matranga, C., Y. Tomari, et al. (2005). "Passenger-strand cleavage facilitates assembly of siRNA into Ago2-containing RNAi enzyme complexes." Cell **123**(4): 607-620.
- Matz, M. V., A. F. Fradkov, et al. (1999). "Fluorescent proteins from nonbioluminescent Anthozoa species." Nat Biotechnol **17**(10): 969-973.
- Mazurier, F., M. Doedens, et al. (2003). "Rapid myeloerythroid repopulation after intrafemoral transplantation of NOD-SCID mice reveals a new class of human stem cells." Nat Med **9**(7): 959-963.
- McCune, J. M., R. Namikawa, et al. (1988). "The SCID-hu mouse: murine model for the analysis of human hematolymphoid differentiation and function." Science **241**(4873): 1632-1639.
- McMahon, B. and H. C. Kwaan (2008). "The plasminogen activator system and cancer." Pathophysiol Haemost Thromb **36**(3-4): 184-194.
- Meister, G. and T. Tuschl (2004). "Mechanisms of gene silencing by double-stranded RNA." Nature **431**(7006): 343-349.
- Melikyan, G. B., R. M. Markosyan, et al. (2000). "Evidence that the transition of HIV-1 gp41 into a six-helix bundle, not the bundle configuration, induces membrane fusion." J Cell Biol **151**(2): 413-423.
- Menendez, P., P. Catalina, et al. (2009). "Bone marrow mesenchymal stem cells from infants with MLL-AF4+ acute leukemia harbor and express the MLL-AF4 fusion gene." J Exp Med **206**(13): 3131-3141.
- Metzler, M., A. Forster, et al. (2006). "A conditional model of MLL-AF4 B-cell tumorigenesis using inverter technology." Oncogene **25**(22): 3093-3103.

- 
- Mezzanotte, L., R. Fazzina, et al. (2009). "In Vivo Bioluminescence Imaging of Murine Xenograft Cancer Models with a Red-shifted Thermostable Luciferase." Mol Imaging Biol.
- Miller, M. D., C. M. Farnet, et al. (1997). "Human immunodeficiency virus type 1 preintegration complexes: studies of organization and composition." J Virol **71**(7): 5382-5390.
- Milne, T. A., S. D. Briggs, et al. (2002). "MLL targets SET domain methyltransferase activity to Hox gene promoters." Mol Cell **10**(5): 1107-1117.
- Miura, Y., Z. Gao, et al. (2006). "Mesenchymal stem cell-organized bone marrow elements: an alternative hematopoietic progenitor resource." Stem Cells **24**(11): 2428-2436.
- Mochizuki, H., J. P. Schwartz, et al. (1998). "High-titer human immunodeficiency virus type 1-based vector systems for gene delivery into nondividing cells." J Virol **72**(11): 8873-8883.
- Mokrejs, M., V. Vopalensky, et al. (2006). "IRESite: the database of experimentally verified IRES structures ([www.iresite.org](http://www.iresite.org))." Nucleic Acids Res **34**(Database issue): D125-130.
- Money Penny, C. G., J. Shao, et al. (2006). "MLL rearrangements are induced by low doses of etoposide in human fetal hematopoietic stem cells." Carcinogenesis **27**(4): 874-881.
- Montini, E., D. Cesana, et al. (2009). "The genotoxic potential of retroviral vectors is strongly modulated by vector design and integration site selection in a mouse model of HSC gene therapy." J Clin Invest **119**(4): 964-975.

- Mori, H., S. M. Colman, et al. (2002). "Chromosome translocations and covert leukemic clones are generated during normal fetal development." Proc Natl Acad Sci U S A **99**(12): 8242-8247.
- Morimoto, M. and R. Kopan (2009). "rtTA toxicity limits the usefulness of the SP-C-rtTA transgenic mouse." Dev Biol **325**(1): 171-178.
- Mullighan, C. G., S. Goorha, et al. (2007). "Genome-wide analysis of genetic alterations in acute lymphoblastic leukaemia." Nature **446**(7137): 758-764.
- N.J. Zeleznik-Lee, A. M. H. a. J. D. R. (1994). "Ilq23 translocations split the AT hook cruciform DNA binding region and the transcriptional repression domain from the activation domain of the MLL gene
- " Proceedings of the National Academy of Science of the U.S.A. **91**: 10610–10614.
- Nadella, R., J. B. Blumer, et al. (2010). "Activator of G Protein Signaling 3 Promotes Epithelial Cell Proliferation in PKD." J Am Soc Nephrol.
- Nakamura, Y., F. Arai, et al. (2010). "Isolation and characterization of endosteal niche cell populations that regulate hematopoietic stem cells." Blood.
- Naldini, L., U. Blomer, et al. (1996). "In vivo gene delivery and stable transduction of nondividing cells by a lentiviral vector." Science **272**(5259): 263-267.
- Nieman, M. T., R. S. Prudoff, et al. (1999). "N-cadherin promotes motility in human breast cancer cells regardless of their E-cadherin expression." J Cell Biol **147**(3): 631-644.
- Nilson I, R. M., Ennas MG, Greim R, Knörr C, Siegler G, Greil J, Fey GH, Marschalek R (1997). "Exon/intron structure of the human AF-4 gene, a member of the AF-4/LAF-4/FMR-2 gene family coding for a nuclear protein with structural alterations in acute leukaemia." Br J Haematol **98**: 157-169.

- Notta, F., S. Doulatov, et al. (2010). "Engraftment of human hematopoietic stem cells is more efficient in female NOD/SCID/IL-2Rgnull recipients." Blood.
- Oelgeschlager, M., J. Larrain, et al. (2000). "The evolutionarily conserved BMP-binding protein Twisted gastrulation promotes BMP signalling." Nature **405**(6788): 757-763.
- Oettinger, M. A., D. G. Schatz, et al. (1990). "RAG-1 and RAG-2, adjacent genes that synergistically activate V(D)J recombination." Science **248**(4962): 1517-1523.
- Ohlmann, T., M. Lopez-Lastra, et al. (2000). "An internal ribosome entry segment promotes translation of the simian immunodeficiency virus genomic RNA." J Biol Chem **275**(16): 11899-11906.
- Ornitz, D. M. and N. Itoh (2001). "Fibroblast growth factors." Genome Biol **2**(3): REVIEWS3005.
- Page, K. A., N. R. Landau, et al. (1990). "Construction and use of a human immunodeficiency virus vector for analysis of virus infectivity." J Virol **64**(11): 5270-5276.
- Palermo, C. M., C. A. Bennett, et al. (2008). "The AF4-mimetic peptide, PFWT, induces necrotic cell death in MV4-11 leukemia cells." Leuk Res **32**(4): 633-642.
- Parker, R. and U. Sheth (2007). "P bodies and the control of mRNA translation and degradation." Mol Cell **25**(5): 635-646.
- Patnaik, M. M., N. Gangat, et al. (2010). "Chromosome 8p11.2 translocations: prevalence, FISH analysis for FGFR1 and MYST3, and clinicopathologic correlates in a consecutive cohort of 13 cases from a single institution." Am J Hematol **85**(4): 238-242.
- Pedersen, F. and M. Duch (2001). "Retroviral Replication"
- " ENCYCLOPEDIA of LIFE SCIENCES: 1-7.

- 
- Pillai, R. S., S. N. Bhattacharyya, et al. (2007). "Repression of protein synthesis by miRNAs: how many mechanisms?" Trends Cell Biol **17**(3): 118-126.
- Pizzato, M., E. Popova, et al. (2008). "Nef can enhance the infectivity of receptor-pseudotyped human immunodeficiency virus type 1 particles." J Virol **82**(21): 10811-10819.
- Pluta, K. and M. M. Kacprzak (2009). "Use of HIV as a gene transfer vector." Acta Biochim Pol **56**(4): 531-595.
- Ponchio, L., L. Duma, et al. (2000). "Mitomycin C as an alternative to irradiation to inhibit the feeder layer growth in long-term culture assays." Cytotherapy **2**(4): 281-286.
- Popovic, R. and N. J. Zeleznik-Le (2005). "MLL: how complex does it get?" J Cell Biochem **95**(2): 234-242.
- Povirk, L. F. (2006). "Biochemical mechanisms of chromosomal translocations resulting from DNA double-strand breaks." DNA Repair (Amst) **5**(9-10): 1199-1212.
- Prasad, R., T. Yano, et al. (1995). "Domains with transcriptional regulatory activity within the ALL1 and AF4 proteins involved in acute leukemia." Proc Natl Acad Sci U S A **92**(26): 12160-12164.
- Prasher, D. C., V. K. Eckenrode, et al. (1992). "Primary structure of the Aequorea victoria green-fluorescent protein." Gene **111**(2): 229-233.
- Prosper, F., K. Vanoverbeke, et al. (1997). "Primitive long-term culture initiating cells (LTC-ICs) in granulocyte colony-stimulating factor mobilized peripheral blood progenitor cells have similar potential for ex vivo expansion as primitive LTC-ICs in steady state bone marrow." Blood **89**(11): 3991-3997.

- Puccetti, E., D. Obradovic, et al. (2002). "AML-associated translocation products block vitamin D(3)-induced differentiation by sequestering the vitamin D(3) receptor." Cancer Res **62**(23): 7050-7058.
- Pui, C. H. and D. Campana (2007). "Age-related differences in leukemia biology and prognosis: the paradigm of MLL-AF4-positive acute lymphoblastic leukemia." Leukemia **21**(4): 593-594.
- Pui, C. H., D. Campana, et al. (2001). "Childhood acute lymphoblastic leukaemia--current status and future perspectives." Lancet Oncol **2**(10): 597-607.
- Pui, C. H. and W. E. Evans (2006). "Treatment of acute lymphoblastic leukemia." N Engl J Med **354**(2): 166-178.
- Pui, C. H. and M. V. Relling (2000). "Topoisomerase II inhibitor-related acute myeloid leukaemia." Br J Haematol **109**(1): 13-23.
- Pui, C. H., M. V. Relling, et al. (2004). "Acute lymphoblastic leukemia." N Engl J Med **350**(15): 1535-1548.
- Pui, C. H., L. L. Robison, et al. (2008). "Acute lymphoblastic leukaemia." Lancet **371**(9617): 1030-1043.
- Reiser, J. (2000). "Production and concentration of pseudotyped HIV-1-based gene transfer vectors." Gene Ther **7**(11): 910-913.
- Reiss, K., T. Maretzky, et al. (2005). "ADAM10 cleavage of N-cadherin and regulation of cell-cell adhesion and beta-catenin nuclear signalling." Embo J **24**(4): 742-752.
- Reya, T., A. W. Duncan, et al. (2003). "A role for Wnt signalling in self-renewal of haematopoietic stem cells." Nature **423**(6938): 409-414.
- Reynolds, A., E. M. Anderson, et al. (2006). "Induction of the interferon response by siRNA is cell type- and duplex length-dependent." RNA **12**(6): 988-993.

- Rhodes, T., H. Wargo, et al. (2003). "High rates of human immunodeficiency virus type 1 recombination: near-random segregation of markers one kilobase apart in one round of viral replication." J Virol **77**(20): 11193-11200.
- Rio, D. C., S. G. Clark, et al. (1985). "A mammalian host-vector system that regulates expression and amplification of transfected genes by temperature induction." Science **227**(4682): 23-28.
- Roecklein, B. A. and B. Torok-Storb (1995). "Functionally distinct human marrow stromal cell lines immortalized by transduction with the human papilloma virus E6/E7 genes." Blood **85**(4): 997-1005.
- Ross, J. and L. Li (2006). "Recent advances in understanding extrinsic control of hematopoietic stem cell fate." Curr Opin Hematol **13**(4): 237-242.
- Ross, J. A. (2000). "Dietary flavonoids and the MLL gene: A pathway to infant leukemia?" Proc Natl Acad Sci U S A **97**(9): 4411-4413.
- Roumiantsev, S., D. S. Krause, et al. (2004). "Distinct stem cell myeloproliferative/T lymphoma syndromes induced by ZNF198-FGFR1 and BCR-FGFR1 fusion genes from 8p11 translocations." Cancer Cell **5**(3): 287-298.
- Saad, J. S., J. Miller, et al. (2006). "Structural basis for targeting HIV-1 Gag proteins to the plasma membrane for virus assembly." Proc Natl Acad Sci U S A **103**(30): 11364-11369.
- Samuels, A. L., V. K. Peeva, et al. (2010). "Validation of a mouse xenograft model system for gene expression analysis of human acute lymphoblastic leukaemia." BMC Genomics **11**(1): 256.
- Schatz, D. G., M. A. Oettinger, et al. (1989). "The V(D)J recombination activating gene, RAG-1." Cell **59**(6): 1035-1048.

- Schmid, M. and T. H. Jensen (2008). "Quality control of mRNP in the nucleus." Chromosoma **117**(5): 419-429.
- Schofield, R. (1978). "The relationship between the spleen colony-forming cell and the haemopoietic stem cell." Blood Cells **4**(1-2): 7-25.
- Schwieger, M., A. Schuler, et al. (2009). "Homing and invasiveness of MLL/ENL leukemic cells is regulated by MEF2C." Blood **114**(12): 2476-2488.
- Seiffert, M., S. Stilgenbauer, et al. (2007). "Efficient nucleofection of primary human B cells and B-CLL cells induces apoptosis, which depends on the microenvironment and on the structure of transfected nucleic acids." Leukemia **21**(9): 1977-1983.
- Sen, G. L. and H. M. Blau (2005). "Argonaute 2/RISC resides in sites of mammalian mRNA decay known as cytoplasmic bodies." Nat Cell Biol **7**(6): 633-636.
- Sheng, Y., C. C. Lin, et al. (2010). "Generation and characterization of a Tet-On (rtTA-M2) transgenic rat." BMC Dev Biol **10**: 17.
- Shih, L. Y., D. C. Liang, et al. (2006). "Characterization of fusion partner genes in 114 patients with de novo acute myeloid leukemia and MLL rearrangement." Leukemia **20**(2): 218-223.
- Shinkai, Y., G. Rathbun, et al. (1992). "RAG-2-deficient mice lack mature lymphocytes owing to inability to initiate V(D)J rearrangement." Cell **68**(5): 855-867.
- Shiozawa, Y., A. M. Havens, et al. (2008). "The bone marrow niche: habitat to hematopoietic and mesenchymal stem cells, and unwitting host to molecular parasites." Leukemia **22**(5): 941-950.
- Shtutman, M., A. Maliyekkel, et al. (2010). "Function-based gene identification using enzymatically generated normalized shRNA library and massive parallel sequencing." Proc Natl Acad Sci U S A **107**(16): 7377-7382.



- Shultz, L. D., S. J. Banuelos, et al. (2003). "Regulation of human short-term repopulating cell (STRC) engraftment in NOD/SCID mice by host CD122+ cells." Exp Hematol **31**(6): 551-558.
- Shultz, L. D., B. L. Lyons, et al. (2005). "Human lymphoid and myeloid cell development in NOD/LtSz-scid IL2R gamma null mice engrafted with mobilized human hemopoietic stem cells." J Immunol **174**(10): 6477-6489.
- Shultz, L. D., P. A. Schweitzer, et al. (1995). "Multiple defects in innate and adaptive immunologic function in NOD/LtSz-scid mice." J Immunol **154**(1): 180-191.
- Silverman, L. B., R. D. Gelber, et al. (2001). "Improved outcome for children with acute lymphoblastic leukemia: results of Dana-Farber Consortium Protocol 91-01." Blood **97**(5): 1211-1218.
- Slany, R. K., C. Lavau, et al. (1998). "The oncogenic capacity of HRX-ENL requires the transcriptional transactivation activity of ENL and the DNA binding motifs of HRX." Mol Cell Biol **18**(1): 122-129.
- Smardon, A., J. M. Spoerke, et al. (2000). "EGO-1 is related to RNA-directed RNA polymerase and functions in germ-line development and RNA interference in *C. elegans*." Curr Biol **10**(4): 169-178.
- Staal, F. J. and T. C. Luis (2010). "Wnt signaling in hematopoiesis: crucial factors for self-renewal, proliferation, and cell fate decisions." J Cell Biochem **109**(5): 844-849.
- Stam, R. W., M. L. Den Boer, et al. (2010). "Association of high-level MCL-1 expression with in vitro and in vivo prednisone resistance in MLL-rearranged infant acute lymphoblastic leukemia." Blood **115**(5): 1018-1025.
- Stong, R. C. and J. H. Kersey (1985). "In vitro culture of leukemic cells in t(4;11) acute leukemia." Blood **66**(2): 439-443.

- 
- Stumpel, D. J., P. Schneider, et al. (2009). "Specific promoter methylation identifies different subgroups of MLL-rearranged infant acute lymphoblastic leukemia, influences clinical outcome, and provides therapeutic options." Blood **114**(27): 5490-5498.
- Suyama, K., I. Shapiro, et al. (2002). "A signaling pathway leading to metastasis is controlled by N-cadherin and the FGF receptor." Cancer Cell **2**(4): 301-314.
- Svoboda, P., P. Stein, et al. (2000). "Selective reduction of dormant maternal mRNAs in mouse oocytes by RNA interference." Development **127**(19): 4147-4156.
- T. Pe'ery and M. B. Mathews (2000). Viral translational strategies and host defense mechanisms. Translational Control of Gene Expression. New York, C.S.H.L Press (Ed.): 371-424.
- Tabara, H., M. Sarkissian, et al. (1999). "The rde-1 gene, RNA interference, and transposon silencing in *C. elegans*." Cell **99**(2): 123-132.
- Taichman, R. S. (2005). "Blood and bone: two tissues whose fates are intertwined to create the hematopoietic stem-cell niche." Blood **105**(7): 2631-2639.
- Takeichi, M. (1991). "Cadherin cell adhesion receptors as a morphogenetic regulator." Science **251**(5000): 1451-1455.
- Taussig, D. C., F. Miraki-Moud, et al. (2008). "Anti-CD38 antibody-mediated clearance of human repopulating cells masks the heterogeneity of leukemia-initiating cells." Blood **112**(3): 568-575.
- Theisen, C. S., J. K. Wahl, 3rd, et al. (2007). "NHERF links the N-cadherin/catenin complex to the platelet-derived growth factor receptor to modulate the actin cytoskeleton and regulate cell motility." Mol Biol Cell **18**(4): 1220-1232.

- Thomas, M., A. Gessner, et al. (2005). "Targeting MLL-AF4 with short interfering RNAs inhibits clonogenicity and engraftment of t(4;11)-positive human leukemic cells." Blood **106**(10): 3559-3566.
- Tomlinson, I. P., R. Roylance, et al. (2001). "Two hits revisited again." J Med Genet **38**(2): 81-85.
- Tracey, L., C. J. Streck, et al. (2010). "NF-kappaB activation mediates resistance to IFN beta in MLL-rearranged acute lymphoblastic leukemia." Leukemia **24**(4): 806-812.
- Traggiai, E., L. Chicha, et al. (2004). "Development of a human adaptive immune system in cord blood cell-transplanted mice." Science **304**(5667): 104-107.
- van der Loo, J. C., H. Hanenberg, et al. (1998). "Nonobese diabetic/severe combined immunodeficiency (NOD/SCID) mouse as a model system to study the engraftment and mobilization of human peripheral blood stem cells." Blood **92**(7): 2556-2570.
- Vormoor, J., T. Lapidot, et al. (1994). "SCID mice as an in vivo model of human cord blood hematopoiesis." Blood Cells **20**(2-3): 316-320; discussion 320-312.
- Wang, J. C. and J. E. Dick (2005). "Cancer stem cells: lessons from leukemia." Trends Cell Biol **15**(9): 494-501.
- Wang, Y., A. V. Krivtsov, et al. (2010). "The Wnt/beta-catenin pathway is required for the development of leukemia stem cells in AML." Science **327**(5973): 1650-1653.
- Weinreich, M. A., I. Lintmaer, et al. (2006). "Growth factor receptors as regulators of hematopoiesis." Blood **108**(12): 3713-3721.
- Whetton, A. D. and G. J. Graham (1999). "Homing and mobilization in the stem cell niche." Trends Cell Biol **9**(6): 233-238.

- Wianny, F. and M. Zernicka-Goetz (2000). "Specific interference with gene function by double-stranded RNA in early mouse development." Nat Cell Biol **2**(2): 70-75.
- Wiemels, J. L., G. Cazzaniga, et al. (1999). "Prenatal origin of acute lymphoblastic leukaemia in children." Lancet **354**(9189): 1499-1503.
- Williams, E. J., G. Williams, et al. (2001). "Identification of an N-cadherin motif that can interact with the fibroblast growth factor receptor and is required for axonal growth." J Biol Chem **276**(47): 43879-43886.
- Williams, J. M., S. H. Oh, et al. (2010). "The role of the Wnt family of secreted proteins in rat oval "stem" cell-based liver regeneration: Wnt1 drives differentiation." Am J Pathol **176**(6): 2732-2742.
- Wilson, A., M. J. Murphy, et al. (2004). "c-Myc controls the balance between hematopoietic stem cell self-renewal and differentiation." Genes Dev **18**(22): 2747-2763.
- Wu, X., Y. Li, et al. (2003). "Transcription start regions in the human genome are favored targets for MLV integration." Science **300**(5626): 1749-1751.
- Xia, Z. B., M. Anderson, et al. (2003). "MLL repression domain interacts with histone deacetylases, the polycomb group proteins HPC2 and BMI-1, and the corepressor C-terminal-binding protein." Proc Natl Acad Sci U S A **100**(14): 8342-8347.
- Xie, Y., T. Yin, et al. (2009). "Detection of functional haematopoietic stem cell niche using real-time imaging." Nature **457**(7225): 97-101.
- Yan, Y., E. A. Wieman, et al. (2009). "Autonomous growth potential of leukemia blast cells is associated with poor prognosis in human acute leukemias." J Hematol Oncol **2**: 51.

- Yi, R., Y. Qin, et al. (2003). "Exportin-5 mediates the nuclear export of pre-microRNAs and short hairpin RNAs." Genes Dev **17**(24): 3011-3016.
- Yu, W. J., W. H. Yang, et al. (2008). "[Application of NOD/SCID mice in research of experimental hematology - review]." Zhongguo Shi Yan Xue Ye Xue Za Zhi **16**(4): 964-968.
- Zamore, P. D., T. Tuschl, et al. (2000). "RNAi: double-stranded RNA directs the ATP-dependent cleavage of mRNA at 21 to 23 nucleotide intervals." Cell **101**(1): 25-33.
- Zhang, J., C. Niu, et al. (2003). "Identification of the haematopoietic stem cell niche and control of the niche size." Nature **425**(6960): 836-841.
- Zhao, Y., J. F. Ransom, et al. (2007). "Dysregulation of cardiogenesis, cardiac conduction, and cell cycle in mice lacking miRNA-1-2." Cell **129**(2): 303-317.
- Zhi, L., M. Wang, et al. (2010). "Enrichment of N-Cadherin and Tie2-bearing CD34(+)/CD38(-)/CD123(+) leukemic stem cells by chemotherapy-resistance." Cancer Lett.
- Zhou, J., Z. Yu, et al. (2009). "Lentivirus-based DsRed-2-transfected pancreatic cancer cells for deep in vivo imaging of metastatic disease." J Surg Res **157**(1): 63-70.
- Zhou, X., J. Symons, et al. (2007). "Improved single-chain transactivators of the Tet-On gene expression system." BMC Biotechnol **7**: 6.
- Zhou, X., M. Vink, et al. (2006). "Modification of the Tet-On regulatory system prevents the conditional-live HIV-1 variant from losing doxycycline-control." Retrovirology **3**: 82.
- Zufferey, R., D. Nagy, et al. (1997). "Multiply attenuated lentiviral vector achieves efficient gene delivery in vivo." Nat Biotechnol **15**(9): 871-875.

Zuo, Y. X., L. P. Zhang, et al. (2010). "[Clinical characteristics of children with B cell type acute lymphoblastic leukemia carrying different fusion gene]." Zhongguo Dang Dai Er Ke Za Zhi **12**(3): 172-176.

# Appendix

## cDNA array data

97 most significantly altered genes from the cDNA array fold change >2

genes >2 are genes upregulated more than 2 fold

genes < 0.5 are genes downregulated more than 2 fold

Gene	Fold change	Gene	Fold change	Gene	Fold change
ACSL3	0.49	GABPB2	0.47	SEMA3B	0.48
ALDOC	0.33	GLG1	0.36	SERPINE2	0.20
ANTXR2	0.46	GNA15	0.49	SERPINE2	0.21
APP	0.37	INSIG1	0.39	SLC12A7	0.46
ATP2B3	0.45	IRX3	0.39	SLC20A1	0.27
B3GNT1	0.32	ISLR	0.44	SLC2A3	0.49
BMI1	0.29	KIAA0828	0.43	SLC2A5	0.36
BMP4	0.50	LAPTM5	0.34	STS-1	0.38
BNIP3	0.33	LRIG1	0.51	TERF2	0.49
BNIP3L	0.48	MEF2C	0.23	TMP21	0.37
BUB3	0.48	MT1F	0.48	TRA2A	0.49
C17orf27	0.50	MT1X	0.50	UBE1DC1	0.47
C6orf33	0.41	MYO6	0.41	UBL3	0.45
C7orf36	0.37	MYST2	0.41	VAV3	0.39
C9orf91	0.50	NAP1L4	0.36	VPS39	0.50
CAMK2D	0.41	NDUFB6	0.51	AMICA1	1.97
CAT	0.47	NR3C1	0.41	ATAD3B	3.59
CD38	0.31	NR3C1	0.50	CACNA1B	2.80
CD69	0.27	P2RY5	0.47	DAAM1	2.09
CDH2	0.43	PDE7A	0.36	FBL	1.97
CHI3L2	0.47	PEL1	0.42	FLJ13639	2.66
DHRS3	0.22	PLAT	0.46	LMCD1	2.07
DTL	0.36	PLXNC1	0.31	LZTS2	2.29
DUSP6	0.20	PSAP	0.21	MAGED1	2.54
ECE1	0.40	PSMB2	0.43	NME1	1.96
EGLN1	0.46	PTPRC	0.34	PRCP	2.47
EMR3	0.35	PTPRG	0.42	RAB9P40	2.04
ENO2	0.42	RAB3IL1	0.32	REEP3	2.65
ETV5	0.29	RAB6A	0.31	RPS6KA3	2.33
EZH2	0.50	RBP5	0.48	SYT4	2.37
FBXL11	0.51	RGS16	0.50	VEZATIN	2.14
FGFR1	0.43	SCD	0.43		
FGFR1	0.49	SDCBP	0.49		

**oligo array data**

genes analysed by MAS with a fold change &gt;4


Dowregulated Genes					Upregulated Genes		
CA3	KCNJ4	KRT5	NAT8B	ABCC9	UBR4	VCPIP1	GLRA3
UGT2A3	LECT2	LAMA2	NEUROD1	ACOX1	PIK3R4	LOC10028	PDLIM4
AKAP9	LOC29034	MAPK4	NR2F2	ACVR1B	TSPAN12	DENND2A	CAMK2A
DHRS7	PBX1	MYT1	NRXN2	AMOTL2	RASSF4	IGL@	SLC4A10
IBTK	PGR	NAP1L3	RNF6	ARHGEF16	C9	ADH1B	KCNJ4
MSX2	POFUT1	PSG1	ROR1	ATP1B4	MCHR1	RNF39	MCF2
MSTN	PPYR1	CACNA1D	SMR3B	C5AR1	DDX28	COL1A1	CD163
PYY	TMEM47	CCDC102B	TBX3	CLDN4	HRK	SLC22A6	LIN28
CD300A	AVPR1A	CLCA2	CDC42BPA	DSTYK	PCDH9	CREB5	MAGEA11
KCNH6	CYP1B1	CXCL2	DLGAP1	FLJ13197	TECTA	CLDN11	PDLIM3
ATP2B3	EFNB1	DOK4	DSCR6	GNAL	VPS13D	ADAM28	NFX1
GRK5	FAM20B	IL5	DST	KCNA2	KYNU	GPR107	LIFR
HCG4	FXD2	KIDINS220	EPHB2	KCND3	REPS1	GRK4	FAM198B
KCNK2	GRM8	KLHL23	ERN2	KCNJ8	AZU1	IFNW1	STMN2
NUDT7	IL18R1	LOC90925	FCAR	LOC10013401	CLEC5A	LAMC2	ZNF174
TEF	IL1RAP	NUP54	GREB1	NEDD4L	EHBP1	SLC13A1	SIX3
B3GALT2	NRL	PCDHGB6	HUWE1	RAB11FIP4	AGBL3	SNRK	ZNF329
CLCA3	SULF1	PPEF2	KBTBD11	RBMY2FP	LPPR3	CYP4F11	ST3GAL6
CYP4F8	AKAP13	TIMM17A	MICALL2	SCT	NMU	LIMCH1	SLC9A3R2
IL9	ANKRD1	ZNF236	PGCP	SH3TC2	OR1D4	APC	LOC64596
RAI2	ARHGEF12	ADRB3	PTCH1	TMX4	DSC1	GRM1	SOX2
SUSD5	CH25H	BTF3L1	SEMG2	USP22	MYH6	SSX2	NDUFB7
TIGD6	HOXD13	DUX3	TBX6	ZNF814	ERC2	SULT1C2	TNC
FCN3	IL24	GPR172B	USP46		TM4SF1	KITLG	MEP1B
GRM5	IL26	INVS	ABCC6		DCT	TTY2	PID1
IFNA8	LOC100288413	MUC5AC	ALAS2		SLC16A6	SLC16A5	TRIL
INVS	LOC392555	MYOF	CALCR		POMC	HGF	PSEN2
NPIPL3	NACAD	NMNAT2	CCND2		SLC28A1	ARMC9	ZNF141
PRSS50	SF4	PDZD2	CD28	up	MAP9	COL10A1	STEAP4
RALGPS2	SLC25A31	PTGIS	CLC	FAM131B	IGHM	LHX2	KIF24
TRPM1	TP53AIP1	PTPN12	CR2	PTGER2	APOE	NR5A2	TF
CD47	ABI3BP	RHBDF1	DACH1	SSTR1	CCL21	SP2	C5ORF4
CEP290	BAZ1B	SERPINB2	GARNL3	DGKB	MYL10	CNOT4	TIMM8A
EPB41L4A	GCM2	SHOX2	GPC5	MYH7B	WNT4	GRIK2	OLFM4
FBXO40	GPR161	TEK	HSPG2	LARGE	C10ORF92	PRR16	ALDH5A1
GH2	MT1M	AIM1L	IFIH1	CDR1	APOA4	POU5F1	C7ORF44
IRGC	PRDM2	CHI3L1	MAB21L2	PDLIM5	C22ORF31	PTPRF	TDGF1
MGAT4C	SPTLC3	CHRN3	POSTN	DAZ1	AMELY	KCNJ13	ASCL1
NID1	THBS1	DOCK9	PTHLH	DTNA	DHRS12	SIGLEC8	USP29
NPAS2	CDC42BPA	DYSF	RAB40AL	AFAP1	SCN7A	CCL27	LRR8B
PLCE1	F13B	ELAVL2	RUNDC3A	EHF	ASPH	THSD7A	MAGIX
SLC26A3	GREM2	EXOSC6	SERPINA3	TPM1	FZD10	LOC94431	CORIN
CDC42BPA	GSTA1	FUT9	SFRP5	APOF	HLF	PHF15	RALGPS1
CPE	HGF	IKZF1	SLC22A2	GPR37	ABCG5	ZNF80	CNTNAP2
DDC	HLA-DOB	KIAA1310	SPRR2B	STON1	TEF	PTPRT	FXD6
DHX34	IGHG1	LZTS1	VCL	SLC26A3	SASH1	TEX12	DRD4
DOPEY1	KERA	MIA	ZNF384	SIM1	TLX2	CRCT1	IRF4



## Conferences

Postgraduate conference Newcastle, September 2007


Poster:



# Identification and characterisation of possible MLL-AF4 target genes

**Lars Buechler**

Northern Institute for Cancer Research, Paul O'Gorman Building,  
Medical School, Newcastle University, Newcastle upon Tyne, NE2 4HH.



---

### Introduction

Blood cancer or leukaemia is the most common cancer in children. Depending on their haematopoietic progenitor cell, the blood cells can be subdivided into two major groups: lymphoid cells, which include B-cells, T-cells and natural killer cells, and myeloid cells which include granulocytes, monocytes, erythrocytes and megakaryocytes. One form of this cancer is Acute Lymphoblastic Leukaemia (ALL), in which the haematopoiesis of lymphoid cells is disrupted, resulting in large numbers of immature lymphoid progenitor cells that block and displacement of other blood cells. This rapidly progressing disease commonly affects the immune system and other functions of the blood. The most common variant ALL type is B-ALL, in which an aberrant translocation event occurs between chromosomes 4 and 11 (Fig. 1a) that fuses the MLL gene with the AF4 gene, giving rise to the chimeric gene MLL-AF4 (Fig. 1a). This fusion gene leads to a biologically distinct ALL. We aim to further the understanding the biology of this relatively therapy-resistant childhood leukaemia in order to help find a better treatment and cure.

### Results

Genes significantly altered by MLL-AF4 down-regulation were identified via oligo and cDNA arrays. Their functions and involved pathways as well as their interactions were investigated. Figure 3 summarises the cancer relevant functions of the 50 genes showing the greatest change in expression following MLL-AF4 knockdown. These are involved in malignancies (35%), proliferation (22%), differentiation (16%), metabolism (11%) and more. Twenty genes were concordantly altered in the cDNA and the oligo-array.

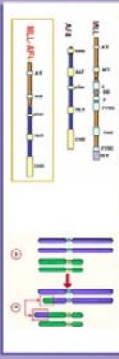


Fig 1a. MLL-AF4 and MLL-AF4

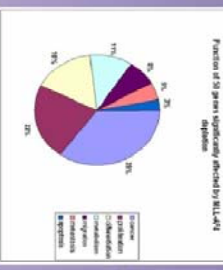


Fig 2. Chart of gene function

### Methods

Cell cultures of leukemic SKM1 (ALL) cells with MLL-AF4 fusion gene) in RPMI + 10% FCS + 1% GM in 37°C, 5% CO<sub>2</sub>. Cells were disrupted with sDNA (Inger + 2 controls) followed by lysis in lysis buffer in the ovate and a 30 fold dilution in medium. RT-PCR: Isolation of RNA via RNeasy columns (Qiagen), cDNA synthesis: RT-PCR, with SYBR green mix and primer against MLL-AF4 fusion transcript.

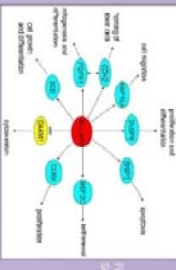


Fig 3. Network of genes significantly altered by MLL-AF4

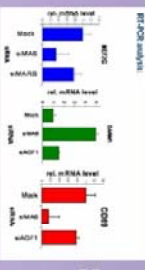


Fig 4. Expression levels of validated genes




Fig 5. Gene ontology of genes significantly altered by MLL-AF4

### Conclusions

- Possible target genes of MLL-AF4 were identified and validated
- Gene expression pattern and level of genes affected by MLL-AF4 down-regulation were analysed
- Biological functions of possible MLL-AF4 target genes have been assigned and a interaction model hypothesized

### References


Thomas M, Groll J, Hakkarin S, O'Gorman M. Targeting leukemic fusion proteins with small interfering RNAs. *Mol Pharmacol* 2006; 70(3): 173-81.

Thomas M, et al. Targeting MLL-AF4 with short interfering RNAs inhibits clonogenicity and upregulates p21<sup>CIP1</sup> in primary human leukemic cells. *Blood* 2005; 106(10): 3598-96.

### This Work Was Sponsored By:

Deutscher-Joel-Carreras-Leukämie-Stiftung

NIHCC, North of England Children's Cancer Research Fund



LRF stem cell meeting London, November 2007

XX. Conference of the Kind-Philipp-Stiftung for leukaemia research in Wilsede (Hamburg), June 2007

Presentation: Identification and Characterisation of MLL-AF4 target Genes

## **Publication**

Manuscript accepted in *Leukaemia*, June 2009

Leukemic fusion genes *MLL/AF4* and *AML1/MTG8* support leukaemic self-renewal by controlling expression of the telomerase subunit TERT

\*Andreas Gessner<sup>1</sup>, \*Maria Thomas<sup>2,5</sup>, Patricia Garrido Gastro<sup>1</sup>, Lars Büchler<sup>1</sup>, Tim Brümmendorf<sup>4,6</sup>, Natalia Martinez Soria<sup>2,7</sup>, Josef Vormoor<sup>1</sup>, Johann Greil<sup>3</sup> and Olaf Heidenreich<sup>1</sup>

### Abstract

Leukemia relapse and persistence of leukemic cells are greatly dependent on the self-renewal capacity of leukemic cells. Telomerase plays an important role in self-renewal in both malignant and non-malignant cells. However, the underlying molecular mechanisms and genes involved in malignant self-renewal remain incompletely understood. *MLL/AF4* and *AML/MTG8* represent two leukemic fusion genes, which are most frequently found in infant acute lymphoblastic leukemia (ALL) and acute myeloid leukemia (AML), respectively. By using RNA interference, we examined more precisely the influence of *MLL/AF4* and *AML1/MTG8* fusion genes on the expression of

*TERT* coding for the telomerase protein subunit, and subsequently telomerase activity in t(4;11)-positive ALL and t(8;21)-positive cell lines, respectively. *MLL/AF4* suppression diminished telomerase activity and expression of *TERT*. Blocking pro-apoptotic caspase activation in conjunction with *MLL/AF4* knockdown enhanced the inhibition of *TERT* gene expression, which suggests that *MLL/AF4* depletion does not reduce *TERT* expression levels by inducing apoptosis. Knockdown of *HOXA7*, a direct transcriptional target of *MLL/AF4* fusion gene, caused a reduction of telomerase and *TERT* to an extent similar to that observed with *MLL/AF4* suppression. Chromatin immunoprecipitation of SEM cells, using ectopically expressed FLAG-tagged Hoxa7, indicate *HOXA7* binding site in the *TERT* promoter region. Furthermore, suppression of the *AML1/MTG8* fusion gene was associated with severely reduced clonogenicity, induction of replicative senescence, impaired *TERT* expression and accelerated telomere shortening. We thus present findings that demonstrate a mechanistic link between leukemic fusion proteins, essential for development and maintenance of leukemia, and telomerase, a key element of both normal and malignant self-renewal.

## **Courses**

Endnote

Document Management 1+2

Animal course module 1-3

personal licence (Home office)